INFORMATION TO USERS

This manuscript has been reproduced from the microfilm master. UMI films the text directly from the original or copy submitted. Thus, some thesis and dissertation copies are in typewriter face, while others may be from any type of computer printer.

The quality of this reproduction is dependent upon the quality of the copy submitted. Broken or indistinct print, colored or poor quality illustrations and photographs, print bleedthrough, substandard margins, and improper alignment can adversely affect reproduction.

In the unlikely event that the author did not send UMI a complete manuscript and there are missing pages, these will be noted. Also, if unauthorized copyright material had to be removed, a note will indicate the deletion.

Oversize materials (e.g., maps, drawings, charts) are reproduced by sectioning the original, beginning at the upper left-hand corner and continuing from left to right in equal sections with small overlaps.

ProQuest Information and Learning
300 North Zeeb Road, Ann Arbor, MI 48106-1346 USA
800-521-0600

Université de Sherbrooke

Modélisation moléculaire de la protéine "Steroidogenic Acute Regulatory" (StAR) et du cytochrome P450 17α-hydroxylase/17,20-Lyase (P450c17): Une approche moléculaire pour comprendre les mécanismes de la stéroïdogenèse.

par

Axel Patrick Mathieu

Département de Biochimie

Thèse présentée à la Faculté de Médecine

en vue de l'obtention du grade de

Philosophiae Doctor (Ph.D.)

Janvier 2002

À ma jolie femme et mes enfants, pour leur montrer que tout est possible si nous le désirons et que le support de la famille peut nous mener à des chemins de découvertes inimaginables.

TABLE OF CONTENTS

List of Figures

Chapter 2.2.

Chapter 3.1.

Chapter 3.2.

Chapter 3.3.

List of Abbreviations

3β-HSD ..... 3β-Hydroxysteroid dehydrogenase

AI, AII, and AIII ..... Angiotensin I, II, and III respectively

ACE ..... Angiotensin converting enzyme

ACTH ..... Adrenocorticotropin hormone

AT1 and AT2 ..... AII receptors type 1 and 2 respectively

AVP ..... Arginine vassopressin

Bu2-cAMP (cAMP) ..... Dibutyryl adenosine-3',5'-cyclic monophosphate

CAH ..... Congential adrenal hyperplasia

CRH ..... Corticotropin releasing hormone

DAG 1,2-Diacylglycerol

DHEA ..... Dehydropeiandrosterone

DHEAS ..... Dehydroepiandrosterone Sulfate

G-proteins ..... Guanosine triphosphate-binding proteins

HMG-CoA ..... 3-Hydroxy-3-methylglutaryl-coenzyme A

HPA ..... Hypothalamus-pituitary-adrenal axis

IP_3 ..... Inositol 1,4,5-triphosphate

IUPAC ..... International Union of Pure and Applied Chemistry

LCAH ..... Lipoid congenital hyperplasia

^{32}P ..... ^{32}Phosphorus

P450aldo ..... Cytochrome P450 aldosterone synthase

P450c11 ..... Cytochrome P450 11β-hydroxylase

P450c17 ..... Cytochrome P450 17α-Hydroxylase/17,20-Lyase

P450c21 ..... Cytochrome P450 21-hydroxylase

P450scc ..... Cytochrome P450 side-chain cleavage

PIP_2 ..... Phosphatidylinositol-4,5-bisphosphate

PKA ..... Protein kinase A

PKC ..... Protein kinase C

POMC ..... Pro-opiomelanocortin

RAS ..... Renin-angiotensin system

SDS ..... Sodium Dodecyl Sulphate Poly Acrylamide Gel Electrophoresis

SR-B1 ..... Scavenger, class B, type 1 receptor

StAR ..... Steroidogenic acute regulatory protein

Preface

I would like to take this oportunity to make several notes regarding the presentaion of my thesis. First, it is important to note that my thesis is presented much in the same flow as steroidogenesis. Since I worked on two distinctive projects, it was decided to present these works individually under the common theme of molecular modeling, headed by the StAR protein and followed by the P450c17. This was intended to represent the overall steroidogenesis pathway such that P450c7 has no role in steroidogenesis if StAR cannot transfer cholesterol inside mitochondria. Yet, the most part of my studies was spent on the analysis of the P450c17, which originated all this work. Second, all the articles are presented as exact copies of those sent for review in the specified journals. This results in a slight discrepancy in terms of the overall format, but should not distress the reader to a great extent. And finally, I participated in the composition of a review article after the original submission of my thesis; thus this article has been added in the appendices as supplementary documentation.

Sommaire

Au fil des années, beaucoup de travail a été accompli pour comprendre les mécanismes gouvernant le métabolisme des stéroïdes. Malheureusement, plusieurs maladies stéroïdogéniques existent et sont directement reliées à la dysfonction des enzymes responsables du métabolisme des stéroïdes. En particulier, l'hyperplasie lipoïde surrénalienne congénitale a été attribuée à la protéine «*steroidogenic acute regulatory*» (StAR) portant des mutations qui inhibent sa fonction primaire; StAR est responsable du transport du cholestérol dans les mitochondries permettant la première étape stéroïdogénique enzymatique, transformant le cholestérol en pregnénolone. Plusieurs mutations de la StAR ont été caractérisées dans le but de comprendre le mode d'action de cette protéine sur le transport du cholestérol dans la mitochondrie. Cependant, à date nous sommes toujours incapables d'en comprendre le mécanisme exact. Nous avons donc entrepris des démarches pour clarifier le mécanisme d'action de la StAR en utilisant des techniques à la fine pointe de la technologie, telle que la modélisation moléculaire.

Nous avons développé un modèle StAR basé sur les données cristallographiques de la protéine MLN64 humaine. Nous démontrons par notre modèle que StAR possède une cavité hydrophobe et non un tunnel tel qu'observé pour la molécule MLN64. Cette cavité a une surface de 783.9 $Å^2$, assez large pour maintenir une molécule de cholestérol. De plus, nous avons identifié un pont salin unique dans cette cavité, responsable de la liaison du cholestérol *via* une molécule d'eau; ceci suggère que le cholestérol se lie à l'intérieur de la StAR. En considérant que des cavités à l'intérieur des protéines déstabilisent les structures des protéines natives, et que la cavité de StAR doit s'ouvrir pour être accessible au cholestérol, nous avons exploré la possibilité que StAR existe sous forme

probablement associée au vieillissement. Or, il est important d'élucider le mécanisme d'action du P450c17 pour comprendre son contrôle différentiel lors du vieillissement.

Nous démontrons que trois mutants, T202N, D240N, et D407H, modulent l'activité du P450c17 de manières différentes dépendant de leurs effets structuraux.. Ceci supporte le concept que le P450c17 est contrôlé par des facteurs post traductionnels qui modifieraient aussi sa structure, tel que la phosphorylation. Notre modèle du P450c17 de hamster révèle une structure légèrement différente de celle du modèle du P450c17 humain, ce qui n'est pas surprenant puisqu'ils possèdent des d'activités différentes. Dans ce contexte notre modèle est utilisable pour l'étude du mécanisme d'action du P450c17.

En couplant la modélisation moléculaire et la mutagénèse dirigée, nous avons donc créé des systèmes testables *in silico* nous permettant d'obtenir d'importantes informations et de suggérer de nouveaux mécanismes d'action.

1. Introduction:

1.1. The Adrenal Gland:

1.1.1. History and Histology: The initial description of the adrenal gland seems to have been in 1563 by Eustachius as the "*glandulae renis incumbentes*". Unfortunately, his results were only published in 1714, as edited by Lancisius (Eustachius, 1774). The adrenal gland was then shown to be separated into two distinct zones due to differential staining in 1856 by Vulpian (Vulpian, 1856); these zones are the cortex and the *medulla*, basically representing two glands in one. Although both zones are important for normal physiological function, only the cortex is of interest for this presentation. Ten years after the discovery of the cortex and *medulla*, the cortex was then subdivided into three layers termed *zonae glomerulosa*, *fasciculata* and *reticularis* (Arnold, 1866) each of which secretes a particular steroid subfamily due to distinct expression of steroidogenic enzymes (see "The Steroidogenesis Pathway" below).

Regrettably, associating function to the adrenal gland remained unclear for a long period of time since the discovery of the adrenal gland. In 1849, Addison first published the results of abnormal adrenal glands in three deceased patients with anemia (Addison, 1849), but it wasn't until 1855 that he described chronic adrenal insufficientcy (Addison, 1855), now referred to as Addison's disease. The year after, Brown-Séquard demonstrated that adrenal glands were essential for life as bilateral adrenalectomy on various animal species caused death (Brown-Séquard, 1856). Since, many disorders have been characterized describing different adrenal function deficiencies. In particular, Cushing described a disease involving excessive and prolonged secretion of

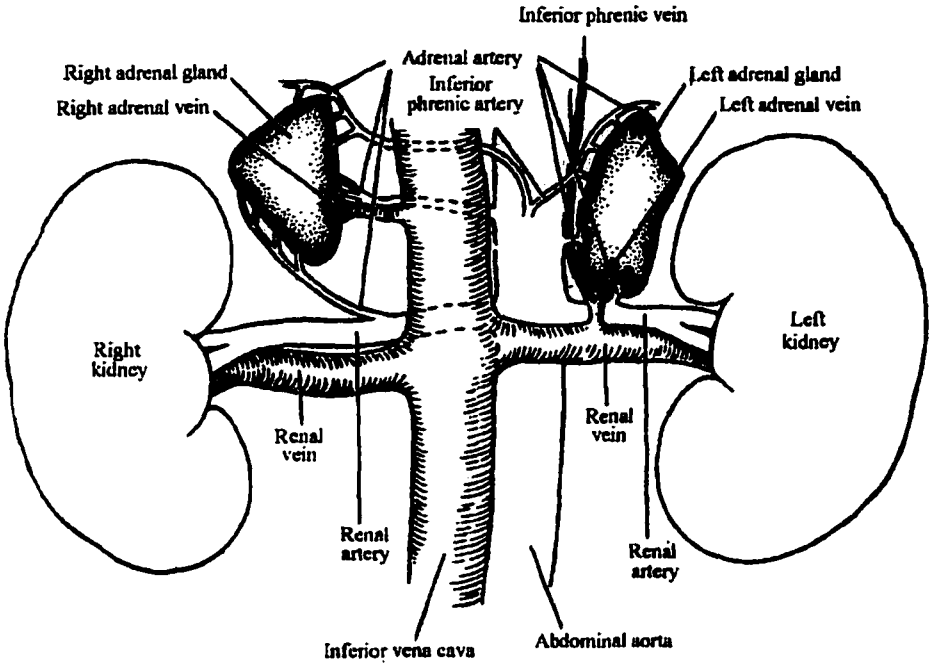

Fig. 1. Location of the adrenal glands. Of particular interest, both adrenal glands are properly supplied with blood (not distinctly shown in this diagram) and each adrenal gland is directly attached to a principal vein; the right adrenal vein empties into the inferior vena cava and the left adrenal gland into the renal vein. This "connectivity" is required for appropriate release of steroids into the blood flow (Greenspan, 1991).

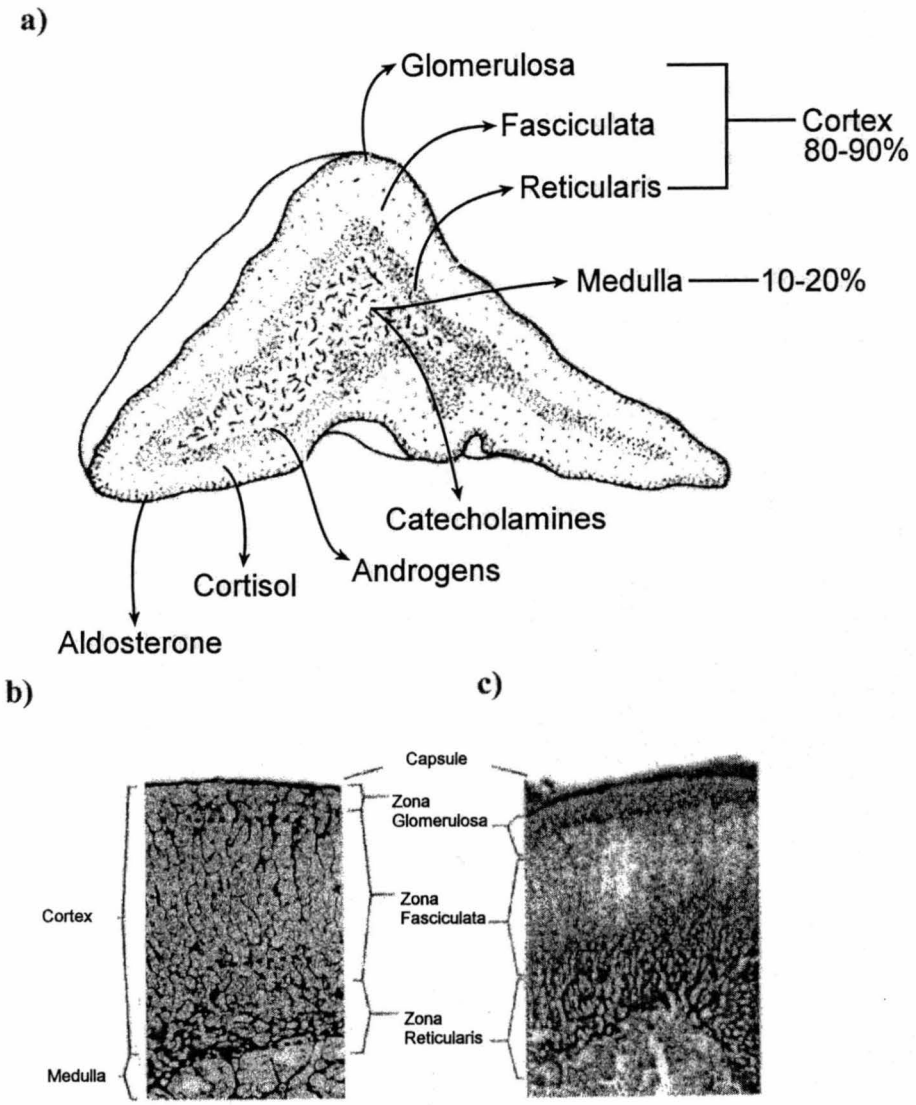

Fig. 2. Adrenal gland zones. a) The adrenal gland is composed of two distinct zones: the cortex and the *medulla* representing approximately 85% and 15% of the total adrenal gland weight respectively. Each zone is responsible for the secretion of a particular hormone (Griffin and Ojeda, 1992). Histological cuts of the hamster (b) and human (c) adrenal glands also demonstrate the subdivision of the cortex in zones called *zonae glomerulosa*, *fasciculata* and *reticularis* (Dulbecco, 1991).

1.2. Hormonal Steroids:

1.2.1. History: Cholesterol, the mother of all steroids, was apparently first discovered in gallstones in 1763 (DeFourcroy, 1789). Thereafter, all compounds discovered with the basic cyclopentanoperhydrophenanthrene structure (Fig. 3) were termed steroids (also known as hormonal steroids). Estrogen was structurally defined in 1932, followed by progesterone in 1934, testosterone in 1935, and aldosterone in 1953. Today, hundreds of steroids produced from various steroidogenic tissues have been identified contributing to their field of study, termed endocrinology.

1.2.2. Classification and Nomenclature: The adrenal steroids can be classified into two distinct groups according to their structures: androstanes and pregnanes. A cyclopentanoperhydrophenanthrene core with two additional methyl groups attached at positions 13 and 10 (carbons respectively numbered 18 and 19) are androstanes, while pregnanes are androstanes with an additional ethyl group at position 17 (respectively carbons 20 and 21). Although, adrenal steroids can also be classified according to their secretion patterns and biological functions: mineralocorticoids, glucocorticoids, and androgens. Basically, mineralocorticoids are steroids secreted from the *zona glomerulosa* whose primary function is to regulate plasma ion homeostasis and ultimately lead to plasma volume and tension regulation. Glucorticoids on the other hand, are mainly secreted from the *zona fasciculata* and generally perceived as stress mediators broadly implicated in a variety of biological responses. These include increased gluconeogenesis, relaxation of blood vessels in the vicinity of skeletal muscle, and decreased immunity response. In contrast, androgens are secreted from the *zona reticularis* and serve as precursors to sexual hormones. All these steroids are derived from cholesterol and their

nomenclature follows either of two possibilities: nomenclature established by the International Union of Pure and Applied Chemistry (IUPAC) (International Union of Pure and Applied Chemistry, 1972 – also at http://www.chem.qmw.ac.uk/iupac/steroid/) or trivial names based on biological properties (some examples given in Table 1); for simplicity, trivial names are used here.

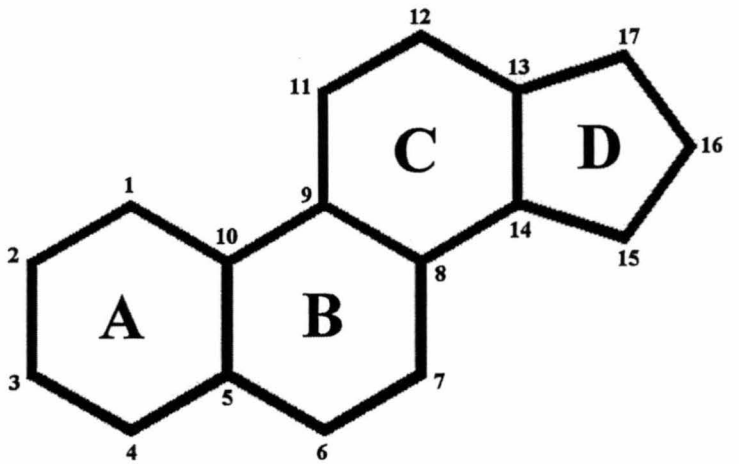

Fig. 3. Cyclopentanoperhydrophenanthrene. Basic structural core for all steroids. Rings are labelled A-D while each carbon is numbered.

Table 1. Trival and IUPAC names of serveral adrenal steroids.

Trivial	IUPAC
Aldosterone	Pregn-4-ene-11β,21-diol-3,18,20-trione
Androstenedione	Androst-4-ene-3,17-dione
Cortisol	Pregn-4-ene-11β,17α,21-triol-3,20-dione
Dehydroepiandrosterone	Androst-5-ene-3β-ol-17-one
Deoxycorticosterone	Pregn-4-ene-21-ol-3,20-dione
Pregnenolone	Pregn-5-ene-3β-ol-20-one
Progesterone	Pregn-4-ene-3,20-dione

1.3. The Adrenal Steroidogenic Pathway:

The adrenal steroidogenic pathway consists of many steroidogenic enzymes responsible for the metabolism of cholesterol to various hormonal steroids. Figure 4 depicts the classical steroidogenic pathway in the adrenal gland. One has to keep in mind that the adrenal steroidogenic pathway is different in species, dependent on the expression of the steroidogenic enzymes. Here, a general perception of the adrenal steroidogenic pathway is introduced and as such, makes no distinction of species-specific steroidogenesis. This will be discussed later.

Cytochromes P450 make up the majority of adrenal steroidogenic enzymes. These enzymes contain a single heme prosthetic group (Fig. 5), which the maximum absorbance is displaced from 420 nm to 450 nm when reduced and bound to carbon monoxide (Nebert and Gonzalez, 1987), effectively and efficiently differentiating them from other heme-bound proteins. These enzymes mostly consist of approximately 500 amino acids and with electrons provided by NADPH, can reduce atmospheric oxygen in the following manner:

$$NADPH + H^{+} + O_2 + R\text{-}H \xrightarrow[R=Steroid]{P450} R\text{-}OH + H_2O + NADP^{+}$$

Most P450's are of hepatic origin responsible for the catabolism of a huge number of toxins, medication, and polluents (Nebert and Gonzalez, 1987). Since only a few hundred P450's are available for this catabolism, it is not surprising that the P450's have evolved to accommodate and be reactive to more than one substrate. This applies to all adrenal P450's that recognize more than one substrate and have more than one catalytic activity.

In adrenal gland cells, two types of P450's exist: mitochondrial and microsomal. These are evidently characterized by their location, but also by their electron transport mechanisms. Mitochondrial P450's require adrenodoxin and adrenodoxin reductase in order to complete the reduction reaction (Fig. 6). In mitochondria, the electron transport system is located in the inner mitochondrial membrane, facing the matrix. Adrenodoxin reductase oxidizes NADPH and adrenodoxin serves as an electron shuttle, transporting one electron at a time from adronodoxin reductase to the target acceptor P450. Microsomal P450's on the other hand, directly obtain their electrons sequentially from the NADPH reductase located on the cytosolic side of the endoplasmic reticulum membrane (Fig. 6).

Before any steriodogenesis can occur, cholesterol first has to be localized in the steroidogenic tissue. There are two sources of cholesterol: circulating plasma lipoproteins and *de novo* synthesis. Circulating lipoproteins provide the majority of the cholesterol (~80%) utilized for steroidogenesis (Bolté *et al.*, 1967; Borkowski *et al.*, 1967; Gwynne and Strauss, III, 1982). Particularily, low-density lipoproteins are endocytosed through coated pits, degraded by lysozymes, and the esterified cholesterol is stored in lipid droplets until utilisation (Fig. 7). High-density lipoproteins also transfer cholesterol to steroidogenic tissue, although through a non-degradation pathway using the scavenger, class B, type 1 receptor (SR-B1) (Williams *et al.*, 2000). Endogenous sources of cholesterol require synthesis from acetate; the rate-limiting step of cholesterol synthesis is the conversion of 3-hydroxy-3-methylglutaryl-coenzyme A (HMG-CoA) to mevalonate though the HMG-CoA reductase (Gibson and Paker, 1987). Before utilisation, lipid droplet esterified cholesterol has to be desterified though the activity of cholesterol

esterase, and transported to the mitochondria outer membrane *via* various possible candidates (Sviridov, 1999). Once at the mitochondrial outer mitochondria membrane, the hydrophobic cholesterol necessitates a transport mechanism to cross the mitochondrial hydrophilic intermembrane space; this transport mechanism has been identified as the steroidogenic acute regulatory protein (StAR).

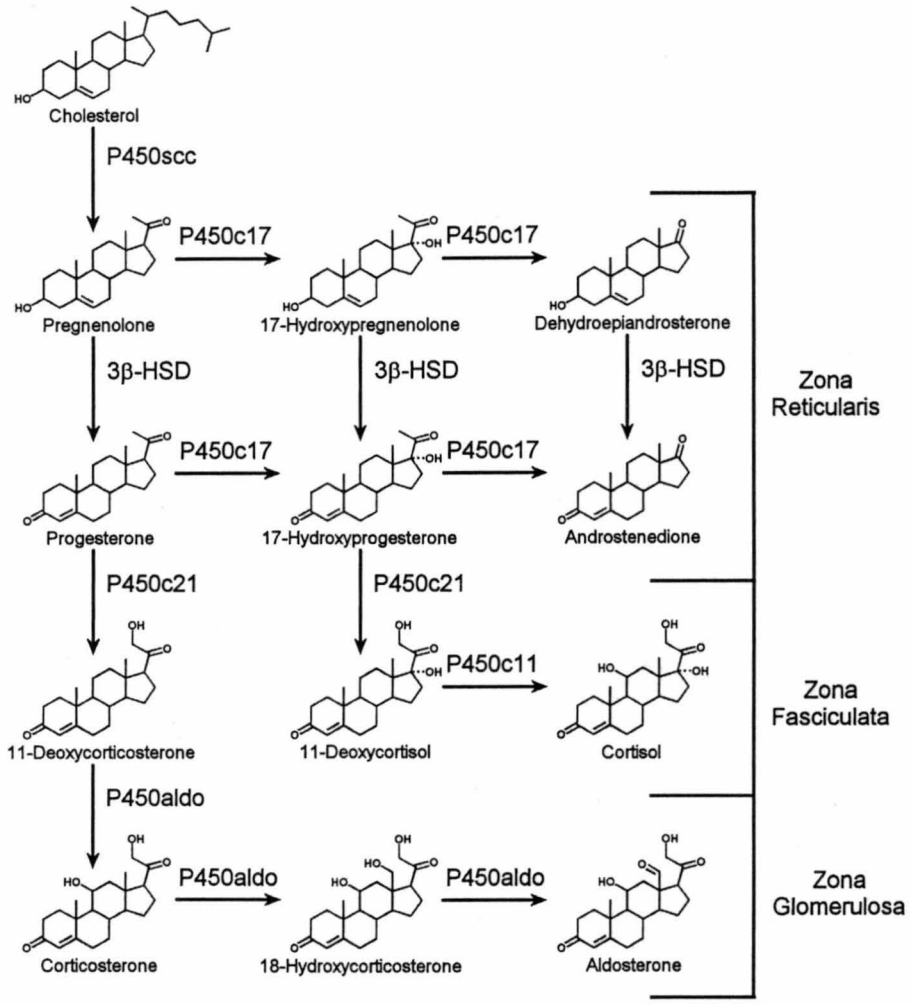

Fig. 4. Classic adrenal steroidogenesis.

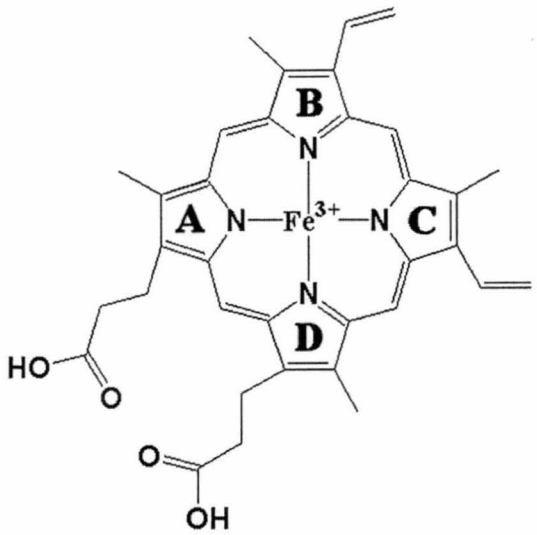

Fig. 5. Heme prosthetic group for the P450 enzymes. The heme prosthetic group for the family of P450 enzymes is of type b, characterized by a propionate and methyl group on the A and D rings, and a methyl and ethene group on the B and C rings.

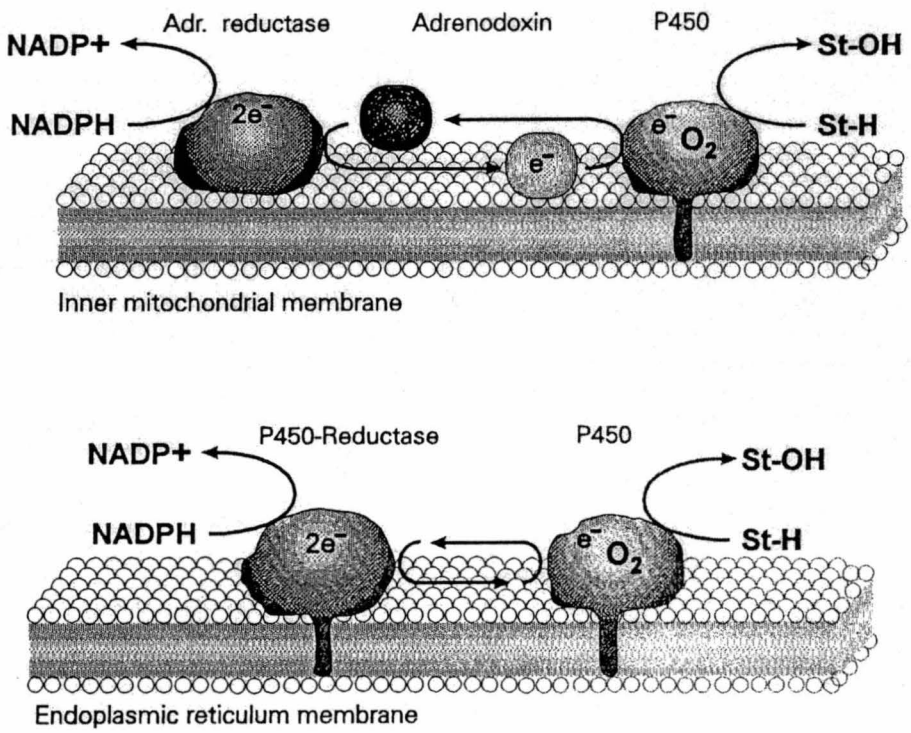

Fig. 6. Models for the electron transport system of mitochondrial and microsomal P450's. Adr. Reductase, adenodroxin reductase; St, Steroid (Hanukoglu, 1992).

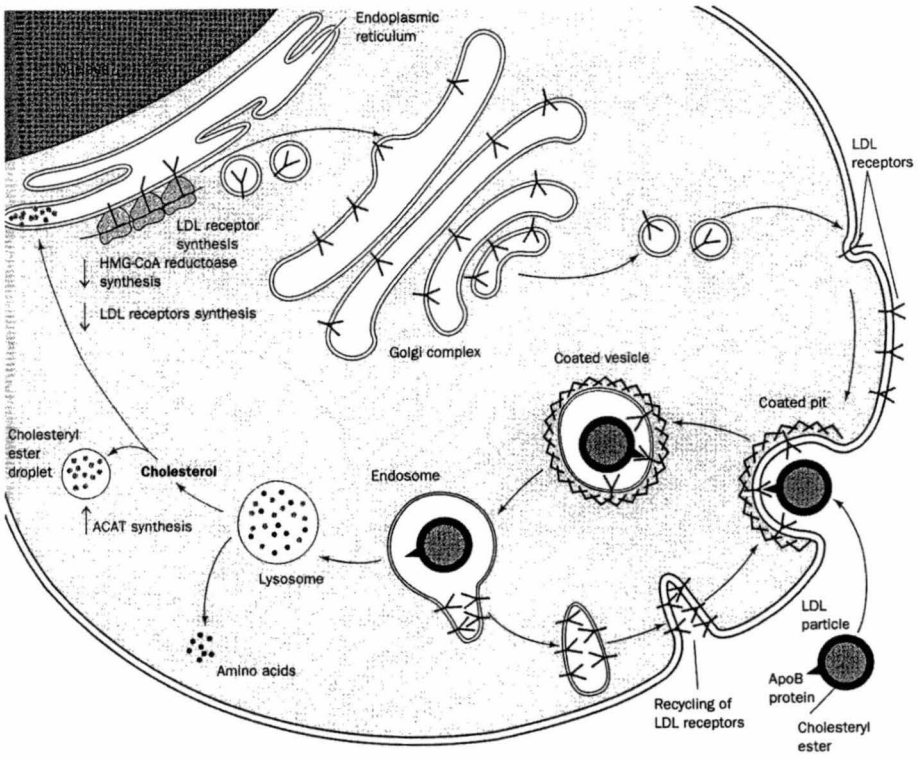

Fig. 7. Cholesterol supply to endocrine cells by low-density lipoproteins (LDL). LDL from the blood flow is endocytosed through clatherin-coated pits, degraded by lysosomes, and the cholesterol is stored in lipid droplets until utilisation (Voet and Voet, 1990).

1.3.1. Steroidogenic Acute Regulatory Protein (StAR): It has long been believed that the rate-limiting step in steroidogenesis was the conversion of cholesterol to pregnenolone by the protein P450 side-chain cleavage (P450scc) in view of the fact that it is the first enzyme-dependent step in steroidogenesis (Farkash *et al.*, 1986). Relatively recently, it has been demonstrated that the true rate-limiting step in steroidogenesis is the protein-dependent transfer of cholesterol to the matrix side of the inner mitochondrial membrane where P450scc is located (Epstein and Orme-Johnson, 1991b; Privalle *et al.*, 1983). Basically, cycloheximide-inhibition of *de novo* protein synthesis inhibited both steroidogenesis and the transfer of cholesterol inside mitochondria, although the identity of the protein responsible for such a task remained a mystery for many years. The discovery of StAR by Clark, B.J. and collaborators (Clark *et al.*, 1994) in the MA-10 mouse Leydig tumor cell line, identified the best candidate for the protein responsible for the adrenocorticotropin hormone (ACTH – see below) stimulated steroidogenesis described by Orme-Johnson and colleagues (Alberta *et al.*, 1989; Epstein and Orme-Johnson, 1991a; Epstein and Orme-Johnson, 1991b; Hartigan *et al.*, 1995;Pon *et al.*, 1986; Pon and Orme-Johnson, 1988). Many experimental results support StAR's implication in the protein-dependent transfer of cholesterol inside mitochondria, but the most bolstering result is the StAR knock-out mouse (Caron *et al.*, 1997) displaying lipoid congenital hyperplasia (LCAH – see below). Mutational analyses of StAR also demonstrated that a dysfunctional StAR was responsible for the defective steroidogenesis in patients with LCAH (Bose *et al.*, 1996; Bose *et al.*, 1997; Fujieda *et al.*, 1997; Lin *et al.*, 1995; Nakae *et al.*, 1997; Tee *et al.*, 1995). Yet, the exact mechanism of StAR in the transfer of cholesterol inside mitochondria is controversial.

Three mechanisms for StAR action have been proposed: 1) desorption (Stocco and Clark, 1996), 2) molten glubule acting on the outer mitochondrial membrane (Bose *et al.*, 1999), and 3) intermembrane shuttle (Tsujishita and Hurley, 2000). Several key observations are in support of these contradicting mechanisms. First, StAR has a mitochondrial leader peptide targeting it to mitochondria and mediating its entry. The desorption model (Stocco and Clark, 1996) suggests that as StAR enters mitochondria *via* its targeting leader peptide, contact sites are created between the outer and inner mitochondria membranes, effectively ablating the intermembrane space, and thus allowing large amounts of cholesterol to flow from the outer to inner mitochondrial membrane. The greatest downfall of this mechanism is the fact that it has been shown that StAR lacking the first 46 amino acids (lacking the mitochondrial targeting peptide) can still transfer cholesterol inside mitochondria (Arakane *et al.*, 1996; Arakane *et al.*, 1998). Second, loss of StAR tertiary structure without loss of secondary structure was observed at low pH (3.5-4.0), suggesting that a molten globular form is important for StAR function (Bose *et al.*, 1999). Taken together with the observation that the N-terminally cleaved StAR can still function, these authors suggest that StAR functions as a molten globule remaining in contact with the cytosol side of the outer mitochondria membrane. Although it has been shown that an active electrochemical force is necessary for the transfer of cholesterol inside mitochondria (King *et al.*, 1999), an acidic environment immediately adjacent to the outer mitochondrial membrane *in vivo* is speculative and has not been demonstrated to exist. Finally, the crystal structure determination of the human MLN64, a protein believed to replace StAR in tissues lacking StAR such as the placenta, showed the presence of a hydrophobic tunnel large enough to

accommodate one cholesterol molecule resembling other sterol carrier proteins (Tsujishita and Hurley, 2000). In addition, the tunnel openings are not large enough to allow passage of the cholesterol molecule, suggesting that StAR shuttles one cholesterol molecule at a time between the mitochondrial membranes. Unfortunately, this model cannot support the observed rapid cholesterol transfer mechanism inside mitochondria (Artemenko *et al.*, 2001) or the fact that StAR still functions without its mitochondrial leader peptide. It is clear that not one mechanism can account for the true functionality of StAR and thus the idea of an amalgamated mechanism is growing (Stocco, 2000). Regrettably, crytallization of StAR has been unsuccessful, and the closest approximation of the actual StAR structure and mechanism is the crystallized MLN64. Moreover, StAR has been shown to exist as a phosphoprotein and the implication of this phosphorylation in its mechanism remains unclear.

Indeed, StAR phosphorylation was reported well in advance of the identification of StAR as the main constituent responsible for the protein-mediated mitochondrial cholesterol transfer (Alberta *et al.*, 1989; Epstein and Orme-Johnson, 1991a; Epstein and Orme-Johnson, 1991b; Pon *et al.*, 1986; Pon and Orme-Johnson, 1986; Pon and Orme-Johnson, 1988), and mutational analyses of StAR's serine 195 reduced its ^{32}P incorporation and activity by 50% *ex vivo* (Arakane *et al.*, 1997). Although StAR has been shown to have several forms in two-dimensional SDS-PAGE (Arakane *et al.*, 1997; Epstein and Orme-Johnson, 1991a; LeHoux *et al.*, 1999; Pon *et al.*, 1986; Pon and Orme-Johnson, 1988), no systematic phosphorylation/function analyses have been undertaken to explain such observations, and no almagamated mechanism has been methodically verified.

1.3.2.Cytochrome P450 17α-Hydroxylase/17,20-Lyase (P450c17): Once pregnenolone has been formed in mitochondria, it can then be converted into any other steroid through metabolism by many different enzymes. In fact, pregenenolone is located at the apex of a major divergence in the steroidogenic pathway (Fig. 4). P450c17 is a bifunctional endoplasmic reticulum membrane-bound enzyme, displaying two activites in a single active site (Nakajin *et al.*, 1981; Zuber *et al.*, 1986). The first activity is 17α-hydroxylation, adding a hydroxyl group at carbon 17 of the cyclopentanoperhydrophenanthrene core. The second activity, 17,20-lyase, uses the 17α-hydroxylated products previously formed and cleaves the carbon 17 to carbon 20 bond leading to the formation of androstanes. Not only is the P450c17 complex enough with the utilisation of a single active site for two distinct activites, but two sets of substrates can also bind and be reactive in the P450c17. Therefore, four different substrates can bind and be reactive in the P450c17: pregnenolone, progesterone, 17α-hydroxypregnenolone and 17α-hydroxyprogesterone (Fig. 4).

In adrenal glands, P450c17 is usually expressed in the *zonae fasciculata* and *reticularis*, and never in the *zona glomerulosa* ensuing in the observed patterns of steroid secretion (Fig. 2 vs Fig. 4). Moreover, P450c17 expression and reactivity are species-specific (see the section entitled "The Hamster as a Model") and may not even be expressed in the adrenal glands. Without the expression of P450c17, pregnenolone is eventually converted into corticosterone and mineralocorticoids. In the case where P450c17 is expressed, separation of both activites leads to the production of either glucocorticoids or androgens. Due to the complexity of the P450c17 system with species-

specific steroid production, much work is being undertaken to understand the differential functional control of the P450c17 in steroidogenesis.

In order to have a fully functional P450c17, four elements must be present: proper P450c17 binding to the endoplasmic reticulum membrane, heme binding, substrate binding, and electron transfer from NADPH to P450c17. If any one or more of these processes are dysfunctional, impaired P450c17 may result in various clinical symptoms including hypertension, ambiguous genital formation in males, and lack of progression into puberty for females (Auchus, 2001).

Although pregnenolone is produced in mitochondria and the P450c17 is bound to the endoplasmic reticulum, pregnenolone can still attain the P450c17. As a matter of fact, cleavage of cholesterol's hydrophobic side chain by P450scc confers and additional polar group to pregnenolone allowing it to be readily soluable in hydrophilic solvent; the cyclopentanoperhydrophenanthrene ring still maintains the hydrophobic character of steroids allowing the steroids to diffuse across membranes.

1.3.3. Other Steroidogenic Enzymes: Obviously, many enzymes are necessary for the production of all the adrenal steroids (Fig. 4) and are not of particular interest for this thesis. Thus, only a brief description of their activites is presented here. These enzymes can be divided into two groups: mitochondrial and microsomal. Along with P450c17, the 3β-hydroxysteroid dehydrogenase (3β-HSD) and the cytochrome P450 21-hydroxylase (P450c21) are located in the endoplasmic reticulum. 3β-HSD is not a P450 enzyme and is expressed in all three zones of the adrenal cortex (Dupont *et al.*, 1990); various isoforms of 3β-HSD have been identified in a panoply of tissues for a variety of species, including the hamster (Rogerson *et al.*, 1998). In the adrenal, 3β-HSD is responsible for the

conversion of 3β-hydroxy-5-ene steroids into 3-keto-4-ene steroids. Therefore, pregnenolone, 17α-hydroxypregnenolone and DHEA are all substrates for 3β-HSD and are converted into progesterone, 17α-hydroxyprogesterone, and androstenedione respectively (Fig. 4).

The microsomal P450c21 is responsible for the hydroxylation at carbon 21 of the alkyl group of pregnanes, essential for the synthesis of mineralocortiocoids and glucocorticoids. This enzyme is expressed in all three zones of the adrenal cortex (Ishimura and Fujita, 1997) and mediates the conversion of progesterone to 11-deoxycorticosterone and the conversion of 17α-hydroxyprogesterone to 11-deoxycortisol (Fig. 4). Being microsomal, the P450c21 uses the same electron transport system as the P450c17 (Fig. 6).

The remaining steroidogenic enzymes presented here are the mitochondrial cytochromes P450 11β-hydroxylase (P450c11) and P450 aldosterone synthase (P450aldo). Both these enzymes are located on the matrix side of the inner mitochondrial membranes and use the same electron transport mechanism as P450scc. Due to their high homology (>90% in humans), it was believed for a considerable time that these enzymes were in fact only one protein and caused much debate on "its" differential activity regulation in the *zona glomerulosa* versus the *zonae fasciculata* and *reticularis*. As shown in Fig. 4, both the P450c11 and the P450aldo display 11β-hydroxylation, but the P450aldo has additional 18-hydroxylation and 18-oxidation activities to synthesize aldosterone. What then, was the determining factor allowing 18-hydroxylation and 18-oxidation for the corticosterone pathway while inhibiting these activities in the cortisol pathway? It was discovered over time that in actuality, two enzymes were present; the

P450c11 was expressed in the *zonae fasciculata* and *reticularis* while the P450aldo was only expressed in the *zona glomerulosa* explaining the differential activity profiles.

1.4. Deficiencies in Steroidogenic Enzymes:

1.4.1. Congenital Adrenal Hyperplasia (CAH): The term "congenital adrenal hyperplasia" refers to genetic defects hindering cortisol biosynthesis (Orth and Kovacs, 1998). Therefore, any steroidogenic enzyme involved in the production of cortisol from cholesterol can be implicated in this syndrome, including the P450scc, 3β-HSD, P450c17, and P450c21 (Fig. 4.). According to the dysfunctional enzyme present, since no cortisol is produced, there loss of negative feedback inhibition of ACTH production (see Regulation of Steroidogenic Enzyme Expression below) and accumulation of precursor steroids directing various symptoms (Orth and Kovacs, 1998). For example, loss of P450c17 activity causes accumulation of aldosterone and intermediate steroids clinically presenting hypertension, hypokalemia, and hypogonadonism (Fig. 8).

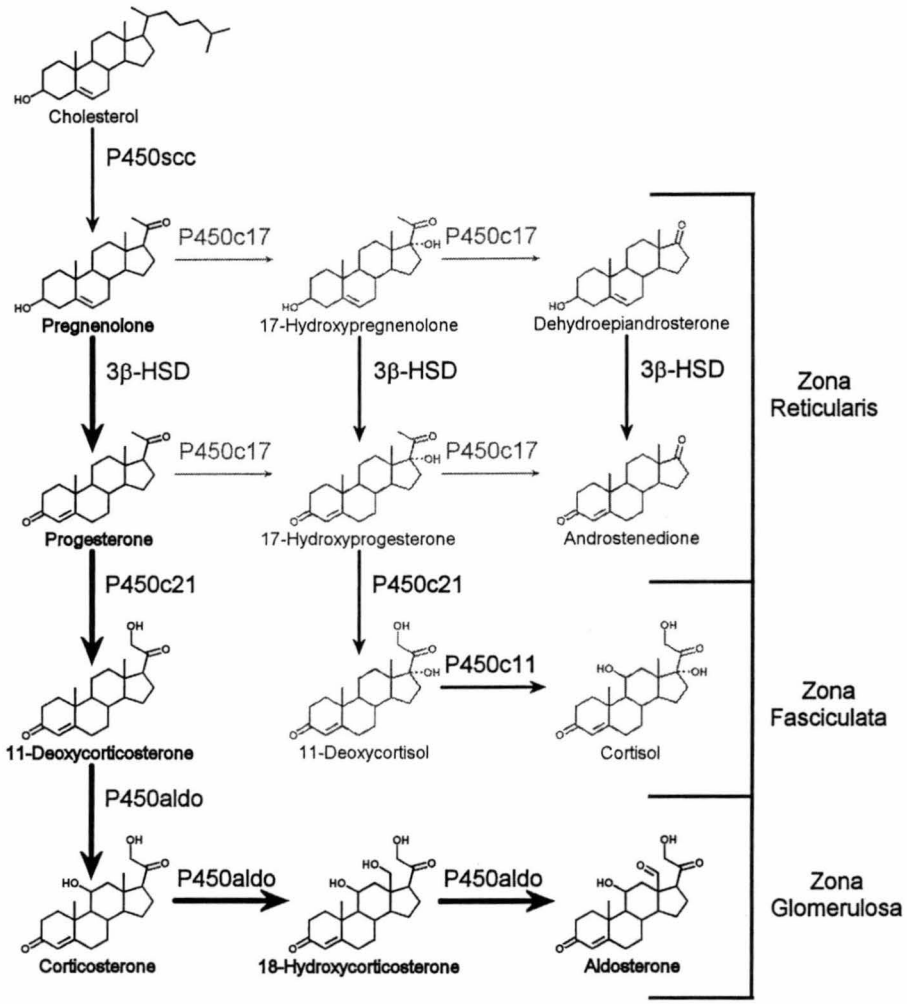

Fig. 8. Congenital Adrenal Hyperplasia manifested by loss of P450c17 activity. Same representation as in Fig. 4 showing the classic steroidogenic pathway in adrenal glands, although with a dysfunctional P450c17. Accumulated steroids are represented by larger arrows and bold names. Inhibited P450c17 activity is represented by small grey arrows, and grey steroid structures and names.

1.4.2. Lipoid Congenital Adrenal Hyperplasia (LCAH): Lipoid CAH is a fatal form of CAH, characterized by a severe adrenal insufficiency and cholesterol accumulation in adrenal glands and gonads; LCAH is manifested by failure to thrive, vomiting, diarrhea, hyponatrimia, and hypokalemia during the prenatal period (Orth and Kovacs, 1998). It was believed that LCAH was due to a dysfunctional P450scc as it is the steroidogenic enzyme responsible for the initial conversion of cholesterol to pregnenolone (Fig. 4), although since the discovery of StAR, all LCAH cases have been attributed to a dysfunctional mutant StAR (Miller, 1997) and is best described by a two-hit model. This model hypothesizes initial loss of steroidogenesis due to the dysfunctional StAR, followed by complete loss of steroidogenesis due to loss of cellular function by the accumulation of cholesterol in lipid droplets (Fig. 9).

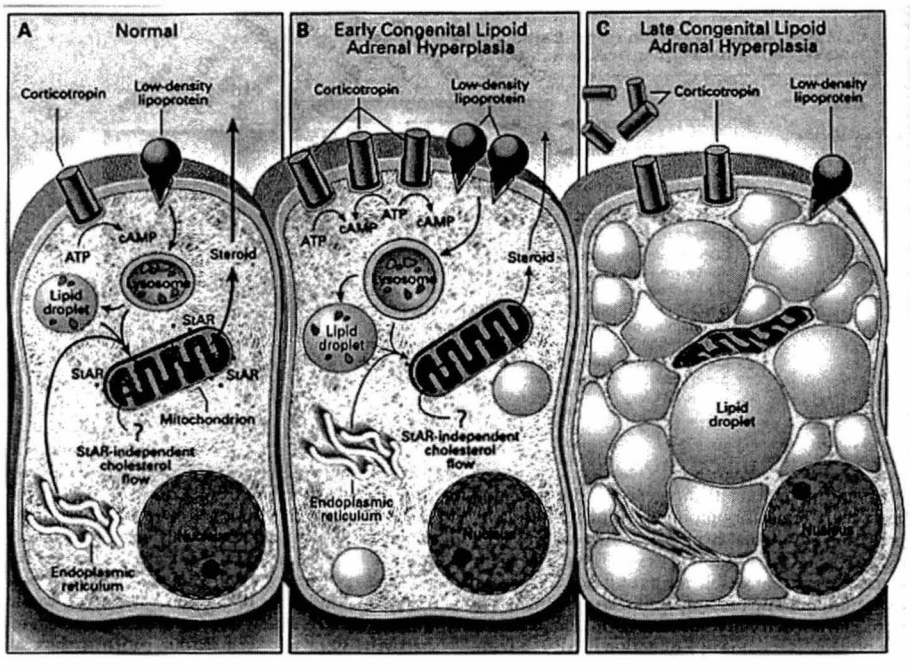

Fig. 9. Lipoid Congenital Adrenal Hyperplasia. A) Normal conditions. B) Initial loss of steroidogenesis by a dysfunctional StAR. C) Complete loss of cellular function and steroidogeneis due to accumulation of cholesterol esters in lipid droplets (Bose *et al.*, 1996).

1.5. Regulation of Adrenal Steroidogenic Enzyme Expression:

1.5.1. Adrenocorticotropin Hormone (ACTH): It has been known for a considerable time that there exists a tight association of the hypothalamus, pituitary, and adrenal glands (Fig. 10); this is called the hypothalamus-pituitary-adrenal axis (HPA). In the 1930's, the existence of a functional pituitary-adrenal axis was documented (Smith, 1930), followed by the demonstration of a negative feedback regulation of the adrenocorticotropic effect of the pituitary gland by adrenal extracts (Ingle and Kendall, 1937). In the decade following 1956, the adrenocorticotropin hormone was identified and its structure determined (Graf *et al.*, 1971). The major factor responsible for the secretion of pituitary ACTH is the corticotropin releasing hormone (CRH) from the hypothalamus; it was characterized in 1981 (Vale *et al.*, 1981). Also of importance, the hypothalamus arginine vassopressin (AVP) can stimulate pituitary ACTH secretion, although it mostly potentiates the action of CRH *in vivo* and *in vitro* (DeBold *et al.*, 1984). Basically, neurological responses such as the circadian rhythm and stress, stimulate CRH and AVP secretion from the hypothalamus. CRH and AVP then stimulate the secretion of the ACTH from the pituitary, which stimulates cortisol secretion from the adrenal glands. Cortisol then negatively regulates both the hypopthalamus and pituitary hormone secretions (Fig. 10).

ACTH is produced by the peptidic cleavage of pro-opiomelanocortin (POMC). Upon stimulation, POMC is expressed in the pituitary gland where it is processed into various peptidic species (Fig. 11) according to the location of the POMC; the anterior lobe processing is responsible for the release of ACTH from POMC. ACTH is a 39 amino acid peptide that binds to the melanocortin-2 receptor on the surface of adrenal cells

(Mountjoy *et al.*, 1992). This binding leads to the formation of cAMP by adenylyl cyclase, ultimately leading to the activation of cAMP-dependent protein kinase (PKA) phosphorylating various proteins for a variety of functions (Gill, 1976). ACTH response can be divided into two categories, acute and chronic (Simpson and Waterman, 1983; Simpson and Waterman, 1988). The acute response is characterized by the rapid conversion of cholesterol into pregnenolone (the first step in steroidogenesis – Fig. 4), mediated through the rapid transport of cholesterol to the inner mitochondrial membrane where the P450scc resides (Lin *et al.*, 1995). The chronic effect on the other hand, involves increased synthesis of most of the steroidogenic enzymes including the P450c17 (Simpson and Waterman, 1983; Simpson and Waterman, 1988). ACTH also increases circulating aldosterone levels, however this is of minor effect (Conaglen *et al.*, 1984; Williams and Dluhy, 1983); aldosterone synthesis is mostly regulated by the renin-angiotensin system (RAS).

Glucocorticoids, such as cortisol, inhibit both the ACTH secretion as well as POMC expression (Lundblad and Roberts, 1988). Also, glucocorticoids decrease CRH and AVP levels, although to a lesser extent (Davis *et al.*, 1986; Itoi *et al.*, 1987). Moreover, as though it wasn't enough, glucocorticoids block the stimulatory effect of CRH on the expression of POMC (Eberwine *et al.*, 1987) and the secretion of ACTH (Oki *et al.*, 1991), as well as inhibit CRH receptor expression in the anterior pituitary (Holmes *et al.*, 1987; Luo *et al.*, 1995). In the rat, the negative glucocorticoid feedback mechanism consists of two distinct steps (Keller-Wood and Dallman, 1984): a fast feedback in the order of seconds to minutes proportional to the rate of glucocorticoid concentration increase, and a latent feedback in the order of hours to days relative to the absolute

concentration of glucocorticoids in plasma. The secretion of ACTH is halted first, followed by the reduction in ACTH synthesis due to reduced CRH dependent POMC expression (Eberwine *et al.*, 1987).

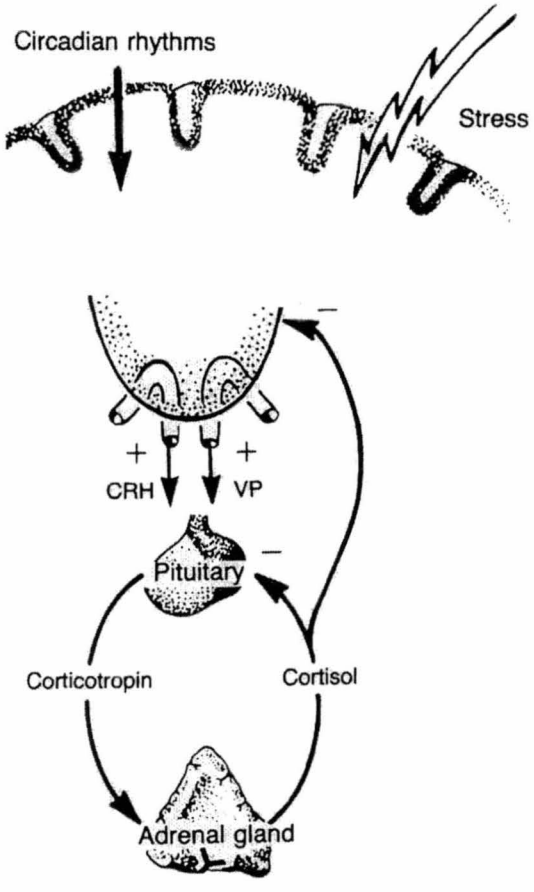

Fig. 10. The Hypothalamus-Pituitary-Adrenal Axis. Neurological effectors stimulate the secretion of corticotropin releasing hormone (CRH) and arginine vassopressin (VP) from the hypothalamus, which in turn stimulate pituitary adenocorticotropin hormone (ACTH) secretion. ACTH then stimulates cortisol production in the adrenal glands, which negatively regulates both the hypothalamus and the pituitary glands (Arnold, 1998).

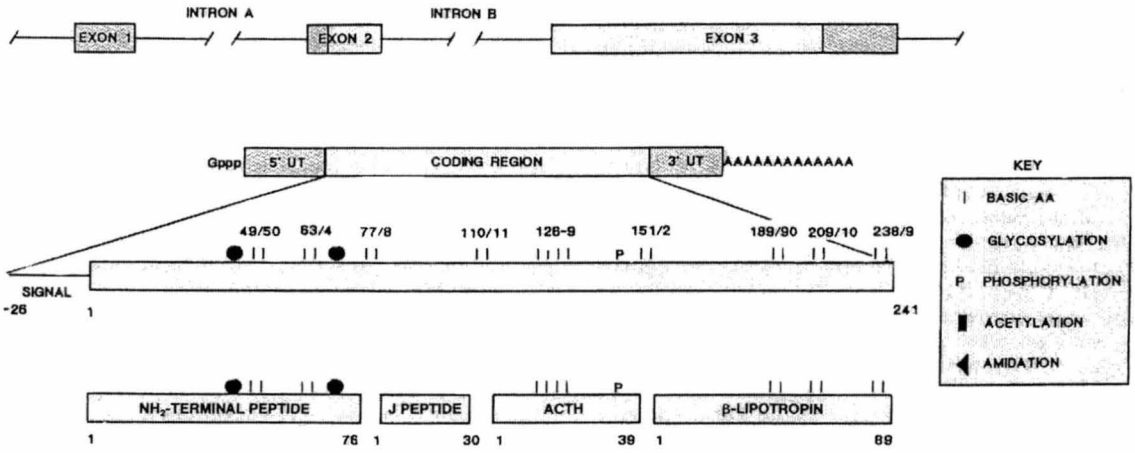

Fig. 11. Structure of the Pro-opimelanocortin (POMC) gene and protein. Once stimulated, the POMC gene expresses the POMC protein which is then proteotically cleaved according to its location in the pituitary. In this example, POMC is cleaved into the NH2-terminal peptide, joining peptide (J Peptide), adenocorticotropin hormone and β-lipotropin in the pituitary anterior lobe (Orth and Kovacs, 1998).

1.5.2. Renin-Angiotensin System (RAS): The RAS is composed of many factors resulting in the production of angiotensin II (AII), the most abundant biologically active angiotensin species in plasma, responsible for maintaining plasma volume and tension (Fig. 12). Renin is an enzyme synthesized in the kidneys, responsible for the conversion of angiotensinogen to angiotensin I (AI) (Gibbons *et al.*, 1984). AI is then rapidly converted to AII by the angiotensin converting enzyme (ACE) in the lung and other tissues including the adrenal gland. AII can then be cleaved to angiotensin III (AIII) by the peptidic cleavage of the N-terminal aspartate; both AII and AIII stimulate the production of aldosterone similarly in the adrenal gland, although AII is more potent as a vasopressor (Blair-West *et al.*, 1980;Gibbons *et al.*, 1984).

Renin is the limiting factor in this system; renin secretion is regulated by blood pressure, sodium concentration in the renal tubular fluid, and by renal sympathetic nerve activity (Gibbons *et al.*, 1984). Renin levels are increased by factors that decrease renal blood flow. For example, hemorrhaging, dehydration, and salt restriction decrease renin secretion. On the flip side, factors that increase the blood pressure, such as high salt intake, decrease renine secretion. Moreover, AII inhibits the secretion of renin by a short-feedback loop (Williams and Dluhy, 1983).

AII mediates its effects on the adrenal gland through specific cell-surface receptors coupled to guanosine triphosphate-binding proteins (G-proteins). Although much work has been accomplished in this area, only a brief description will be given here. Two major types of the AII receptors have been identified in various tissues of species, mediating a variety of responses; these receptors are appropriately termed type 1 and 2 (AT1 and AT2 respectively). Binding of AII on its receptor in the adrenal gland triggers the activation of

phospholypase C responsible for the hydrolysis of phosphatidylinositol-4,5-bisphosphate (PIP_2) to inositol 1,4,5-triphosphate (IP_3) and 1,2-diacylglycerol (DAG). DAG and IP3 are both implicated in the mediation of signal through the protein kinase C (PKC) pathway leading to various cellular responses. In the case of the adrenal cortex, this particularily augments the production of aldosterone.

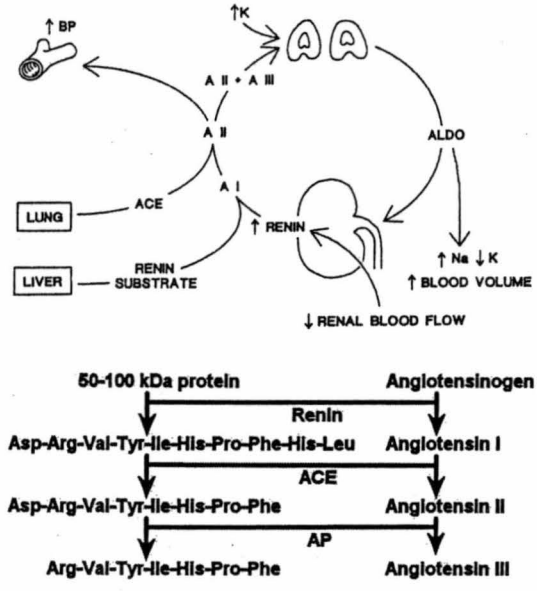

Fig. 12. The Renin-Angiotensin System. Renin from the liver converts the angiotensinogen (renin substrate) in angiotensin I (AI). In lungs, AI is converted to angiotensin II (AII) by angiotensin converting enzyme (ACE). AII can then regulate plasma volume and pressure by stimulating vasoconstriction and the production of aldosterone in the adrenal glands, responsible for the mineral homeostasis of plasma. AII can be converted to angiotensin III (AIII) by aminopeptidase (AP) (Orth and Kovacs, 1998).

1.6. The Hamster as a Model:

1.6.1. Steroidogenesis: In order to understand human endocrinology, a variety of animals have been utilized as models. Yet, not all biological systems are appropriate to relate biological responses to humans. Small laboratory animals, including the rat, mouse and guinea pig, have been used in relation to human endocrinology. Unfortunately, these models are not always desireable due to their steroidogenic enzyme expression and/or activity profiles (particularly for P450c17). We have chosen the hamster as a model to study human endocrinology for a variety of reasons. The two most convincing reasons are: 1) the hamster expresses adrenal P450c17 that resembles more like the human P450c17 activity profile than the other laboratory animals (Brière *et al.*, 1997; Cloutier *et al.*, 1995; Cloutier *et al.*, 1997; LeHoux *et al.*, 1992), and 2) the hamster uses cortisol as its major glucocorticoid like humans (LeHoux *et al.*, 1992; LeHoux and Lefebvre, 1980).

1.6.2. StAR: Since the discovery of the mouse StAR in MA-10 Leydig tumor cell line, StAR has been cloned from human, horse, pig, sheep, cow, rat, mouse, chicken, frog, and raibow and brook trout. We have cloned the cDNA of the hamster StAR and have shown that the transcribed protein has 284 amino acids (Fleury *et al.*, 1998), one less than that of human StAR; the human and hamster StAR are 86% homologous. We have also shown that administrattion of ACTH to hamsters provoked and increase in adrenal StAR content within one hour *in vivo* (Fleury *et al.*, 1998).

1.6.3. P450c17: In humans, the adrenal P450c17 17α-hydroxylates both pregnenolone and progesterone, but DHEA is the preferred final product over androstenedione (AD) (Chung *et al.*, 1987; Lin *et al.*, 1993). The rat and mouse do not express P450c17 in the adrenal glands (Fevold *et al.*, 1989; Namiki *et al.*, 1988; van Weerden *et al.*, 1992;

Youngblood and Payne, 1992), and the gonadal P450c17 preferentially produces AD. The guinea pig on the other hand, does express adrenal P450c17 and although it 17α-hydroxylates both pregnenolone and progesterone, AD is the preferred final product (Provencher *et al.*, 1992; Tremblay *et al.*, 1994). We have previously isolated the hamster adrenal P450c17 cDNA and have compared the activity profile of the hamster P450c17 enzyme to that of the human P450c17.

We have demonstrated that the hamster adrenal 17α-hydroxylates both pregnenolone and progesteone, and produces both DHEA and AD in adrenal cell suspensions, microsomal preparations, and transiently transfected COS-1 cells with the hamster adrenal P450c17 cDNA (Cloutier *et al.*, 1995; Cloutier *et al.*, 1997). Furthermore, we have immunolocalized the hamster P450c17 in the *zonae fasciculata* and *reticularis* of hamster adrenals (Brière *et al.*, 1997), and we have shown that the hamster adrenal P450c17 mRNA is positively regulated by ACTH (LeHoux *et al.*, 1992).

1.7. Specific Objectives:

1.7.1. Understanding StAR: Unfortunately, adrenal dysfuction is a reality. Since the first discovery of adrenal insufficiency by Addison in 1855, much effort has been put in research to understand the structural/functional relationship of the adrenal gland and all its machinery. Dysfunction of practically any adrenal steroidogenic enzyme results in CAH, presenting various symptoms outside of the adrenal gland morphology, even death. LCAH, the most severe type of CAH, is a direct consequence of a genetically dysfunctional StAR abolishing all steroidogenesis with accumulation of cholesterol in lipid droplets in adrenocortical cells, prohibiting normal cellular function. Since the

discovery of StAR in 1994, several mechanisms for its action in cholesterol transfer inside mitochondria have been suggested but none can explain all experimental evidence reported to date and cause much debate. We therefore hypothesized that the actual mechanism of the StAR-dependent cholesterol transfer inside mitochondria was a unified portrayal of these views. With advances in technology, new experimental methods enlighten the deepest recesses of the misunderstood. Hence, we explored the possibility that molecular modeling could shed light on the true StAR mechanism of action. Our specific objectives were:

i. To obtain a realistic molecular model of StAR based on the recently crystallized human MLN64 protein having similar properties to the human StAR;

ii. To utilize the StAR molecular model to explain rational site-directed mutagenesis, particularly those targeting potential phosphorylation sites; and,

iii. To clarify contradicting experimental results, proposing a new mechanism for the StAR-dependent transfer of cholesterol inside mitochondria.

Here, we show that the rational use of homology modeling, coupled to rational mutagenesis can resolve contradicting experimental evidence and we propose a novel mechanism for StAR action.

1.7.2. Understanding P450c17: Molecular modeling is not restrained to sheding light on dysfunctional systems. During the lifespan of man, many developmental stages such as adrenarche, puberty, and aging are surpassed. Throughout these developmental stages,

secretion patterns of the adrenal steroids change due to their differential regulation, particularly for the production of DHEA. DHEA is the most abundant steroid in man (Chung *et al.*, 1987; Lin *et al.*, 1993). It is converted to a sulfated form, DHEA sulphate (DHEAS), in the *zona reticularis* of the human adrenal cortex by a sulphotransferase fittingly termed DHEA sulphotransferase (Kennerson *et al.*, 1983). Adding this sulphate group to the 3β-hydroxyl group of DHEA stabilizes DHEA for transport in the blood flow. In peripheral tissues, DHEAS is hydrolyzed locally by a sulfatase in order to liberate the active form DHEA (Fig. 13) (Wolf and Kirschbaum, 1999). In man, 99% of the circulating DHEA is in the stable DHEAS form (Zumoff *et al.*, 1980), leaving 1% for bioactivity. This miniscule portion has been shown to be metabolically active in aging (Morales *et al.*, 1994), breast cancer (Bulbrook *et al.*, 1971), hypertension in rats (Shafagoj *et al.*, 1992), and immunostimulation (Daynes *et al.*, 1990).

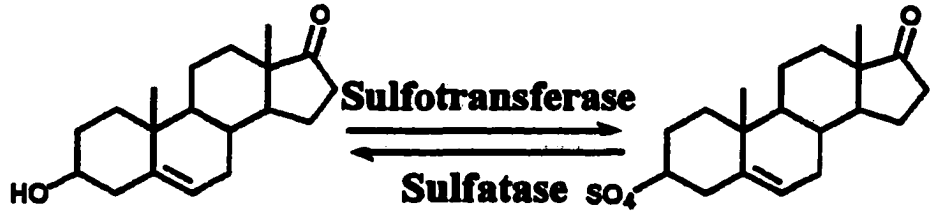

Dehydroepiandrosterone (DHEA) **Dehydroepiandrosterone Sulphate (DHEAS)**

Fig. 13. Conversion of DHEA to DHEAS. In adrenal glands, DHEA is sulphated by a sulfotransferase at the functional hydroxyl group on carbon 3, stabilizing DHEA for transport in the blood flow. In periferal tissues, DHEAS in then converted back to the active form DHEA by a sulfatase.

Interestingly, the secretion pattern of DHEAS with age and gender changes drastically (Fig. 14). Indeed, plasma DHEAS levels are low at birth and begin to rise prior sexual matuation and continue to rise well into the early twenties, only to decrease therafter approximately 10% for every decade (Migeon *et al.*, 1957; Orentreich *et al.*, 1984; Regelson *et al.*, 1994; Regelson and Kalimi, 1994); the increase of DHEAS is termed adrenarche. Moreover, cortisol production in man remains unchanged with aging. The fluctuation in DHEA(S) can be attributable to any steroidogenic enzyme directly or indirectly implicated in the production of DHEA. Predominantly, it is conceivable that a decrease in 3β-HSD and/or P450c21 could lead to augmentation of DHEA production due to increased precursor availability for the P450c17; CAH due to dysfuctional P450c21 causes accumulation of DHEA (White *et al.*, 1987). It was discovered that 3β-HSD expression does decrease in the *zona reticularis* only, simultaneous to observed adrenarche (Gell *et al.*, 1998). On the other hand, this research showed that the adult *zona reticularis* also has a decreased 3β-HSD expression, which cannot explain the observed loss of DHEA production with aging (starting around 25 years old – Fig. 14). This same investigation revealed that P450c21 expression does not change significantly with age under normal circumstances. This is reasonable since the production of cortisol does not change with time in man. Finally, the human P450c17 has been shown to be phosphorylated on serine and threonine (Zhang *et al.*, 1995) and that this phosphorylation can regulate the 17α-hydroxylase/17,20-lyase activity ratio (Biason-Lauber *et al.*, 2000a; Miller, 1999).

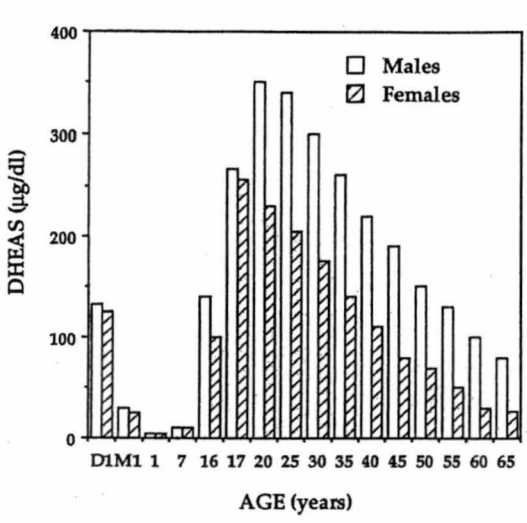

Fig. 14. Human Plasma DHEAS Concentrations. Comparison of the DHEAS levels in men and women with respect to age at day 1 (D1), month 1 (M1) and approxiamately every five years (Nafziger *et al.*, 1991).

It seems therefore, that the adrenal P450c17 is differentially regulated with time in the *zona reticularis*; this is the adrenocortical zone responsible for the secretion of DHEA(S) in man. Since the hamster is an attractive model to study DHEA production with respect to man, yet still presenting a different activity profile, we hypothesized that elements conferring basal activity distinction between the human and hamster P450c17 was directly linked to the amino acid sequences of these forms. Again, our objectives consisted of using molecular modeling to study the structure/function relationship of the hamster P450c17 and explain the activity profiles of the hamster and human P450c17s. Specifically, our objectives were:

i. To identify potentially regulating amino acids in the hamster P450c17 protein conferring its specific activity profile using rational site-directed mutagenesis;

ii. To obtain a rational model of the hamster P450c17 based on the coordinates of the human P450c17 structure;

iii. To utilize the hamster P450c17 model to account for the site-directed mutagenesis results;

iv. To clarify the substrate selectivity of the hamster P450c17 versus the human P450c17; and,

v. To propose a mechanism for substrate selectivity and uptake conferring the observed activity profile of the hamster P450c17.

Briefly, we show that the validated hamster P450c17 model can account for the rational site-directed mutagenesis results altering the hamster P450c17 activity profile, and that substrate selection appears to be important early in substrate uptake inside the hamster P450c17. The P450c17 structures have three key features: 1) amino acids responsible to maintain core elements and structural integrity of the protein; 2) amino acids responsible for the heme binding, redox partner ineteractions, and catalysis; and 3) amino acids responsible for substrate selectivity and uptake. Moreover, any amino acid can participate in one or more of these functions, regulating P450c17 activity. Finally, substrate selectivity and intake requires three distinct steps: 1) recognition of the substrate at the accessible surface of the putative substrate entrance; 2) entrance of the substrate into the active site directed by key hydrogen bonding to particular amino acids in the active site; and 3) rotation of the substrate inside the active site to position the substrates optimally for catalysis.

We have thus developed testable models of two key enzymes in the hamster steoidogenesis, StAR and P450c17, by combining rational mutagenesis and molecular modeling.

2. StAR:

2.1. Mathieu AP. Fleury A. Ducharme L. Lavigne P. LeHoux JG. Insights into StAR-Dependent Cholesterol Transfer in Mitochondria: Evidence from molecular modeling and structure-based thermodynamics supporting the existence of partially unfolded states of StAR. [Journal Article] ***Submitted to The Journal of Molecular Endocrinology 06/2002.***

Contribution: Everything in this article is the product of my work except for the production of the StAR mutants, and their assays. I actively participated in the decision of which mutants to test, and I analysed the results.

Insights into StAR-Dependent Cholesterol Transfer in Mitochondria: Evidence from molecular modeling and structure-based thermodynamics supporting the existence of partially unfolded states of StAR.

Axel P. Mathieu[1], Alain Fleury[1], Lyne Ducharme[1], Pierre Lavigne[2], and Jean-Guy LeHoux[1]*

[1] Department of Biochemistry and the [2] Department of Pharmacology, Faculty of Medicine, Université de Sherbrooke, QC, Canada, J1H 5N4.

Running title: Molecular Modeling of StAR.

* Corresponding authors: Jean-Guy LeHoux, Department of Biochemistry, Faculty of Medicine, Université de Sherbrooke, QC, Canada, J1H 5N4. Tel: (819) 564-5282; Fax: (819) 820-6852; E-mail: jlehou01@courrier.usherb.ca. Pierre Lavigne, Department of Pharmacology, Faculty of Medicine, Universiré de Sherbrooke, QC, Canada, J1H 5N4. Tel: (819) 564-5462; Fax: (819) 564-5400; E-mail: pierre.lavigne@courrier.usherb.ca.

† This work was supported by grants from the Canadian Institutes of Health Research and the Heart and Stroke Foundation of Canada to J.G.L., and from the Natural Sciences and Engineering Research Council of Canada to P.L.; J.G.L. is *chercheur boursier de carrière du Fonds de la recherche en santé du Québec* and P.L. is *chercheur-stratégique du Fonds pour la formation de chercheurs et l'Aide à la recherche.*

ABSTRACT

The steroidogenic acute regulatory protein (StAR) is the major entrance for cholesterol in mitochondria under acute stimulation. Under such circumstances, dysfunctional StAR activity can ultimately lead to lipoid congenital adrenal hyperplasia (LCAH). A complete understanding of the StAR's molecular structure and mechanism is essential to comprehend LCAH. Thus far, there is no mechanistic model that can explain experimental results at the molecular level. This is partly due to the lack of the molecular structure of StAR. The closest approximation to the StAR molecular structure is the human MLN64 which has a similar activity to StAR, has a highly homologous primary structure and for which an X-Ray structure is known. In this context, we have modeled the structure of StAR through standard homology modeling procedures based on the MLN64 structure. Our StAR model shows the presence of a hydrophobic cavity of 783.9 $Å^2$ in surface, large enough to fit one molecule of cholesterol. In addition, we have identified a unique charged pair as in MLN64, lining the surface of the cavity and which could play a key role in the binding of cholesterol through the formation of an H-Bond with the its OH moiety. This suggests that the cholesterol-binding site of StAR is located inside this cavity. Taking into account that internal cavities are destabilizing to native protein structures and that the lining of the cavity has to become accessible in order to allow cholesterol binding, we have explored the possibility that StAR could exist in equilibrium with partially unfolded states. Using a structure-based thermodynamics approach, we show that partially folded states (with an unfolded C-terminal α-helix, and an open cavity) can be significantly populated at

equilibrium and therefore allow cholesterol binding. These results are supported by recent experiments that show a loss of StAR helical character upon binding of an analogue of cholesterol. Moreover, we show that the replacement of the residues involved in the charged-pair located in the binding site, results in the loss of StAR activity supporting a key role for these residues. Taken together, our results are applicable to both a StAR functioning in the mitochondrial intermembrane space as well as outside mitochondria.

Keywords: Steroidogenic acute regulatory protein (StAR), molecular modeling, site-directed mutagenesis, human, hamster, structure-based thermodynamics.

Abbreviations: Steroidogenic acute regulatory protein (StAR), Phosphatidyldylinositol transfer protein α (PITPα), energy minimization (EM), simulated annealing (SA), structure-based thermodynamics calculations (STC), adrenocorticotropin hormone (ACTH), 22-(N-(7-nitrobenz-2-oxa-1,3-diazol-4-yl)amino)-23,24-bisnor-5-cholen-3β-ol (NBD-cholesterol).

INTRODUCTION

Until recently, it was believed that the rate-limiting step in steroid hormone synthesis was the conversion of cholesterol into pregnenolone by the cytochrome P450 side-chain cleavage (P450scc) enzyme in the inner membrane of mitochondria (Farkash *et al.* 1986). However, it was discovered that the true rate-limiting step in steroidogenesis is the transfer of cholesterol from the outer mitochondrial membrane, through the aqueous intermembrane space, to the inner mitochondrial membrane where the P450scc resides (Brownie *et al.* 1972; Crivello and Jefcoate 1980; Privalle *et al.* 1983; Simpson *et al.* 1978).

As potential cholesterol transferring proteins, the best candidate to date is the Steroidogenic Acute Regulatory protein (StAR) first cloned and characterized in the MA-10 mouse Leydig tumor cell line by Clark, BJ *et al.* (Clark *et al.* 1994). Effectively, these authors were the first to identify StAR as being the same 30-kDa protein originally described by Orme-Johnson and colleagues (Alberta *et al.* 1989; Epstein and Orme-Johnson 1991a; Epstein and Orme-Johnson 1991b; Hartigan *et al.* 1995; Pon *et al.* 1986; Pon and Orme-Johnson 1988), responsible for adrenocorticotropin hormone (ACTH) stimulated steroidogenesis. The involvement of StAR in cholesterol translocation is supported through a number of experimental results, the most obvious being the StAR knockout mice (Caron *et al.* 1997) displaying lipoid congenital adrenal hyperplasia (LCAH). Patients with LCAH cannot synthesize adequate amounts of steroids and are characterized by cholesterol accumulation in the adrenal glands and gonads. This potentially lethal condition is now commonly attributed to a dysfunctional StAR, most importantly in the critical C-terminal region as demonstrated by StAR mutants (Bose *et*

al. 1996; Lin *et al.* 1995). In humans, StAR is expressed in adrenal glands, gonads, and brain, and consists of 285 amino acids (Sugawara *et al.* 1995) separated into two functional domains: 1) the mitochondrial import sequence responsible for its localization in mitochondria, and 2) the StAR lipid transfer (START) domain (Ponting *et al.* 1999; Ponting and Aravind 1999) responsible for the transfer of cholesterol into the inner membrane of mitochondria.

START domains have been discovered and characterized for a large variety of proteins with different functions (Homma and Emori 1995; Masucci *et al.* 1996; Ponting *et al.* 1999; Ponting and Aravind 1999; Raya *et al.* 1999). Of these, the human MLN64 protein may have a similar function as the human StAR in the placenta, brain, and non-steroidogenic tissues for the formation of steroids and bile acids (Bieche *et al.* 1996; Moog-Lutz *et al.* 1997; Watari *et al.* 1997). The structure of MLN64 was recently solved by X-Ray crystallography and revealed several interesting features (Tsujishita and Hurley 2000). More importantly, the cholesterol binding site is best described as a hydrophobic tunnel formed predominantly from a U-shaped unclosed β-barrel topped by the parallel C-terminal α-helix. The tunnel completely traverses the entire MLN64 and has been suggested to work as an intermembrane shuttle (Tsujishita and Hurley 2000), although the exact mechanism by which StAR mediates cholesterol transfer is still a subject of intensive research. Several mechanisms have been suggested for the action of cholesterol transfer by StAR. These include desorption, the implication of a molten globule state and the intermembrane shuttle (Stocco 2000; Stocco 2001; Stocco and Clark 1996).

Desorption requires that the inner and outer mitochondrial membranes come into contact as StAR is imported into the mitochondrial matrix by its mitochondrial targeting

sequence (Kallen *et al.* 1998). Then, high volumes of cholesterol can be transferred from the cholesterol-rich outer membrane to the cholesterol-depleted inner membrane. This mechanism does account for localization of mitochondrial imported proteins at contact points (Pon *et al.* 1989; Schwaiger *et al.* 1987; Stocco and Clark 1996), the rapid cholesterol transfer requiring little StAR, and the quick degradation of StAR by mitochondria (Clark *et al.* 1994; Stocco and Clark 1996). It does not however, account for the fact that StAR can still function without its N-terminal import sequence (Arakane *et al.* 1996; Arakane *et al.* 1998). As for the molten globule (Bose *et al.* 2002; Christensen *et al.* 2001), it was shown that StAR looses tertiary structure at low pH (3.5-4.0) while retaining secondary structures, suggesting that partially folded states of StAR are significantly populated at low pH and even at pH values closer to neutrality (Christensen *et al.* 2001). In the latter study, the authors suggest that this "molten globular state" is important for StAR function outside mitochondria (Bose *et al.* 2002). This model is in agreement with the observation that an active electrochemical force is required for the transfer of cholesterol (King *et al.* 1999) but the *in vivo* local acidic environment still remains to be proven. Finally, the intermembrane shuttle states that StAR acts as a sterol carrier, migrating between mitochondrial membranes (Tsujishita and Hurley 2000). The molecular mechanism and structural requirement for the carrier role of StAR is still elusive. On the other hand, it appears that the structure of MLN64 may reveal key features to understand the mode of cholesterol transport by StAR. The X-Ray structure of MLN64 (Tsujishita and Hurley 2000) depicts a hydrophobic tunnel characterized by β-strands forming the floor and sidewalls, topped by a C-terminal α-helix and two loops. Inside the tunnel, there is opening of the cavity such that one

cholesterol molecule may fit. On the other hand, the tunnel openings are not large enough to allow a cholesterol molecule to pass through StAR. Tsujishita & Hurley (Tsujishita and Hurley 2000) suggest that transient conformational changes of the loops and/or the C-terminal α-helix allow cholesterol access to the hydrophobic tunnel, supported by the recent crystallization of the phosphatidyldylinositol transfer protein α (PITPα) open conformation (Schouten *et al.* 2002); PITPα is involved in the regulation of lipid and vesicular trafficking and in lipid-mediated signal transduction pathways (Cockcroft 1999; Cunningham *et al.* 1995). Importantly, in support of the C-terminal α-helix transient conformational changes, it has been recently observed that there is loss of helical content in StAR upon binding of a cholesterol chromophoric analogue, NBD-cholesterol (Petrescu *et al.* 2001).

Following the observation that the C-terminal region of StAR is important for proper StAR activity (Bose *et al.* 1996; Lin *et al.* 1995), that the C-terminal region is suggested to transiently change conformations for cholesterol binding (Tsujishita and Hurley 2000), that loss of StAR helical structure is obtained upon binding of a cholesterol analogue (Petrescu *et al.* 2001), that molten globular states of StAR are possible (Bose *et al.* 1999; Christensen *et al.* 2001), and that the C-terminal α-helix in MLN64 entirely covers the putative cholesterol binding site, we investigated the possible implication of various conformational states of this C-terminal α-helix in the binding of cholesterol to StAR through molecular modeling.

We show that the hamster StAR model has a hydrophobic cavity instead of a tunnel. This cavity is proposed to be the driving force for the unfolding of the C-terminal α-helix revealing the cholesterol binding site. We calculate through structure-based

thermodynamics (Freire 1993);(Lavigne *et al.* 2000) that this partially folded state could be significantly populated and that cholesterol favorably binds to it. We also observe that once cholesterol has bound to StAR, adjacent loops to the opened StAR binding site (loop Ω1 and the loop between β-strands 1 and 2) effectively inhibit the C-terminal α-helix reformation, supporting the observed loss of α-helical structure upon cholesterol binding to StAR thus allowing a rapid cholesterol transfer inside mitochondria. Finally, we show a peculiar salt-bridge in the binding site plays a key role in cholesterol binding. This is supported by new mutagenesis results showing that cholesterol transfer can be abolish by removal of this salt-bridge.

Taken together, these results suggest a rapid unfolded StAR mechanism for the transfer of cholesterol from the outer to the inner mitochondial membranes, driven by the transmembrane cholesterol gradient; our calculations are applicable to both a StAR functioning in the mitochondrial intermebrane space or in the cytosol in proximity of mitochondria. Thus, we propose a plausible common ground for the intermembrane shuttle and molten globule mechanisms.

MATERIALS AND METHODS

Modeling Methodology

All calculations were performed on an SGI Octane 2 workstation and the InsightII (2000) suite of programs (Homology, Discover, Biopolymer, and Builder) to obtain all models. The amino acid sequences for the hamster and human StAR were obtained from Genbank (Accession Numbers AAB06763 and NP_000340 respectively) and aligned to the extracted amino acid sequence of MLN64 by a ClustalW algorithm (Thompson *et al.*

1994), and manually adjusted in Homology. The amino acid side chains of the hamster and human StAR were replaced in the MLN64 coordinate file (PDB ID number 1EM2.). The minimization calculations were performed in the absence of Coulombic potential, cross terms and morse potentials. The consistent valence forcefield (CVFF (Dauber-Osguthorpe *et al.* 1988)) was used for all calculations. Essentially, the minimization was completed in four steps: 1) fixed heavy (all but hydrogens) atoms, 2) fixed backbone atoms with tethered heavy atoms, 3) tethered backbone atoms, and 4) no atoms fixed. Each step was performed as follows: 1) steepest descent for 1000 iterations or until the maximum derivative is less than 0.001 kcal/Å, followed by 2) conjugate gradient for 1000 iterations or until the maximum derivative is less than 0.001 kcal/Å.

To define the cavity, we filled it with water; water molecules were discovered in the MNL64 crystal (Tsujishita and Hurley 2000). First, a 50 Å solvent layer was added to the StAR models, upon which the cavity was placed "over" the water molecules. All the water molecules outside the cavity volume were removed, keeping only the water molecules that fit in the cavity. These water molecules were visually identified by comparing the molecular surfaces of the water molecules as well as the cavity.

For binding studies, a cholesterol molecule was created using the Builder module in the InsightII suite. The initial planar structure was minimized using steepest decent for 1000 iterations or until the maximum derivative is less than 0.001 kcal/Å, fixing nothing and using no Coulombic potential, cross terms and morse potentials. After, the cholesterol molecule was manually and visually placed inside the StAR cavity, as previously suggested (Tsujishita and Hurley 2000). Due to the shape of StAR's cavity, placement of cholesterol was unambiguous. The structures were then minimized as

mentioned above. The cholesterol free native hamster and human models have been deposited in the PDB and have PDB ID numbers 1ILJ and 1IMG respectively.

Free Energy Calculations

In order to calculate the Gibb's free energy difference (ΔG) between the native and partially unfolded states of StAR, we have used an approach called structure-based thermodynamics (Freire 1993) as implemented in the computer program STC (Lavigne *et al.* 2000). This approach has been shown to allow for the identification of partially folded (unfolded) states of proteins in equilibrium with their native states and to allow for the prediction of binding free energy of ligands to proteins (Baker and Murphy 1998; Hilser and Freire 1997).

Briefly, we manually unfolded the C-terminal α-helix of the hamster StAR model using the Biopolymer module of the InsightII suite. As a model for the unfolded state, we have used an extended conformation (ψ and ϕ =180°). Then, the changes in accessible surface area (ΔASA) between the "unfolded states" and the native state were calculated using the CALC_ASA module of STC (Lavigne *et al.* 2000) and separated into polar (N and O atoms) and non-polar (C and S atoms). Using the calculated ΔASA and empirical functions relating changes in heat capacity (ΔCp), enthalpy (ΔH), entropy (ΔS) per unit of ΔASA, ΔG between the different states were calculated using the THERMO module of STC (Lavigne *et al.* 2000). Note that no changes in the protonation states were considered. We also explored loop movement above the opened StAR cavity using this same methodology. Finally, the binding constant between cholesterol and the partially unfolded state was calculated as described elsewhere (Lavigne *et al.* 2000).

Rendering

All the model graphical images were created using either InsightII for molecular surfaces or Ribbons 3.0 for ribbon diagrams.

Materials for Site-Directed Mutagenesis

All restriction and modifying enzymes were purchased from New England Biolabs (Mississauga, ON, Canada). The expression vector pcDNA3.1Myc-His, Lipofectamine and oligonucleotides were purchased from Invitrogen Canada Inc. (Burlington, ON, Canada). All vectors were amplified in XL1 Blue *E coli* competent cells (Stratagene, La Jolla, CA), and purified on Qiagen anion-exchange columns (Qiagen, Chatsworth, CA). TPA and $(Bu)_2$-cAMP (cAMP) were obtained from Sigma-Aldrich (St-Louis, MO).

Hamster StAR Mutagenesis by PCR

Briefly, two series of PCR amplifications were obtained using the following conditions: Hot start of 5 min at 94°C (without DNA polymerase) followed by a touch down of 2°C from 94°C/70°C/72°C to 94°C/50°C/72°C, completed with 30 cycles of 94°C/50°C/72°C and a final 72°C elongation of 15 min. The first series consists of amplifying hamster StAR cDNA in two different reactions. 1) A wild type (WT) upstream (sense) oligonucleotide to the downstream mutant (antisense) oligonucleotide at the site of interest for mutagenesis and 2) a mutant sense oligonucleotide from the site of interest for mutagenesis to a WT antisense oligonucleotide. The second series consists of pooling both PCRs previously obtained, purified by agarose gel electrophoresis, and

amplifying using WT 5' and 3' oligonucleotides. WT-StAR and all mutants were cloned into pcDNA3.1Myc-His using unique *Eco*RI and *Hind*III restriction sites, and entirely sequenced between these restriction sites using T7 sequencing kit from Amersham Pharmacia Biotech (Baie d'Urfé, QC Canada), amplified, and purified on Qiagen anion-exchange columns.

Hamster StAR Expression

Either WT or mutated StAR was transiently transfected into monkey kidney COS-1 cells (American Type Culture Collection, Rockville, MD) using the lipofectamine method. Twenty-four hours before transfection the cells were harvested with pancreatin-EDTA solution (Invitrogen Canada Inc., Burlington, ON, Canada) and plated at an initial density of 3.5×10^5 cells per 10 cm^2 well in 6-well plates. Cells were cultured in DMEM supplemented with 10% fetal bovine serum (FBS), 5.96 g/L HEPES, 2.2 g/L $NaHCO_3$, 1 mM L-glutamine, 100 IU/ml penicillin, and 100 μg/ml streptomycin sulphate. DMEM containing no fetal bovine serum and no antibiotics was used for transfections. Each transfection assay received 1 μg of DNA (500 ng/ml F2 construct (Harikrishna *et al.* 1993) containing cytochrome P450scc/adrenodoxin reductase/adrenodoxin and 500 ng/ml of pcDNA3.1 + pcDNA3.1-StAR) and 10 μg/ml lipofectamine. Twenty two hours after transfection cells were rinsed with PBS. Cells were then incubated for 24 hours in DMEM without phenol red containing 10% dextran-coated charcoal-treated FBS and antibiotics without or with stimulation agents. Media were kept for pregnenolone determination and cells for immunoblotting analyses.

Measurement of the Hamster StAR Activity

In this study, StAR activity is defined as the quantity of pregnenolone formed by transfected COS-1 cells in co-transfection experiments using F2 (Harikrishna *et al.* 1993) and StAR plasmids. Pregnenolone was analyzed by radioimmunoassay (ICN Pharmaceuticals, Diagnostics Division, Orangeburg, NY). This conversion of cholesterol into pregnenolone is directly related to the rate of cholesterol transfer by StAR to P450scc in the inner mitochondrial membrane.

Immunoblotting Analysis

Sodium-dodecyl sulphate polyacrylamide gel electrophoresis (SDS-PAGE) were performed with 20 μg of soluble proteins on a 12% gel and analyzed by immunoblotting (LeHoux *et al.* 1992) using a rabbit polyclonal anti-mouse StAR antibody (kindly given by Dr. Dale Buchanan Hales, Department of Physiology and Biophysics, University of Illinois at Chicago, Chicago, IL) as previously described (LeHoux *et al.* 1996). This immunoglobulin was raised against a GST-fusion protein from a mouse StAR cDNA from a 208-1467 bp fragment (Clark *et al.* 1997). Cells were scraped and directly harvested in hot (100°C) Laemmli buffer. All samples were then passed through a 26 gauge needle, then boiled for 10 min and finally centrifuged at 12000 x g for 2 min. Soluble proteins were determined on the supernatant using the Bio-Rad Protein Assay Dye Reagent (Bio-Rad Laboratories, Ltd. Mississauga, ON, Canada).

Immunoreactive proteins were detected using ECL-PLUS light emitting reagents (Amersham Pharmacia Biotech UK Ltd., Amersham Place, Little Chalfont, Buckinghamshire, UK). Autoradiograms were observed by exposing the blots to Kodax

X-Omat XK films. The results were also visualized and quantified on the optical imager STORM 860 using ImageQuant software version 5.0 (Molecular Dynamics, Sunnyvale, CA).

Statistical Analyses

Differences between experimental groups were analyzed by ANOVA followed by Dunnett's test, using the SigmaStat program for Windows (SPSS Science, Chicago, IL).

RESULTS

Overall Structure of Molecular Models

In order to undertake theoretical molecular modeling of proteins, a suitable alignment between a protein of known three-dimensional structure with the target protein must be obtained. In this case, the alignment of the human MLN64 with the hamster and human StAR proteins is depicted in Fig. 1 and shows a suitable identity of approximately 34% between the sequence of the hamster/human StAR and MLN64. Following the unambiguousness of the alignment, the amino acid residues of the hamster and human StAR proteins were substituted in the MLN64 coordinate file and the potential energy of the model was minimized appropriately (see MATERIALS AND METHODS). The stereochemical quality of the models were checked with the program PROCHECK (Laskowski *et al.* 1993) and was found to be excellent.

As expected, the theoretical models for the hamster and human StAR greatly resembled the crystalline structure of the human MLN64 (Tsujishita and Hurley 2000). As demonstrated in Fig. 2 (only hamster model shown), the prominent feature to the

hamster StAR model is the U-shaped unclosed β-strand barrel, topped by the parallel C-terminal α-helix. Altogether, the structure is composed of 4 α-helices and 9 twisted anti-parallel β-strands like the MLN64. Although, the most significant change in the overall structure of the StAR model as compared to the human MLN64 crystal, is a cholesterol binding site in the shape of an oval cavity matching the size and structure of cholesterol (Fig. 3A – cholesterol not shown); in MLN64, the cholesterol binding site is "tunnel-like" (Tsujishita and Hurley 2000). Amidst the mostly hydrophobic environment of the cavity, there are two charged amino acid residues (Glu168-Arg187, hamster numbering) forming a salt bridge (Fig. 3B) as described previously in MLN64 (Tsujishita and Hurley 2000).

STC Calculations

To get insight into the cholesterol transfer mechanism into the mitochondria, we attempted to calculate the change in free energy of various conformations of the hamster StAR model. STC is one of the very few methods applicable to model partially folded states that has been validated by others (Baker and Murphy 1998; Freire 1993; Hilser and Freire 1997; Lavigne *et al.* 2000). We therefore utilized STC to calculate the change in free energy of the various conformational states of our StAR model and to calculate a theoretical dissociation constant (K_d).

Free Energy of Cavity Formation

Bearing in mind that the binding site of StAR has to become accessible and that cavities inside globular proteins destabilize the native state of proteins (Creighton 1993), we have calculated the ΔG for cavity formation using STC. Moreover, the water

molecules discovered in the MLN64 crystal contribute to the destabilization of the hydrophobic cavity. In order to calculate the ΔG, we manually calculated the ASA inside the binding site of the StAR cavity. Briefly, all atoms directly adjacent the water molecules in the solvated model of the hamster StAR were visually identified. After, the hamster StAR model was "cut" parallel to the oval binding site (Fig. 3C) and each piece was subjected to ASA calculations separately. ΔASA between the "cut state" and the native state was taken to be the solvated ASA (ΔASAnp = 627.8 $Å^2$ and ΔASApol = 156.1 $Å^2$) inside the hydrated cavity. This translates into a ΔG of destabilization (cavity formation) of approximately 12 kcal/mol.

Partial Unfolding of StAR

It is clear that StAR with a closed binding site would have to open to allow cholesterol inside. Supporting evidence for structural changes during cholesterol binding to StAR, and cholesterol transfer inside mitochondria include: 1) the C-terminal region of StAR is important for proper StAR activity (Bose *et al.* 1996; Lin *et al.* 1995); 2) the C-terminal region as well as the loops spatially adjacent to this region, are believed to transiently change conformations for cholesterol binding (Tsujishita and Hurley 2000); 3) molten globular states of StAR are possible (Bose *et al.* 1999); and 4) the C-terminal α-helix of our StAR model entirely covers the putative cholesterol binding site as for the MLN64 crystal (Tsujishita and Hurley 2000) and should be free for movement. Yet, the most convincing discovery supporting StAR conformational changes for proper StAR activity is the loss of StAR helical structure upon the binding of a cholesterol analogue in StAR (Petrescu *et al.* 2001). We therefore conceptualized the opening of the binding site

primarily by the movement of the C-terminal α-helix covering the U-shaped unclosed β-barrel such as could happen in a molten globule state, driven by the ΔG of destabilization caused by the hydrophobic cavity hydration as calculated above. In order to test this hypothesis, we modeled different conformations of the C-terminal α-helix of the hamster StAR model. In absence of cholesterol, three key conformations were considered: A) native, B) opened: C-terminal α-helix still folded but remove from the binding site, and C) partially unfolded: C-terminal α-helix unfolded but with the rest of the molecule native. The free energy change for all the steps are indicated in Fig. 4 (A, B, and C respectively). Note that we have subtracted the ΔG for cavity formation from calculated ΔG change between state A and B; indeed, the destabilization of the native state by the cavity has to be taken into account. The net free energy change between the native state (A) and the partially unfolded state (C) is +2.61 kcal/mol. To a first approximation, *i.e.* considering the population of this state relative to the native state according to the following equation:

$$P = \frac{\exp(-\Delta G / RT)}{1 + \exp(-\Delta G / RT)}$$

we can estimate a significant relative population of approximately 2% for this partially unfolded conformation. Note that state B is less stable than state C, mostly due to the cost in conformational entropy for maintaining the helical conformation of the C-terminal α-helix without tertiary interactions.

Binding of Cholesterol to the Partially Unfolded State

Next, we have calculated the ΔG of binding cholesterol to the partially unfolded state of StAR using STC as described elsewhere (Lavigne *et al.* 2000), and found a relatively weak K_d of 9.44 x10^{-5} M (Fig. 4, C to D). Once cholesterol binds to the partially unfolded state of the hamster StAR protein, the free energy of the complex drops below the free energy of the native state (corrected for the cost of cavity formation). Since is was discovered that there is loss of helical character upon cholesterol binding (Petrescu *et al.* 2001), we simulated movement of the loops adjacent the cholesterol binding site (loop Ω1 and loop between β-strands 1 and 2) such as to inhibit the C-terminal α-helix reformation. These loops are the only structures available for movement in the vicinity of the C-terminal α-helix, as mentioned previously (Tsujishita and Hurley 2000), that could aid in maintaining it in the unfolded state; Fig. 5 (D to E) depicts the movement of these loops and represent a partially refolded state of StAR.

Trapping Cholesterol Inside the Cavity of the StAR Protein

Although it was observed that there is loss of helical structure upon binding of cholesterol inside (Petrescu *et al.* 2001), it is still conceivable that the C-terminal α-helix refolds on top of the bound cholesterol. We thus simulated the refolding of the C-terminal α-helix, trapping cholesterol inside StAR (Fig. 6, D to F to G). A ΔG for a closing reaction of the folded C-terminal α-helix trapping the cholesterol inside was calculated (conformation A to G) to be -17.91 kcal/mol. As one can see, there is a dramatic stabilization of the complex. As discussed below we propose that this reaction could be involved in the shut-off of the transfer.

Cholesterol Binding Site

As mentioned above, the cholesterol binding site of the hamster StAR model took the shape of a hydrophobic cavity and not a hydrophobic tunnel (Fig. 3). We thus investigated the possibility that water molecules could change the binding site conformation since water molecules were discovered inside the MLN64 crystal (Tsujishita and Hurley 2000). The model was then solvated in the binding site as well as surrounding the protein as described in MATERIALS AND METHODS. After minimization, the overall structure of the model and the cholesterol bind site did not alter. A cholesterol molecule was then inserted in the hamster StAR models and minimized accordingly. In the minimized complex, the 3β-OH group of cholesterol localized adjacent to the salt bridge formed by Glu168-Arg187 as we expected (Fig. 7). As seen, the 3β-OH group was localized < 6 Å away, which is a sufficient distance for one water molecule to bridge the 3β-OH of cholesterol and the salt bridge through hydrogen bonding.

Mutant Activity Alterations

The salt bridge mutants of the hamster StAR were expressed in COS-1 cells and verified for activity alterations. In both cases, when either of the amino acids involved in the formation of the salt bridge were changed for a hydrophobic residues of similar volume (*i.e.*: Glu168Leu, and Arg187Met), total loss of StAR activity was obtained in the absence of cAMP-stimulation as compared to the mock transfections (Fig. 8A). Under cAMP-stimulation, an increase in StAR activity was obtained but never higher than the

non-stimulated wild type indicating a critical role for this salt bridge in the StAR-mediated transfer of cholesterol.

Mutant SDS-PAGE Analysis

Whole cell extracts from the mutant hamster StAR-expressing COS-1 cells were analyzed by SDS-PAGE (Fig. 8B). Under non-stimulated conditions, wild type and mutant hamster StAR is expressed in similar proportions as seen by the ensemble of three experiments (Fig. 8C). Under cAMP-stimulation, protein concentrations were markedly increased, similarly for all preparations. The control empty vector pcDNA3.1 did not produce detectable StAR protein but a basal StAR-independent cholesterol transfer into mitochondria was obtained (Bose *et al.* 1996). Unexpectedly, different migratory patterns were obtained for the hamster StAR mutant Glu168Leu (E168L) preparations, which remain unexplained.

DISCUSSION

Molecular Modeling and Mutagenesis

As expected, the structure of the hamster and human StAR models greatly resemble the human MLN64 crystal structure. The most surprising structural difference compared to the MLN64 crystal structure was the loss of the hydrophobic tunnel replaced by a hydrophobic cavity in our StAR models, matching the overall structure of cholesterol. The cavity can be imagined as the driving force allowing StAR to open, exposing the binding site to incoming cholesterol molecules. Indeed, trapping water molecules inside this hydrophobic cavity, as those co-crystallized in the MLN64 (Tsujishita and Hurley

2000), greatly costs to StAR stability. According to our structure-based thermodynamic calculations, this hydration destabilizes StAR by approximately 12 kcal/mol, driving the unfolding of the C-terminal α-helix in solution. With a net difference of 2.61 kcal/mol between the original empty folded state and the open unfolded state of StAR, we can expect approx. 2% of the StAR population to be in partially unfolded state.

The salt bridge inside the cavity can be conceptualized as having two major functions: 1) allowing cholesterol to bind in the proper orientation inside the well defined cavity, and 2) maintaining minimal StAR folding for optimal cholesterol binding. The first function is clearly demonstrated through cholesterol docking analyses in the presence of one water molecule. After all, the salt bridge is located opposite the moveable C-terminal α-helix at the bottom of the hydrophobic pocket, where it will not move and to which the 3β-OH group of cholesterol can interact as it binds to StAR.

Although molten globular states are possible for StAR, a minimal structure must be maintained to mediate StAR function. Therefore, the salt bridge can be visualized as a key component to maintain StAR in a conformation such that cholesterol will bind. This is supported by our mutational analyses of the salt bridge, as well as the presence of a peptidase-resistant domain in the human StAR, which includes this salt bridge (Bose *et al.* 1999). In the case where the salt bridge is replaced by hydrophobic residues of similar volume (hamster E168L-R187M), total loss of StAR-dependent cholesterol transfer into mitochondria is obtained as compared to the mock transfections. This is most likely due to non-specific interactions of the hydrophobic amino acids and thus could lead to improper StAR folding altogether (Bose *et al.* 1996); the residual cholesterol transfer inside mitochondria is StAR-independent (Bose *et al.* 1996).

Serine185 was thought to be a potential phosphorylation site and was thus changed into an alanine that cannot be phosphorylated; total loss of StAR-dependent cholesterol transfer was also obtained (Fleury *et al.*, unpublished results). To further test the hypothesis that S185 is indeed phosphorylated, we mutated S185 into aspartate and glutamate mimicking phosphorylation, and no gain in StAR activity was obtained. The only recuperation of StAR activity was obtained with the mutant S185C, where cysteine greatly resembles serine both in volume and hydrophilicity but still cannot be phosphorylated. Moreover, 2D-PAGE analyses of the S185A mutant did not reveal any differences to wild type StAR. This clearly indicates that S185 is not phosphorylated and its control on StAR activity comes from structural alterations. Upon a closer look, S185 is located directly beneath the salt bridge, inaccessible to solvent. It thus becomes clear that not only the salt bridge is important, but also its immediate environment leading to its proper positioning. Therefore in summary, removal of the salt bridge by mutagenesis can not only reduce cholesterol affinity to the StAR binding site due to loss of orientation, but could also result in improper folding of StAR altogether as demonstrated for the human StAR mutant E169G (Bose *et al.* 1998).

Cholesterol Translocation

The major reason for modeling StAR is to visualize its environment, hopefully leading to an understanding of the cholesterol translocation into mitochondria. Now, two mechanisms are widely accepted: the molten globule, and the intermembrane shuttle. Here, we demonstrate the possibility of structural changes in the hamster StAR supported

by theoretical molecular thermodynamics, in accordance with either of these mechanisms.

As one looks at the energy profile of the proposed states of StAR (Fig. 9), two possible mechanisms become clear to account for either the intermembrane shuttle or the molten globular states acting outside mitochondria (Fig. 10). First, if in the mitochondrial intermembrane space, StAR is mainly in the native state (Fig. 9, A) in equilibrium with approximately 2% in the partially unfolded state (Fig. 9, C). Upon stimulation (i.e.: cAMP), cholesterol is mobilized to the outer mitochondrial membrane, increasing the chemical potential between the inner and outer mitochondrial membranes (Jefcoate *et al.* 1987). This increased chemical gradient should be sufficient to increase the amount of cholesterol bound StAR, shifting the equilibrium between native and partially unfolded StAR states, towards the partially unfolded state (Fig. 10C). This is because the cholesterol bound partially unfolded StAR is more stable than empty native StAR (Fig. 9, C vs 9, A). Upon cholesterol binding, StAR partially closes through the movement of the loops (loop Ω1 and the loop between β-strands 1 and 2 – Fig. 5E) and maintains the observed loss of helical structure upon cholesterol binding (Petrescu *et al.* 2001). This partially "refolded" state (E) then rotationally translates on itself (Fig. 10, step III), now positioning the opened cholesterol-bound cavity towards the inner mitochondrial membrane to allow cholesterol to be transferred. Once flipped, StAR releases the cholesterol in the inner mitochondrial membrane and returns to the outer mitochondrial where it can bind another cholesterol molecule for transfer (Fig. 10, D). In the event that the cholesterol gradient across the mitochondrial membranes is insufficient to drive the transfer of cholesterol inside mitochondria, refolding of the C-terminal α-helix competes

with the release of cholesterol and the recycling of StAR. In other words, if the release of cholesterol is disfavored due to a lowered chemical gradient, cholesterol remains bound to StAR long enough due to no net cholesterol transfer inside mitochondria. This allows enough time for the C-terminal α-helix to refold on top of cholesterol; it is widely accepted that refolding of a helix is much slower than transient movement of loops in solvent. Yet, it is impossible at the moment to estimate the differences in energy threshold between the refolding of the C-terminal α-helix and the recycling of StAR to the native state after cholesterol release (Fig. 5, steps 4a vs 4b, and Fig. 10, steps Va and Vb). In virtue of the large stabilization of the closed C-terminal α-helix on top of the bound cholesterol in StAR (Fig. 9, G), this step can be visualized as a rapid shut off mechanism halting StAR function, as it is irreversible. Even though these various StAR states can be located throughout the mitochondrial intermembrane, this mechanism will only function if in close proximity of "contact sites". In support of this, the complete human StAR has been located in the intermembrane space and the inner mitochondrial membrane facing the intermembrane space by immunoelectron microscopy (King *et al.* 1995), and at mitochondrial contact sites by immunoblotting (Cherradi *et al.* 1997).

Since our STC calculations have been performed in an aqueous solvent, these StAR partially unfolded states are also applicable to StAR in the cytosol (Bose *et al.* 2002). In this case, StAR functions similarly to that of the intermembrane mechanism with the exception that StAR does not rotationally translate upon itself. On the other hand, it would seem that StAR needs another unidentified factor to transfer cholesterol inside mitochondria as it does not enter mitochondria itself other than to be degraded. Recently, it has been shown that the peripheral benzodiazepine receptor (PBR) is located

preferentially at approx. 70 Å from StAR on the mitochondrial cytosolic surface (West *et al.* 2001), suggestive of a close interaction for cholesterol transfer inside mitochondria. Therefore, cytosolic StAR mediates cholesterol transfer inside mitochondria by "shuttling" cholesterol from the cholesterol rich outer mitochondrial membrane to another factor (*i.e.:* PBR) for subsequent cholesterol transfer inside mitochondria (Fig. 11); this mechanism may still be dependant on the cholesterol gradient across the outer and inner mitochondrial membranes. In this case moreover, it is not inconceivable that cholesterol may be fed to StAR directly from the cytosol cholesterol carriers, such as the sterol carrier protein-2 (SCP-2) (Gallegos *et al.* 2001).

The Pros and Cons

The largest downfall from our mechanism is the fact that the first 65 amino acids are unaccounted; this N-terminal region is presently surrounded by controversy. On one hand, it permits cholesterol transfer in the desorption mechanism (Kallen *et al.* 1998). On the other hand, it has absolutely nothing to do with cholesterol transfer (Arakane *et al.* 1996; Arakane *et al.* 1998; Tsujishita and Hurley 2000). Yet not too long ago, it was demonstrated by 2D-PAGE and 2-phased analyses of cholesterol metabolism, that newly synthesized complete StAR is rapidly processed to the N-terminally cleaved StAR, the form that mediates cholesterol access to P450scc (Artemenko *et al.* 2001).

Combining the observation that removal of the first 46 N-terminal amino acids only slightly affected protein concentrations and not StAR activity (Fleury *et al.*, unpublished results), that N-terminally cleaved StAR is the active form of StAR mediating cholesterol access to P450scc (Artemenko *et al.* 2001), and that through modeling we can justify the

existence of molten globular StAR states, further support our mechanism. Therefore, in the case of the intermembrane shuttle, an import sequence independent internalization of StAR into the mitochondrial intermembrane space is necessary and could be possible (Derman *et al.* 1993). In the event where StAR functions outside mitochondria, StAR interactions with mitochondrial proteins are key for proper StAR function and still remain to be clearly identified.

Petrescu *et al.* (Petrescu *et al.* 2001) have recently observed four novel characteristic of StAR lacking the first 62 amino acids: 1) NBD-cholesterol bound at two distinct sites, 2) loss of StAR α-helical structure when bound with NBD-cholesterol, 3) an average K_d near 32 nM for both binding sites, and 4) NBD-cholesterol binds inside the StAR "tunnel". First, the authors suggest that there is room inside the "tunnel" for two NBD-cholesterol molecules. Following our modeling, the replacement of the tunnel by the cavity restrains its volume to only permit one cholesterol molecule. In addition, this is contradictory to previous results showing molar cholesterol binding to the human MLN64 and StAR (Tsujishita and Hurley 2000). Therefore the second "cholesterol" binding site seems to be an artifact from the intrinsic polar properties of NBD-cholesterol chromophoric side-chain.

Second, a nanomolar K_d is unlikely for StAR. Although this strong association of "cholesterol" to StAR could explain the dissociation of cholesterol from the outer mitochondrial membrane as Petrescu *et al.* (Petrescu *et al.* 2001) suggested, it cannot explain how cholesterol is released to the inner mitochondrial membrane. Furthermore, such strong interactions are against a rapid cholesterol transfer, as they would slow down StAR efficiency. On the other hand, a K_d in the micromolar proportions, such as our

theoretical calculated $K_d \sim 95$ μM validated by STC, supports a rapid release of cholesterol by StAR.

Our STC calculations can account for several key points in the StAR-dependent cholesterol mechanism. First, the N-terminal mitochondrial sequence is not required for cholesterol transfer (Arakane *et al.* 1996; Arakane *et al.* 1998) either inside the intemembrane space or outside mitochondrial in the cytosol. Second, a significant population of molten globular StAR is possible (Bose *et al.* 1999; Christensen *et al.* 2001) under normal conditions for both mechanisms. Third, the hydrophobic tunnel is inexistent but rather replaced by a hydrophobic pocket that opens through the molten globule; according to the MLN64 crystal, it was argued that the openings were too small to allow cholesterol to pass though the hydrophobic tunnel (Tsujishita and Hurley 2000). Forth, the intermembrane shuttle becomes extremely rapid for the transfer of a great amount of cholesterol in a short period of time (Artemenko *et al.* 2001) through StAR partially unfolded states. Fifth, there is loss of StAR helical structure upon "cholesterol" binding (Petrescu *et al.* 2001). Sixth, the C-terminal region of StAR is critical for StAR activity (Bose *et al.* 1996; Lin *et al.* 1995). Finally, shutting off StAR-dependent cholesterol transfer inside mitochondria by irreversibly trapping cholesterol inside StAR is in agreement with the dependence of cholesterol transfer on newly synthesized StAR (Artemenko *et al.* 2001). Finally, our proposed StAR unfolding is entirely consistent with similar C-terminal movement and unfolding of PITPα, discovered by crystallization, to allow substrate binding (Schouten *et al.* 2002).

In conclusion, we were able to enlarge our understanding of the elusive StAR-dependent cholesterol transfer into mitochondria through molecular modeling and

structure-based thermodynamics. This is supported by our experimental and validated computational (Freire 1993) results presented here, and those of others (Lin *et al.* 1995). It is now possible to envision a global mechanism accounting for previously contradicting results.

ACKNOWLEDGEMENTS

We would like to thank Dr. Dale Buchanan Hales (University of Illinois at Chicago) for the anti-StAR antibody and Dr. Walter L. Miller (University of California at San Francisco) for the F2 construct.

REFERENCES

Alberta JA, Epstein LF, Pon LA & Orme-Johnson NR 1989 Mitochondrial localization of a phosphoprotein that rapidly accumulates in adrenal cortex cells exposed to adrenocorticotropic hormone or to cAMP. *Journal of Biological Chemistry* **264** 2368-2372.

Arakane F, Kallen CB, Watari H, Foster JA, Sepuri NB, Pain D, Stayrook SE, Lewis M, Gerton GL & Strauss JF, III 1998 The mechanism of action of steroidogenic acute regulatory protein (StAR). StAR acts on the outside of mitochondria to stimulate steroidogenesis. *Journal of Biological Chemistry* **273** 16339-16345.

Arakane F, Sugawara T, Nishino H, Liu Z, Holt JA, Pain D, Stocco DM, Miller WL & Strauss JF, III 1996 Steroidogenic acute regulatory protein (StAR) retains activity in the absence of its mitochondrial import sequence: implications for the mechanism of

StAR action. [see comments]. *Proceedings of the National Academy of Sciences of the United States of America* **93** 13731-13736.

Artemenko IP, Zhao D, Hales DB, Hales KH & Jefcoate CR 2001 Mitochondrial processing of newly synthesized StAR, but not total StAR, mediates cholesterol transfer to P450scc in adrenal cells. *Journal of Biological Chemistry* M107815200-

Baker BM & Murphy KP 1998 Prediction of binding energetics from structure using empirical parameterization. *Methods in Enzymology* **295** 294-315.

Bieche I, Tomasetto C, Regnier CH, Moog-Lutz C, Rio MC & Lidereau R 1996 Two distinct amplified regions at 17q11-q21 involved in human primary breast cancer. *Cancer Research* **56** 3886-3890.

Bose H, Lingappa VR & Miller WL 2002 Rapid regulation of steroidogenesis by mitochondrial protein import. *Nature* **417** 87-91.

Bose HS, Baldwin MA & Miller WL 1998 Incorrect folding of steroidogenic acute regulatory protein (StAR) in congenital lipoid adrenal hyperplasia. *Biochemistry* **37** 9768-9775.

Bose HS, Sugawara T, Strauss JF, III & Miller WL 1996 The pathophysiology and genetics of congenital lipoid adrenal hyperplasia. International Congenital Lipoid Adrenal Hyperplasia Consortium. *New England Journal of Medicine* **335** 1870-1878.

Bose HS, Whittal RM, Baldwin MA & Miller WL 1999 The active form of the steroidogenic acute regulatory protein, StAR, appears to be a molten globule.

Proceedings of the National Academy of Sciences of the United States of America **96** 7250-7255.

Brownie AC, Simpson ER, Jefcoate CR, Boyd GS, Orme-Johnson WH & Beinert H 1972 Effect of ACTH on cholesterol side-chain cleavage in rat adrenal mitochondria. *Biochemical & Biophysical Research Communications* **46** 483-490.

Caron KM, Soo SC, Wetsel WC, Stocco DM, Clark BJ & Parker KL 1997 Targeted disruption of the mouse gene encoding steroidogenic acute regulatory protein provides insights into congenital lipoid adrenal hyperplasia. *Proceedings of the National Academy of Sciences of the United States of America* **94** 11540-11545.

Cherradi N, Rossier MF, Vallotton MB, Timberg R, Friedberg I, Orly J, Wang XJ, Stocco DM & Capponi AM 1997 Submitochondrial distribution of three key steroidogenic proteins (steroidogenic acute regulatory protein and cytochrome p450scc and 3beta-hydroxysteroid dehydrogenase isomerase enzymes) upon stimulation by intracellular calcium in adrenal glomerulosa cells. *Journal of Biological Chemistry* **272** 7899-7907.

Christensen K, Bose HS, Harris FM, Miller WL & Bell JD 2001 Binding of steroidogenic acute regulatory protein to synthetic membranes suggests an active molten globule. *Journal of Biological Chemistry* **276** 17044-17051.

Clark BJ, Combs R, Hales KH, Hales DB & Stocco DM 1997 Inhibition of transcription affects synthesis of steroidogenic acute regulatory protein and steroidogenesis in MA-10 mouse Leydig tumor cells. *Endocrinology* **138** 4893-4901.

Clark BJ, Wells J, King SR & Stocco DM 1994 The purification, cloning, and expression of a novel luteinizing hormone-induced mitochondrial protein in MA-10 mouse Leydig tumor cells. Characterization of the steroidogenic acute regulatory protein (StAR). *Journal of Biological Chemistry* **269** 28314-28322.

Cockcroft S 1999 Mammalian phosphatidylinositol transfer proteins: emerging roles in signal transduction and vesicular traffic. *Chem.Phys.Lipids* **98** 23-33.

Creighton TE 1993 Proteins: Structure and Molecular Properties. **2nd**

Crivello JF & Jefcoate CR 1980 Intracellular movement of cholesterol in rat adrenal cells. Kinetics and effects of inhibitors. *Journal of Biological Chemistry* **255** 8144-8151.

Cunningham E, Thomas GM, Ball A, Hiles I & Cockcroft S 1995 Phosphatidylinositol transfer protein dictates the rate of inositol trisphosphate production by promoting the synthesis of PIP2. *Curr.Biol.* **5** 775-783.

Dauber-Osguthorpe P, Roberts VA, Osguthorpe DJ, Wolff J, Genest M & Hagler AT 1988 Structure and energetics of ligand binding to proteins: *E. coli* dihydrofolate reductase-trimethoprim, a drug-receptor system. *Proteins: Structure, Function and Genetics* **4** 31-47.

Derman AI, Puziss JW, Bassford PJ, Jr. & Beckwith J 1993 A signal sequence is not required for protein export in prlA mutants of Escherichia coli. *EMBO Journal* **12** 879-888.

Epstein LF & Orme-Johnson NR 1991a Acute action of luteinizing hormone on mouse Leydig cells: accumulation of mitochondrial phosphoproteins and stimulation of testosterone synthesis. *Molecular & Cellular Endocrinology* **81** 113-126.

Epstein LF & Orme-Johnson NR 1991b Regulation of steroid hormone biosynthesis. Identification of precursors of a phosphoprotein targeted to the mitochondrion in stimulated rat adrenal cortex cells. *Journal of Biological Chemistry* **266** 19739-19745.

Farkash Y, Timberg R & Orly J 1986 Preparation of antiserum to rat cytochrome P-450 cholesterol side chain cleavage, and its use for ultrastructural localization of the immunoreactive enzyme by protein A-gold technique. *Endocrinology* **118** 1353-1365.

Freire E 1993 Structural thermodynamics: prediction of protein stability and protein binding affinities. [Review] [16 refs]. *Archives of Biochemistry & Biophysics* **303** 181-184.

Gallegos AM, Atshaves BP, Storey SM, Starodub O, Petrescu AD, Huang H, McIntosh AL, Martin GG, Chao H, Kier AB & Schroeder F 2001 Gene structure, intracellular localization, and functional roles of sterol carrier protein-2. *Prog.Lipid Res.* **40** 498-563.

Harikrishna JA, Black SM, Szklarz GD & Miller WL 1993 Construction and function of fusion enzymes of the human cytochrome P450scc system. *DNA & Cell Biology* **12** 371-379.

Hartigan JA, Green EG, Mortensen RM, Menachery A, Williams GH & Orme-Johnson NR 1995 Comparison of protein phosphorylation patterns produced in adrenal cells by

activation of cAMP-dependent protein kinase and Ca-dependent protein kinase. *Journal of Steroid Biochemistry & Molecular Biology* **53** 95-101.

Hilser VJ & Freire E 1997 Predicting the equilibrium protein folding pathway: structure-based analysis of staphylococcal nuclease. *Proteins* **27** 171-183.

Homma Y & Emori Y 1995 A dual functional signal mediator showing RhoGAP and phospholipase C-delta stimulating activities. *EMBO Journal* **14** 286-291.

Jefcoate CR, DiBartolomeis MJ, Williams CA & McNamara BC 1987 ACTH regulation of cholesterol movement in isolated adrenal cells. *Journal of Steroid Biochemistry* **27** 721-729.

Kallen CB, Billheimer JT, Summers SA, Stayrook SE, Lewis M & Strauss JF, III 1998 Steroidogenic acute regulatory protein (StAR) is a sterol transfer protein. *Journal of Biological Chemistry* **273** 26285-26288.

King SR, Liu Z, Soh J, Eimerl S, Orly J & Stocco DM 1999 Effects of disruption of the mitochondrial electrochemical gradient on steroidogenesis and the Steroidogenic Acute Regulatory (StAR) protein. *Journal of Steroid Biochemistry & Molecular Biology* **69** 143-154.

King SR, Ronen-Fuhrmann T, Timberg R, Clark BJ, Orly J & Stocco DM 1995 Steroid production after in vitro transcription, translation, and mitochondrial processing of protein products of complementary deoxyribonucleic acid for steroidogenic acute regulatory protein. *Endocrinology* **136** 5165-5176.

Laskowski RA, MacArthur MW, Hutchinson EG & Thornton JM 1993 PROCHECK: A program to check the stereochemical quality of protein structures. *Journal of Applied Crystallography* **26** 283-291.

Lavigne P, Bagu JR, Boyko R, Willard L, Holmes CF & Sykes BD 2000 Structure-based thermodynamic analysis of the dissociation of protein phosphatase-1 catalytic subunit and microcystin-LR docked complexes. *Protein Science* **9** 252-264.

LeHoux JG, Lefebvre A, Ducharme L, Lehoux J, Martel D & Briere N 1996 Some effects of a low sodium intake on the expression of P450 aldosterone synthase in the hamster adrenal cortex: immunoblotting, immunofluorescent and immuno-gold electron microscopic studies. *Journal of Endocrinology* **149** 341-349.

LeHoux JG, Mason JI & Ducharme L 1992 In vivo effects of adrenocorticotropin on hamster adrenal steroidogenic enzymes. *Endocrinology* **131** 1874-1882.

Lin D, Sugawara T, Strauss JF, III, Clark BJ, Stocco DM, Saenger P, Rogol A & Miller WL 1995 Role of steroidogenic acute regulatory protein in adrenal and gonadal steroidogenesis. [see comments]. *Science* **267** 1828-1831.

Masucci JD, Rerie WG, Foreman DR, Zhang M, Galway ME, Marks MD & Schiefelbein JW 1996 The homeobox gene GLABRA2 is required for position-dependent cell differentiation in the root epidermis of Arabidopsis thaliana. *Development* **122** 1253-1260.

Moog-Lutz C, Tomasetto C, Regnier CH, Wendling C, Lutz Y, Muller D, Chenard MP, Basset P & Rio MC 1997 MLN64 exhibits homology with the steroidogenic acute

regulatory protein (STAR) and is over-expressed in human breast carcinomas. *International Journal of Cancer* **71** 183-191.

Petrescu AD, Gallegos AM, Okamura Y, Strauss JF & Schroeder F 2001 Steroidogenic acute regulatory protein binds cholesterol and modulates mitochondrial membrane sterol domain dynamics. *Journal of Biological Chemistry* **276**-36970-36982.

Pon L, Moll T, Vestweber D, Marshallsay B & Schatz G 1989 Protein import into mitochondria: ATP-dependent protein translocation activity in a submitochondrial fraction enriched in membrane contact sites and specific proteins. *Journal of Cell Biology* **109** 2603-2616.

Pon LA, Hartigan JA & Orme-Johnson NR 1986 Acute ACTH regulation of adrenal corticosteroid biosynthesis. Rapid accumulation of a phosphoprotein. *Journal of Biological Chemistry* **261** 13309-13316.

Pon LA & Orme-Johnson NR 1988 Acute stimulation of corpus luteum cells by gonadotrophin or adenosine 3',5'-monophosphate causes accumulation of a phosphoprotein concurrent with acceleration of steroid synthesis. *Endocrinology* **123** 1942-1948.

Ponting CP & Aravind L 1999 START: a lipid-binding domain in StAR, HD-ZIP and signalling proteins. *Trends in Biochemical Sciences* **24** 130-132.

Ponting CP, Schultz J, Milpetz F & Bork P 1999 SMART: identification and annotation of domains from signalling and extracellular protein sequences. *Nucleic Acids Research* **27** 229-232.

Privalle CT, Crivello JF & Jefcoate CR 1983 Regulation of intramitochondrial cholesterol transfer to side-chain cleavage cytochrome P-450 in rat adrenal gland. *Proceedings of the National Academy of Sciences of the United States of America* **80** 702-706.

Raya A, Revert F, Navarro S & Saus J 1999 Characterization of a novel type of serine/threonine kinase that specifically phosphorylates the human goodpasture antigen. *Journal of Biological Chemistry* **274** 12642-12649.

Schouten A, Agianian B, Westerman J, Kroon J, Wirtz KW & Gros P 2002 Structure of apo-phosphatidylinositol transfer protein alpha provides insight into membrane association. *EMBO J.* **21** 2117-2121.

Schwaiger M, Herzog V & Neupert W 1987 Characterization of translocation contact sites involved in the import of mitochondrial proteins. *Journal of Cell Biology* **105** 235-246.

Simpson ER, McCarthy JL & Peterson JA 1978 Evidence that the cycloheximide-sensitive site of adrenocorticotropic hormone action is in the mitochondrion. Changes in pregnenolone formation, cholesterol content, and the electron paramagnetic resonance spectra of cytochrome P-450. *Journal of Biological Chemistry* **253** 3135-3139.

Stocco DM 2000 Intramitochondrial cholesterol transfer. [Review] [92 refs]. *Biochimica et Biophysica Acta* **1486** 184-197.

Stocco DM 2001 Tracking the role of a star in the sky of the new millennium. [Review] [78 refs]. *Molecular Endocrinology* **15** 1245-1254.

Stocco DM & Clark BJ 1996 Regulation of the acute production of steroids in steroidogenic cells. [Review] [268 refs]. *Endocrine Reviews* **17** 221-244.

Sugawara T, Holt JA, Driscoll D, Strauss JF, III, Lin D, Miller WL, Patterson D, Clancy KP, Hart IM & Clark BJ 1995 Human steroidogenic acute regulatory protein: functional activity in COS-1 cells, tissue-specific expression, and mapping of the structural gene to 8p11.2 and a pseudogene to chromosome 13. *Proceedings of the National Academy of Sciences of the United States of America* **92** 4778-4782.

Thompson JD, Higgins DG & Gibson TJ 1994 CLUSTAL W: improving the sensitivity of progressive multiple sequence alignment through sequence weighting, position-specific gap penalties and weight matrix choice. *Nucleic Acids Research* **22** 4673-4680.

Tsujishita Y & Hurley JH 2000 Structure and lipid transport mechanism of a StAR-related domain. [see comments]. *Nature Structural Biology* **7** 408-414.

Watari H, Arakane F, Moog-Lutz C, Kallen CB, Tomasetto C, Gerton GL, Rio MC, Baker ME & Strauss JF, III 1997 MLN64 contains a domain with homology to the steroidogenic acute regulatory protein (StAR) that stimulates steroidogenesis. *Proceedings of the National Academy of Sciences of the United States of America* **94** 8462-8467.

West LA, Horvat RD, Roess DA, Barisas BG, Juengel JL & Niswender GD 2001 Steroidogenic acute regulatory protein and peripheral-type benzodiazepine receptor associate at the mitochondrial membrane. *Endocrinology* **142** 502-505.

FIGURE LEGENDS

FIGURE 1. Alignment of the hamster and human StAR, and human MLN64 amino acid sequences used for homology modeling.

FIGURE 2. Ribbon diagram of the final hamster StAR model. The same overall structure was obtained for the human StAR and is therefore not shown. Helices in red, strands in blue, and loops in yellow. There is "fog" in the image for depth perception. All structural elements have been labeled according to the human MLN64 crystal structure.

FIGURE 3. Hamster StAR model cholesterol binding site. A, Ribbon diagram of the hamster StAR with a solvated binding site. The solvent is represented as Connolly surface dots with the water molecules as black sticks. The black and gray areas show where the model has been "opened" to allow surface area calculations of the cholesterol binding site. In black, the major feature is the C-terminal α-helix which tops the binding site; in gray, the major feature is the U-shaped β-barrel forming the bottom of the binding site, along with the majority of the remaining amino acids. B, Connolly surface representation of the "opened" hamster StAR model, as depicted from A. Left, U-shaped β-barrel as seen from above the cholesterol binding site. Right, C-terminal α-helix seen

from below (as though in the cholesterol binding site). Color scheme: hydrophobic atoms in gray, potentially polar atoms in yellow, and charged atoms in red (oxygens) and blue (nitrogens). The cholesterol binding site salt bridge is circled in orange. C, Same representation as in B except everything in white but the atoms directly in contact to the cholesterol binding site in black.

FIGURE 4. Molecular mechanism of cholesterol binding in StAR. The cholesterol binding site of StAR is opened through two movements of the C-terminal α-helix (dark gray) from the original folded conformation (A): step 1) opened (B): completely removed from the cholesterol binding site, and step 2) partially unfolded (C): all of the α-helical structure of the C-terminal α-helix is lost. Once open, cholesterol can bind to StAR (D) as indicated in step 3; a theoretical K_d of 94.4 μM was calculated with STC. StAR is represented as a ribbons diagram while cholesterol is depicted as van der Waals radii. StAR is white with the C-terminal α-helix dark gray, and cholesterol dark gray. ΔG is the change in Gibb's free energy in kcal/mol.

FIGURE 5. Representation of loop mobility upon cholesterol binding to StAR. Cholesterol binding was simulated in the partially unfolded StAR (Fig. 4, D); after cholesterol binding, the loops immediately adjacent to the unfolded C-terminal α-helix (loop Ω1 and the loop between β-strands 1 and 2) cover the bound cholesterol (E), inhibiting the refolding of the C-terminal α-helix. D; partially unfolded StAR (same as in Fig. 4, D), E; partially refolded StAR with loops "closed". Main StAR structure drawn as white ribbons

with the exception of the moveable loops in dark gray; cholesterol represented as van der Waals radii, also in dark gray. ΔG is the change in Gibb's free energy in kcal/mol.

FIGURE 6. Cholesterol solvation by StAR. Closure of the cholesterol bound StAR active site can take either of two pathways: 1) closure of the loops adjacent the open binding site (loop Ω1 and the loop between β-strands 1 and 2), resulting in a partially refolded state where C-terminal α-helix refolding is inhibited (step 4a, D to E to G); and 2) C-terminal α-helix refolding in the opposite direction of Fig. 4, resulting in the trapping of cholesterol inside StAR (steps 4b and 5, D to F to G). The color code is the same as for Fig. 6 with the exception of the closed loop partially folded cholesterol bound StAR (F) colored dark gray, distinguishing it from the partially unfolded cholesterol bound StAR (D).

FIGURE 7. Cholesterol binding inside StAR. Surface diagram of the StAR U-shaped β-barrel with representation of cholesterol as sticks without hydrogens. One water molecule is depicted as a thick stick, allowing hydrogen bonding of the cholesterol's 3β-OH with Arg187. The color scheme is the same as in Fig. 3B: hydrophobic atoms in gray, potentially polar atoms in yellow, and charged atoms in red (oxygens) and blue (nitrogens).

FIGURE 8. Altered StAR activity of salt bridge mutants. COS-1 cells co-transfected with F2 and different StAR-pcDNA3.1 plasmids were incubated without (Ctr) and with $(Bu)_2$-cAMP (cAMP) for 24 hours. A) Relative StAR activity compared to Ctr-WT; values are

the mean of three different experiments. B) After electrophoresis and transfer on membranes, proteins were revealed using a mouse anti-StAR antibody: results are from three different homogenate preparations. C) Quantification of the protein bands obtained in B. *$p < 0.05$ compared to their own control value; †$p < 0.05$ compared to Ctr-WT.

FIGURE 9. Profile of the change in free Gibb's energy. Graphical representation of the results obtained in Figs. 4 and 6; the letters represent the same conformations as in these figures. Under normal conditions, StAR is in equilibrium between to the native and partially unfolded states (A vs C). Approx. 2% of the StAR population is expected to be in the partially unfolded state. Note that the opened state B should not be existent other than to go change from the native to partially unfolded state and vice versa (A to C and C to A). Upon cholesterol binding, the cholesterol bound partially unfolded StAR is slightly more stable than the native state (D vs A, respectively) therefore shifting the equilibrium of the population of StAR to the partially unfolded state. Half of the partially unfolded cholesterol bound StAR population has the loops closed on top of the cholesterol (E; $population^{D} = population^{E}$). The partially refolded StAR (E) can then return to the partially unfolded empty StAR (C) if cholesterol is released, or irreversibly trap cholesterol inside StAR's cholesterol binding site if cholesterol is not released (G). In the latter case, the transient refolded C-terminal α-helix with the open binding site (F) is not believe to exist other than to allow the transition from the partially unfolded to native cholesterol bound StAR. Threshold activation between conformational states are arbitrary and do not represent experimental data. ΔG is the change in Gibb's free energy sequentially obtained from Figs. 4 and 6.

FIGURE 10. Proposed StAR mechanism in the mitochondrial intermembrane space. Cholesterol is transferred into mitochondria through the flipping of StAR from the outer mitochondrial membrane (OMM) to the inner mitochondrial membrane (IMM). In the intermembrane space at contact sites, the cholesterol deprived native StAR opens and unfolds through the movement of the C-terminal α-helix (step I, A to C). Close to the cholesterol rich OMM, maybe even interacting with it, cholesterol binds to the exposed StAR binding site and the loops adjacent the binding site (loop Ω1 and the loop between β-strands 1 and 2) close, covering cholesterol (step II, C to E). The StAR-cholesterol complex then flips on itself to release cholesterol in the IMM after the loops open to expose cholesterol (steps III and IV, E to D). If cholesterol is released in the IMM, then it can be recycled back to the native/partially unfolded state equilibrium for transport of another cholesterol molecule (step Va, D to C). In the event where no cholesterol gradient exists to drive the transport of cholesterol inside the IMM, the C-terminal α-helix of the partially unfolded cholesterol-bound StAR can then refold on top of cholesterol, irreversibly trapping cholesterol inside StAR (step Vb, D to G) and shutting off StAR function; equilibrium between the native and partially unfolded state of StAR is re-established (step I, A to C). The structures, their colors, and their labels are identical to Figs. 4 and 6 for consistency.

FIGURE 11. Proposed StAR mechanism in the cytosol. Cholesterol enters mitochondria through the concerted action of a cytosolic StAR with an unidentified factor (?). In this case, StAR unfolding is identical to the case where StAR is located in the mitochondrial

intermembrane space (Fig. 10), with the exception that StAR now shuttles cholesterol from the cholesterol-rich outer mitochondrial membrane to the unidentified mitochondrial factor. StAR supposedly remains outside mitochondria until it is marked for degradation inside mitochondria. For consistency, the structures, their colors, and their labels are identical to Figs. 4, 6, and 10. OMM: outer mitochondrial membrane; IMM: inner mitochondrial membrane.

FIG 1

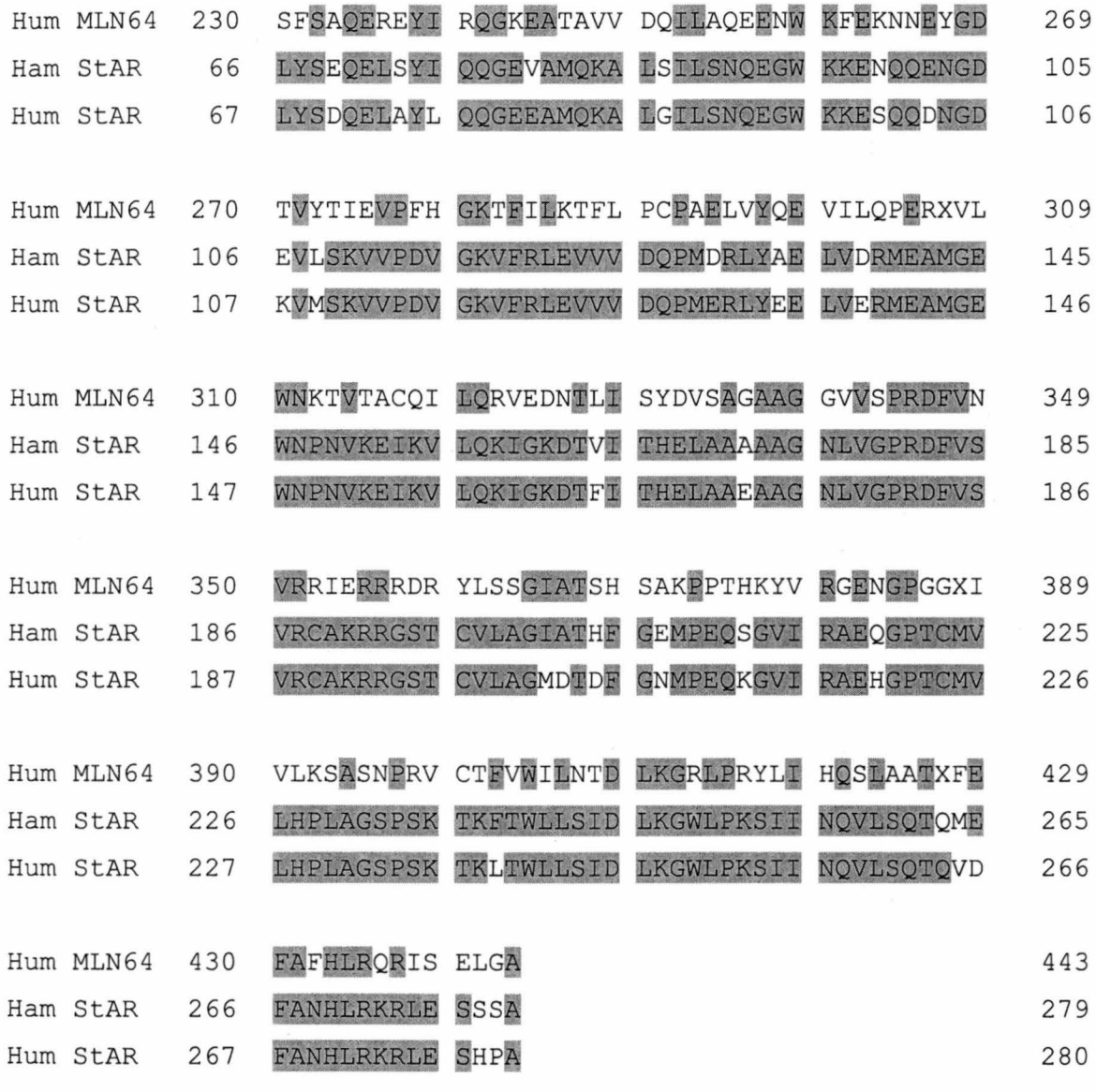
Hum MLN64 230 SFSAQEREYI RQGKEATAVV DQILAQEENW KFEKNNEYGD 269
Ham StAR 66 LYSEQELSYI QQGEVAMQKA LSILSNQEGW KKENQQENGD 105
Hum StAR 67 LYSDQELAYL QQGEEAMQKA LGILSNQEGW KKESQQDNGD 106
Hum MLN64 270 TVYTIEVPFH GKTFILKTFL PCPAELVYQE VILQPERXVL 309
Ham StAR 106 EVLSKVVPDV GKVFRLEVVV DQPMDRLYAE LVDRMEAMGE 145
Hum StAR 107 KVMSKVVPDV GKVFRLEVVV DQPMERLYEE LVERMEAMGE 146
Hum MLN64 310 WNKTVTACQI LQRVEDNTLI SYDVSAGAAG GVVSPRDFVN 349
Ham StAR 146 WNPNVKEIKV LQKIGKDTVI THELAAAAAG NLVGPRDFVS 185
Hum StAR 147 WNPNVKEIKV LQKIGKDTFI THELAAEAAG NLVGPRDFVS 186
Hum MLN64 350 VRRIERRRDR YLSSGIATSH SAKPPTHKYV RGENGPGGXI 389
Ham StAR 186 VRCAKRRGST CVLAGIATHF GEMPEQSGVI RAEQGPTCMV 225
Hum StAR 187 VRCAKRRGST CVLAGMDTDF GNMPEQKGVI RAEHGPTCMV 226
Hum MLN64 390 VLKSASNPRV CTFVWILNTD LKGRLPRYLI HQSLAATXFE 429
Ham StAR 226 LHPLAGSPSK TKFTWLLSID LKGWLPKSII NQVLSQTQME 265
Hum StAR 227 LHPLAGSPSK TKLTWLLSID LKGWLPKSII NQVLSQTQVD 266
Hum MLN64 430 FAFHLRQRIS ELGA 443
Ham StAR 266 FANHLRKRLE SSSA 279
Hum StAR 267 FANHLRKRLE SHPA 280

FIG 2

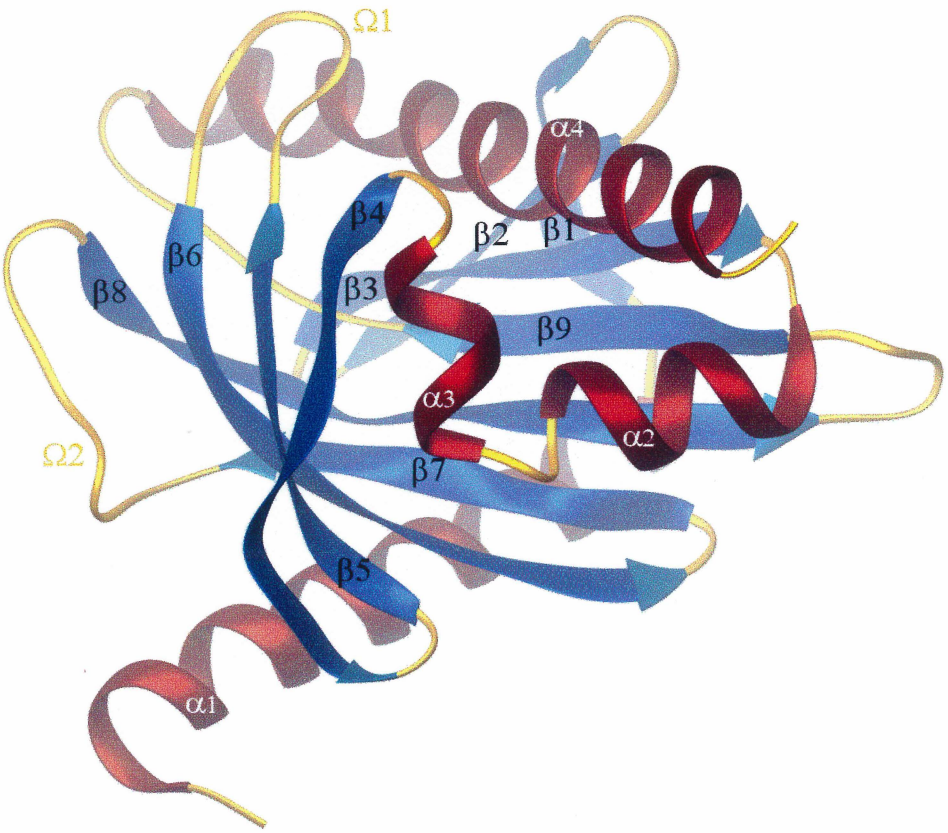

FIG 3

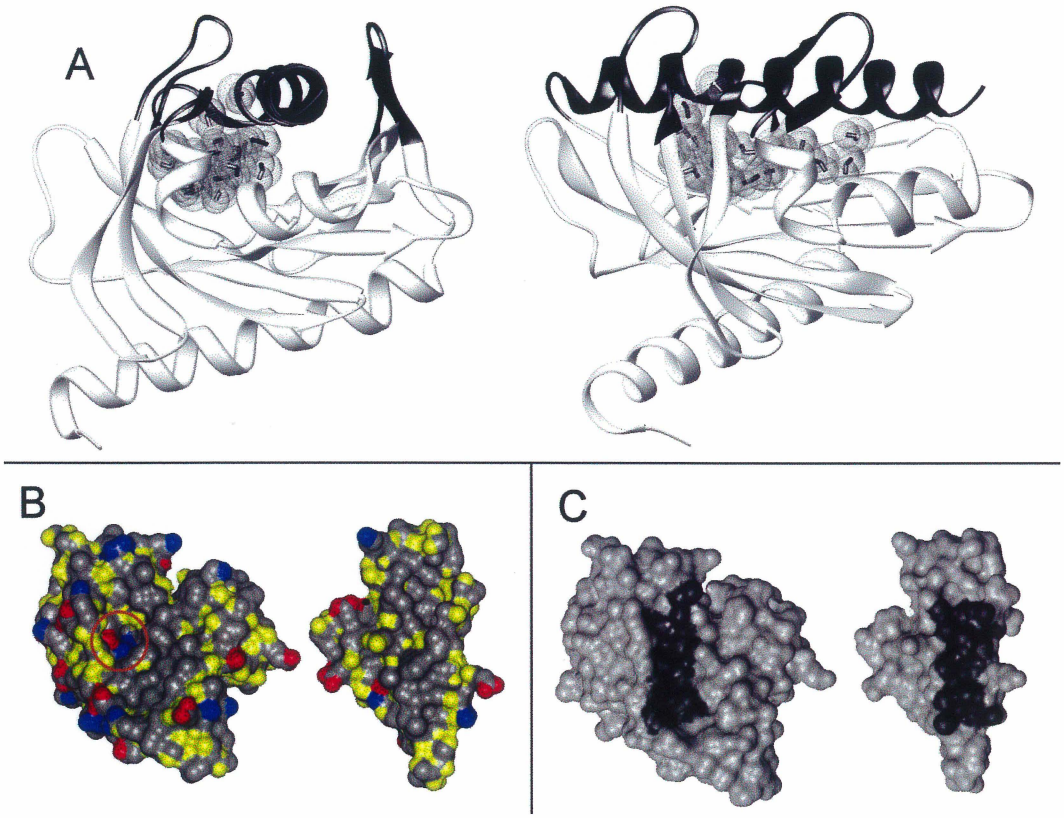

FIG 4

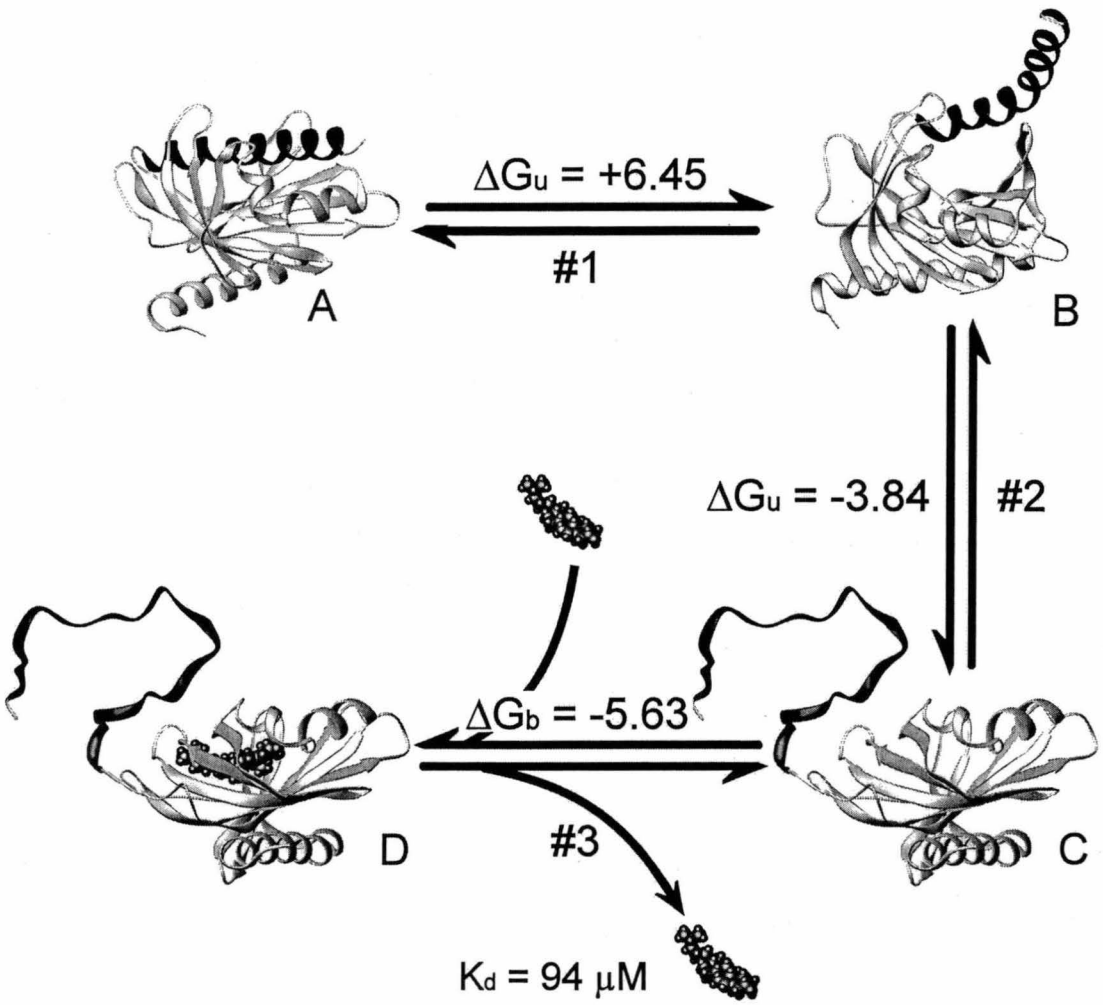

FIG 5

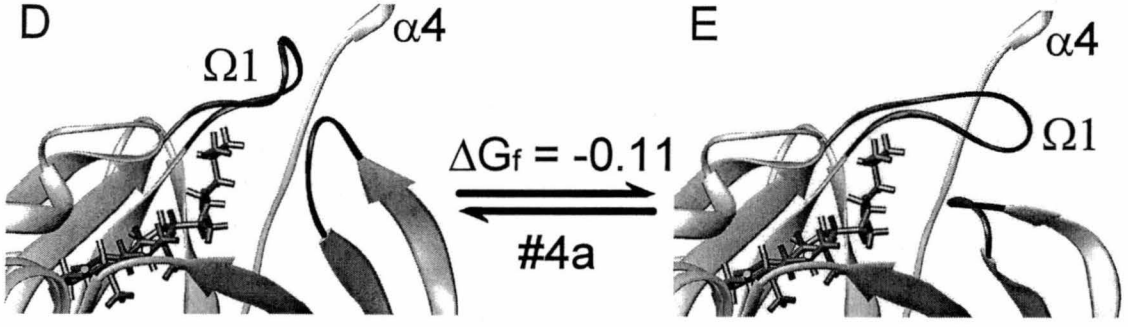

FIG 6

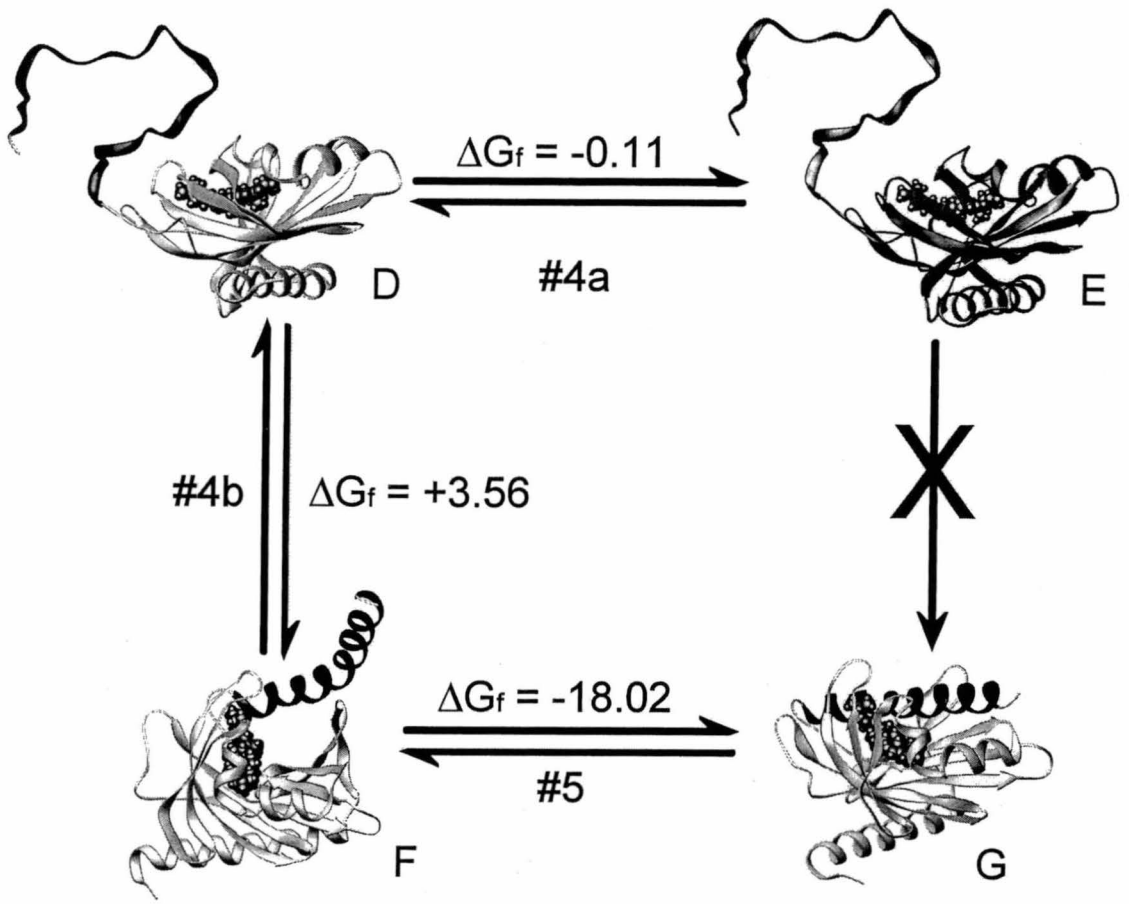

FIG 7

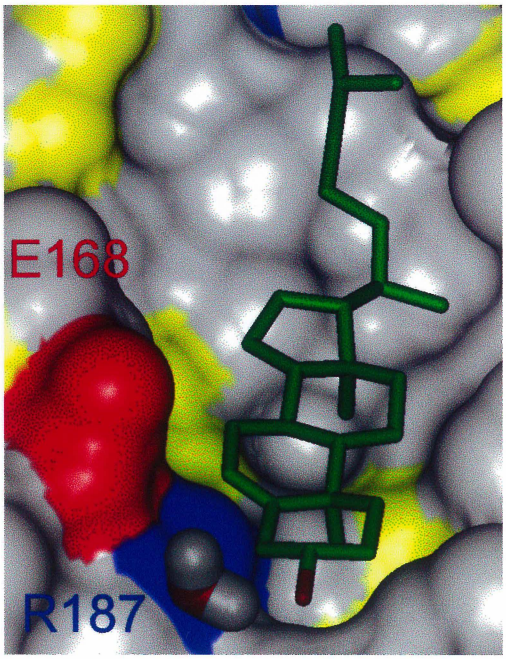

FIG 8

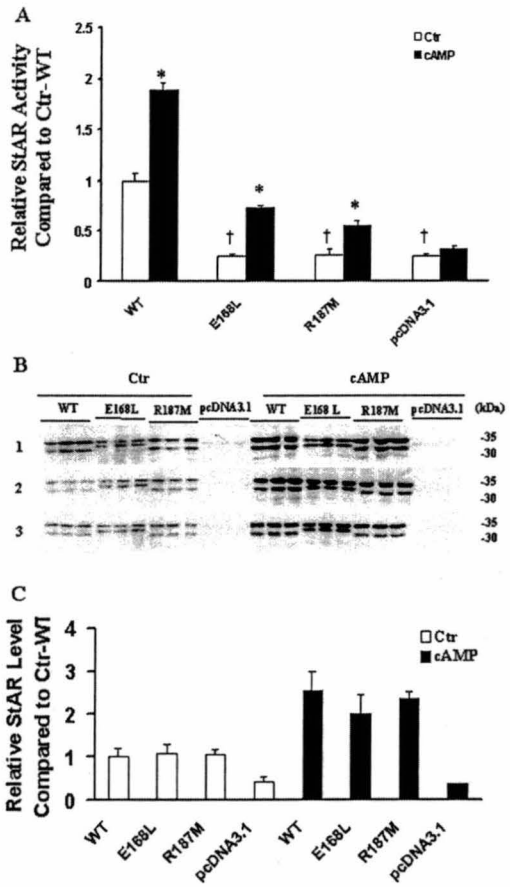
A
Relative StAR Activity Compared to Ctr-WT
Ctr
cAMP
WT
E168L
R187M
pcDNA3.1
B
Ctr
cAMP
WT
E168L
R187M
pcDNA3.1
WT
E168 L
R187M
pcDNA3.1
(kDa)
1
2
3
-35
-30
C
Relative StAR Level Compared to Ctr-WT
Ctr
cAMP
WT
E168L
R187M
pcDNA3.1

FIG 9

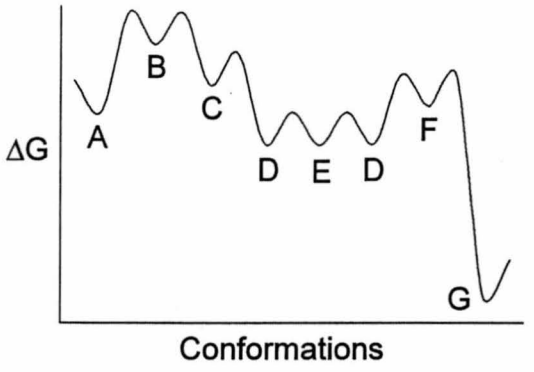

FIG 10

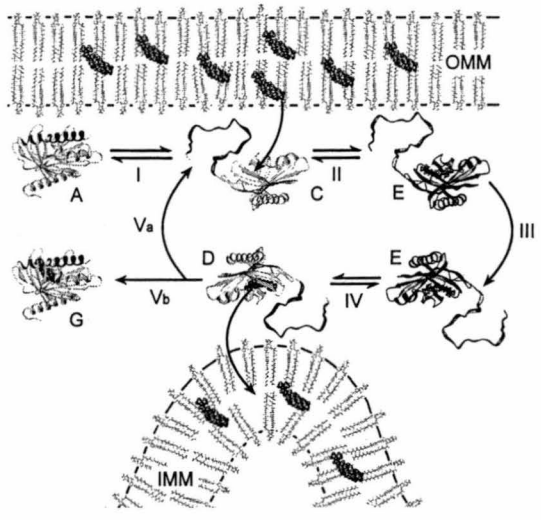

FIG 11

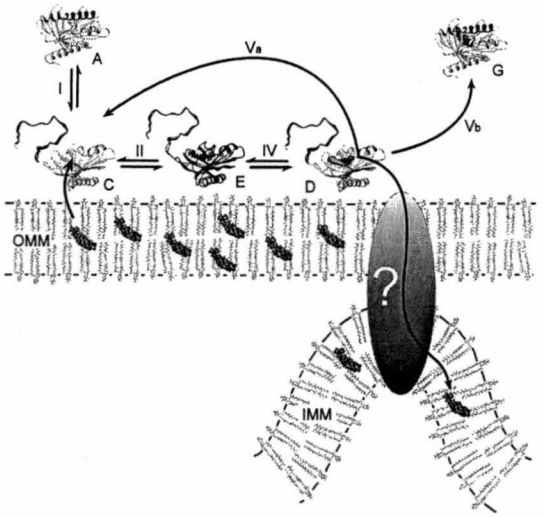

2.2. Fleury A. Mathieu AP. Ducharme L. Hale DB. LeHoux JG. Phosphorylation and Function of the Hamster Adrenal Steroidogenic Acute Regulatory Protein. [Journal Article] ***Submitted to The Journal of Biological Chemistry 10/2001 – To be revised.***

Contribution: My greatest contribution in this paper was the molecular modeling analysis of the putative phophorylation sites, actively participating in the decision of which mutants to test, and their analyses.

Phosphorylation and Function of the Hamster Adrenal Steroidogenic Acute Regulatory Protein (StAR)*.

Alain Fleury, Axel P. Mathieu, Lyne Ducharme, Dale Buchanan Hales and Jean-Guy LeHoux‡

From the Department of Biochemistry (A.F., A.P.M., L.D., J.G.L.), Faculty of Medicine, University of Sherbrooke, Sherbrooke, Quebec, Canada, J1H 5N4, and Department of Physiology and Biophysics (D.B.H.), University of Illinois at Chicago, Chicago, Illinois 60612-7342.

Running title: Hamster StAR Structure and Function

Key words: Hamster, adrenal, ACTH, angiotensin, TPA, StAR, cyclic AMP, 2D-PAGE

*This work was supported by a grant from the Medical Research Council of Canada, grant MT-10983 (to J.-G.L.), and the Heart and Stroke Foundation of Canada (to J.-G.L.). J.G.L. is *Chercheur boursier de carrière* du *Fonds de la recherche en santé du Québec.*

‡To whom correspondence should be addressed: Department of Biochemistry, Faculty of Medicine, University of Sherbrooke, Sherbrooke, Quebec, Canada, J1H 5N4. Phone: (819) 564-5282; Fax: (819) 820-6852

E-mail: jlehou01@courrier.usherb.ca.

The steroidogenic acute regulatory protein (StAR) undergoes post-translational changes that modify its activity, defined as the quantity of pregnenolone synthesized in co-transfection experiments of COS-1 cells using F2 (P450scc-adrenodoxin reductase-adrenodoxin) and StAR plasmids. Eleven putative phosphorylation sites were mutated in the hamster StAR. Decreases of 30%, 81% and 95% in basal activity were found only for the mutants S13A, S185A and S194A respectively. The $(Bu)_2$-cAMP stimulated activities of the mutants S185A and S194A were 40% and 89% lower than other preparations. Control and $(Bu)_2$-cAMP stimulated activities of the S194A mutant were significantly lower than those of the S194A/S13A and S194A/S185A double mutants. The 2D-PAGE migration patterns of stimulated preparations revealed many low pI StAR species, presumably phosphorylated, in WT, S13A and S185A, but absent in S194A preparations. Substitution of S185 by D or E residues to mimic phosphorylation resulted in decreased activity, and since the quantity of expressed StAR was similar between preparations, we can conclude that S185 is not a site of phosphorylation. According to a 3D-model of StAR, S194 is located at the exterior of the molecule and accessible to kinases, whereas S185 is hidden inside the protein and not accessible to kinases. However, S185 is located near a saline bridge that may be involved in the mechanism of cholesterol binding since it is the only hydrophilic component of the cholesterol-binding site. This suggests that mutation of S185 alters the binding site environment, changing its affinity for cholesterol and consequently decreasing StAR activity.

The rate limiting step of steroidogenesis is the delivery of cholesterol to the matrix side of inner mitochondria membrane where resides the cholesterol side-chain cleavage cytochrome P450 (P450scc)[1], the enzyme catalyzing the transformation of cholesterol to pregnenolone (1). The transfer of cholesterol into mitochondria across the inter-membrane aqueous space and steroidogenesis are both inhibited by the protein synthesis inhibitor cycloheximide (2;3).

In lipoid congenital adrenal hyperplasia, mutations in the steroidogenic acute regulatory protein (StAR) gene were shown to be responsible for defective steroidogenesis (4-9). *In vitro*, the expression of StAR was shown to induce steroidogenesis without hormonal stimulation (1). Furthermore, impaired steroidogenesis and lipid accumulation in steroidogenic tissues was obtained in StAR gene nullizygous mice produced by homologous recombination with identical phenotype (10). This genetic and biochemical evidence has indicted StAR as a key molecule in regulating cholesterol transfer across the mitochondria membrane and consequently in controlling the transformation of cholesterol to pregnenolone.

Up to now three models have been proposed to describe the mechanism of action of StAR on the cholesterol entry into mitochondria. One model suggests cholesterol desorption from the outer side of the outer membrane to the inner membrane (11). The second model proposes that StAR is active as a molten globule (12). In the third model, cholesterol is transferred via an intermembrane shuttle mechanism (13).

Two main factors are regulating steroidogenesis in the adrenal cortex, adrenocorticotropin hormone (ACTH) and angiotensin II (AII), both regulating steroid formation at the site of transformation of cholesterol to pregnenolone (14). We have demonstrated that ACTH administration (15-17) and sodium restriction (18) *in vivo* affected the formation of different species of StAR in rat (16-18) and hamster (15) adrenals.

The labeling of phosphoproteins upon ACTH and gonadotropin treatment of steroidogenic cells were reported well before their identification as StAR (2;19-25) and recently using ^{35}S-methionine or ^{32}P-orthophosphate, Arakane *et al.* (26) showed that ACTH and AII affected the labeling of 30 kDa phosphoproteins in steroidogenic cells. Moreover, using COS-1 cells to express human StAR, a mutation of a potential site for protein kinase A-mediated phosphorylation at serine 195 to alanine (S195A) reduced ^{32}P incorporation from labeled ATP to StAR. The capacity of that mutant to induce pregnenolone production was reduced by 50%, indicating the importance of phosphorylation as part of the mechanism of action of this protein to control steroidogenesis. Up to now, the remaining capacity of transfected COS-1 cells by the S195A to synthesize pregnenolone has not been attributed to other phosphorylation sites and no systematic studies have been completed to cover this aspect.

Since the first report on the mouse StAR cDNA (1), StAR cDNA were cloned from twelve other animal species including the hamster (15). By alignment analysis of the amino acid sequences of all these StARs, we have found that eleven putative phosphorylation sites were conserved among most animal species. In order to determine if these putative phosphorylation sites were part of the mode of action of StAR, we have mutated these eleven conserved sequences in the hamster StAR and studied their effect on pregnenolone synthesis in transfected COS 1 cells.

EXPERIMENTAL PROCEDURES

Materials-All restriction and modifying enzymes were purchased from New England Biolabs (Mississauga, ON, Canada). The expression vector pcDNA3.1Myc-His, Lipofectamine and

oligonucleotides were purchased from Invitrogen Canada Inc. (Burlington, ON, Canada). All vectors were amplified in XL1 Blue E. coli competent cells (Stratagene, La Jolla, CA), and purified on anion-exchange columns (Qiagen, Chatsworth, CA). TPA and $(Bu)_2$-cAMP were obtained from Sigma-Aldrich (St-Louis, MO).

Hamster StAR mutagenesis by PCR-The hamster StAR cDNA was isolated and cloned as previously described (15). StAR sequences of man (27), horse (28), pig (29), sheep (30), cow (31), rat (32), mouse (1), hamster (15), chicken (33), frog (33), zebra fish (33), rainbow trout (34) and brook trout (35) were obtained from Genbank and aligned by Clustal method using Lasergene software from DNASTAR Inc. Madison WI. Putative phosphorylation sites were determined using PhosphoBase v2.0, a database of phosphorylation sites provided by Center for Biological Sequence Analysis at the Technical University of Denmark (http://www.cbs.dtu.dk/databases/PhosphoBase). Site-directed mutagenesis was performed by PCR (36). Briefly, two series of PCR amplifications were obtained using the following conditions: Hot start of 5 min at 94°C (without DNA polymerase) followed by a touch down of 2°C from 94°C/70°C/72°C to 94°C/50°C/72°C, completed with 30 cycles of 94°C/50°C/72°C and a final 72°C elongation of 15 min. The first series consists of amplifying hamster StAR cDNA in two different reactions. 1) A wild type (WT) upstream (sense) oligonucleotide to the downstream mutant (antisense) oligonucleotide at the site of interest for mutagenesis and 2) a mutant sense oligonucleotide from the site of interest for mutagenesis to a WT antisense oligonucleotide. The second series consists of pooling both PCRs previously obtained, purified by agarose gel electrophoresis, and amplifying using WT 5' and 3' oligonucleotides. WT-StAR and all mutants were cloned into pcDNA3.1Myc-His using unique Eco RI and Hind III restriction sites, and

entirely sequenced between these restriction sites using T7 sequencing kit from Amersham Pharmacia Biotech (Baie d'Urfé, QC Canada), amplified, and purified on Qiagen anion-exchange columns.

Hamster StAR expression-Either WT or mutated StAR was transiently transfected into monkey kidney COS-1 cells (American Type Culture Collection, Rockville, MD) using the lipofectamine method. Twenty-four hours before transfection, the cells were harvested with pancreatin-EDTA solution (Invitrogen Canada Inc., Burlington, ON, Canada) and plated at an initial density of 3.5 x 10^5 cells per 10 cm^2 well in 6-well plates, or 1.6 x 10^6 cells in 78.5 cm^2 Petri dishes. Cells were cultured in DMEM supplemented with 10% fetal bovine serum (FBS), 5.96 g/L HEPES, 2.2 g/L $NaHCO_3$, 1mM L-glutamine, 100 IU/ml penicillin, and 100 µg/ml streptomycin sulphate. DMEM containing no fetal bovine serum and no antibiotics was used for transfections. Each transfection assay received 1 µg of DNA (500 ng F2 construct (37) containing P450scc-adrenodoxin reductase-adrenodoxin and 500 ng of pcDNA3.1 + pcDNA3.1-StAR) and 10 µg lipofectamine in one ml of media. Twenty-two hours after transfection cells were rinsed with PBS. Cells were then incubated for 24 hours in DMEM without phenol red containing 10% dextran-coated charcoal-treated FBS and antibiotics with or without stimulating agents. Media were kept for pregnenolone quantification and cells for immunoblotting analyses.

Measurement of the hamster StAR activity-In this study, StAR activity is defined as the quantity of pregnenolone formed by co-transfected COS-1 cells with F2 and StAR plasmids. Pregnenolone formation was analyzed by radioimmunoassay (ICN Pharmaceuticals, Diagnostics Division, Orangeburg, NY).

Immunoblotting analysis-For 1D-SDS-PAGE analyses, cells were scraped and directly harvested in hot (100°C) Laemmli buffer. All samples were then passed through a 26 gauge needle, then boiled for 10 min and finally centrifuged at 12000 x g for 2 min. Protein levels were determined on the supernatant using the Bio-Rad Protein Assay Dye Reagent (Bio-Rad Laboratories, Ltd. Mississauga, ON, Canada). For 2D-PAGE analyses, cells were scraped and harvested in the homogenization buffer containing 50 mM Tris pH 7.4, 0.25 M sucrose, 5 mM EDTA and complete protease inhibitor cocktail tablets (Roche Diagnostics Canada, Laval, QC, Canada). For mitochondria preparations, cells were suspended in the homogenization buffer and were sonicated for 7 seconds. The degree of cell rupture was verified under microscope. When totally ruptured, the cell preparation was centrifuged 10 min at 900 x g, only the supernatant was kept and centrifuged at 15 min at 9500 x g. The mitochondria pellet was resuspended in 75 µl homogenization buffer and 25 µl Laemmli buffer (4X) (38).

For 1D-SDS-PAGE, soluble proteins were electrophoresed on 12% polyacrylamide gels and analyzed by immunoblotting as previously described (39;40) using a rabbit polyclonal anti-mouse StAR antibody (41).

Immunoreactive proteins were detected using ECL-PLUS light emitting reagents (Amersham Pharmacia Biotech UK Ltd., Amersham Place, Little Chalfont, Buckinghamshire, UK). Autoradiograms were observed by exposing the blots to Kodax X-Omat XK films. The results

were also visualized and quantified on the optical imager STORM 860 using ImageQuant software version 5.0. (Molecular Dynamics, Sunnyvale, CA). For 2D-PAGE, gel rods (110 mm x 4 mm) were made with 8M urea, 4.5% polyacrylamide, 2% triton X-100 and 2% ampholines (0.67% pH 3-10 and 1.33% pH 5-7). Prefocusing (0.66mA per gel rod) was performed during 1 h with a 500 V maximum limit in NaOH 0.1N (catholyte) and 0.06% phosphoric acid (anolyte). Soluble proteins from mitochondria preparations were diluted with two volumes of sample dilution buffer which contained: 9.5 M urea, 10% triton X-100, 2% ampholines, and 5% β-mercaptoethanol (v/v). Samples were loaded and overlaid with 5M urea, 2% triton X-100 and 2% ampholines. Constant 400 V were applied for 9000-10000 Volt•hours. Gel rods were equilibrated 2 x 20 min in a reducing buffer (62.5mM Tris, pH 6.8, 5% β-mercaptoethanol, 3% SDS, 0.01% bromophenol blue). Reduced rods may be stored at –80 °C until used. Thawed rods were fixed with 1% agarose in upper buffer (125mM Tris, pH 6.8, 0.1% SDS). Sodium dodecyl sulfate-PAGE and immunoblotting were performed as described above. Isoelectric points (pI) were determined using 2D-PAGE standards # 161-0320 from Bio-Rad Laboratories (Mississauga, ON, Canada). In addition, in some experiments, standards and adrenal preparations were mixed and ran on the same gel. After transferring on membranes, standards were stained and StAR was detected as described for 1D-SDS-PAGE.

Statistical analyses-Differences between experimental groups were analyzed by one way ANOVA using the SigmaStat program for Windows (SPSS Science, Chicago IL).

RESULTS

A strong amino acid sequence identity exists between StAR indexed from thirteen different vertebrate species. These StARs undergo post-translational changes, which can modify protein activity. Indeed, StAR contains putative phosphorylation sites for protein kinases A (PKA), protein kinase C (PKC), and casein kinase 2 (CK2). StAR amino acid sequences were thus analyzed *in silico* to determine putative phosphorylation sites conserved among species. Out of nineteen putative sites discovered, eleven of them were shown to be conserved among most mammal species including the hamster (Table 1). The hamster StAR serines (S) 13, S55, S56, S60, S68, S90, S185, S194, S276, threonines (T) 5 and T262 putative phosphorylation sites were thus mutated; T by valine (V) and S by alanine (A) respectively, in order to systematically study their role in StAR activity.

To test StAR activity (defined as the quantity of pregnenolone formed by transfected cells), COS-1 cells were co-transfected with the expression plasmid F2 (harboring P450scc-adrenodoxin reductase-adrenodoxin) and pcDNA3.1-StAR. Fig.1 shows the enhancing effect of increasing concentrations of wild type (WT) StAR DNA in transfection media on StAR activity. In this series of experiments, basal activity of cells co-transfected with the empty pcDNA3.1 vector and F2 was 47 ng pregnenolone / 3 x 10^5 cells, and this activity was increased to 348 ng in the presence of 75 ng pcDNA3.1-WT-StAR. At this DNA concentration $(Bu)_2$-cAMP further stimulated the production of pregnenolone to 1037 ng whereas TPA appeared to have no enhancing effect on basal StAR activity (results not shown). A background corresponding to 27 ng pregnenolone in COS-1 cells transfected with F2 and pcDNA3.1 plasmids was subtracted to experimental values.

In the next series of experiments, COS-1 cells were co-transfected with the F2 construct and either the WT-StAR or mutated-StAR plasmids. Compared to WT, basal StAR activity was not affected for mutants T5V, S55A, S56A, S60A, S68A, S90A, T262V and S276A (Fig.2A). However, StAR activity was significantly decreased by 30%, 81% and 95% with the mutants S13A, S185A and S194A respectively. When $(Bu)_2$-cAMP was added to the incubation media, the activity of all preparations was increased. Increases observed for the mutants were comparable to that of WT except for mutants S185A and S194A (Fig.2B). Indeed, the increase in activity of these two mutants was 40% and 89% lower than that of stimulated WT. Interestingly, the $(Bu)_2$-cAMP stimulated activity of the mutant S13A was comparable to that of the WT. Compared to their own control, the presence of TPA in incubation media did not change StAR activity of any preparation (Fig.2C).

Fig.3 shows the effects of the double mutations S185A/S194A and S13A/S194A, and of the triple mutation S13A/S185A/S194A on StAR activity. The double mutant S185A/S194A and triple mutant S13A/S185A/S194A had practically no StAR activity, pregnenolone formed being similar to that of the empty pcDNA3.1 vector. Ctr-S13A StAR activity values were significantly different from Ctr-S194A values; Ctr-S194A values were significantly different from Ctr-S194A/S13A values; $(Bu)_2$-cAMP-S13A values were significantly ($p< 0.05$) different from $(Bu)_2$-cAMP-S194A values and $(Bu)_2$-cAMP-S194A values were significantly different from $(Bu)_2$-cAMP-S194A/S13A values. Compared to other preparations, the stimulated StAR activity levels of the mutants decreased in the following order: WT > S13A > S194A > S194A/S13A > S185A/S194A = S13A/S185A/S194A = pcDNA3.1. In this series of experiments, the presence of TPA in incubation media did not enhance StAR activity of WT or mutants (not shown).

We have further studied the implication of S194 amino acid residue on StAR activity after deleting the first 46 amino acid residues forming the N-terminal mitochondrial import leader sequence. For better immunoblotting analysis, 200 ng of StAR pcDNA3.1 plasmid were used in subsequent co-transfection experiments. Fig.4A shows that both full length and truncated StAR were expressed in transfected COS-1 cells. As expected, the truncated protein migrated faster on 1D-SDS-PAGE than its full-length counterpart. One main StAR band was revealed for the truncated protein in comparison of two for the full-length. The intensity of protein bands from the full-length S194A preparations was similar to that of its full-length control WT. Higher StAR levels were found for the full-length S194A and WT preparations when cells were stimulated by $(Bu)_2$-cAMP. Similarly the intensity of protein bands from the truncated N46-S194A preparations was similar to its control N46-WT. Higher StAR levels were found for the truncated N46-S194A and N46-WT preparations when cells were stimulated by $(Bu)_2$-cAMP, although the levels of StAR were once again similar in both preparations. The full-length and the truncated 'N46-WT' proteins had similar basal and $(Bu)_2$-cAMP stimulated activities respectively (Fig.4B). The basal activity of the full-length S194A mutant was significantly decreased compared to the full-length WT confirming results shown in preceding figures. In contrast, the N46-S194A mutant basal activity did not differ from that of the truncated N46-WT although its activity was only slightly increased by $(Bu)_2$-cAMP.

Fig.5A compares the levels of StAR expression between truncated N46-S185A, N46-S194A and N46-S185A/S194A; Fig.5B shows their relative StAR activities. Control experiments were also performed using full-length StAR cDNAs. The basal protein expression levels of the full-length WT and mutants preparations were similar and these were similarly increased with $(Bu)_2$-cAMP. Also, the basal protein expression levels of the truncated N46-WT and N46-mutants

preparations were increased with $(Bu)_2$-cAMP. Data obtained for StAR activity of full-length-WT and -mutant preparations confirm results shown in preceding figures. However, in contrast to the N46-S194A mutant, the basal activities of the N46-S185A and N46-S185A/S194A mutants were lower than the activity of their full-length counterparts. Dibutyryl-cAMP slightly but significantly increased the activity of the N46-S194A mutant (Fig.4B) and had no effect on the N46-S185A nor on the N46-S185A/S194A double mutant. These results indicate that both S185 and S194 amino acid residues are important for StAR activity although when mutated they appear to affect differently StAR activity.

Upon phosphorylation, StAR becomes more acidic generating species with different pI. Phosphorylated species can be separated on two-dimensional polyacrylamide gels (2D-PAGE) by first using isoelectrofocusing and then electrophoresis.

When proteins from whole COS-1 cells were analysed by 2D-PAGE and Western two main StAR immunoreactive bands were revealed for Ctr-WT cells with pI of 5.9 and 5.7 and migrating in the 30 kDa area (Fig.6A). These two bands are common to all other preparations shown on this figure. Other paler bands were also revealed as seen on the right of the figure. Almost identical patterns were observed when Ctr-StAR and mutated S13A, S185A and S194A preparations were analyzed (not shown).

The addition of $(Bu)_2$-cAMP to the incubation media however, resulted in the formation of many StAR species circled in black in Fig.6B. Among the mutant preparations S194A, S185A, S13A, it is the migration pattern of the S194A mutant that differed the most from WT. Empty circles show the location of the main low pI StAR species present in WT (Fig.6B) but absent in the S194A mutant (Fig.6C). An additional band pointed by an arrow was revealed for the S194A mutant (Fig.6C). Empty circles in panels D and E also show the location of bands revealed in

$(Bu)_2$-cAMP-WT and absent in S185A, S13A preparations. Furthermore three additional StAR species were revealed in the S13A preparation pointed by the three arrows.

Isolated mitochondria and supernatant preparations from transfected COS-1 cells with WT-StAR-pcDNA3.1 and stimulated with $(Bu)_2$-cAMP were analyzed by Western using an anti-StAR antibody. StAR was found nearly exclusively in mitochondria preparations (not shown). Therefore, in order to improve the resolution on 2D-PAGE, we have used StAR enriched mitochondria preparations to compare WT and mutant electrophoresis profiles. When mitochondria preparations were separated by 2D-PAGE and analyzed by immunoblotting, four StAR bands were revealed for the control-WT (Fig.7A). The two right protein bands migrated in the 33-34 kDa area, and for the two lower bands which have pI values of 5.9 and 5.4 respectively, migrated in the 29-30 kDa area. These two latter species indicated by arrows are common to all other preparations shown on this figure. Very similar patterns were observed when mutated StAR (S185A and S194A) was analyzed (not shown). However, the addition of $(Bu)_2$-cAMP to the incubation media of transfected cells resulted in the formation of many acidic StAR species as shown for the WT (Fig.7B). The migration pattern of the S194A mutant incubated with $(Bu)_2$-cAMP greatly differed from the WT. Empty circles show the location of the main low pI StAR species present in WT but absent in the S194A mutant (Fig.7C). In contrast, the migration pattern of the S185A mutant preparation stimulated by $(Bu)_2$-cAMP did not differ a great deal from WT although proteins appeared more clustered in the 33-34 kDa area (Fig.7D). Circles effectively show that absent protein bands for the S194A mutant are present in the S185A mutant preparation. The double mutation S185A/S194A lead to a migration pattern (Fig.7E) resembling that of the S194A mutant, also suggesting that the loss of acidic species

could be attributed to the S194A mutation. These results indicate that the mutation of serine 194 prevents the formation or entry of low pI StAR species into mitochondria.

Two-dimensional analyses were also performed on mitochondria preparations of StAR from transfected COS-1 cells incubated with TPA. In this situation, StAR activity was not increased in WT and mutant preparations as compared to their own control (Fig.2C). The electrophoretic patterns of TPA-WT, TPA-S185A and TPA-S194A mitochondria preparations (Fig8.B-D) were similar. However, the intensity of the four left StAR bands circled on panels B-D appeared stronger in TPA treated than in control samples. Moreover, an additional band was detected in the TPA treated samples when compared to control, as shown by the left-circled species in the B-D panels. These results indicate that TPA did not enhance the presence of StAR into mitochondria as much as did $(Bu)_2$-cAMP. They also indicate that TPA did not favor the formation or presence of low pI StAR species into mitochondria as did $(Bu)_2$-cAMP (see Fig.7B).

The hamster StAR amino acid residue S194 corresponds to the conserved S195 in human and Arakane *et al.* (26) have efficiently demonstrated that this amino acid residue was phosphorylated upon $(Bu)_2$-cAMP stimulation. Yet, nothing is known about the putative phosphorylation site S185 in the hamster, which is the equivalent to the conserved S186 in human. To confirm that the hamster S185 could effectively be phosphorylated, we have done three additional mutations. We have substituted the serine to the charged glutamic acid (E) or aspartic acid (D) residues in order to mimic phosphorylation. We have also substituted the serine into a cysteine (C), effectively replacing the serine OH group by a SH group. The SH group has similar properties to the OH group but cannot be phosphorylated. Compared to WT, S185E and S185D mutants had a decreased basal StAR activity similar to that of the S185A mutant

(Fig.9B). In addition, the activity of these two mutants was not stimulated by $(Bu)_2$-cAMP. In contrast to these, the substitution of S185 by a cysteine residue resulted in a partial recovery of basal StAR activity; this activity was stimulated by $(Bu)_2$-cAMP. As analyzed by Western, the basal and $(Bu)_2$-cAMP stimulated levels of StAR expression were not decreased by the mutations S185A, S185E, S185C (Fig.9A) and S185D (not shown). This indicates that the change in StAR activity by the mutants was due to the amino acid substitutions and not to differences in protein levels. These results also demonstrate that S185 is not a site of phosphorylation for the hamster StAR.

DISCUSSION

A strong homology exists between StAR amino acid sequences of the thirteen vertebrate species indexed in Table 1. We took advantage of the fact that many phosphorylation consensus sites were conserved among these species to elaborate a strategy to study putative StAR phosphorylation sites on the hamster StAR. In order to verify StAR activity alterations, we have used a previously validated StAR activity test model (37). In this series of experiments this test consisted in the measure of cholesterol conversion into pregnenolone by COS-1 cells co-transfected with expression plasmid F2 and pcDNA3.1-StAR. We have established (Fig.1) that a ratio StAR plasmid / F2 plamid in the range of 75-200ng / 500ng was suitable for the assay with or without $(Bu)_2$-cAMP stimulation. Furthermore, differences in StAR activity that we observed between Ctr-WT, $(Bu)_2$-cAMP-WT and TPA-WT preparations was not due to a difference in the level of P450scc-adrenodoxin reductase-adrenodoxin expression. Indeed, the expression levels of this protein complex, as analyzed by Western blotting using either an anti-P450scc antibody or

an anti-adrenodoxin antibody, were found similar under control and stimulated conditions (not shown), therefore showing that the cholesterol side chain cleavage system was not causing the changes in StAR activity under $(Bu)_2$-cAMP stimulation.

The basal activity of cells co-transfected with the empty pcDNA3.1 vector and F2 plasmid was not increased by the presence of $(Bu)_2$-cAMP indicating that a certain quantity of cholesterol was transformed into pregnenolone in the absence of StAR. This also indicates that $(Bu)_2$-cAMP alone did not act on the passive entry of cholesterol inside mitochondria. Bose *et al.* (6) have also mentioned StAR independent entry of cholesterol into mitochondria.

In this study, the three most important changes in StAR activity were induced by the mutations of S194, S185 and S13 (Fig.2) demonstrating the importance of these sites. On the other hand, differences in the inhibition intensity were noticeable between these three mutants. Mutation S194A affected the StAR activity the most, followed in a decreasing order by mutations S185A and S13A. Another difference is that $(Bu)_2$-cAMP was able to enhance the activity of S185A well above the WT basal activity whereas the stimulated activity of the S194A mutant remained under the WT basal activity (Figs 2-5). This shows the relative importance of these two amino acid residues on StAR activity.

The smaller but significant decrease (30%) in the basal activity of StAR induced by the mutation S13A suggests that this amino acid residue also plays a role in the mode of action of this protein. This role is emphasized by the fact that the double mutant S13A/S194A had significant ($p < 0.05$) lower basal and $(Bu)_2$-cAMP stimulated activity respectively than that of the mutant S194A. Yet, we cannot interpret the fact that no significant difference in activity was found between S13A mutant and WT StAR when $(Bu)_2$-cAMP was added to both incubation media. It is possible that other mechanisms overrule the importance of this site under acute

stimulation by $(Bu)_2$-cAMP. Another possibility is that experimental variations between samples is too large to obtain a significant decrease in StAR activity between $(Bu)_2$-cAMP stimulated S13A and WT preparations. The other putative phosphorylation sites tested involving T5, S55, S56, S60, S68, S90, T262 and S276 are not likely involved in StAR activity since removal of the putative phosphorylation sites of these amino acid residues did not affect StAR activity (Fig.2) nor their level of expression (not shown). In COS-1 cell transfection experiments in the presence of [γ-^{32}P] ATP, mutation of the human StAR serine residues 57 and 195 by alanine decreased ^{32}P incorporation into the molecule (26). The S195A mutation resulted in a decrease whereas mutation S57A had no effect on pregnenolone synthesis in transfected COS-1 cells. In agreement with these authors, mutation of the hamster StAR S56 corresponding to the human S57, had no effects, whereas mutation of the hamster StAR S194 corresponding to the human S195, decreased pregnenolone synthesis in transfected COS-1 cells.

Deleting the N-terminal first 46 amino acid residues including the mitochondrial import sequence resulted in the formation of only one main StAR band migrating on 1D-SDS-PAGE (Fig.4), having a molecular weight lower than the two main bands revealed for the full-length molecule preparation (in the 29 kDa vs 31 and 33-34 kDa regions). The calculated molecular weight of the full-length and the cleavage site products of the hamster StAR-Myc-His are 34 315, 29 979 and 29 265 Daltons respectively, which are close to our obtained experimental data. The fact that the truncated protein migrated faster than the second band of the full-length preparation could be due to the presence of two protease cleavage sites in the leader peptide of the hamster StAR (15), and that in COS-1 cells, StAR was presumably processed predominately at the first N-terminus proteolytic site between amino acids 38 and 39 of the full-length preparation.

The decrease in basal StAR activity of the S194A mutant was not due to a difference in the quantity of proteins since the intensity of StAR bands from the full-length Ctr-S194A preparations was similar to that the full-length Ctr-WT (see histograms, Figs 4A and 5A). Similarly, the quantities of proteins were comparably increased when both preparations were stimulated by $(Bu)_2$-cAMP. These results clearly indicate that the mutation *per se*, and not the protein expression level was the cause of the decrease in activity of the S194A mutant. The double mutation S185A/S194A completely abolished basal and $(Bu)_2$-cAMP stimulated StAR activity of the full-length and N46 truncated preparations (Fig.5) indicating that the protein had been considerably altered by these two modifications. Once again, under identical incubation conditions, the quantities of proteins were comparable between WT and mutated preparations confirming that activity changes were not due to differences in protein levels.

From the results of the N46-truncated proteins, we observed that the Ctr-'N46-WT' activity was equal to the full-length Ctr-WT (Figs.4B and 5B), both preparations being similarly stimulated by $(Bu)_2$-cAMP. This confirms that the presence of the mitochondrial import sequence is not mandatory for full StAR activity. Our results are in agreement with those of Arakane *et al.* (42) that show that recombinant StAR lacking the import sequence promoted steroid production in a cell-free system containing mitochondria.

Interestingly, the mutation S194A in the N46-truncated protein only lowered the basal StAR activity slightly compared to the great inhibition observed for its full-length counterpart (Fig.4B). Again, no difference in the quantity of proteins was found compared to their relative control. However, StAR activity of the N46-S194A was not stimulated much in the presence of $(Bu)_2$-cAMP although the quantity of immunoreactive proteins was doubled compared to its own control and was equal to that of the $(Bu)_2$-cAMP stimulated 'N46-WT'. These results confirm

again that an increased quantity of StAR *per se* is not sufficient to explain changes in StAR activity and also stresses the importance of an intact S194 amino acid residue for the development of full activity.

Then, how to explain that basal StAR activity of Ctr-N46-S194A is equal to that of the full-length Ctr-WT, and higher than that of the full-length Ctr-S194A? One explanation could be that the elimination of the first 46 amino acid residues would expose a StAR surface area favorable to the interaction of the molecule with the outer mitochondrion membrane and to the entry of cholesterol. Indeed, according to Tsujisita *et al.* (13) the START architecture appears well designed to bind and solubilize a lipid monolayer.

Therefore, one can speculate that the intact S194 residue in the full-length WT would serve at least two functions. One function of the phosphorylated S194 amino acid residue would be to overcome the rigidity conferred to the molecule by the presence of the mitochondrial import sequence under basal conditions. The second function of the phosphorylated S194 amino acid residue would be to favor the transfer of cholesterol into the mitochondrion. This is evidenced by the fact that, although equally expressed, the StAR activity of N46-S194 is lower than that of the 'N46-WT' (Fig.4A). It is possible that the S194 phosphorylation would produce conformational changes of the StAR molecule that could enhance cholesterol transfer into mitochondria.

Another possible mode of action of the phosphorylation of S194 could be through increasing StAR stability. Using Y1 cells and mutant Kin-8 cells lacking PKA expression, Clark *et al.* (43) proposed that phosphorylation of StAR by PKA might contribute to protein stability. Their conclusion was based on the fact that upon $(Bu)_2$-cAMP stimulation, increased StAR protein synthesis was observed for both cell types, but in contrast to Y1 cells, without a relative corresponding increase in steady state levels of StAR protein in Kin-8 cells. In this respect, the

increased StAR levels we observed when transfected cells were stimulated by $(Bu)_2$-cAMP (Figs 4A, 5A and 8A) could be due to an increased StAR stability since no general increase in total cell proteins was found (not shown) under these experimental conditions.

Using fluorescence energy transfer analysis, West *et al.* (30) reported that StAR and Peripheral-type Benzodiazepine Receptor (PBR) are closely associated in mitochondrial membranes and that these molecules may interact in the transportation of cholesterol. However, the interaction between StAR and PBR is yet to be definitely established and experiments performed up to now to demonstrate any interaction between StAR and mitochondrial membrane proteins have not been conclusive. In fact, Kallen *et al.* (44) demonstrated that StAR could promote cholesterol transfer to mitochondria in which the outer membrane proteins have been removed by partial proteolysis with trypsin. This suggests that StAR does not have protein binding partners on the outer mitochondrial membrane and can instead interact directly with membrane phospholipids.

Another interesting observation is that the full-length S185A mutant could be stimulated by $(Bu)_2$-cAMP but not its N46-truncated counterpart. This suggests that StAR was dramatically altered by the mutation S185A in the absence of the mitochondrial import sequence in a way that the mutant activity could not be even partially rescued by phosphorylation of S194.

StAR becomes more acidic upon phosphorylation giving rise to species with different pI which can be separated by 2D-PAGE and revealed by immunoblotting. The 2D-profiles did not differ much between unstimulated WT and mutants S13A, S185A and S194A using either whole COS-1 cell proteins or isolated mitochondrial preparations. Under $(Bu)_2$-cAMP stimulation however, many StAR species were revealed on immunoblots (Figs 6 and 7). These results are in agreement with those of Kim Y-C *et al.* (45) who identified eight StAR species migrating in the

28 and 30 kDa region in bovine adrenal cell mitochondrial preparations upon hormonal stimulation. Similarly, many species were also revealed in mitochondrial preparations of rats injected with ACTH (18).

The 2D-profiles of WT and S194A preparations differed in many aspects under $(Bu)_2$-cAMP stimulation. Many acidic species were missing in the S194A (Figs 6 and 7) suggesting that less phosphorylation had occurred in these preparations compared to WT. Fig.6E demonstrates that mutation of S13 could affect the 2D-migration pattern of StAR: two species present in WT being absent in the mutant and three new species being generated. It thus appears that S13 could be involved somehow in the control of StAR action through phosphorylation.

Surprisingly the 2D-profile of the $(Bu)_2$-cAMP stimulated mutant S185A, which greatly affected StAR activity, did not differ much from that of the WT. Most of the low pI species were revealed in both preparations (Fig.7C vs. Fig.7B). This result indicates that the mutation S185A affected StAR activity by another mean than phosphorylation. Indeed, in subsequent experiments, we have demonstrated that the decreased activity of the mutant S185A was not due to a blockage of phosphorylation at this position. Substituting the amino acid S185 by either glutamic acid or aspartic acid in order to mimic the presence of a negatively charged group on S185 resulted in no increase, but rather a decrease in StAR activity. Moreover, substitution of S185 by a cysteine residue, to replace the serine OH group by a SH group having similar characteristics, nearly fully restored basal and $(Bu)_2$-cAMP stimulated activities (Fig.9B). These results thus clearly showed that S185 is not a phosphorylation site.

If S185 is not a site of phosphorylation for the hamster StAR, then how can we explain that mutating this serine inhibited StAR activity? One explanation could be that mutations of S185 created StAR conformational changes resulting in a decrease in its binding affinity for

cholesterol. This explanation is based on the fact that the activity of non-stimulated WT differs from that of the S185A mutant although they were expressed at similar levels. This is reinforced by the observation that although the $(Bu)_2$-cAMP stimulated WT and S185A mutant were similarly expressed and similarly processed by the mitochondrial machinery, the mutant activity remained much lower than the WT. Moreover the activity of the WT was comparable to S185C, a mild mutation created by the substitution of an OH by a SH group suggesting that only a small conformation change had occurred. The conformation change produced by the mutations S185D and S185E however, should have been more drastic to result in the complete abolition of basal as well as $(Bu)_2$-cAMP stimulated activity.

To fully comprehend the effect of the mutations on the hamster StAR, we have constructed a molecular model for the hamster StAR. This model was elaborated according to crystallographic data of the human protein MLN64 (13). MLN64 possesses a StAR related lipid transfer (START) domain found in StAR and in other proteins (46).

The details of the hamster StAR modeling are given in an article by Axel Mathieu *et al.* (47). Coordinates of the hamster StAR model are available at http://www.rcsb.org, PDB ID number 1ILJ. Briefly, the generated StAR model was very similar to the MLN64 model issued from crystallographic data. Like MLN64, the StAR model shows nine antiparallel β-sheet and four α-helices. Unlike the MLN64 crystallographic data, our model has a hydrophobic pocket instead of a hydrophobic tunnel. This tunnel was proposed to be the site of cholesterol binding in MLN64 (13). According to the graphic model, the hamster StAR serine 194 is located to the exterior of the molecule and thus accessible to kinases. As mentioned earlier the hamster StAR amino acid residue S194 corresponds to the conserved S195 in human and Arakane *et al.* (26) have demonstrated well that this amino acid residue was phosphorylated upon $(Bu)_2$-cAMP stimulation.

In contrast, S185 is hidden inside the protein and consequently is not accessible to kinases (Fig.10). However, S185 is located near a saline bridge formed by amino acid residues glutamic acid (E) 168 and arginine (R) 187. It is possible that this salt bridge is involved in the mechanism of cholesterol movement since it is the only hydrophilic component of the cholesterol-binding site. This suggests that mutating S185, especially in the case of S185D and S185E, could have resulted in a perturbation of the saline bridge environment, which would explain the inhibition of StAR activity.

TPA did not induce any changes in StAR activity (Fig.2C) and did not favor the formation or presence of StAR low pI species in mitochondria as did $(Bu)_2$-cAMP (Fig.8B). This indicates that under the experimental conditions used, the protein kinase C pathway was not involved in controlling StAR activity in COS-1 cells. It is also possible that PKC isoforms necessary for StAR phosphorylation may not be expressed in COS-1 cells. Indeed in bovine adrenal glomerulosa cells, the PKC signaling pathway was effective in inducing StAR phosphorylation (48). Similarly, we have found an enhanced StAR expression *in vivo* in the adrenal zona glomerulosa of rats fed a low sodium diet (18) which increases angiotensin II (14). The inhibitor TPA was also shown to increase the expression of StAR in NCI-H295 cells (49). More work will thus be necessary to clarify the real role played by PKC if any in controlling StAR activity.

In conclusion, we have found that in the hamster StAR, the serine amino acid residue 194 available to kinases is the most important site of phosphorylation supporting StAR activity. The serine residue 13 appears to play a minor role in maintaining basal StAR activity. We also found that mutations of amino acid serine 185, replacing serine by aspartic acid or glutamic acid, are most likely to produce perturbations at a nearby salt bridge formed by amino acid residue glutamic acid 168 and arginine 187.

ACKNOWLEDGEMENTS

F2 plasmid was a generous gift from Dr. Walter L Miller, University of California at San Francisco. We would like to acknowledge Dr. Pierre Lavigne for his valuable insight on the StAR modeling.

REFERENCES

1. Clark, B. J., Wells, J., King, S. R., and Stocco, D. M. (1994) *Journal of Biological Chemistry* **269,** 28314-28322

2. Epstein, L. F. and Orme-Johnson, N. R. (1991) *Journal of Biological Chemistry* **266,** 19739-19745

3. Privalle, C. T., Crivello, J. F., and Jefcoate, C. R. (1983) *Proceedings of the National Academy of Sciences of the United States of America* **80,** 702-706

4. Lin, D., Sugawara, T., Strauss, J. F., III, Clark, B. J., Stocco, D. M., Saenger, P., Rogol, A., and Miller, W. L. (1995) *Science* **267,** 1828-1831

5. Tee, M. K., Lin, D., Sugawara, T., Holt, J. A., Guiguen, Y., Buckingham, B., Strauss, J. F., and Miller, W. L. (1995) *Human Molecular Genetics* **4,** 2299-2305

6. Bose, H. S., Sugawara, T., Strauss, J. F., and Miller, W. L. (1996) *New England Journal of Medicine* **335,** 1870-1878

7. Nakae, J., Tajima, T., Sugawara, T., Arakane, F., Hanaki, K., Hotsubo, T., Igarashi, N., Igarashi, Y., Ishii, T., Koda, N., Kondo, T., Kohno, H., Nakagawa, Y., Tachibana, K.,

Takeshima, Y., Tsubouchi, K., Strauss, J. F., III, and Fujieda, K. (1997) *Human Molecular Genetics* **6,** 571-576

8. Bose, H. S., Pescovitz, O. H., and Miller, W. L. (1997) *Journal of Clinical Endocrinology & Metabolism* **82,** 1511-1515

9. Fujieda, K., Tajima, T., Nakae, J., Sageshima, S., Tachibana, K., Suwa, S., Sugawara, T., and Strauss, J. F., III (1997) *Journal of Clinical Investigation* **99,** 1265-1271

10. Caron, K. M., Soo, S. C., Wetsel, W. C., Stocco, D. M., Clark, B. J., and Parker, K. L. (1997) *Proceedings of the National Academy of Sciences of the United States of America* **94,** 11540-11545

11. Stocco, D. M. and Clark, B. J. (1996) *Endocrine Reviews* **17,** 221-244

12. Bose, H. S., Whittal, R. M., Baldwin, M. A., and Miller, W. L. (1999) *Proceedings of the National Academy of Sciences of the United States of America* **96,** 7250-7255

13. Tsujishita, Y. and Hurley, J. H. (2000) *Nature Structural Biology* **7,** 408-414

14. LeHoux, J. G., Bernard, H., Ducharme, L., Lefebvre, A., Shapcott, D., Tremblay, A., and Véronneau, S. (1996) The regulation of the formation of glucocorticoids and mineralocorticoids *in vivo* . In Jefcoate, C. R., editor. *Advances in Molecular and Cell Biology*, JAI Press Inc., London, England

15. Fleury, A., Ducharme, L., and LeHoux, J. G. (1998) *Journal of Molecular Endocrinology* **21,** 131-139

16. Fleury, A., Ducharme, L., Hales, D. B., Stocco, D. M., and LeHoux, J. G. (1998) *Endocrine Research* **24,** 571-574

17. LeHoux, J. G., Fleury, A., and Ducharme, L. (1998) *Endocrinology* **139,** 3913-3922

18. LeHoux, J. G., Hales, D. B., Fleury, A., Briere, N., Martel, D., and Ducharme, L. (1999) *Endocrinology* **140,** 5154-5164

19. Pon, L. A. and Orme-Johnson, N. R. (1988) *Endocrinology* **123,** 1942-1948

20. Pon, L. A., Epstein, L. F., and Orme-Johnson, N. R. (1986) *Endocrine Research* **12,** 429-446

21. Pon, L. A., Hartigan, J. A., and Orme-Johnson, N. R. (1986) *Journal of Biological Chemistry* **261,** 13309-13316

22. Pon, L. A. and Orme-Johnson, N. R. (1986) *Journal of Biological Chemistry* **261,** 6594-6599

23. Krueger, R. J. and Orme-Johnson, N. R. (1988) *Endocrinology* **122,** 1869-1875

24. Alberta, J. A., Epstein, L. F., Pon, L. A., and Orme-Johnson, N. R. (1989) *Journal of Biological Chemistry* **264,** 2368-2372

25. Epstein, L. F. and Orme-Johnson, N. R. (1991) *Molecular & Cellular Endocrinology* **81,** 113-126

26. Arakane, F., King, S. R., Du, Y., Kallen, C. B., Walsh, L. P., Watari, H., Stocco, D. M., and Strauss, J. F., III (1997) *Journal of Biological Chemistry* **272,** 32656-32662

27. Sugawara, T., Holt, J. A., Driscoll, D., Strauss, J. F., III, Lin, D., Miller, W. L., Patterson, D., Clancy, K. P., Hart, I. M., and Clark, B. J. (1995) *Proceedings of the National Academy of Sciences of the United States of America* **92,** 4778-4782

28. Kerban, A., Boerboom, D., and Sirois, J. (1999) *Endocrinology* **140,** 667-674

29. Pilon, N., Daneau, I., Brisson, C., Ethier, J. F., Lussier, J. G., and Silversides, D. W. (1997) *Endocrinology* **138,** 1085-1091

30. West, L. A., Horvat, R. D., Roess, D. A., Barisas, B. G., Juengel, J. L., and Niswender, G. D. (2001) *Endocrinology* **142,** 502-505

31. Rust, W., Stedronsky, K., Tillmann, G., Morley, S., Walther, N., and Ivell, R. (1998) *Journal of Molecular Endocrinology* **21,** 189-200

32. Ariyoshi, N., Kim, Y. C., Artemenko, I., Bhattacharyya, K. K., and Jefcoate, C. R. (1998) *Journal of Biological Chemistry* **273,** 7610-7619

33. Bauer, M. P., Bridgham, J. T., Langenau, D. M., Johnson, A. L., and Goetz, F. W. (2000) *Molecular & Cellular Endocrinology* **168,** 119-125

34. Todo, T., Kusakabe, M., McQuillan, J., and Young, G. Molecular cloning of steroidogenic acute regulatory (StAR) protein cDNA from rainbow trout. 2000. Ref Type: Unpublished Work

35. Goetz, F. W. Characterization of the brook trout StAR and MLN64 homologs. 2000. Ref Type: Unpublished Work

36. Dulau, L., Cheyrou, A., Dubourdieu, D., and Aigle, M. (1989) *Nucleic Acids Research* **17,** 2873

37. Harikrishna, J. A., Black, S. M., Szklarz, G. D., and Miller, W. L. (1993) *DNA & Cell Biology* **12,** 371-379

38. Laemmli, U. K. (1970) *Nature* **227,** 680-685

39. LeHoux, J. G., Mason, J. I., and Ducharme, L. (1992) *Endocrinology* **131,** 1874-1882

40. LeHoux, J. G., Lefebvre, A., Ducharme, L., Lehoux, J., Martel, D., and Briere, N. (1996) *Journal of Endocrinology* **149,** 341-349

41. Clark, B. J., Combs, R., Hales, K. H., Hales, D. B., and Stocco, D. M. (1997) *Endocrinology* **138,** 4893-4901

42. Arakane, F., Kallen, C. B., Watari, H., Foster, J. A., Sepuri, N. B., Pain, D., Stayrook, S. E., Lewis, M., Gerton, G. L., and Strauss, J. F., III (1998) *Journal of Biological Chemistry* **273,** 16339-16345

43. Clark, B. J., Ranganathan, V., and Combs, R. (2000) *Endocrine Research* **26,** 681-689

44. Kallen, C. B., Billheimer, J. T., Summers, S. A., Stayrook, S. E., Lewis, M., and Strauss, J. F., III (1998) *Journal of Biological Chemistry* **273,** 26285-26288

45. Kim, Y. C., Ariyoshi, N., Artemenko, I., Elliott, M. E., Bhattacharyya, K. K., and Jefcoate, C. R. (1997) *Steroids* **62,** 10-20

46. Ponting, C. P. and Aravind, L. (1999) *Trends in Biochemical Sciences* **24,** 130-132

47. Mathieu, A. P., Fleury, A., Ducharme, L., Lavigne, P., and LeHoux, J. G. Molecular Modeling of the Human and Hamster Adrenal Steroidogenic Acute Regulatory (StAR) Protein: Insight on cholesterol Transfer Into Mitochondria. 2001.

48. Betancourt-Calle, S., Calle, R. A., Isales, C. M., White, S., Rasmussen, H., and Bollag, W. B. (2001) *Molecular & Cellular Endocrinology* **173,** 87-94 .

49. Clark, B. J., Pezzi, V., Stocco, D. M., and Rainey, W. E. (1995) *Molecular & Cellular Endocrinology* **115,** 215-219

[1]The abbreviations used are: StAR, Steroidogenic Acute Regulatory Protein; $(Bu)_2$-cAMP, Dibutyryl cAMP; TPA, 12-O-Tetradecanoylphorbol 13-acetate; SDS-PAGE, sodium dodecyl sulfate-polyacrylamide gel electrophoresis; P450scc, cytochrome P450 side chain cleavage; A, alanine; S, serine; D, aspartic acid; E, glutamic acid.

FIGURE LEGENDS

FIG. 1 COS-1 cells co-transfected with the F2 construct (500 ng) and increasing concentrations of WT StAR-pcDNA3.1 and pcDNA3.1 (to a total of 1000 ng of DNA), were incubated without (Ctr) or with $(Bu)_2$-cAMP (cAMP) (1 mM) for 24 hours. Pregnenolone was analyzed by RIA. Results are mean ± SD of values obtained from three different preparations performed in triplicate.

FIG. 2 COS-1 cells co-transfected with the F2 plasmid (500 ng), different StAR-pcDNA3.1 plasmids (75 ng) and pcDNA3.1 (425 ng), were incubated without or with $(Bu)_2$-cAMP (cAMP) (1 mM) or TPA (32 nM) for 24 hours. A) Basal StAR activity. B) The Ctr-WT was incubated without $(Bu)_2$-cAMP. C) Ctr values are the same as in panel A. Results are mean ± SEM of three different experiments performed in triplicate, except for TPA where the values are the mean of two experiments performed in triplicate. In this series of experiments, pcDNA3.1 values were subtracted to other preparation values. A:*$p < 0.05$ compared to Ctr-WT; B:*$p < 0.05$ compared to $(Bu)_2$-cAMP stimulated WT.

FIG. 3 COS-1 cells co-transfected with the F2 construct (500 ng), different StAR-pcDNA3.1 plasmids (75 ng) and pcDNA3.1 (425 ng), were incubated without (Ctr) or with $(Bu)_2$-cAMP (cAMP) (1 mM) for 24 hours. Values are the mean ± SEM obtained from three different experiments performed in triplicate using three different plasmid preparations. In this series of experiments, pcDNA3.1 values were subtracted to other preparation values. Interestingly, Ctr-S13A StAR activity values were significantly ($p < 0.05$) different from Ctr-S194A values, Ctr-S194A values were significantly different from Ctr-S194A/S13A values, $(Bu)_2$-cAMP-S13A values were significantly different from $(Bu)_2$-cAMP-S194A values and $(Bu)_2$-cAMP-S194A values were significantly different from $(Bu)_2$-cAMP-S194A/S13A values.

FIG.4 COS-1 cells co-transfected with the F2 construct (500 ng), different StAR-pcDNA3.1 plasmids (200 ng) and pcDNA3.1 (300 ng), were incubated without or with $(Bu)_2$-cAMP (cAMP) (1 mM) for 24 hours. A) Immunoblotting analysis is from three different preparations performed in duplicate. Twenty μg of proteins from total COS-1 cell were used in each lane. B)

Relative StAR activity, mean ± SEM of seven different experiments performed in triplicate. *p < 0.05 compared to Ctr-WT.

FIG.5 COS-1 cells co-transfected with the F2 construct (500 ng), different StAR-pcDNA3.1 plasmids (200 ng) and pcDNA3.1 (300 ng), were incubated without or with $(Bu)_2$-cAMP (cAMP) (1 mM) for 24 hours. A) Immunoblotting analysis of three different plasmid preparations. Twenty μg of total COS-1 cell proteins were used in each lane. C = Ctr; A = $(Bu)_2$-cAMP. B) Relative StAR activity compared to Ctr-WT. Values are the mean ± SD obtained from three different plasmid preparations performed in triplicate.

FIG.6 COS-1 cells co-transfected with F2 construct (500 ng), different StAR-pcDNA3.1 plasmids (75) and pcDNA3.1 (425 ng), were incubated without or with $(Bu)_2$-cAMP (cAMP) (1 mM) for 24 hours. One hundred μg total COS-1 cell proteins of each preparation were separated on 2D-polyacrylamide gels, first by electrofocusing and then electrophoresis. Proteins were then transferred on membranes and revealed by an anti-StAR antibody.

FIG. 7 COS-1 cells co-transfected with the F2 construct (500 ng), different StAR-pcDNA3.1 plasmids (200 ng) and pcDNA3.1 (300 ng), were incubated without or with $(Bu)_2$-cAMP (cAMP) (1 mM) for 24 hours. Fifty μg mitochondrial proteins of each preparation were separated on 2D-polyacrylamide gels first by electrofocusing and then electrophoresis. Proteins were then transferred on membranes and revealed by an anti-StAR antibody.

FIG. 8 COS-1 cells co-transfected with the F2 construct (500 ng), different StAR-pcDNA3.1 plasmids (200 ng) and pcDNA3.1 (300 ng), were incubated without or with TPA (32nM) for 24 hours. Fifty μg mitochondrial proteins of each preparation were separated on 2D-polyacrylamide gels first by electrofocusing and then electrophoresis. Proteins were then transferred on membranes and revealed by an anti-StAR antibody. Ctr-Wt values are the same as in Fig.7A).

FIG. 9 COS-1 cells co-transfected with the F2 construct (500 ng), different StAR-pcDNA3.1 plasmids (200 ng) and pcDNA3.1 (300 ng), were incubated without or with $(Bu)_2$-cAMP (cAMP) (1 mM) for 24 hours. A) Immunoblotting was done in duplicate on three different total COS-1 cell preparations (20 μg proteins) using an anti-StAR antibody. B) Relative StAR activity. Values are the mean ± SEM of three different experiments performed in triplicate. *$p < 0.05$ compared to Ctr-WT.

FIG.10 Localization of serine 185 and serine 194 on the hamster StAR molecular model. Alpha-helices in red, β-sheets in blue, loops in white, and S185 and S194 in pink and yellow respectively. Left: the model is shown as a ribbon diagram with S185 and S194 as wireframes. Right: same representation as on the left, but as an accessible surface diagram. S194 is clearly accessible for kinases, yet S185 is not.

TABLE I

Putative phosphorylation sites in StAR from various animal species

StAR sequences were obtained from Genbank and aligned by Clustal method using Lasergene software from DNASTAR Inc. Madison WI. Putative phosphorylation sites were determined using PhosphoBase v2.0, a database of phosphorylation sites provided by Center for Biological Sequence Analysis at the Technical University of Denmark (http://www.cbs.dtu.dk/databases/PhosphoBase). PKA, protein kinase A; PKC, protein kinase C; CK2, casein kinase II; -, absence and +, presence of a phosphorylation consensus sequence.

Position	T5	S13	S55 / S56	S56 / S57	S60 / S61	S68 / S69	S90 / S91	S185/ S186	S194 / S195	T262/ T263	S276/ S277
Kinase	**PKC**	**PKC**	**PKA**	**PKA**	**CK2**	**CK2**	**CK2**	**PKC**	**PKA**	**CK2**	**PKA**
Hamster	+	+	+	+	+	+	+	+	+	+	+
Mouse	+	+	+	+	+	+	-	+	+	+	-
Rat	+	+	+	+	+	+	-	+	+	+	+
Human	+	+	+	+	+	+	+	+	+	+	+
Porcine	+	+	+	+	+	+	+	-	+	+	+
Bovine	+	+	-	+	+	+	-	+	+	+	+
Ovine	+	+	-	+	+	+	-	+	+	+	+
Horse	+	+	+	+	+	+	-	+	+	+	+
Chicken	+	-	+	+	+	+	-	+	+	+	-
Frog	+	+	-	+	+	-	-	+	+	+	+
Rainbow Trout	+	+	+	-	+	-	-	+	+	+	-
Brook Trout	+	+	+	+	-	-	-	+	+	+	-
Zebra Fish	+	+	+	-	-	-	-	-	T194	-	-

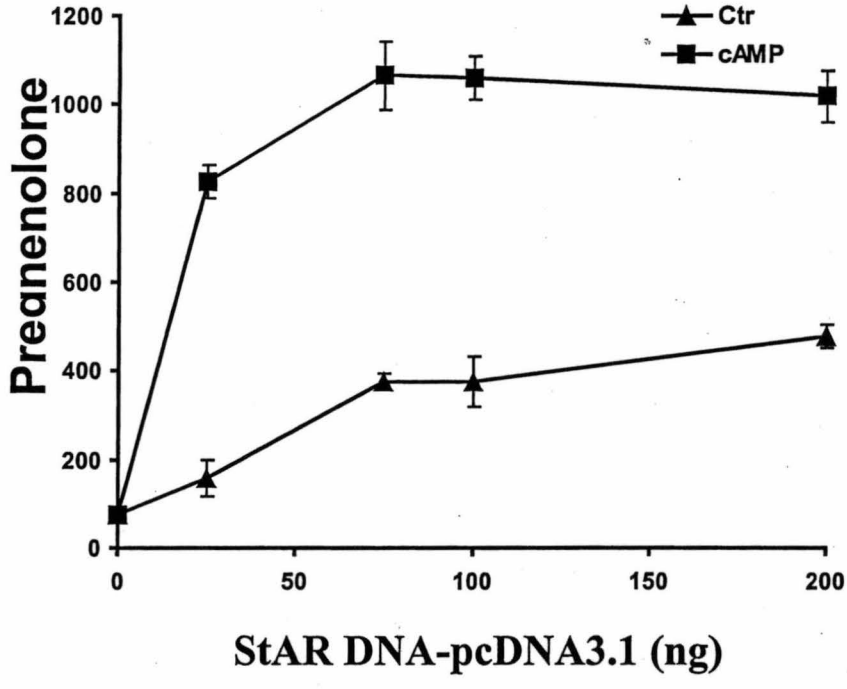
Ctr
cAMP
Preanenolone
1200
1000
800
600
400
200
0
0
50
100
150
200
StAR DNA-pcDNA3.1 (ng)

Fig.1

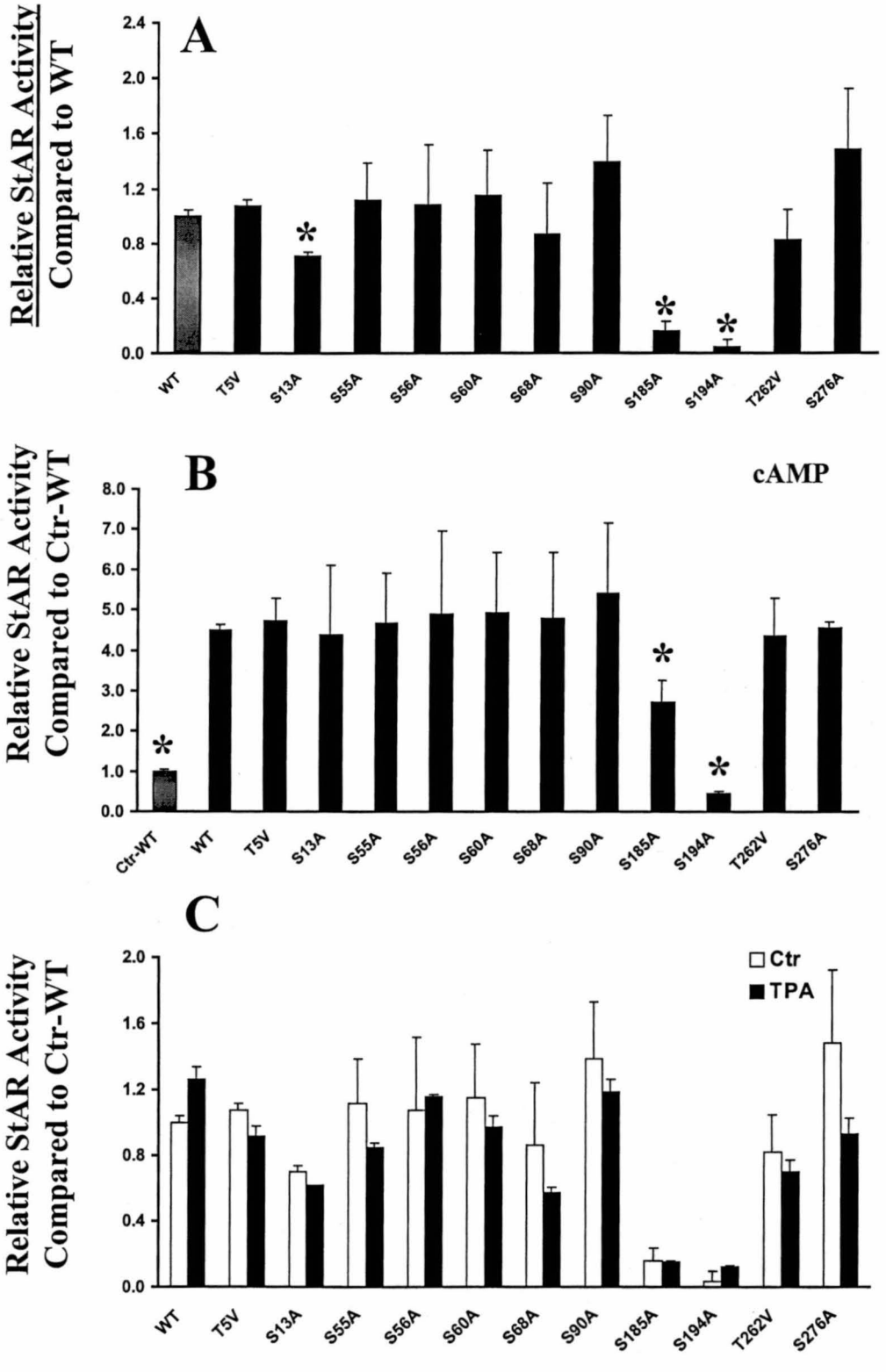
A
Relative StAR Activity
Compared to WT
2.4
2.0
1.6
1.2
0.8
0.4
0.0
WT
T5V
S13A
S55A
S56A
S60A
S68A
S90A
S185A
S194A
T262V
S276A
B
cAMP
Relative StAR Activity
Compared to Ctr-WT
8.0
7.0
6.0
5.0
4.0
3.0
2.0
1.0
0.0
Ctr-WT
WT
T5V
S13A
S55A
S56A
S60A
S68A
S90A
S185A
S194A
T262V
S276A
C
Ctr
TPA
Relative StAR Activity
Compared to Ctr-WT
2.0
1.6
1.2
0.8
0.4
0.0
WT
T5V
S13A
S55A
S56A
S60A
S68A
S90A
S185A
S194A
T262V
S276A

Fig.2

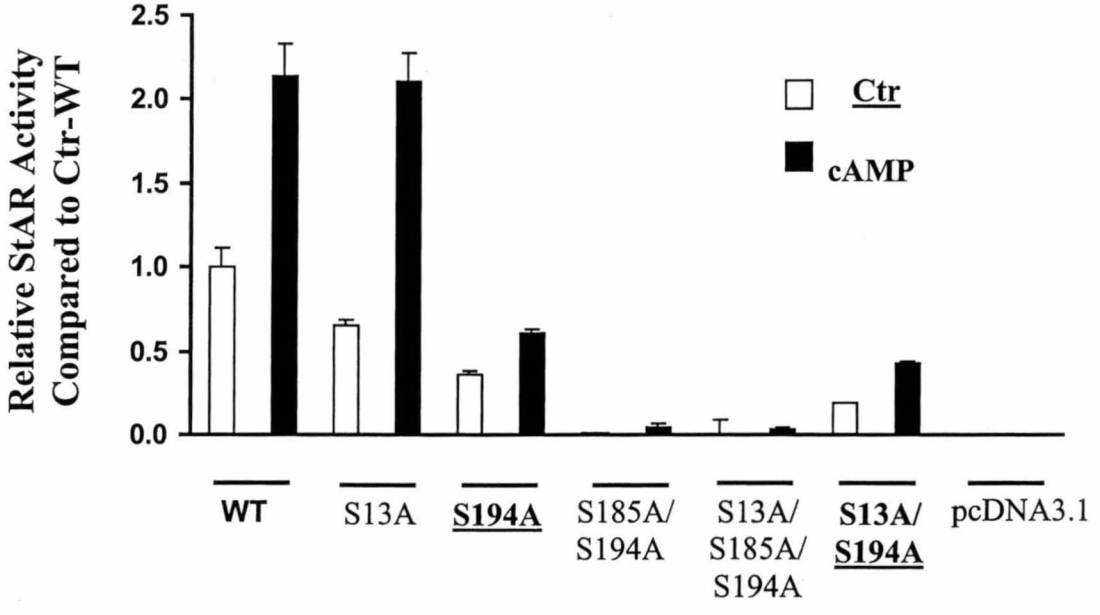
Relative StAR Activity
Compared to Ctr-WT
2.5
2.0
1.5
1.0
0.5
0.0
Ctr
cAMP
WT
S13A
S194A
S185A/
S194A
S13A/
S185A/
S194A
S13A/
S194A
pcDNA3.1

Fig.3

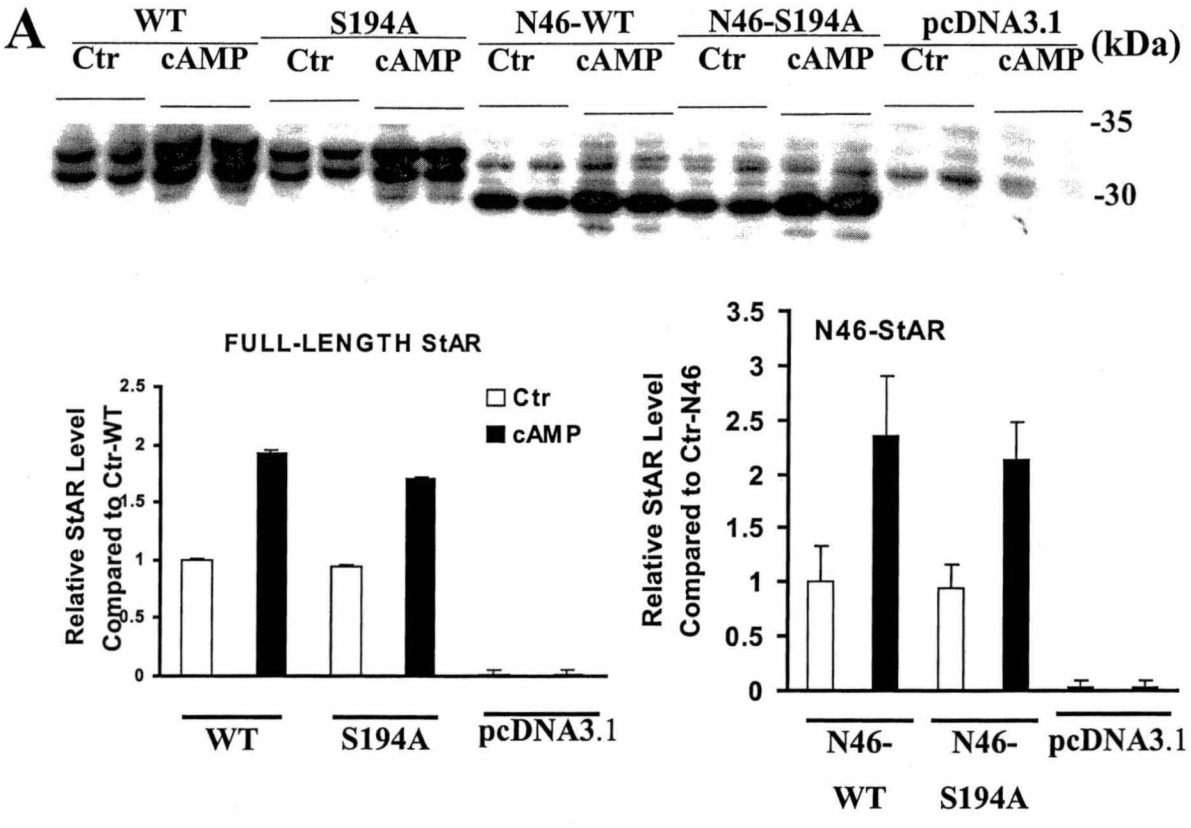
A
WT
S194A
N46-WT
N46-S194A
pcDNA3.1
Ctr
cAMP
(kDa)
-35
-30
FULL-LENGTH StAR
Relative StAR Level
Compared to Ctr-WT
Ctr
cAMP
WT
S194A
pcDNA3.1
N46-StAR
Relative StAR Level
Compared to Ctr-N46
N46-WT
N46-S194A
pcDNA3.1

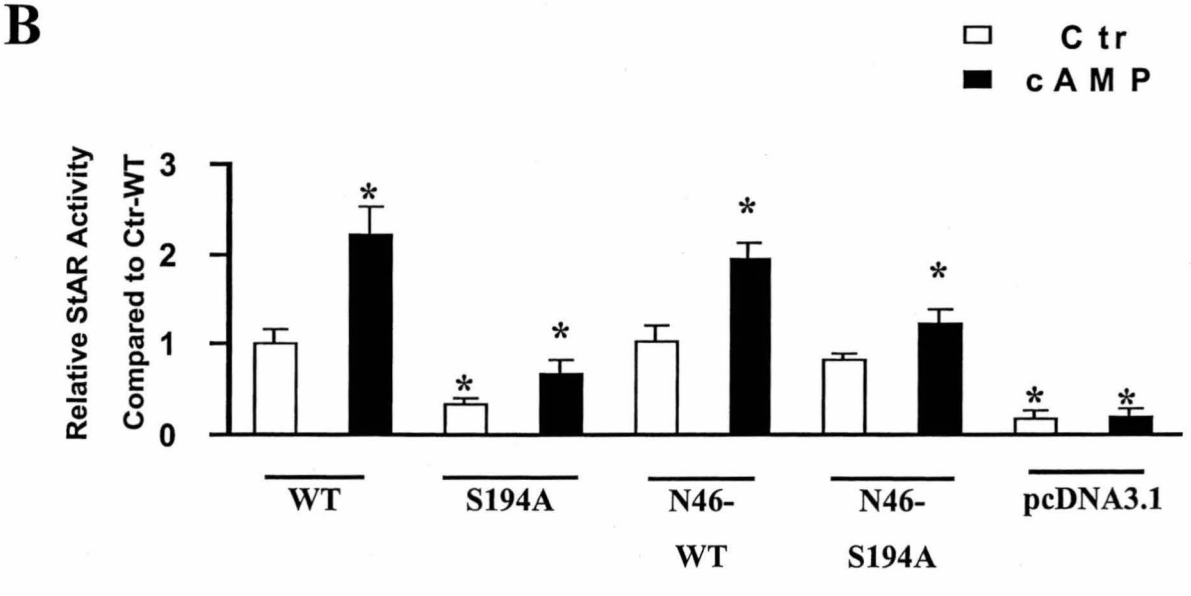
B
Ctr
cAMP
Relative StAR Activity
Compared to Ctr-WT
WT
S194A
N46-WT
N46-S194A
pcDNA3.1

Fig.4

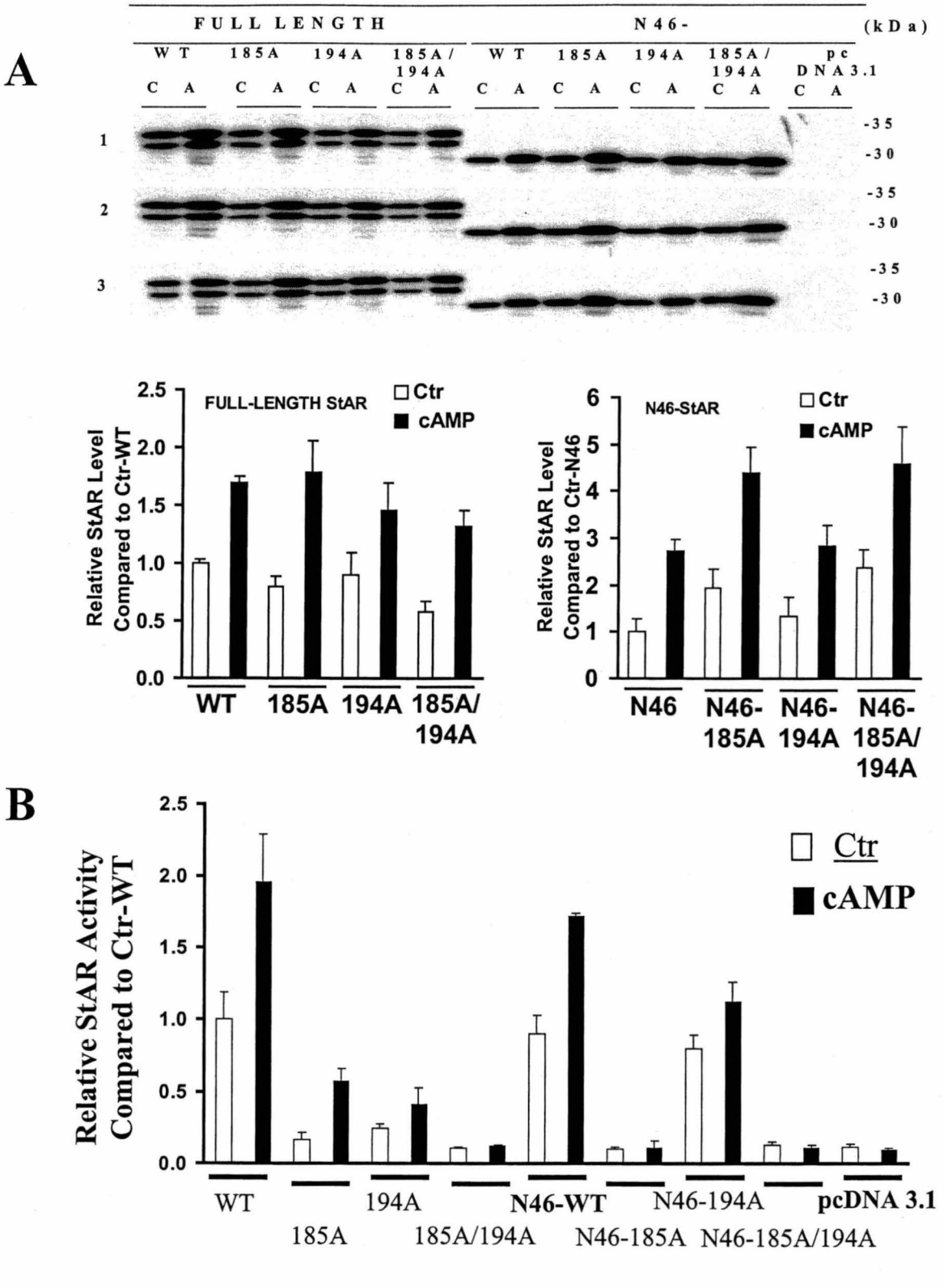
A
FULL LENGTH
N46-
(kDa)
WT 185A 194A 185A/194A
pcDNA3.1
C A C A C A C A C A C A C A C A C A
1
2
3
-35
-30
-35
-30
-35
-30
FULL-LENGTH StAR
Ctr
cAMP
Relative StAR Level Compared to Ctr-WT
WT 185A 194A 185A/194A
N46-StAR
Relative StAR Level Compared to Ctr-N46
N46 N46-185A N46-194A N46-185A/194A
B
Relative StAR Activity Compared to Ctr-WT
WT
185A
194A
185A/194A
N46-WT
N46-185A
N46-194A
N46-185A/194A
pcDNA 3.1

Fig.5

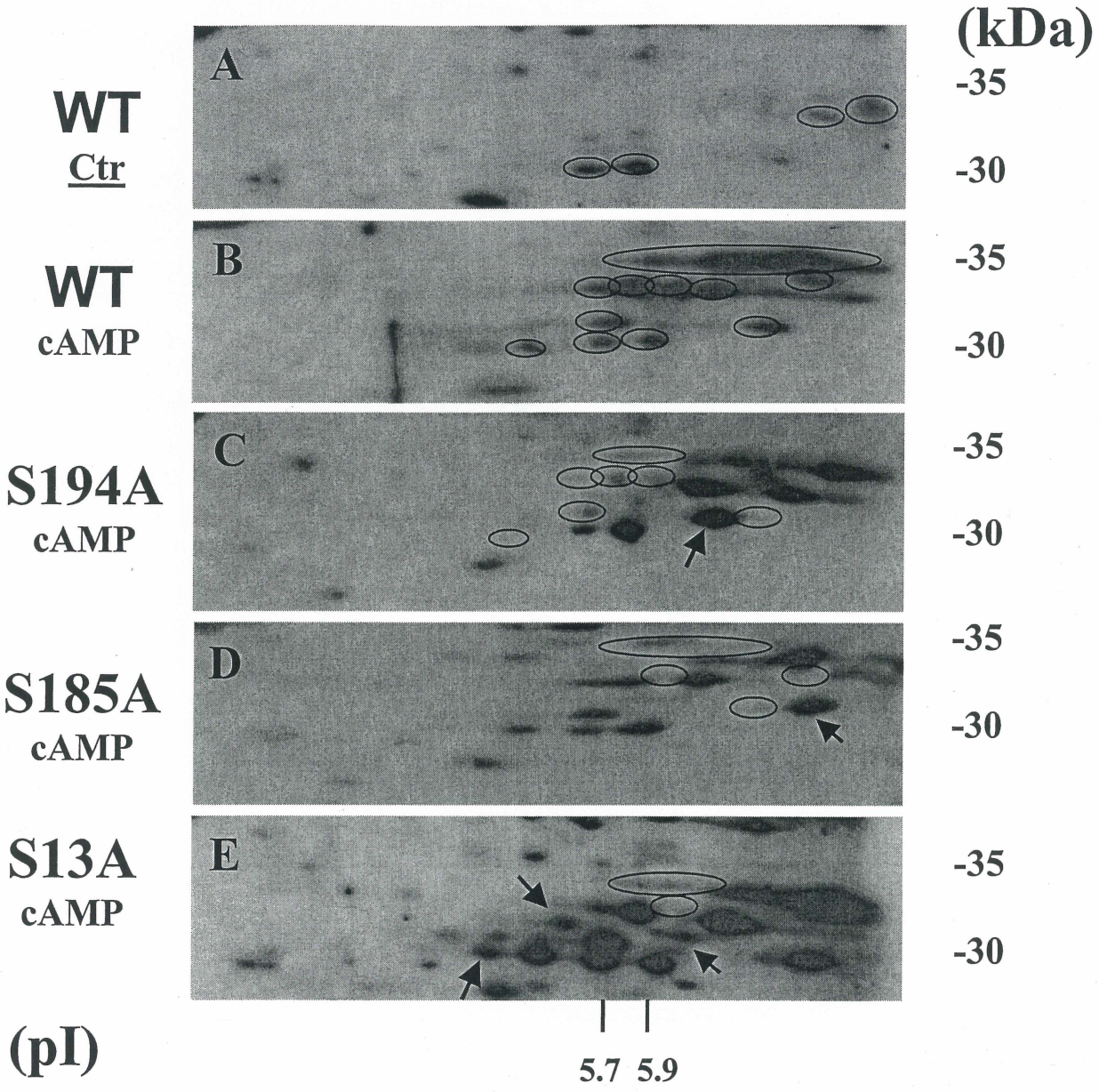
(kDa)
WT
Ctr
A
-35
-30
WT
cAMP
B
-35
-30
S194A
cAMP
C
-35
-30
S185A
cAMP
D
-35
-30
S13A
cAMP
E
-35
-30
(pI)
5.7
5.9

Fig.6

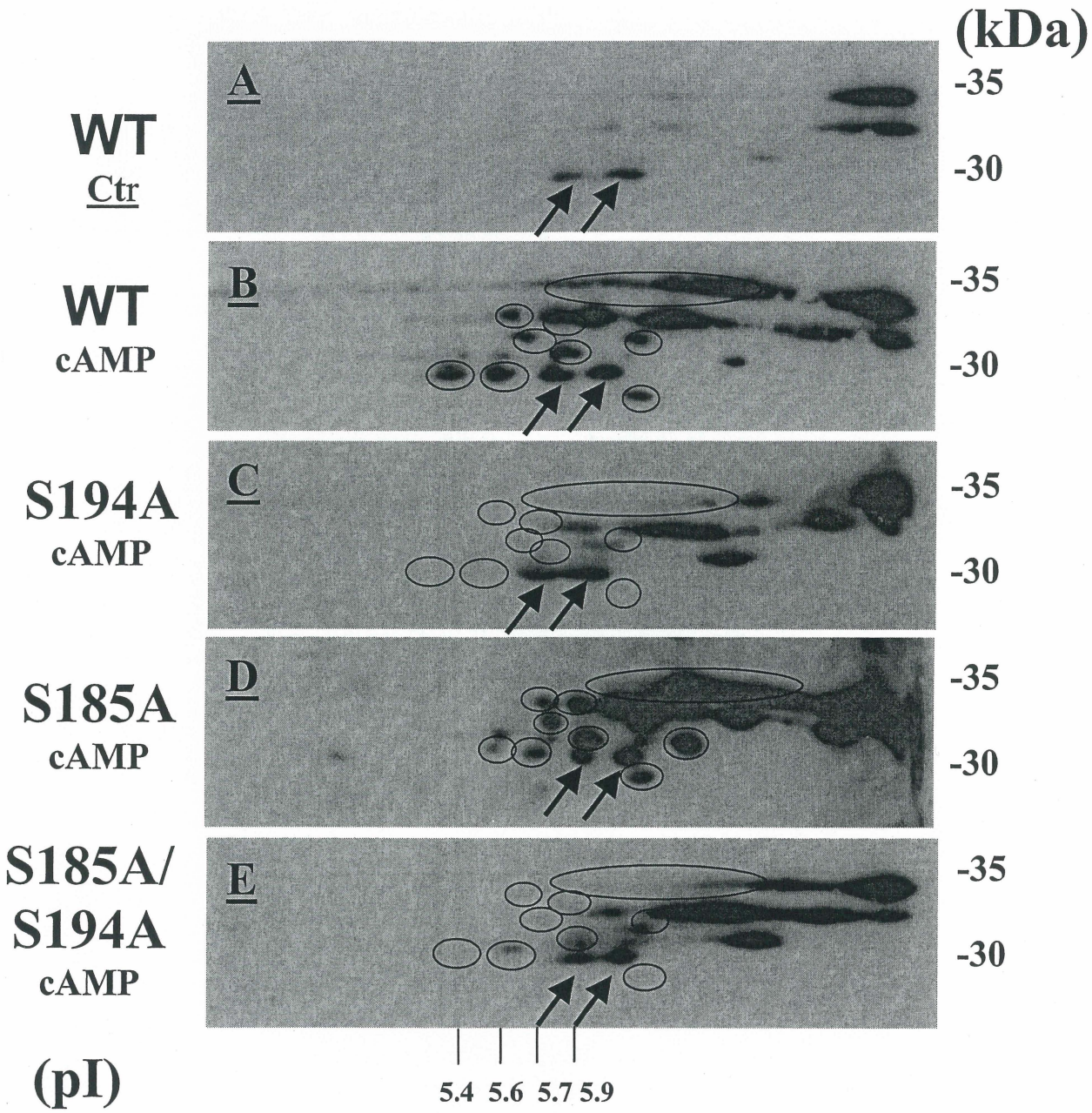
(kDa)
A
WT
Ctr
-35
-30
B
WT
cAMP
-35
-30
C
S194A
cAMP
-35
-30
D
S185A
cAMP
-35
-30
E
S185A/
S194A
cAMP
-35
-30
(pI)
5.4 5.6 5.7 5.9

Fig.7

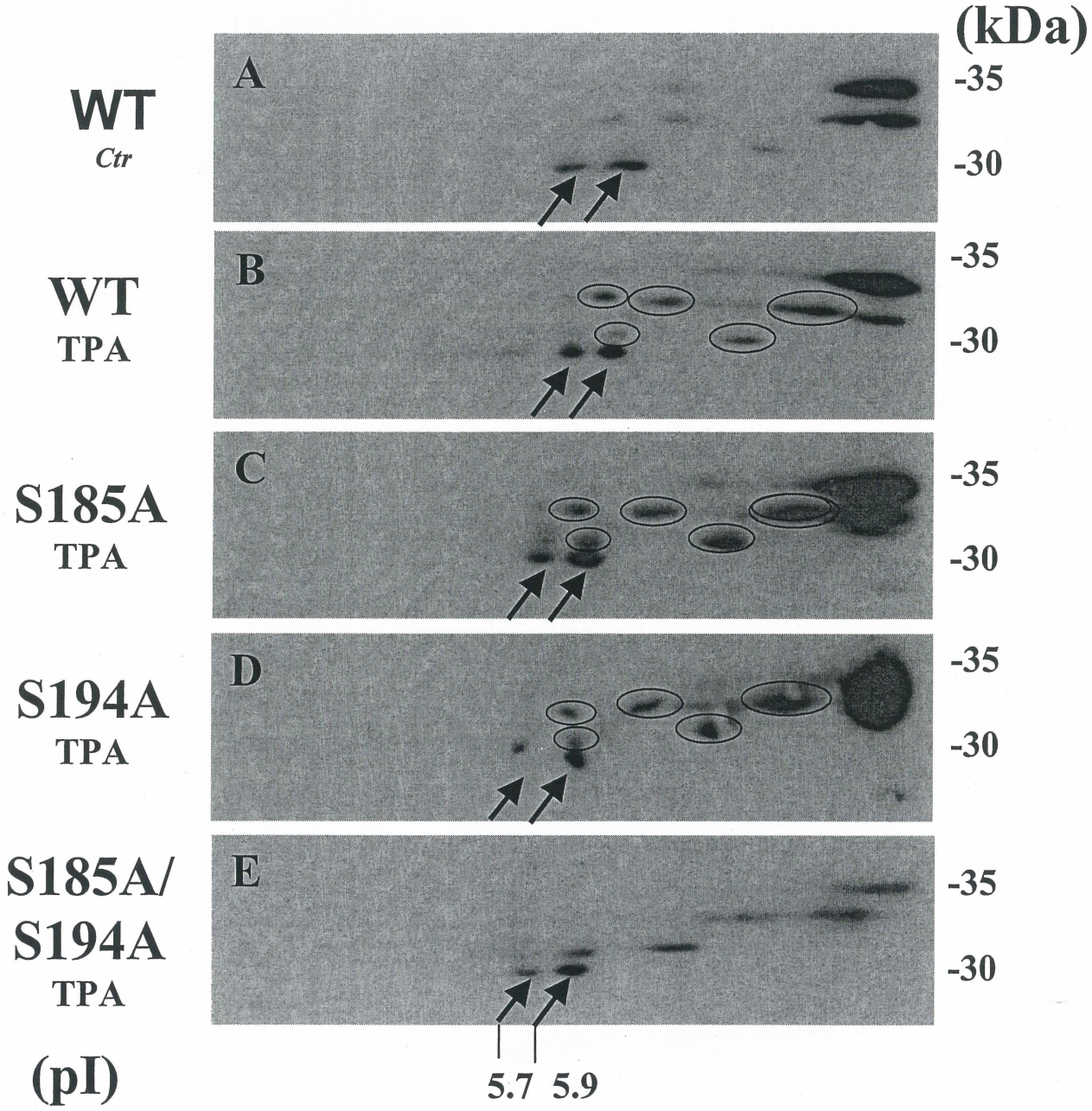
(kDa)
WT
Ctr
A
-35
-30
WT
TPA
B
-35
-30
S185A
TPA
C
-35
-30
S194A
TPA
D
-35
-30
S185A/
S194A
TPA
E
-35
-30
(pI)
5.7
5.9

Fig.8

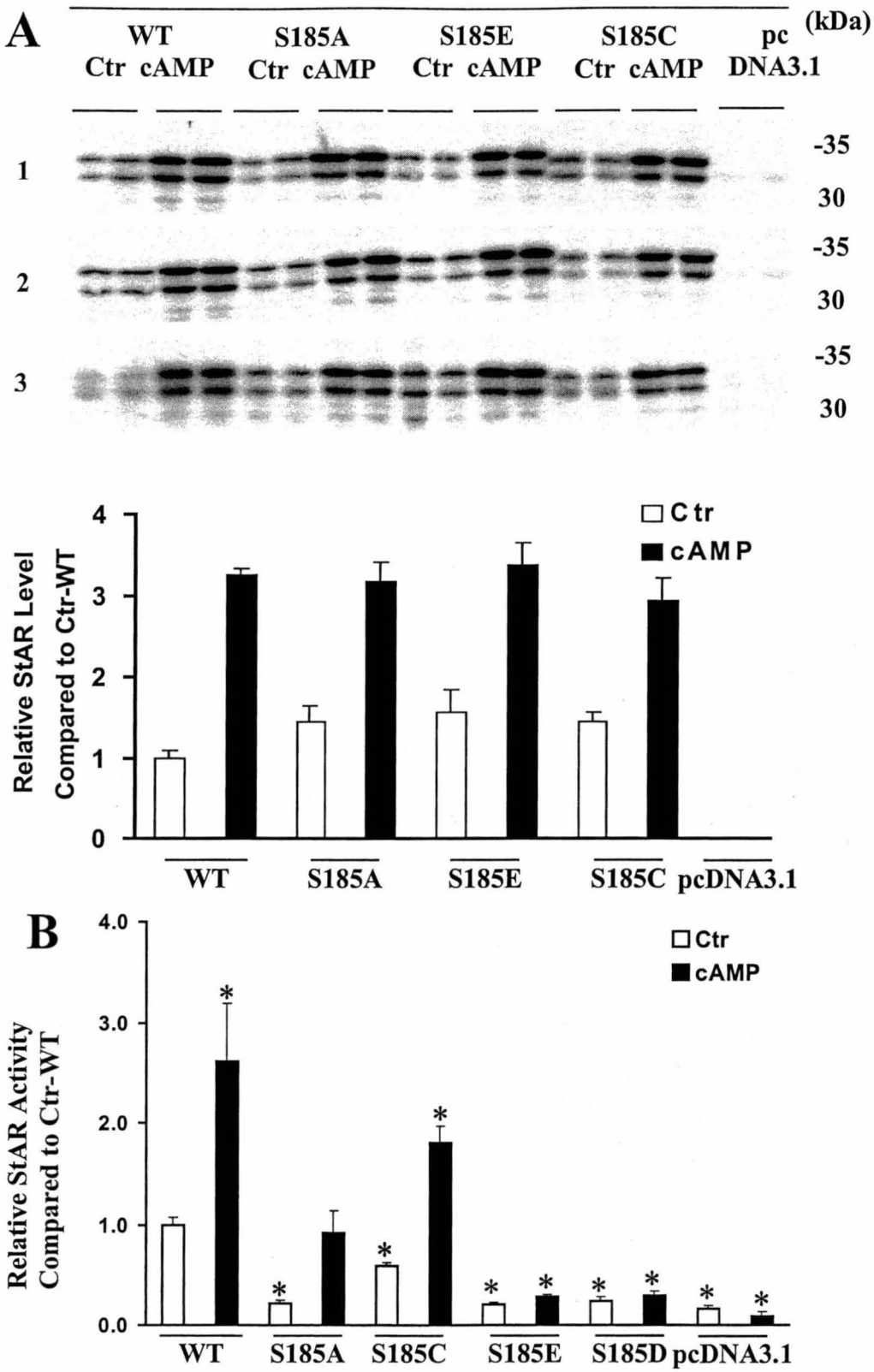
A
WT
Ctr cAMP
S185A
Ctr cAMP
S185E
Ctr cAMP
S185C
Ctr cAMP
pc
DNA3.1
(kDa)
1
2
3
-35
30
-35
30
-35
30
Relative StAR Level
Compared to Ctr-WT
Ctr
cAMP
WT
S185A
S185E
S185C
pcDNA3.1
B
Relative StAR Activity
Compared to Ctr-WT
Ctr
cAMP
WT
S185A
S185C
S185E
S185D
pcDNA3.1

Fig.9

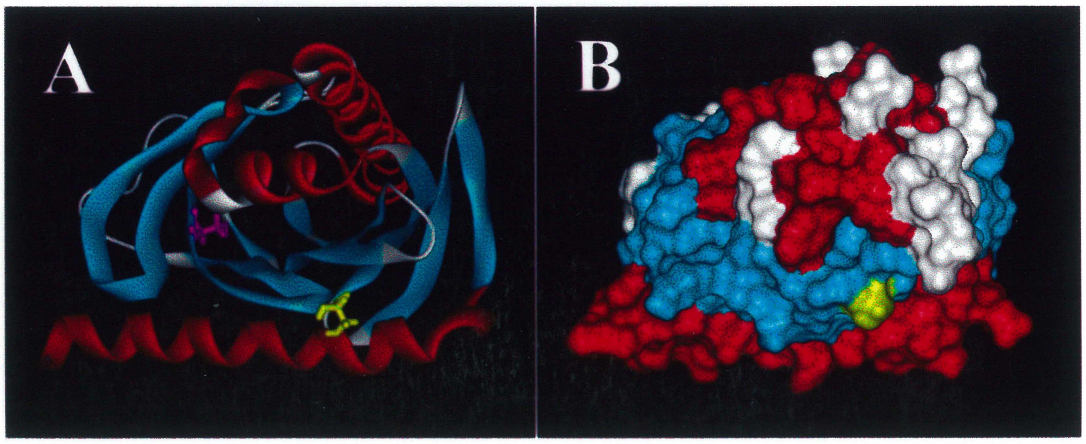

Fig.10

3. P450c17:

3.1. Mathieu AP. Auchus RJ. LeHoux JG. Molecular Modeling of the Hamster Adrenal P450C17. [Journal Article] ***Endocrine Research. 26(4):723-8, 2000 Nov.***

Contribution: Everything in this article is the product of my work.

MOLECULAR MODELING OF THE HAMSTER ADRENAL P450C17

Axel P Mathieu[1], Richard J. Auchus[2], Jean-Guy LeHoux[1]

[1]Department of Biochemistry, Faculty of Medicine, University of Sherbrooke, Sherbrooke, Quebec, Canada, J1H 5N4. [2]Division of Endocrinology and Metabolism, UT Southwestern Medical Center, Dallas, Texas, USA, 75390-8857

ABSTRACT

The cytochrome P450C17 (C17) is the steroidogenic enzyme responsible for the conversion of pregnenolone and progesterone to dehydroepiandrosterone (DHEA) and Δ^4-androstenedione (AD) respectively. This conversion is achieved by two enzymatic activities, 17α-hydroxylase and 17,20-lyase, located at the same active site. In man, the adrenal C17 basically only produces DHEA. We have shown that

the hamster adrenal C17 produces DHEA as well as AD. Moreover, the hamster like man produces cortisol as its major glucocorticoid. We can thus compare the hamster's and man's adrenal C17, and use their differences in order to elaborate a strategy for structure-function studies. We have thus engineered hamster adrenal C17 mutants which possess modified enzymatic activities. We also proceeded to elaborate a three-dimensional model of the hamster C17 to visualise the structural impact of these mutations. This model demonstrates that the mutations created are not localised at the active site, but rather in surrounding regions. These could affect the conformation of the active site, in turn, modulating the 17α-hydroxylase and 17,20-lyase activities. For example, the mutation T202N is located next to Val 482 and Val 483 which compose the roof of the active site. This mutation decreased both 17α-hydroxylase and 17,20-lyase activities, indicating the importance of the roof of the active site for general functionality of the C17.

INTRODUCTION

The specificity of the cytochrome P450C17 (C17) towards its substrates differs among species. In human and bovine adrenals, C17 hydroxylates both pregnenolone and progesterone but selectively produces dehydroepiandrosterone (DHEA) in a more abundant concentration than for Δ^4-androstenedione (AD) (1-3). In the case of the guinea pig adrenals, both substrates are hydroxylated but AD is the preferred final product (4, 5). In rats and mice adrenals, C17 is not

expressed but the C17 expressed in the gonads preferentially produces AD (6-9). In contrast to other laboratory animals, and like man, the hamster expresses adrenal C17 and produces cortisol as its major glucocorticoid (10, 11). We have isolated the hamster adrenal C17 and demonstrated that it produces both DHEA and AD in transiently transfected COS 1 cells, adrenal cell suspensions, and microsomal preparations (12, 13). Moreover the hamster adrenal C17 is inducible by adrenocorticotropin hormone (11).

Due to the importance of the C17 for the production of cortisol, DHEA, and sex steroids, we have decided to study the structure/activity of the hamster enzyme. We also elaborated a 3-dimensional model of the hamster C17 based on the previously published human C17 model (14).

MATERIAL AND METHODS

All energy minimization and molecular dynamic studies were performed on "Socrates" in San Francisco using AMBER 5.0 program suit, through Secure Shell Protocol (http://www.ssh.org/). All Brookhaven files were renamed using "fixatname" of Midas Plus 2.1 in order to be visualized, and the structures were visualized with either Midas Plus 2.1 or RasMol 2.7.1; all images were created with RasMol (http://www.klaatu.oit.umass.edu/microbio/rasmol/). The hamster C17 amino acid sequence was compared to the human C17 amino acid sequence by manually aligning them. Due to the explicit alignment, the human C17

sequence was immediately replaced by the amino acid side-chains of the hamster C17 using Midas Plus 2.1. This initial model was then subjected to energy minimization (1000 cycles) and asymmetrically solvated within a radius of 65 Å. The asymmetric solvated protein excluded the hydrophobic membrane bound region. After the initial 10 picoseconds (ps) molecular dynamics of the solvent molecules only, the entire model was subjected to another 100 ps of molecular dynamics. The final model represents an average structure of the last 40 ps of molecular dynamics, energy minimized for another 1000 cycles using the steepest descent method. For more information, examine references 14 and 15.

RESULTS AND DISCUSSION

The hamster C17 model obtained (Fig 1) greatly resembles the human C17 model (14). First of all, there is conservation of characteristic features of P450 crystallized proteins (16): A) the formation of a β-sheet rich region, B) the intersecting I-Helix with the adjacent heme prosthetic group, and C) the α-helix rich region. In terms of comparison to the human model, three subtle alterations are observed in the hamster C17 model, when compared to the human: 1) consolidation of the membrane attachment domain, 2) protrusion of the J'-helix, and 3) slight modification of the hamster C17 model active site.

First, the membrane attachment domain defined by the A-, F-, and G-helices, along with the β-sheets (sheets) 1.1-1.3 and 2.1-2.2, is consolidated

predominantly by the internalisation of two loops, the first between the F- and G-helices, and the second between sheets 2.1 and 2.2. Although, the F-G loop is likely to be disordered as in P450terp. In addition, the F- and G-helices in the hamster C17 model run more parallel than in the human C17 model.

Secondly, the J'-helix seems to have been extended from its end, causing flattening of the helical structure and rotation of its axis, resulting in a net protrusion of the helix outwards from the protein. This affects the region defined by the J-J'-loop, J'-helix, and the C-D loop located on the cytoplasmic exposed area, opposite the membrane attachment domain. The significance of this protrusion remains to be elucidated.

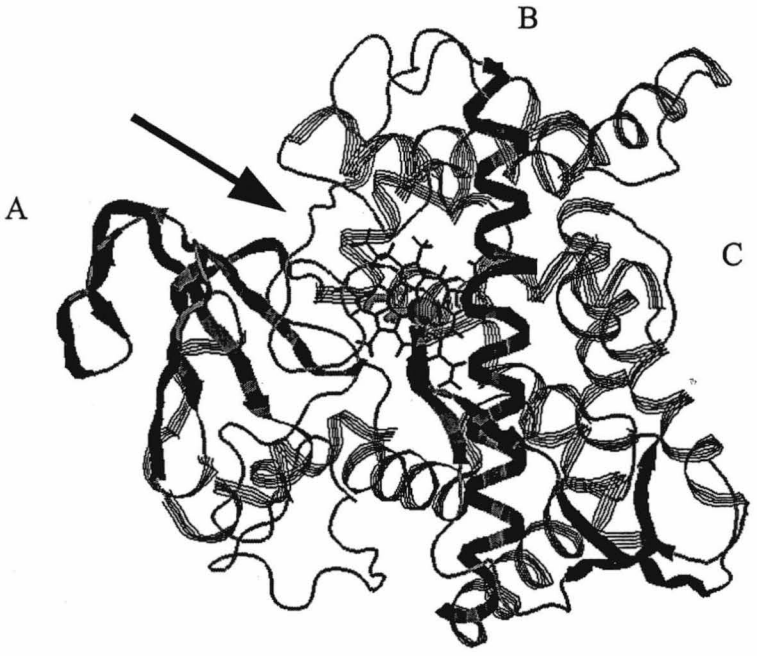

FIGURE 1.

Three Dimensional Model of the Hamster P450C17. Representation of the hamster P450C17 model as seen from above the protein. A, β-Sheet rich region; B, I-helix with prosthetic heme group; C, α-Helix rich region; Arrow: substrate entrance. Heme prosthetic shown in black wireframe, β-sheets as black cartoon arrows, α-helices in black strands, and I-helix in black cartoon strand.

Finally, in the hamster C17 model active site compared to the human C17 model, the I-helix has a large bulge at position Lys302 and kinking at the N-terminus causing the Thr306 (17, 18) to be located slightly higher from the heme prosthetic group, and allowing the H-I loop to shift closer to the substrate entrance defined by sequence between β-sheet 1.5 and B'-C loop. Thus, slight alterations in the active site as seen here, appear to define the activity specificity of the C17 in various species (1-9).

Much like the human C17 model (14), the hamster model explains the functionality of various mutants. For example, the mutant T202N reduced the overall activity of the hamster C17 for both Δ^5 and Δ^4-substrates (15). This

threonine is located adjacent to the 482 and 483 valines, composing the roof of the active site. The change of the threonine to an asparagine in the hamster, results in "kinking" of the G-helix, resulting to the overall shifting of the active site approximately 0.7 Å deeper, closer to the I-helix (15). In conclusion, shifting such as obtained by the T202N mutation, certainly results in displacement of the substrates such that reactivity is not optimal suggesting that more information about activity specificity of the C17 of various species is to be obtained by mutations surrounding the active site rather than directly in the active site.

ACKNOWLEDGMENTS

This work was supported by grants from the Medical Research Council of Canada (MT-10983) (to JGL), and from the Heart and Stroke Foundation of Canada (to JGL). A P Mathieu was a recipient of a studentship from the Medical Research Council of Canada, and JG LeHoux was chercheur-boursier de carrière du Fonds de la recherche en santé du Québec.

REFERENCES

1. Chung BC, Picado-Leonard J, Haniu M, Bienkowski M, Hall PF, Shively JE, Miller WL 1987 Proc Natl Aca Sci USA 84: 407-411.

2. Lin D, Black SM, Nagahama Y, Miller WL 1993 Endocrinology 132: 2498-2506.

3. Fevold HR, Ivanovitch JD, Zanger UM, Waterman MR 1993 Mol.Cell Endocrinol 95: 95-100.

4. Provencher PH, Tremblay Y, Bélanger A 1992 J.Endocrinol. 132: 269-276.

5. Tremblay Y, Fleury A, Beaudoin C, Vallée M, Bélanger A 1994 DNA Cell Biol 13: 1199-1212.

6. Namiki M, Kitamura M, Buczko E, Dufau ML 1988 Biochem Biophys Res Commun 157: 705-712.

7. Fevold HR, Lorence MC, McCarthy JL, Trant JM, Kagimoto M, Waterman MR, Mason JI 1989 Mol.Endocrinol 3: 968-975.

8. van Weerden WM, Bierings HG, van Steenbrugge GJ, de Jong FH, Schroder FH 1992 Life Sci 50: 857-861.

9. Youngblood GL, Payne AH 1992 Mol.Endocrinol 6: 927-934.

10. LeHoux JG, Lefebvre A 1980 J.Steroid Biochem 12: 479-485.

11. LeHoux JG, Mason JI, Ducharme L 1992 Endocrinology 131: 1874-1882.

12. Cloutier M, Fleury A, Courtemanche J, Ducharme L, Mason JI, LeHoux JG 1995 Ann.N.Y.Acad.Sci. 774: 294-296.

13. Cloutier M, Fleury A, Courtemanche J, Ducharme L, Mason JI, LeHoux JG 1997 DNA Cell Biol 16: 357-368.

14. Auchus RJ, Miller WL 1999 Mol Endocrinol 13:1169-1182

15. Mathieu AP, Auchus RJ, LeHoux, JG. 2000 (submitted for publication)

16. Graham-Lorence S, Peterson JA 1996 In: Adv Mol and Cell Biol (Bittar, EE, Jefcoate GR eds) 14: 57-79.

17. Lee-Robichaud P, Akhtar ME, Akhtar M 1998 Biochem J 330: 967-974.

18. Poulos TL, Finzel BC, Howard AJ 1987 J Mol Biol 195: 687-700.

3.2. Mathieu AP. Auchus RJ. LeHoux JG. Comparison of the Hamster and Human Adrenal P450c17 (17α-hydroxylase/17,20-lyase) Using Site-Directed Mutagenesis and Molecular Modeling. [Journal Article] ***Journal of Steroid Biochemistry and Molecular Biology. 80(1): 99-107, 2002 Jan.***

Contribution: Everything in this article is the product of my work.

Comparison of the Hamster and Human Adrenal P450c17 (17α-hydroxylase/17,20-lyase) Using Site-Directed Mutagenesis and Molecular Modeling°

AXEL P. MATHIEU [1], RICHARD J. AUCHUS [2], AND JEAN-GUY LEHOUX [1]*

[1] Department of Biochemistry, Faculty of Medicine, University of Sherbrooke, QC, Canada, J1H 5N4.

[2] Division of Endocrinology and Metabolism, UT Southwestern Medical Center, Dallas, TX, USA, 75390-8857

* Address all correspondence to Jean-Guy LeHoux, Department of Biochemistry, Faculty of Medicine, University of Sherbrooke, Sherbrooke, QC, Canada, J1H 5N4. TEL: (819) 564-5282; FAX: (819) 820-6852; E-mail: jlehou01@courrier.usherb.ca

° This work was presented in abstract form at the Ninth Adrenal Cortex Conference in Toronto, Ontario, Canada, June 2000.

Abstract

In order to understand the activity specificity of the hamster cytochrome P450 17α-hydroxylase/17,20-lyase (P450c17), we have studied its structure/activity using three hamster P450c17 recombinant mutants (T202N/D240N/D407H). In transiently transfected COS-1 cells, the mutation T202N reduced 17α-hydroxylation of pregnenolone and progesterone to 24% and 44% of wild type, respectively, followed by reduced 17,20-cleavage to 71% and 67%, respectively. On the other hand, the mutation D240N decreased specifically 17,20-lyase activity to 61% of wild type when incubated with pregnenolone while the mutation D407H only decreased 17α-hydroxylation to 46% when incubated with progesterone.

To comprehend the altered activity profiles of these hamster P450c17 mutants, we have elaborated a three-dimensional model of the hamster P450c17 and compared it to our preceding model of the human P450c17. Analysis of the mutants with this model showed that, without direct contact to the substrates, these mutations transmit structural changes to the active site. By analogy, these results support the concept that any cellular changes modifying the external structure of P450c17, such as phosphorylation, could have influence on its active site and enzymatic activities.

Keywords: Cytochrome P450c17, CYP17, 17alpha-hydroxylase, 17,20-lyase, 3D modeling, hamster, human, site-directed mutagenesis, mutants, adrenals.

Abbreviations: Cytochrome P450 17α-hydroxylase/17,20-lyase (P450c17), dehydroepiandrosterone (DHEA), androstenedione (AD), 17α-hydroxypregnenolone (17OHpreg), 17α-hydroxyprogesterone (17OHprog), Polymerase chain reaction (PCR), wild type (WT), thin-layer chromatography (TLC), energy minimization (EM) and molecular dynamics (MD), amino acids (AAs), aspartate (Asp-D), asparagine (Asn-N), arginine (Arg-R), cysteine (Cys-C), histidine (His-H), isoleucine (Ile-I), lysine (Lys-K), phenylalanine (Phe-F), proline (Pro-P), threonine (Thr-T), tryptophan (Trp-W), valine (Val-V).

Running Title: Molecular Modeling of the Hamster Adrenal Cytochrome P450c17.

1. Introduction

The cytochrome P450 17α-hydroxylase/17,20-lyase (P450c17, the gene product of *CYP17*) is a major branch point in steroidogenesis in the adrenal glands and the gonads. In humans, P450c17 is necessary for the production of the major glucocorticoid, cortisol, and for the production of androgens via dehydroepiandrosterone (DHEA). A non-functional or reduced P450c17 activity results in a diminution of sex steroid production in males and can lead to ambiguous genital formation, and in females, lack of progression into puberty [1,2].

P450c17 is an endoplasmic reticulum membrane bound multifunctional enzyme [3,4] that exhibits 17α-hydroxylase and 17,20-lyase activities. The first activity, 17α-hydroxylase, converts pregnenolone and progesterone into their respective 17α-hydroxylated products 17OHpreg and 17OHprog, and the second activity, 17,20-lyase, can cleave the steroid side chain to yield their respective androgens, DHEA and androstenedione (AD). The specificity of the P450c17 towards its substrates differs in various species and tissues. In human and bovine adrenals, P450c17 17α-hydroxylates both pregnenolone and progesterone but selectively produces DHEA in greater quantities than for AD [5-7]. P450c17 is not expressed in the adrenal glands of rats [8-10] and mice [11] but the gonadal P450c17 in these species preferentially produces AD. In the case of the guinea pig adrenals, both substrates are also 17α-hydroxylated whereas AD is the preferred final product [12,13]. In contrast to other small laboratory animals, the hamster also expresses P450c17 in the adrenal and produces cortisol as its major glucocorticoid [14,15].

We have isolated the hamster adrenal P450c17 cDNA and have demonstrated that this enzyme produces both DHEA and AD in transiently transfected COS-1 cells, adrenal cell suspensions, and microsomal preparations [16,17]; AD is the favoured product. Moreover, we have immunolocalized the hamster P450c17 in the *zona fasciculata* and *reticularis* of the hamster adrenals [18], and we have shown that the hamster P450c17 mRNA is inducible by adrenocorticotropin hormone [15]. Because of these similarities between the hamster and human adrenal P450c17 enzymes, the hamster is an attractive animal model to study how P450c17 regulates steroidogenesis in human beings.

Due to the small number of discrete differences in the enzymology of the hamster and human P450 enzymes, we have attempted to compare the structures and activities of the hamster and human enzymes. First, from sequence comparison of various species, amino acids (AAs) that might be responsible for the unique activities of the different P450c17 enzymes were identified, substituted, and studied in transiently transfected COS-1 cells. The substitution of the amino acids were based entirely on their conserved patterns in the sequence alignment. For example, a threonine conserved in AD producing animals (rat, mice, guinea pig, and hamster), was substituted for a conserved asparagine in DHEA producing animals (ex: T202N). Of all the possibilities, three have retained our attention: T202N, D240N, and D407H. Second, we have elaborated a molecular model of the hamster P450c17 in an effort to comprehend altered activity profiles of the selected mutants and ultimately describe their activity distinctions. By combining rational mutagenesis with molecular graphics, we have developed testable models of regions of the P450c17 protein that might be responsible for the difference in substrate utilization amongst species.

2. Materials and methods

2.1. Materials

All restriction and modifying enzymes were purchased from Pharmacia Biotech (Baie d'Urfé, QC, Canada). Oligonucleotides were either purchased from BRL Life Technologies (Gaithersburg, MD) or Biosource International (Camarillo, CA). The expression vector pSVSPORT•1 was obtained from BRL Life Technologies, amplified in XL1 Blue *E coli* competent cells (Statagene, La Jolla, CA), and purified on Qiagen anion-exchange columns (Qiagen, Chatsworth, CA). HPLC-purified [7-^{3}H]pregnenolone (21.0 Ci/mmol) was purchased from Mandel Scientific (Guelph, ON, Canada), while [1,2,6,7-^{3}H]progesterone (95.0 Ci/mmol) was purchased from Amersham Canada (Oakville, ON, Canada). Pregnenolone and progesterone were purchased from Sigma-Aldrich (Oakville, ON, Canada). Polymerase chain reaction (PCR) reagents were obtained from Roche Molecular Biochemicals (*Pwo* DNA polymerase - Laval, QC, Canada).

2.2. Hamster P450c17 mutagenesis by PCR

The hamster P450c17 cDNA was isolated and cloned into the vector pSV-SPORT•1 as previously described [16]. P450c17 sequences of man, cow, pig, sheep, guinea pig, mouse, and rat were obtained from Genbank and aligned by Clustal method using DNA STAR software. Various AAs were determined as potential sites of activity control. Site-

directed mutagenesis was obtained by PCR. Briefly, two series of PCR amplifications were obtained using the following conditions: Hot start of 5 min at 94°C (without DNA polymerase) followed by a touch down of 2°C from 70-50°C, completed with 30 cycles of 94°C/50°C/72°C and a final 72°C elongation of 15 min. The first series consists of amplifying pSV-hamP450c17 in two different reactions: 1) a wild type (WT) upstream (sense) oligonucleotide to the downstream mutant (antisense) oligonucleotide at the site of interest for mutagenesis and 2) a mutant sense oligonucleotide from the site of interest for mutagenesis to a WT antisense oligonucleotide. The second series consists of pooling both PCRs previously obtained, purified by agarose gel electrophoresis, and amplifying using WT 5' and 3' oligonucleotides. The WT upstream oligonucleotide used was termed "486" with the sequence 5'-GGAGTCCAT*AGATCT*TTCCG-3' containing a *Bgl*II restriction site indicated in *italics*. The wild type downstream oligonucleotide used was T7Hot with the sequence 5'-AATTGTAATACGACTCACTATAGGG-3'. All mutants were cloned into recombinant pSV-hamP450c17 using unique *Bgl*II and *Xho*I (just upstream from the T7Hot oligonucleotide) restriction sites, sequenced entirely between these restriction sites using T7 sequencing kit from Pharmacia Biotech, amplified, and purified on Qiagen anion-exchange columns.

2.3. Hamster P450c17 expression

Either WT or mutated pSV-hamP450c17 was transiently transfected into monkey kidney COS-1 cells (American Type Culture Collection, Rockville, MD) using the calcium phosphate method [19]. Twenty-four hours before transfection, the cells were

harvested with trypsin-EDTA solution (GIBCO BRL, Burlington, ON, Canada) and plated at an initial density of $4.0x10^5$ cells per 10.0 cm^2 well in 6-well plates. Cells were cultured in DMEM supplemented with 10% dextran-coated charcoal-treated fetal bovine serum (FBS), 2.2 g/L $NaHCO_3$, 1mM L-glutamine, 100 IU/ml penicillin, and 50 μg/ml streptomycin sulphate. Each transfection assay received 8 μg of DNA.

2.4. Measurement of the hamster P450c17 activity

Forty-eight hours after the COS-1 cells were transiently transfected, each well of cells was incubated for 1 hour with 2.5 μM of pregnenolone or progesterone containing 1.45μCi of [^{3}H]-steroid. The reactions were stopped with 50 μL of 0.5 N acetic acid. The steroids were extracted twice with diethyl ether, applied on silica gel-coated thin-layer chromatography (TLC) plates with unlabelled standards for identification, and developed with chloroform/ethyl acetate (3:1 v/v) three times for pregnenolone reactions and once for progesterone reactions. The TLC plates were then dried overnight and exposed to ^{3}H-sensitive STORM 860 (Molecular Dynamics, Sunnyvale, CA) screens for 24 hours. The results were visualized and quantified on the optical imager STORM 860 using ImageQuant software version 5.0.

2.5. Statistical analyses

All data were analysed using SigmaStat (Jandel Corporation, San Rafael, CA) software. One-way ANOVA statistical analyses were performed between groups in order

to obtain significant results as compared to hamster P450c17 WT. All experiments were performed using three DNA preparations, each in triplicate (n = 3).

2.6. Modeling of the hamster P450c17

All AA side-chain alterations were performed using the Midas Plus 2.1 Graphics program [20] on a Silicon Graphics Octane workstation. Energy minimization (EM) and molecular dynamics (MD) were accomplished using the Amber 5.0 suite of programs [21] remotely on the Digital Equipment Corp. AlphaServer host *socrates* at the UC San Francisco Computer Graphics Laboratory.

In order to be able to compare the human and hamster models, EM and MD calculations for the hamster model were performed following the same protocol as for the human P450c17 modeling. Basically, the hamster model was subjected to 1000 cycles of EM in the SANDER module of Amber 5.0. The favourable energetics at this stage (-5.0766 x 10^3 kcal/mol) allowed us to proceed immediately with the solvation of the hamster molecule. Solvation was performed asymmetrically with a sphere of radius 33.65 Å by means of the EDIT module of AMBER 5.0. This asymmetric solvation excludes the hydrophobic, presumed membrane-bound N-terminal region of the P450c17. The water molecules were then pre-equilibrated for 10 ps and a temperature gradient of 100K to 300K using the BELLY option in the SANDER module. Once achieved, MD calculations were performed on the whole model, including the water molecules, for an additional 100 ps with a rapid temperature gradient of 200K to 300K. An average structure was captured

for the last 40 ps using the CARNAL module of Amber 5.0 and subjected to another 1000 cycles of EM using the steepest-descent method of the SANDER module.

Modeling of the mutants was obtained as mentioned above with the desired altered AA side chains following the same protocol as for the WT modeling. Protein database files were generated using Amber 4.1 "ambpdb" program, and visualized with either Midas Plus 2.1 or RasMol 2.7.1. All images were created with the RasMol 2.7.1. visualization program (http://klaatu.oit.umass.edu/microbio/rasmol/).

3. Results

3.1. Hamster P450c17 mutagenesis

Three recombinant hamster P450c17 mutants were constructed and tested, based on the homology analysis of the AA sequences of eight species: hamster, mouse, rat, guinea pig, human, sheep, bovine, and porcine. As mentioned previously, P450c17 isozymes from different species have different reactivity; small laboratory animals generally produce AD while larger animals such as cows produce DHEA like humans *in vivo*. Thus substituting specific residues that consistently track with different P450c17 activities into hamster P450c17, we hypothesized that we would identify important AAs for the reaction specificity displayed by the various species.

Using this approach, the hamster P450c17 was mutated at three different positions to resemble the human sequence (Table 1). At position 202 of the hamster P450c17, the conserved thr (T) in the hamster, mouse, rat, and guinea pig (all species with high Δ^4

lyase activity) was mutated to asn (N), conserved in human, sheep, cow, and pig P450c17s (all species with high Δ^5 lyase activity), yielding mutant T202N. D240N is an AA alteration from an asp (D) in the hamster P450c17, to an N conserved in rat, human, sheep, cow, and pig at position 240 of the hamster P450c17 sequence. Finally, a D at position 407 of the hamster P450c17, also conserved in the mouse, rat, and guinea pig, was changed into a his (H) found in human P450c17 only.

To compare the activities of mutant and WT hamster P450c17 enzymes, transiently transfected COS-1 cells were incubated with 2.5 μM of substrate for 1 h, since the substrate utilization was linear with time under such conditions (data not shown). The hamster T202N showed decreased 17α-hydroxylase and 17,20-lyase activities for both the Δ^5- and Δ^4-pathways. When incubated with pregnenolone, a 32% decrease in 17OHpreg accumulation was observed, with a 70% decrease in DHEA production (Fig. 1 and Table 2). Similarly, incubation with progesterone resulted in a 46% reduction in 17OHprog production and 66% reduction in AD.

The hamster D240N and D407H mutations are unique in their effects to the hamster P450c17 since they decreased specifically a single activity or pathway. D240N only decreased DHEA and AD formation to 60% and 18% of the wild-type enzyme, respectively (Fig. 1 and Table 2). In contrast, the D407H mutant only decreased 17α-hydroxylase activity for the Δ^4-pathway by 46%, leading to a comparable decrease in AD formation (51% - Fig. 1 and Table 2) which can be almost entirely attributed to the reduced production of the intermediate 17OHprog.

It becomes difficult to hypothesize why these single AA substitutions alter the activity profiles of the hamster P450c17 as observed. Therefore, to have a more complete

understanding of the effects of the site-directed mutagenesis, we thus elaborated 3D-models of wild type and mutant hamster P450c17.

3.2. Hamster P450c17 three-dimensional modeling

3.2.1. HamsterP450c17 wild type modeling

The hamster P450c17 AA sequence was manually aligned to the human P450c17 sequence [22]. Fig. 2 shows perfect alignment between both species of the highly conserved residues: C-helix Trp (W), catalytically important T in the I-helix (T306), the ExxR sequence in the K-helix, and the axial heme-liganding cys (C442). Because the hamster and human AA sequences align perfectly without discrepancies in lengths, the first process (graphics) was unambiguous. The side-chains of the hamster P450c17 sequence were substituted in the human model [22], and the EM and MD were performed following the same protocol as for the human P450c17 modeling in order to be able to compare the models. The final hamster P450c17 model is represented in Fig. 3.

At first glance, there are three noticeable global dissimilarities between the hamster and human models (Fig. 4). The most obvious difference of these global dissimilarities is in the consolidation of the hydrophobic domain described by the α-helices (helices) A, F, and G along with the β-sheets (sheets) 1.1-1.3 and 2.1-2.2. This consolidation is due to the internalization of the F-G loop in addition to the loop between sheets 2.1 and 2.2 (Fig. 4A and B). However, the F-G loop of P450c17 is likely to be disordered as in P450terp [23], so this motion is to be expected. The F- and G-helices have also slightly changed in position with respect to each other: in the human model, they tend to cross each other in

the plane of view in Fig. 4A, but run parallel when observed from above the molecule (not shown); in the hamster model, these helices run parallel in both views.

The second difference between the hamster and human models is in the positioning of the J'-helix (Fig. 4A and B). The hamster J'-helix (Fig. 4B) seems to have been pulled by its ends as compared to the human J'-helix, causing a slight flattening of the helix as well as a slight rotation of the helix axis. This causes the J'-helix in the hamster to protrude from the protein more than in the human model. The affected region is the domain structured by the J-J' loop, J'-helix, and the C-D loop.

Finally, the active sites of the hamster and human P450c17 are also different due to more subtle changes in amino acid positioning. In each case, the active site is the volume delimited by the heme, which forms the floor of the pocket; the Val (V) 482 and 483 which form the roof; the I-helix forming the far wall, running next to the heme; the K-helix, β-sheet 1.4, and loop between them, which form the right wall (as viewed in Fig. 4C and D); the β-sheet 1.5, B'-helix, and the loop between these two, forming the front wall; and the B'-C loop, specifically the Ile (I) 112, forming the left wall. The substrate entrance is shaped by the β-sheet 1.5, loop between sheet 1.5 and B'-helix, B'-helix, and B'-C loop.

The first difference between the hamster and human active sites is the larger bulge at position Lys (K) 302 in the hamster I-helix which, when compared to the human model, displaces the catalytic important T306 higher from the heme. The methyl hydrogen on this T in the human model is located at 4.049 Å from the heme iron and 2.806 Å from the V483 methyl group, while it is displaced to 4.537 and 2.862 Å, respectively, in the hamster model. Thus, this "bulge" could have an implication in the overall reactivity of

the protein. Another difference in the active sites is that the hamster I-helix has a kink towards the heme at its N-terminal which changes the orientation of the H-I loop with respect to the B'-C loop of the substrate entrance, as well as creating some distortion in the B'-helix C-terminal. This "kink" allows the H-I loop to interact more closely with the B'-C loop, changing its conformation. The significance of this new interaction is unknown but suggests the implication of the substrate entrance in the protein's reaction specificity, since this is the major difference in the hamster and human active sites.

3.2.2. Hamster P450c17 mutant modeling

Modeling of the mutants without the substrates suggests explanations for the activities of mutants T202N, D240N, and D407H. T202N is located in the F-helix directly above the substrate, interacting with residues V482 and V483 that form the roof of the active site (Fig. 5). In this case, all activities of the hamster P450c17 are decreased (Table 2). These data are consistent with the model of V482 and V483 forming the roof of the active site [22], and surrounding residues stabilizing the position of these valines. Although H-bonding still occurs between N202 and V482 as seen in the WT, the interactions of N202 with V482 shifts the active site pocket by approximately 0.7 Å closer to I-helix with respect to the substrate entrance. Also, the amide nitrogen of I112 in the T202N model is located about 0.6 Å closer to the heme group than in the WT. This I112 displacement is caused by the bending of the F-helix (where residue 202 is located), which distorts the G-helix. So the twisting displacement of the active site pocket with respect to the heme group, created by differential H-bonding of N202 to V482 and the AAs in the substrate entrance, appears to interfere with the positioning of the active site

and with substrate entrance sufficiently enough to reduce both 17α-hydroxylase and 17,20-lyase activities of the hamster P450c17.

D240N however, is located in the mid-portion of the G-helix, near the junction of the I- and B'-helices close to the H-I loop. Alteration in this position also modified the active site pocket, further lowering I112 closer to the heme and elevating T306 due to kinking of the I-helix similarly. Importantly, Arg (R) 96 and R440 have also changed in position. R96 and R440 are approximately 1.0 and 1.5 Å closer to the heme than in the WT model, which twists and shrinks the active site pocket. Since R96 is located in the substrate entrance (between sheet 1.5 and B'-helix) and since R440 is directly under R96 just beyond the opening, displacement of these arginines would be expected to interfere with the substrate entrance conformation and overall reactivity of the P450c17. In this case, the resultant reduction in 17,20-lyase activity (Table 2) seems to be due to decreased 17α-hydroxysteroid access to the active site because of the reduced substrate entrance, and reduced active site pocket volume.

On the other hand, it is less apparent why mutation D407H, located remotely from the active site, specifically reduces the reactivity of the hamster P450c17 towards the progesterone pathway. Once again, the model obtained for this mutation has a greater kink of the I-helix, but this change alone is unlikely to account for the selective Δ^4 activity loss. Given that Asp407 is upstream the heme binding C442 in the meander, the Asp→Asn change in this position alters the conformation of the heme binding AA sequence leading to a shift of the heme and a change in active site volume, which might specifically reduce reactivity of the hamster P450c17 when progesterone is the substrate.

Taken together, these single AA substitutions appear to alter P450c17 reactivity by transmitting structural changes from their positions to the active site as demonstrated through molecular modeling. Other examples have also demonstrated similar results through molecular modeling supporting our findings. Of which, the most pertaining examples are the human P450c17 [22] and mineralocorticoid receptor [24] models where molecular modeling coupled with experimental data can sufficiently explain activity alterations.

4. Discussion

4.1. Hamster P450c17 mutagenesis

Since T202, D240, and D407 were mutated in the hamster to resemble the corresponding human AAs, we hypothesized that the mutations would engineer hamster P450c17 to act more like the human enzyme, shifting the relative rates of 17,20-lyase activity towards increased DHEA production. However, these single AA substitutions alone cannot explain activity differences between the hamster and human P450c17s.

The T202N AA alteration resulted in a greater reduction in 17α-hydroxylase activity for the Δ^4-pathway than for the Δ^5-pathway, although the overall final product formation is similar for both pathways. Since in both pathways the final product formation is decreased to a greater extent than the 17α-hydroxylated intermediate, these data suggest that this mutation affects all activities for both pathways. In contrast, Beaudoin *et al* [25] have studied the nearby mutant R200N in the guinea pig P450c17 that exhibits increased

hydroxylation of pregnenolone but decreased 17,20-lyase activity of 17OHprog. Their double mutant R200N/T202N did not result in further reactivity alteration.

The D240N mutant specifically decreased 17,20-lyase activity for both Δ^5-and Δ^4-pathways. No structure/function data are available from previous studies of mutations in this region; the only documented mutant in this region is a stop codon leading to a truncated human P450c17 protein conferring combined 17α-hydroxylase/17,20-lyase deficiency [26,27]. Since the D240N mutation alters the positioning of R96 and R440 in 3D space, it is likely that this mutation affects the P450c17 enzymatic activities through these AAs. The mutation of the conserved R96 to W in human P450c17 has been shown to virtually abolish all reactivity [28], consistent with the role of R96 in substrate entrance, and the conserved R440 has been demonstrated to be crucial for heme binding and positioning [29,30].

Analogously for the mutant D407H, a splice site mutation causing exon 7 to be excised and leading to a frame shift and a premature stop codon at position 410 was described [31] abolishing P450c17 reactivity. In addition, Lam *et al.* recently reported that the mutation of Pro(P) 409R causes 17α-hydroxylase deficiency [32], emphasizing the importance of the meander region for all activities. Consistent with these reports we have observed specific but not complete loss of 17α-hydroxylase activity in the hamster P450c17 with the nearby D407H mutation, suggesting that this region of the protein distant from the active site is an important determinant of substrate utilization.

5. Conclusions

At this time, we have been unable to identify single AA substitutions that account for the difference in activities of the P450c17 enzymes from various species such as the hamster and the human. Although specific AA substitutions within the active site would be expected to alter the catalytic activities of the P450c17, our results also indicate that changes in surrounding or "second tear" residues [33] can also modulate active site geometry. We therefore conceptualize P450c17 structures as having three key features: 1) residues that constitute the core elements and preserve the structural integrity of the enzyme; 2) residues that participate directly in heme binding, redox partner interactions, and catalysis; and 3) residues that directly or indirectly influence active site geometry and hence substrate selection. Furthermore, any given residue may participate in one or more of these functions, and these functions can also be modified by mutagenesis or post-translational modification(s). Therefore any cellular alterations leading to the modification of the P450c17 external structure, such as phosphorylation, could directly modulate its activities through the conformational transformation of its active site.

Acknowledgements

We thank A. Lefebvre, L. Ducharme, J. Courtemanche, and A. Fleury for their assistance, and T. Bardati for her editorial skills. We also thank the UCSF Computer Graphics Laboratory for use of host Socrates. A.P. Mathieu was a recipient of a studentship from the Medical Research Council of Canada, and this work was supported by a grant from the Medical Research Council of Canada #MT-10983 (to J.G.L.) and

NIH grant #K08DK02387 (to R.J.A.). J.G. LeHoux is a "chercheur boursier de carrière du FRSQ". A.P.M. and J.G.L. would like to thank the University of Texas Southwestern Medical Center to have allowed the initiation of this work in collaboration with R.J.A.

References

[1] C.E. Kater, E.G. Biglieri, Disorders of steroid 17 alpha-hydroxylase deficiency, Endocrinol. Metab. Clin. North Am. 23 (1994) 341-357.

[2] T. Yanase, 17 alpha-Hydroxylase/17,20-lyase defects, J. Steroid Biochem. Mol. Biol. 53 (1995) 153-157.

[3] S. Nakajin, J.E. Shively, P.M. Yuan, P.F. Hall, Microsomal cytochrome P-450 from neonatal pig testis: two enzymatic activities (17 alpha-hydroxylase and c17,20-lyase) associated with one protein, Biochemistry 20 (1981) 4037-4042.

[4] M.X. Zuber, E.R. Simpson, M.R. Waterman, Expression of bovine 17 alpha-hydroxylase cytochrome P-450 cDNA in nonsteroidogenic (COS 1) cells, Science 234 (1986) 1258-1261.

[5] B.C. Chung, J. Picado-Leonard, M. Haniu, M. Bienkowski, P.F. Hall, J.E. Shively, W.L. Miller, Cytochrome P450c17 (steroid 17 alpha-hydroxylase/17,20 lyase): cloning of human adrenal and testis cDNAs indicates the same gene is expressed in both tissues, Proc. Natl. Acad. Sci. U. S. A. 84 (1987) 407-411.

[6] J.D. Fevold, J.D. Ivanovitch, U.M. Zanger, M.R. Waterman, The sequence of the 5'-end of the rat CYP17 gene, the transcription initiation site and a comparison with the homologous genes of other species, Mol. Cell Endocrinol. 95 (1993) 95-100.

[7] D. Lin, S.M. Black, Y. Nagahama, W.L. Miller, Steroid 17 alpha-hydroxylase and 17,20-lyase activities of P450c17: contributions of serine106 and P450 reductase, Endocrinology 132 (1993) 2498-2506.

[8] M. Namiki, M. Kitamura, E. Buczko, M.L. Dufau, Rat testis P-450(17)alpha cDNA: the deduced amino acid sequence, expression and secondary structural configuration, Biochem. Biophys. Res. Commun. 157 (1988) 705-712.

[9] H.R. Fevold, M.C. Lorence, J.L. McCarthy, J.M. Trant, M. Kagimoto, M.R. Waterman, J.I. Mason, Rat P450(17 alpha) from testis: characterization of a full-length cDNA encoding a unique steroid hydroxylase capable of catalyzing both delta 4- and delta 5-steroid-17,20-lyase reactions, Mol. Endocrinol. 3 (1989) 968-975.

[10] W.M. van Weerden, H.G. Bierings, G.J. van Steenbrugge, F.H. de Jong, F.H. Schroder, Adrenal glands of mouse and rat do not synthesize androgens, Life Sci. 50 (1992) 857-861.

[11] G.L. Youngblood, A.H Payne, Isolation and characterization of the mouse P450 17 alpha-hydroxylase/C17-20-lyase gene (Cyp17): transcriptional regulation of

the gene by cyclic adenosine 3',5'-monophosphate in MA-10 Leydig cells, Mol. Endocrinol. 6 (1992) 927-934.

[12] P.H. Provencher, Y. Tremblay, A. Bélanger, Effects of C19 steroids on adrenal steroidogenic enzyme activities and their mRNA levels in guinea-pig fasciculata-glomerulosa cells in primary culture, J. Endocrinol. 132 (1992) 269-276.

[13] Y. Tremblay, A. Fleury, C. Beaudoin, M. Vallée, A. Bélanger, Molecular cloning and expression of guinea pig cytochrome P450c17 cDNA (steroid 17 alpha-hydroxylase/17,20 lyase): tissue distribution, regulation, and substrate specificity of the expressed enzyme, DNA Cell Biol. 13 (1994) 1199-1212.

[14] J.G. LeHoux, A. Lefebvre, De novo synthesis of corticosteroids in hamster adrenal glands, J. Steroid Biochem. 12 (1980) 479-485.

[15] J.-G. LeHoux, J.I. Mason, L. Ducharme, In vivo effects of adrenocorticotropin on hamster adrenal steroidogenic enzymes, Endocrinology 131 (1992) 1874-1882.

[16] M. Cloutier, A. Fleury, J. Courtemanche, L. Ducharme, J.I. Mason, J.G. LeHoux, Cloning and expression of hamster adrenal cytochrome P450C17 cDNA, Ann. N. Y. Acad. Sci. 774 (1995) 294-296.

[17] M. Cloutier, A. Fleury, J. Courtemanche, L. Ducharme, J.I. Mason, J.G. LeHoux, Characterization of the adrenal cytochrome P450C17 in the hamster, a small animal model for the study of adrenal dehydroepiandrosterone biosynthesis, DNA Cell Biol. 16 (1997) 357-368.

[18] N. Brière, D. Martel, M. Cloutier, J.G. LeHoux, Immunolocalization and biochemical determination of cytochrome P450C17 in adrenals of hamsters treated with ACTH, J. Histochem. Cytochem. 45 (1997) 1409-1416.

[19] F. L. Graham, A.J. Eb, A new technique for the assay of infectivity of human adenovirus 5 DNA, Virology 52 (1973) 456-467.

[20] T.E. Ferrin, C.C. Huang, L.E. Jarvis, R. Langridge, The MIDAS display system, J. Mol. Graphics 6 (1998) 13-27.

[21] T.L. Pearlman, D.A. Case, J.W. Caldwell, W.S. Ross, T.E. Cheatham, D.M. Ferguson, G.L. Seibel, U.C. Sing, P.K. Weiner, P.A. Kollman, Amber 4.1 User manual. University of California at San Fransisco, San Francisco, CA, (1995).

[22] R.J. Auchus, W.L. Miller, Molecular modeling of human P450c17 (17alpha-hydroxylase/17,20-lyase): insights into reaction mechanisms and effects of mutations, Mol. Endocrinol. 13 (1999) 1169-1182.

[23] C.A. Hasemann, K.G. Ravichandran, J.A. Peterson, J. Deisenhofer, Crystal structure and refinement of cytochrome P450terp at 2.3 A resolution, Journal of Molecular Biology 236 (1994) 1169-1185.

[24] G.S. Geller, A. Farhi, N. Pinkerton, M. Fradley, M. Mortitz, A. Spitzer, G. Meinke, F.T. Tsai, P.B. Sigler, R.P. Lifton, Activating mineralocorticoid receptor mutation in hypertension exacerbated by pregnancy, Science 289 (2000) 119-123.

[25] C. Beaudoin, B. Lavallée, Y. Tremblay, D.W. Hum, R. Breton, Y. de Launoit, A. Bélanger, Modulation of 17alpha-hydroxylase/17,20-lyase activity of guinea pig cytochrome P450c17 by site-directed mutagenesis, DNA Cell Biol. 17 (1998) 707-715.

[26] R. Ahlgren, T. Yanase, E.R. Simpson, J.S. Winter, M.R. Waterman, Compound heterozygous mutations (Arg 239----stop, Pro 342----Thr) in the CYP17 (P45017 alpha) gene lead to ambiguous external genitalia in a male patient with partial combined 17 alpha-hydroxylase/17,20-lyase deficiency, J. Clin. Endocrinol. Metab. 74 (1992) 667-672.

[27] G. Rumsby, C. Skinner, H.A. Lee, J.W. Honour, Combined 17 alpha-hydroxylase/17,20-lyase deficiency caused by heterozygous stop codons in the cytochrome P450 17 alpha-hydroxylase gene, Clin. Endocrinol. (Oxf.) 39 (1993) 483-485.

[28] N. Laflamme, J.F. Leblanc, J. Mailloux, N. Faure, F. Labrie, J. Simard, Mutation R96W in cytochrome P450c17 gene causes combined 17 alpha-hydroxylase/17-20-lyase deficiency in two French Canadian patients, J. Clin. Endocrinol. Metab. 81 (1996) 264-268.

[29] K.G. Ravichandran, S.S. Boddupalli, C.A. Hasermann, J.A. Peterson, J. Deisenhofer, Crystal structure of hemoprotein domain of P450BM-3, a prototype for microsomal P450's, Science 261 (1993) 731-736.

[30] C.E. Fardella, D.W. Hum, J. Homoki, W.L. Miller, Point mutation of Arg440 to His in cytochrome P450c17 causes severe 17 alpha-hydroxylase deficiency, J. Clin. Endocrinol. Metab. 79 (1994) 160-164.

[31] H. Yamaguchi, M. Nakazato, M. Miyazato, K. Kangawa, S. Matsukura, A 5'-splice site mutation in the cytochrome P450 steroid 17alpha-hydroxylase gene in 17alpha-hydroxylase deficiency, J. Clin. Endocrinol. Metab. 82 (1997) 1934-1938.

[32] C.W. Lam, W. Arlt, C.K. Chan, J.W. Honour, C.J. Lin, S.F. Tong, K.W. Choy, W.L. Miller, Mutation of Proline 409 to Arginine in the Meander Region of Cytochrome P450c17 Causes Severe 17alpha-Hydroxylase Deficiency, Mol. Genet. Metab 72 (2001) 254-259.

[33] H. Yeom, S.G. Sligar, Oxygen activation by cytochrome P450BM-3: effects of mutating an active site acidic residue, Arch. Biochem. Biophys. 337 (1997) 209-216.

Fig. 1.

A

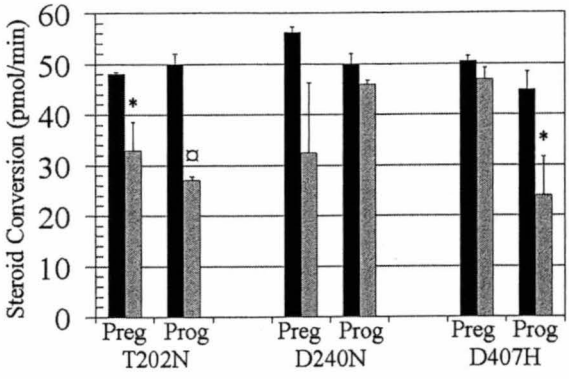
Steroid Conversion (pmol/min)
60
50
40
30
20
10
0
*
¤
*
Preg
Prog
T202N
Preg
Prog
D240N
Preg
Prog
D407H

B

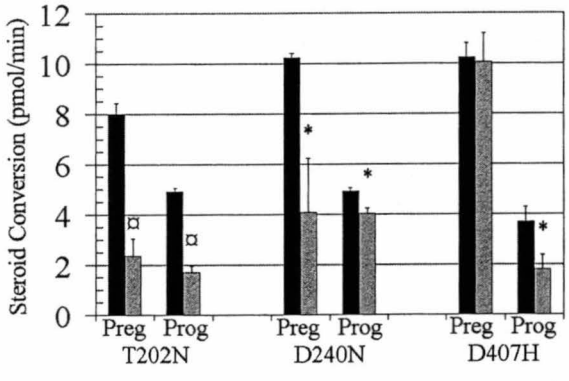
Steroid Conversion (pmol/min)
12
10
8
6
4
2
0
¤
¤
*
*
*
Preg
Prog
T202N
Preg
Prog
D240N
Preg
Prog
D407H

Fig. 2.


A 1.1 1.2 B 1.5
Hum HMHNNFFKLQKKY G PIYSVRM GT KTTVIV G HHQLAKEVLI KKG KDFSG R 96
Ham HPHVNFFKLQEKY G PIYSLRL GS TTTVII G QYQLAKEVLV KKG KEFSG R 96
B′ C
Hum PQMATLDIASNN RKGIAFADS GAHWQLHRRLAMA TFALFKDGDQK 141
Ham PHMVTLGLLSDQ GKGIAFADS GGSWQLHRKLALS SFALFRDGNQK 141
D 3.1 E
Hum LEKIICQEISTLCDMLATH NGQ SIDI SF PVFVAVTNVISLICF NTSYKNGD 192
Ham LEKIICQKASSLCDFLLTH NEE SIDL SE PIFNSITNIICIICF GISYENRD 192
F G
Hum PELNVIQNYNEGIIDNLSK DSLVDLVPWLKIF PNKTLEKLKSHVKIRNDLLNKILENYKEK 253
Ham PILATIKSFTEGILNSLGN DHLVDIFPWLTIF PNKTVDMIKKNVKIRDEVLSGILEKCKEK 253
H I
Hum FRSDSIT NMLDTL MQAKMNSDNGNAGPDQDSELLS DNHILTTIGDIFGAG 303
Ham FNSDSIS SLMDLL IQAKTNADNNNTSEGQGSNAFS DMHILATIADIFGAG 303
I J J′ K
Hum VETTTSVVKWTLAFLLH NPQVKKKLYEEIDQNV GFSRT PTISDRNR LLLLEATI 357
Ham IETTASVLSWIIAFLLH NPEVKKKIQKEIDQNI GFSRT PTFNDRNH LLMLEATI 357
K 1.4 2.1 2.2 1.3 K′
Hum REVLRLR PVA PMLIPHK A NVDSS IG EFAVD K GTEVIIN LWALH HNEKEW 406
Ham REVLRIR PVA PMLIPHR A NSDMS IG EFSIP K FTPVIIN LWALH HSEKEW 406
Meander HB L
Hum HQPDQFMPER FLNPAGTQLISPSVSYL PFGAGPRSCI GEILARQELFLIMAWLLQ 461
Ham DQPDRFMPER FLDPTGSHLITPSLSYL PFGAGARSCI GEVLARQELFLFMAHLLQ 461
3.3 4.1 4.2 3.2

Fig. 3.

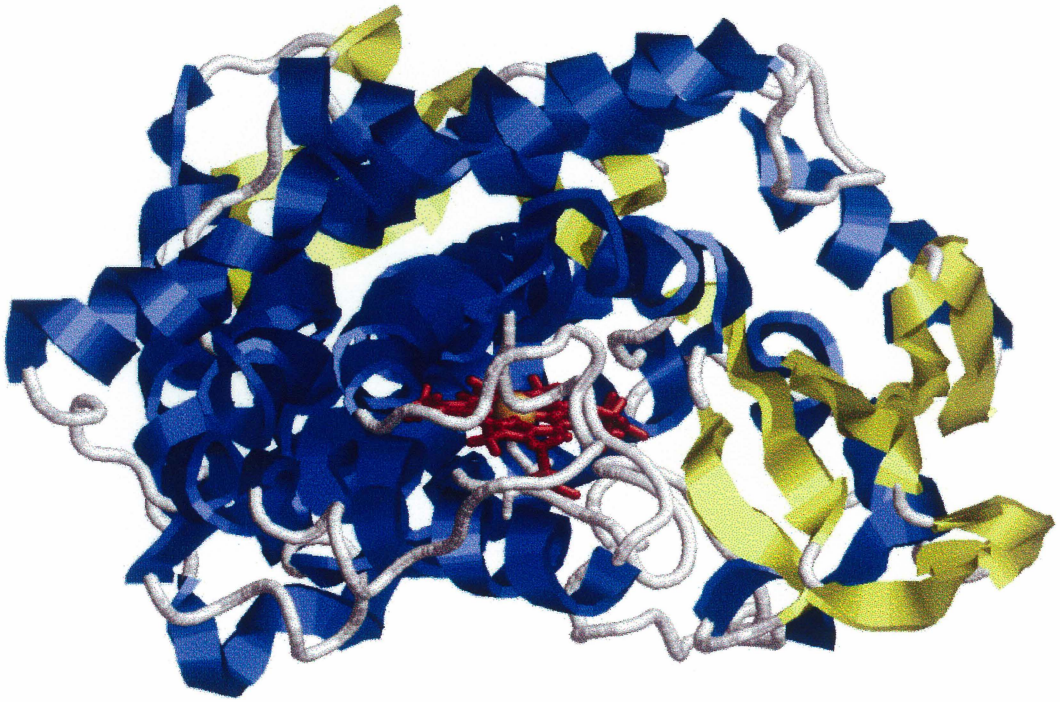

Fig. 4.

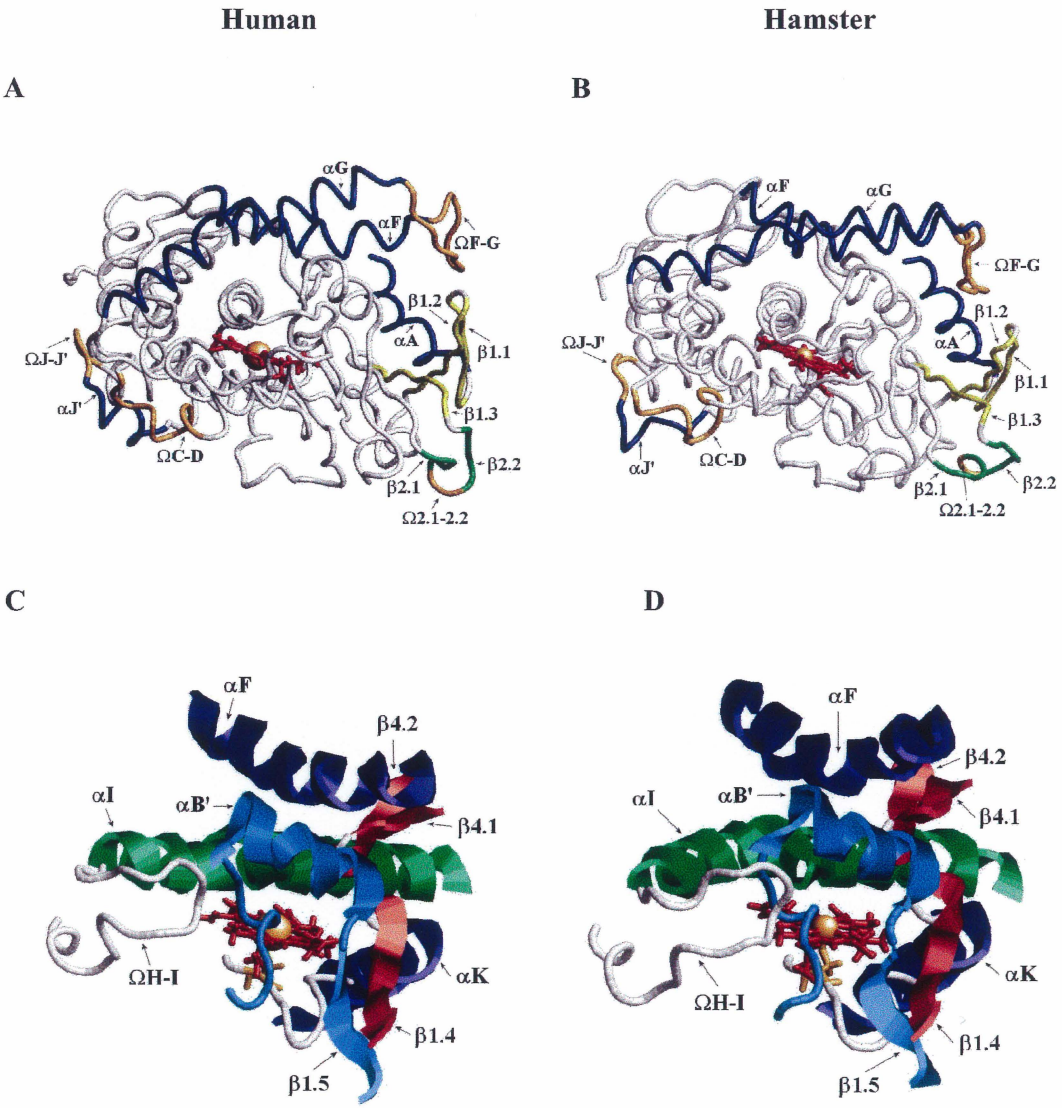
Human
Hamster
A
B
αG
αF
ΩF-G
β1.2
αA
β1.1
ΩJ-J'
αJ'
β1.3
ΩC-D
β2.2
β2.1
Ω2.1-2.2
C
D
αI
αB'
β4.2
β4.1
ΩH-I
αK
β1.4
β1.5

Fig. 5.

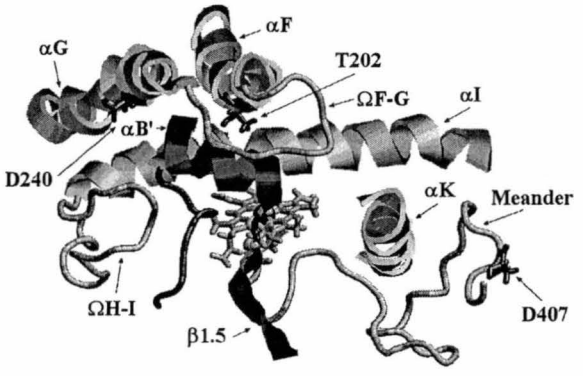

Table 1. Sequence alignment of P450c17 of various species.

Mutation :	T202N	D240N	D407H
Hamster	SF **T** EG	IR **D** EV	EW **D** QP
Mouse	TF **T** EG	IR **E** KT	EW **D** QP
Rat	TF **T** EG	VR **N** EV	EW **D** QP
G. Pig	RF **T** TG	IR **G** AM	EW **D** RP
Human	NY **N** EG	IR **N** DL	EW **H** QP
Aries	NV **N** DG	TR **N** EL	EW **Q** QP
Bovine	NV **N** DG	TR **N** EL	EW **Q** HP
Porcine	NF **N** DG	MR **N** EL	EW **L** RP

Table 2. Summary of activity alterations by site-directed mutagenesis, compared to wild type hamster P450c17.

	Pregnenolone		Progesterone	
	17OH[a]	17,20[b]	17OH	17,20
T202N	-32%	-70%	-46%	-66%
D240N	=[c]	-60%	=	-18%
D407H	=	=	-46%	-51%

[a]17OH is 17α-hydroxylase activity
[b]17,20 is 17,20-lyase activity
[c]= no significant change in activity

Fig. 1. Mutant Activity Alterations of the Hamster P450c17.

A, 17α-hydroxylase activity; B, 17,20-lyase activity. Wild type hamster P450c17 in black solid bars; light grey solid bars, mutants as designated by x-axis; SEM denoted by lines; * representing statistically significant results (*$p<0.05$ and ¤$p<0.01$, 3 experiments performed in triplicate).

Fig. 2. Alignment of the Hamster (Ham) and Human (Hum) P450c17 Amino Acid Sequences.

The models begin at amino acid position 48 and terminate at position 501. Residues belonging to structured elements are in ***boldface type*** with the highly conserved residues (C-helix tryptophan, catalytic threonine in the I-helix, the ExxR sequence in the K-helix, and the axial heme-liganding C442) *underlined.* Alpha-helices are alphabetically identified and the β-sheets are numbered. HB, Heme-binding.

Fig. 3. Final Hamster P450c17 Model.

The molecule is shown as a ribbon diagram with the α-helices in light blue, the β-sheets in yellow, the loops in white, the heme and axial C442 in red, and the heme iron in gold.

Fig. 4. Comparison of the Human and Hamster P450c17 Models.

A, Trace diagram of the human P450c17 model. The heme is shown in red with the gold iron atom, α-helices blue, β-sheets yellow or green, notable loops in orange, and the rest of the molecule in white. B, Same representation as in panel A but for the hamster P450c17 model. C, Ribbon diagram of the human P450c17 model's active site. The heme

is shown in red with the gold iron atom and axial C442, substrate entrance composed of β-sheet 1.5, B'-helix and adjacent loops in cyan, and remaining loops in white. D, Same representation as in panel C, but for the hamster P450c17 model's active site. α = α-helix, β = β-sheets, Ω = loops.

Fig. 5. Localisation of the mutants.

Ribbon diagram of the wild type hamster P450c17 model viewed from the substrate entrance, demonstrating localization of the mutants created: T202N, D240N, and D407H. Substrate entrance and mutant positions in dark grey; everything else in light grey but the heme iron in black. α = α-helix, β = β-sheets, Ω = loops.

3.3. Mathieu AP. LeHoux JG. Auchus RJ. Molecular Dynamics of Substrate Complexes With Hamster P450c17: Mechanistic Approach to Understanding Substrate Binding and Activities. [Journal Article] ***Biochemica Biophysica ACTA – Revised 01/2002.***

Contribution: Everything in this article is the product of my work.

Molecular dynamics of substrate complexes with hamster cytochrome P450c17 (CYP17): mechanistic approach to understanding substrate binding and activities

Axel P. Mathieu[a], Jean-Guy LeHoux[a], and Richard J. Auchus[b]*

[a] Department of Biochemistry, Faculty of Medicine, University of Sherbrooke, QC, Canada, J1H 5N4.

[b] Division of Endocrinology and Metabolism, UT Southwestern Medical Center, Dallas, TX, USA, 75390-8857

* Corresponding Author. Division of Endocrinology and Metabolism, UT Southwestern Medical Center, 5323 Harry Hines Blvd., Dallas, TX, USA, 75390-8857. Phone: (214) 648-6751; FAX: (214) 648-8917; E-mail: richard.auchus@UTsouthwestern.edu

Keywords: Cytochrome P450c17 (CYP17), 17α-hydroxylase/17,20-lyase, hamster adrenal glands, computer modeling, molecular dynamics, steroid hormones

Abstract

The cytochrome P450c17 isoforms from various animal species have different substrate selectivity, especially for 17,20-lyase activity. In particular, the human P450c17 selectively produces dehydroepiandrosterone with little androstenedione. Hamster P450c17, on the other hand, produces both of these steroids at comparable rates. We thus investigated if computational analysis could explain the difference in activity profiles. Therefore, we inserted the four P450c17 substrates—pregnenolone, progesterone, and their 17α-hydroxylated forms—inside our hamster P450c17 model, which we derived from our human P450c17 model based on the crystal structure of P450BMP. We performed molecular dynamics simulations on the complexes and analyzed the resultant trajectories to identify amino acids that interact with substrates. Starting with substrates in two different orientations, we obtained two sets of binding trajectories in each case. The first set of trajectories reveal structural rearrangements that occur during binding, whereas the second set of trajectories reflects substrate orientations during catalysis. Our modeling suggests that three distinct steps are required for substrate selectivity and binding to the hamster P450c17: 1) recognition of the substrate at the putative substrate entrance, characterized by a pocket at the surface of the hamster P450c17 containing charged residues R96 and D116; 2) entry of the substrate into the active site, in an intermediate position directed by possible hydrogen bonding of the substrates with the heme D-ring propionate group, R96, R440, and T306; followed by 3) 90° counter-clockwise rotation of the substrates, positioning them in optimal position for reactivity, a process that may be directed by hydrogen bonding to the 110-112 region of the hamster P450c17. With some substrates, we obtained trajectories which suggest that major

distortions in the I-helix and opening of the H-I loop occur during substrate binding. In conclusion, these modeling exercises provide insight to possible structural reorganizations that occur during substrate binding and suggest that amino acids that participate in three distinct steps of this process may all contribute to substrate binding and activity.

Abbreviations: Cytochrome P450 17α-hydroxylase/17,20-lyase (P450c17), dehydroepiandrosterone (DHEA), androstenedione (AD), 17α-hydroxypregnenolone (17OHPreg), 17α-hydroxyprogesterone (17OHProg), energy minimization (EM), molecular dynamics (MD), carbon 17 (C_{17}), carbon 20 (C_{20}), hydroxy oxygen on C_{17} (O_{C17}), heme iron (Fe), heme oxene oxygen (O_{Fe}) the 3β-hydroxyl group (C_3-O), C_{20} ketone (C_{20}=O), C_3 ketone oxygen (C_3=O), backbone nitrogen (N_b), backbone oxygen (O_b), the C_{17} hydrogen to heme ferryl oxygen distance (H_{C17}-O_{Fe}), and the C_{17} oxygen to heme iron oxygen distance (O_{C17}-O_{Fe}).

Running Title: Molecular dynamics P450c17-substrate complexes

1. Introduction

The cytochrome P450 17α-hydroxylase/17,20-lyase (P450c17) plays a central role in the control in steroid hormone metabolism, regulating the flux of precursors to glucocorticoids and androgens. P450c17 is an endoplasmic reticulum membrane-bound bi-functional enzyme harboring two distinct activities in a unique active site. The first activity of the P450c17 is 17α-hydroxylation, which hydroxylates both pregenenolone and progesterone at the steroid carbon 17 (C_{17}). The 17α-hydroxyprogesterone (17OHProg) can then be converted into cortisol, the major glucocorticoid in humans, through the activities of other steroidogenic enzymes. Both the 17α-hydroxypregenenolone (17OHPreg) and 17OHProg can be converted to their 17,20-cleaved products, dehydroepiandrosterone (DHEA) and androstenedione (AD) respectively, by the 17,20-lyase activity of P450c17. In humans however, the 17,20-lyase activity for the production of AD is approximately 50 times less efficient than for the production of DHEA [1;2].

P450c17 is expressed from a single gene (*CYP17*) in human adrenal glands and gonads [3], but the adrenal 17,20-lyase activity, and hence DHEA formation, is subjected to developmental regulation (adrenarche) [4]. Adrenal expression of the *CYP17* gene is stimulated by adrenocorticotropic hormone (ACTH), which in turn is negatively regulated by cortisol, creating a tight control of P450c17 expression [5;6]. Contrary to humans, rats [7-10] and mice [11;12] do not express adrenal P450c17; corticosterone is the major glucocorticoid in these species. Moreover, since rat and mouse P450c17 preferentially produce AD instead of DHEA, these animal models are not ideally suited for the study of human steroidogenesis. However, we have demonstrated that the hamster

does express adrenal P450c17 [13;14] and that hamster P450c17 is located in the adrenal smooth endoplasmic reticulum [15]. Unlike the human and bovine isoforms, hamster P450c17 exhibits comparable 17,20-lyase activity for both Δ^4 and Δ^5 pathways, producing both AD and DHEA from their respective precursors in abundant quantities [14]. Moreover, as in humans, cortisol is the major glucocorticoid in the hamster [16;17]. Recently, we have modeled hamster P450c17 using the human P450c17 coordinate file as template and have shown that rational site-directed mutagenesis can specifically alter the activities of hamster P450c17 [18]. Moreover, our analysis of the structural differences between the human and hamster models identified regions, most notably the I-helix, that might account for differences in substrate specificity of the two enzymes. The hamster P450c17 model showed a bulge near the catalytically important T306 and a kinking of the H-I loop, allowing the latter to interact with the B'-C loop of the putative substrate entrance. This analysis suggests at least two determinants of substrate selectivity: T306 and residues near the substrate entrance. We thus investigated if molecular dynamics of substrates bound to the hamster P450c17 model could explain the contrasting activity profile of the hamster and human P450c17 isoforms. Here, we modeled the four P450c17 substrates—pregnenolone, progesterone, and their 17α-hydroxylated forms—inside our hamster P450c17 model and performed molecular dynamics on the docked complexes. Our results suggest that the mechanism of substrate selectivity and intake into the hamster P450c17 requires several steps: 1) recognition of the substrate at the putative substrate entrance by the residues R96 and D116; 2) entry of the substrate in a temporary conformation, directed by possible hydrogen bonding (H-bonding) of the substrates with the heme D-ring propionate group, R96, R440, and T306; followed by 3) a 90° counter-

clockwise rotation, settling the substrates in an optimal position for reactivity, directed by H-bonding to the residues in the 110-112 region.

2. Material and methods

2.1 Instrumentation

All the substrates were manually docked inside the hamster P450c17 model using the Midas Plus 2.1 Graphics program [19] on a Silicon Graphics Octane workstation. All energy minimization (EM) and molecular dynamic (MD) calculations were accomplished using the Amber 5.0 suite of programs [20] remotely on the Digital Equipment Corp. AlphaServer host *socrates* at the University of California at San Francisco (UCSF) Computer Graphics Laboratory.

2.2 Substrate docking and molecular modeling

The hamster model (PDBID: 1JO9, [18]) was constructed by amino acid substitution on our human P450c17 model (PDBID: 2C17, [21]), which, in turn, used the crystal structure of P450BMP as template (PDBID: 2HPD, [22]). These models delete the membrane-spanning amino-termini and start at residues 48, corresponding to the first structured element of P450BMP. The hamster model was overlaid on a pregnenolone-docked human model by superimposing the heme nitrogens to allow proper substrate positioning. The hamster P450c17 heme was modeled as the ferryl oxene species using files and parameters develop for the human P450c17 model [21]. Other substrates were then substituted for pregnenolone, taking care not to overlap any atoms in the hamster model. The substrates were placed in similar positions with the carbon-17 (C_{17}) above the

heme iron. The substrates were then fixed in space as the protein was allowed to adjust to accommodate the docked steroids during 200 cycles of EM using the BELLY option of the Sander module. The models were then solvated as previously described [18], with a solvent sphere radius of 25 Å in order to completely solvate the area surrounding the active site. Then, the docked complexes were subjected to MD, first pre-equilibrating the water molecules for 10 ps, and then running the entire solvated structure for another 100 ps. Average structures were obtained as previously described [18].

2.3 Rendering

All images were rendered using WebLab Viewer (www.accelrys.com) for the tube and stick snapshots, and InsightII (www.accelrys.com) for all the accessible surfaces.

3. Results

3.1 Comparison to human P450c17 model and generation of two sets of trajectories

In order to understand the reaction specificity of the different P450c17s, we compared the active sites with the appropriate substrates bound. Upon visualization of the resultant model for the progesterone-docked hamster P450c17 model, we realized that progesterone had caused a depression of the heme and an elevation of the H-I loop compared to the substrate-free model, leading to the distortion of the I-helix (Fig. 1). Since this distortion had not been previously observed during MD of substrate complexes with the human P450c17 model [21], we carefully compared the docking of substrate to the two models. Upon re-examination, the starting positioning of progesterone was different in the hamster and human P450c17 substrate-docked models. In the human model, the progesterone A-ring was located above the heme D-ring, to the right of the

propionate group as viewed from the putative substrate entrance (as in Fig 1C). In the first series of the hamster P450c17 substrate-docked models, in contrast, the steroid A-ring was located to the left of the propionate group of the same heme D-ring (Fig. 1B). This difference positioned the steroid A-ring closer to the substrate entrance and caused the heme D-ring propionate group to settle in the plane of the heme, rather than upwards as in the human model. In order to verify that the observed distortion of the I-helix was a consequence of the substrate positioning on the active site conformation, we obtained a second series of substrate-docked hamster-P450c17 models (Fig. 1C).

In the second series, the substrates were docked with the steroid A-ring to the right of the heme D-ring propionate group and lifted from the heme, being careful to not overlap atoms in the "roof" of the active site, thus leaving more space for the heme propionate group. The second set of models was then subjected to EM, solvation, and MD as for the first models.

3.2 Progesterone-docked hamster P450c17

A great deal of model distortion occurred in the first attempt to dock progesterone in the hamster P450c17 model. In this distorted conformation (Fig. 1B and Fig. 2A), the C_{20} carbonyl (C_{20}=O) can H-bond with the γ-hydroxyl of T306 (2.73Å) and lies near the backbone oxygen (O_b) of G303 (3.37Å); the C_3 carbonyl oxygen (C_3=O) interacts with R96 and R440 guanidinium groups (3.61Å and 4.09Å, respectively). Interaction with T306 is unlikely to be maintained because during catalysis, because T306 is believed to be involved in oxygen homolysis [23]. In the second series of models (Fig 1C and Fig. 2B), the progesterone settled after a quarter turn counter-clockwise above the heme. The closest polar group for C_3=O in this position is the backbone nitrogen (N_b) of L370

(3.60Å). The counter-clockwise rotation of progesterone causes the C_{17} hydrogen to be closer to the heme iron: the C_{17} hydrogen to heme ferryl oxene distance (H_{C17}-O_{Fe}) decreased by 1.07 Å from 3.55Å to 2.48Å.

3.3 Pregnenolone-docked hamster P450c17

When pregnenolone was docked into the hamster P450c17 model, the initial model only had slight distortion of the I-helix (data not shown). The heme remained fixed relative to the I-helix, and the N-terminus of the I-helix kinked only slightly as compared to the initial progesterone-docked hamster P450c17 model. In this case, pregnenolone remains in position by possible interaction of C_{20}=O to the T306 hydroxyl group and/or N_b of V366 (4.01Å and 5.16Å respectively – Fig. 2C). The 3β-hydroxyl group (C_3-OH) could interact with R440 and/or R96 guanidinium groups (3.29Å and 3.11Å respectively – Fig. 2C), but the heme D-ring propionate group is closer than these polar groups (2.88Å), suggesting that the heme itself may help to position pregnenolone through H-bonding. In the second series of models (Fig. 2D), pregnenolone also rotated a quarter turn counter-clockwise as viewed from above the heme. In this position, the C_{20}=O is surrounded by the R440 guanidinium nitrogens (2.79Å). However, the C_3-OH does not appear to be anchored by any specific interactions; the closest polar atoms are the N_b of A367 and P321 (4.22Åand 4.46Å, respectively – Fig. 2D). Curiously, the only H-bonding obtained in these pregnenolone-docked models is the bonding of pregnenolone to the heme propionate groups seen also in the first model series. Through the change from the first to the second model series, the H_{C17}-O_{Fe} ranged from 2.40Å to 4.20Å.

3.4 Docking of 17OHPreg and 17OHProg in the hamster P450c17

When 17OHPreg and 17OHProg are inserted in the hamster P450c17 model, they both greatly resemble the models obtained for the progesterone-docked hamster P450c17. In the first 17OHPreg model (Fig. 2E), the 17OHPreg is restrained in position by H-bonding of C_{20}=O to the ε-amino group of K110 (2.92Å) and by H-bonding of C_3-OH to N_b of R96 (3.39Å). The C_3-OH however, can also H-bond to the heme D-ring propionate group (2.84Å) or to the guanidinium group of R440 (4.32Å). After the counter-clockwise rotation (Fig. 2F), only C_{20}=O H-bonding is maintained; C_{20}=O can H-bond to the N_b of G111 or I112 (3.12Å and 3.15Å respectively), while the C_3-OH could interact with the O_b of M369 (2.78Å). The rotation of the 17OHPreg inside the active site of the hamster P450c17 brings the C_{17} center closer to the heme iron; the C_{17}-O to the ferryl oxene (O_{C17}-O_{Fe}) distance is brought closer from 2.48Å to 2.43Å.

Docked 17OHProg (Fig. 2G) is maintained in position by possible H-bonding of the C_3=O to R96 (2.79Å) and the C_{20}=O to T306 (2.73Å). Moreover, other polar groups are accessible to C_3=O, such as the guanidinium group of R440 (3.2Å) and the hydroxyl group of S94 (4.03 Å). After the counter-clockwise rotation (Fig. 2H), no H-bonding is observed, although the C_3=O is near N_b of L370 (4.63Å). The C_{20}=O is located near the K111 amino group (2.75Å) and the N_b of G303 and A302 (3.60Å and 3.88Å, respectively). The O_{C17}-O_{Fe} distance is reduced from 2.75Å to 2.41Å after the counter-clockwise rotation.

3.5 Molecular surface of the putative substrate entrance and of the hamster P450c17 active site

The molecular surface of the substrate-free hamster P450c17 putative substrate entrance was investigated for possible features that might facilitate substrate uptake into the active site. The first observation is that the putative substrate entrance forms a cleft in the hamster P450c17 surface, characterized by a mostly hydrophobic surface with the exception of two charged residues: R96 and D116 (Fig. 3A and 3B). As viewed in Fig. 3A, R96 and D116 align with T306 located in the middle of the I helix immediately across the substrate binding site, and these two residues are perfectly placed to orient entering substrates close to and parallel to the heme. This analysis therefore suggests that these amino acids are not only important for restraining the substrates in the hamster P450c17 active site, but might also participate in the mechanism of substrate uptake and selectivity, placing steroids inside the active site pocket. This participation in substrate selection could be driven by the polar C_{20}=O common to most P450c17 substrates. The hamster P450c17 active site pocket itself is mostly hydrophobic with the exception of the R96 and R440 closing the substrate entrance and T306 hydroxyl group located directly opposite these residues (Fig. 3C). Interestingly, as the substrate enters the active site (Fig. 3C), distortion of the I-helix and movement of the 110-112 region creates space adjacent to the entering substrate allowing the substrate to reposition by a counterclockwise rotation. This process is shown in the close-up view in Fig. 3E, depicted by the "empty" volume immediately adjacent the C_{20}=O (next to I112 in grey), which may permit or direct the substrate to rotate counter-clockwise a quarter turn (Fig. 3D and 3F).

4. Discussion

For each docked substrate inside the hamster model, we obtained two sets of molecular dynamics trajectories depicting two possible binding modes of the substrates inside the hamster P450c17 binding site. It was previously predicted that P450c17 would have a bi-lobed active site, based on initial models based on structures of P450cam [24;25] and P450BMP [26]. On the other hand, the tight association of the substrates in the active site of a more recent and more carefully validated human P450c17 model suggested that only one binding conformation was possible [21] and that perpendicular binding of substrates to the heme in the P450c17 is not possible. Here, tight association of the substrates inside the hamster P450c17 model is also obtained; perpendicular binding of the substrates is impossible as there is insufficient space in the substrate-binding pocket [18]. The first set of models and the trajectories obtained during MD, in which the active site opens somewhat, appear to reflect conformational changes that occur during substrate binding rather than catalysis. The second set of substrate-bound models show substrate orientation during catalysis. This conclusion is supported by the fact that, with the exception of pregnenolone, all substrates' H_{C17} (or O_{C17}) moved closer to the heme reactive ferryl oxene (Table 1) after the counter clockwise rotation in the second set of models. The unexpectedly discordant interactions observed in the two sets of models, despite only subtle differences in starting substrate orientation, also illustrates the importance of careful substrate positioning when conducting MD calculations on docked complexes.

Interestingly, the C_3-OH of pregnenolone and 17OHPreg seem to be H-bonding to the heme D-ring propionate group (Table 2), which suggests that the heme may participate in

positioning of the Δ^5-substrates in the active site. These interactions were not observed with the progesterone substrates, as these steroids do not have the required hydroxyl group at C_3 to donate a H-bond to the heme propionate group. This H-bonding may provide sufficient substrate stabilization for mutation D240N to retain nearly normal 17α-hydroxylase activity with pregnenolone, despite impaired 17, 20-lyase activity for 17OHPreg, presumably due to active site crowding [18].

Careful investigation of the substrate entrance and binding site inside hamster P450c17 reveals key residues that may mediate different stages of substrate binding. The exterior surface of the entrance is composed of two charged residues, R96 and D116, aligned directly with the active site. Previously, the mutation R96W has been demonstrated to abolish all activity in human P450c17, supporting its role in substrate recognition and binding [27], and we note that the hamster and human enzymes are nearly identical in the region of residues 90-120:

Hamster	G KEFSGRPHMV TLGLLSDQGK GIAFADSGGS
Human	G KDFSGRPQMA TLDIASNNRK GIAFADSGAH

We have also demonstrated that the mutation D240N in hamster P450c17 alters R96 positioning, which may account for the specific reduction in 17,20-lyase activity observed in this mutation [18]. Thus, complete removal of the charged group on R96 abolishes P450c17 activity, and improper positioning of this residue alters substrate selectivity. Therefore, the functional domain composed of the substrate entrance (i.e.: β-sheet 1.5, the loop from β-sheet 1.5 to α-helix B', α-helix B', and the B'-C loop to amino acid D116) all contribute to substrate entry.

Independent molecular dynamics studies of P450s –cam, –BMP, and –eryF have likewise suggested a role of buried arginine residues in guiding substrate expulsion and entry [28]. In the case of P450BMP, R47 forms a salt bridge with the carboxyl group of the substrate palmitoleic acid at the opening of the active site cleft. The R47 side chain rotates outward during substrate expulsion, guiding and neutralizing the negatively charged carboxylate out of the active site cavity. Our molecular dynamics simulations suggest an analogous role of R96 in forming hydrogen bonds with substrate oxygen atoms during the docking process. Residue R96 of P450c17 is located adjacent to K72 (which corresponds to R47 in P450BMP), three strands away on the same β-sheet and somewhat closer to the interior of the protein. Since steroid molecules are more compact than palmitoleic acid in its extended conformation, it is not surprising that the adjacent but more buried R96 side chain, rather than K72, participates more extensively in substrate transit for P450c17.

Two additional sets of residues are identified from the two sets of models that appear to be responsible for directing the substrates into the active site and for properly orientating the substrates for catalysis. The amino acids clustered around T306 and R96 appear to direct or guide substrate entry. In this process, K110, G303, T306, and V366 interact with C_{20}=0, and the heme D-ring propionate group, S94, R96, and R440 are positioned to H-bond with C_3-OH (Table 2). Residues that appear to directly interact with substrate during catalysis include amino acids are amino acids A302-G303, K110-I112, and R440 (at C_{20}=O), and P321 and A367-L370 (at C_3-OH). This analysis of substrate dynamics during binding may explain why some mutations distant from the active site also destroy activity—by interfering with earlier steps in the binding process.

These results are consistent with previously reported human P450c17 mutants. For instance, the mutations R96W [27], S106P [29], and I112 duplication (I112dup) [30] have all been reported to abolish all P450c17 activity. R96W was previously implicated in active site formation; here we present evidence that the specific function of R96W in substrate recognition involves initiating substrate entrance. Moreover, mutations I112dup and S106P have been directly implicated in substrate binding in the human P450c17. Our results also support the importance of the amino acids 110-112 in substrate positioning during catalysis.

Obviously, certain amino acids are not constrained to one function but may participate in several stages of binding and turnover. Specifically, G303, K110, and R440 are located at positions that allow for several functions. G303 and K110 are located adjacent to residues that interact with C_{20}=0 during the latter stages of substrate entry and catalysis, while R440 is located near residues that interact with either C_{20}=O or with C_3-OH. Thus, due to their positioning in the active site, these amino acids can participate at different stages of substrate binding and catalysis in the hamster P450c17. Moreover, T306 and R440 have been previously reported to be important for proton donation [31] and heme binding [32], respectively. Here, our results suggest that T306 and R440 may also participate in substrate alignment during active site entry at C_{20}=O and C_3-OH respectively. Although we were not able to clearly identify the structural basis for the similar and high 17,20-lyase activities for both 17OHProg and 17OHPreg in hamster P450c17, we suspect that differences in the interactions of Δ^4 steroids with T306 may contribute to substrate discrimination.

In conclusion, we conceptualize that the substrate selectivity and intake into hamster P450c17 requires three distinct steps using three sets of residues (Fig. 3): 1) recognition of the substrate at the membrane interface with the solvent accessible surface in the putative substrate entrance by residues R96 and D116; 2) entrance of the substrate into the active site, directed by possible interactions or H-bonding to the heme D-ring propionate group, R96 and R440 at the C_3 oxygen and by T306 at the C_{20}=O; followed by 3) counter-clockwise rotation of the substrate in the active site for optimal positioning allowing reactivity.

Acknowledgements

We want to thank the UCSF Computer Graphics Laboratory (supported by NIH grant P41 RP-01081) for use of host *socrates* and Pierre Lavigne for access to the modeling workstations and InsightII. A.P. Mathieu was a recipient of a studentship from the Medical Research Council of Canada, and this work was supported by a grant from the Medical Research Council of Canada #MT-10983 (to J.G.L.) and NIH grant K08DK02387 (to R.J.A.). J.G. LeHoux is a "*chercheur boursier de carrière du FRSQ*".

References

[1] R.J. Auchus, T.C. Lee, W.L. Miller, Cytochrome b5 augments the 17,20-lyase activity of human P450c17 without direct electron transfer, J. Biol. Chem. 273 (1998) 3158-3165.

[2] P. Lee-Robichaud, J.N. Wright, M.E. Akhtar, M. Akhtar, Modulation of the activity of human 17 alpha-hydroxylase-17,20-lyase (CYP17) by cytochrome b5: endocrinological and mechanistic implications, Biochem. J. 308 (1995) 901-908.

[3] B.C. Chung, J. Picado-Leonard, M. Haniu, M. Bienkowski, P.F. Hall, J.E. Shively, W.L. Miller, Cytochrome P450c17 (steroid 17 alpha-hydroxylase/17,20 lyase): cloning of human adrenal and testis cDNAs indicates the same gene is expressed in both tissues, Proc. Natl. Acad. Sci. U. S. A 84 (1987) 407-411.

[4] C.A. Sklar, S.L. Kaplan, M.M. Grumbach, Evidence for dissociation between adrenarche and gonadarche: studies in patients with idiopathic precocious puberty, gonadal dysgenesis, isolated gonadotropin deficiency, and constitutionally delayed growth and adolescence, J. Clin. Endocrinol. Metab 51 (1980) 548-556.

[5] T. Yanase, E.R. Simpson, M.R. Waterman, 17 alpha-hydroxylase/17,20-lyase deficiency: from clinical investigation to molecular definition, Endocr. Rev. 12 (1991) 91-108.

[6] R.J. Auchus, The genetics, pathophysiology, and management of human deficiencies of P450c17, Endocrinol. Metab Clin. North Am. 30 (2001) 101-119.

[7] M. Namiki, M. Kitamura, E. Buczko, M.L. Dufau, Rat testis P-450(17)alpha cDNA: the deduced amino acid sequence, expression and secondary structural configuration, Biochem. Biophys. Res. Commun. 157 (1988) 705-712.

[8] M. Nishihara, C.A. Winters, E. Buzko, M.R. Waterman, M.L. Dufau, Hormonal regulation of rat Leydig cell cytochrome P-45017 alpha mRNA levels and

characterization of a partial length rat P-45017 alpha cDNA, Biochem. Biophys. Res. Commun. 154 (1988) 151-158.

[9] H.R. Fevold, M.C. Lorence, J.L. McCarthy, J.M. Trant, M. Kagimoto, M.R. Waterman, J.I. Mason, Rat P450(17 alpha) from testis: characterization of a full-length cDNA encoding a unique steroid hydroxylase capable of catalyzing both delta 4- and delta 5-steroid-17,20-lyase reactions, Mol. Endocrinol. 3 (1989) 968-975.

[10] W.M. van Weerden, H.G. Bierings, G.J. van Steenbrugge, F.H. de Jong, F.H. Schroder, Adrenal glands of mouse and rat do not synthesize androgens, Life Sci. 50 (1992) 857-861.

[11] L.M. Perkins, A.H. Payne, Quantification of P450scc, P450(17) alpha, and iron sulfur protein reductase in Leydig cells and adrenals of inbred strains of mice, Endocrinology 123 (1988) 2675-2682.

[12] G.L. Youngblood, C. Sartorius, B.A. Taylor, A.H. Payne, Isolation, characterization, and chromosomal mapping of mouse P450 17 alpha-hydroxylase/C17-20 lyase, Genomics 10 (1991) 270-275.

[13] M. Cloutier, A. Fleury, J. Courtemanche, L. Ducharme, J.I. Mason, J.G. LeHoux, Cloning and expression of hamster adrenal cytochrome P450C17 cDNA, Ann. N. Y. Acad. Sci. 774 (1995) 294-296.

[14] M. Cloutier, A. Fleury, J. Courtemanche, L. Ducharme, J.I. Mason, J.G. LeHoux, Characterization of the adrenal cytochrome P450C17 in the hamster, a small animal model for the study of adrenal dehydroepiandrosterone biosynthesis, DNA Cell Biol. 16 (1997) 357-368.

[15] K. Ishimura, The mechanisms of corticoids biosynthesis revealed by immunohistochemistry and in situ hybridization, Kaibogaku Zasshi 73 (1998) 111-118.

[16] S.A. Ortlip, S.A. Li, J.J. Li, Characterization of specific glucocorticoid receptor in the Syrian hamster testis, Endocrinology 109 (1981) 1331-1338.

[17] N.E. Dunlap, W.E. Grizzle, Golden Syrian hamsters: a new experimental model for adrenal compensatory hypertrophy, Endocrinology 114 (1984) 1490-1495.

[18] A.P.Mathieu, R.J.Auchus, J.G.LeHoux, Comparison of the hamster and human adrenal P450c17 (17alpha-hydroxylase/17,20-lyase) using site-directed mutagenesis and molecular modeling, J. Steroid Biochem. Mol. Biol. 80 (2002) 99-107.

[19] T.E. Ferrin, C.C. Huang, L.E. Jarvis, R. Langridge, The MIDAS display system, Journal of Molecular Graphics 6 (1998) 13-27.

[20] T.L.Pearlman, D.A.Case, J.W.Caldwell, W.S.Ross, T.E.Cheatham, D.M.Ferguson, G.L.Seibel, U.C.Sing, P.K.Weiner, P.A.Kollman, Amber 4.1 User manual, (1995) University of California at San Francisco, San Francisco, CA.

[21] R.J. Auchus, W.L. Miller, Molecular modeling of human P450c17 (17alpha-hydroxylase/17,20-lyase): insights into reaction mechanisms and effects of mutations, Mol. Endocrinol. 13 (1999) 1169-1182.

[22] K.G. Ravichandran, S.S. Boddupalli, C.A. Hasermann, J.A. Peterson, J. Deisenhofer, Crystal structure of hemoprotein domain of P450BM-3, a prototype for microsomal P450s, Science 261 (1993) 731-736.

[23] P. Lee-Robichaud, M.E. Akhtar, M. Akhtar, An analysis of the role of active site protic residues of cytochrome P-450s: mechanistic and mutational studies on 17alpha-hydroxylase-17,20-lyase (P-45017alpha also CYP17), Biochem. J. 330 (1998) 967-974.

[24] D. Lin, L.H. Zhang, E. Chiao, W.L. Miller, Modeling and mutagenesis of the active site of human P450c17, Mol. Endocrinol. 8 (1994) 392-402.

[25] C.A. Laughton, S. Neidle, M.J. Zvelebil, M.J. Sternberg, A molecular model for the enzyme cytochrome P450(17 alpha), a major target for the chemotherapy of prostatic cancer, Biochem. Biophys. Res. Commun. 171 (1990) 1160-1167.

[26] D.F. Burke, C.A. Laughton, S. Neidle, Homology modelling of the enzyme P450 17 alpha-hydroxylase/17,20-lyase--a target for prostate cancer chemotherapy--from the crystal structure of P450BM-3, Anticancer Drug Des. 12 (1997) 113-123.

[27] N. Laflamme, J.F. Leblanc, J. Mailloux, N. Faure, F. Labrie, J. Simard, Mutation R96W in cytochrome P450c17 gene causes combined 17 alpha-hydroxylase/17-20-lyase deficiency in two French Canadian patients, J. Clin. Endocrinol. Metab. 81 (1996) 264-268.

[28] P.J. Winn, S.K. Ludemann, R. Gauges, V. Lounnas, R.C. Wade, Comparison of the dynamics of substrate access channels in three cytochrome P450s reveals different opening mechanisms and a novel functional role for a buried arginine, Proc. Natl. Acad. Sci. U. S. A. 99 (2002) 5361-5366.

[29] D. Lin, J.A. Harikrishna, C.C. Moore, K.L. Jones, W.L. Miller, Missense mutation serine106→proline causes 17 alpha-hydroxylase deficiency, J. Biol. Chem. 266 (1991) 15992-15998.

[30] T. Imai, H. Globerman, J.M. Gertner, N. Kagawa, M.R. Waterman, Expression and purification of functional human 17 alpha-hydroxylase/17,20-lyase (P450c17) in Escherichia coli. Use of this system for study of a novel form of combined 17 alpha-hydroxylase/17,20-lyase deficiency, J. Biol. Chem. 268 (1993) 19681-19689.

[31] T.L. Poulos, B.C. Finzel, A.J. Howard, High-resolution crystal structure of cytochrome P450cam, J. Mol. Biol. 195 (1987) 687-700.

[32] C.E. Fardella, D.W. Hum, J. Homoki, W.L. Miller, Point mutation of Arg440 to His in cytochrome P450c17 causes severe 17 alpha-hydroxylase deficiency, J. Clin. Endocrinol. Metab. 79 (1994) 160-164.

Figure Legends:

Fig. 1. Distortion of the hamster P450c17 active site upon progesterone binding. Panel A, Unliganded hamster P450c17 model as previously obtained [18]. Panel B, First model obtained upon progesterone binding, demonstrating distortion of the I-helix. Panel C, Second model obtained upon progesterone binding, demonstrating a counter-clockwise rotation of the progesterone in the active site, settling in a similar position as previously described for the human P450c17 model [21]. The I-helix backbone is shown in tubular form with the heme and progesterone as stick diagrams. Color code: I-helix, heme, and progesterone in dark, medium, and light grey, respectively.

Fig. 2. Enzyme-substrate interactions in the hamster P450c17 active site. Two sets of substrate-bound models were obtained: the first series of models are depicted in panels A, C, E, and G, while the second series are depicted in panels B, D, F, and H. Bound substrates: progesterone (Prog) in panels A and B; pregnenolone (Preg) in panels C and D; 17α-hydroxypregnenolone (17OHPreg) in panels E and F; 17α-hydroxyprogesterone (17OHProg) in panels G and H. The heme is rendered as an accessible surface. Color code: Carbon in grey, oxygen in red, nitrogen in blue, distance monitors in green, and labels in yellow. Hydrogen atoms are not shown.

Fig. 3. Accessible surfaces of the hamster P450c17 putative substrate entrance and active site. Panel A, Ribbon representation of the hamster P450c17 without substrate, depicting the location of important structures: I-helix in red, heme in yellow sticks, putative substrate entrance (composed of β-sheet 1.5, the loop from β-sheet 1.5 to α-helix

B', α-helix B', and the B'-C loop to amino acid D116) in blue, and the amino acids R96 and D116 in green sticks, circled in blue and red respectively. Panel B, Accessible surface representation of Panel A. Panel C, Accessible surface representation of the hamster P450c17 active site with bound progesterone, as obtained in the first series of substrate-bound models. Panel D, Same representation as in panel C but after the counter clockwise rotation (second series of substrate bound models). Panels E and F, Identical representations as in C and D but at a closer perspective. Note that in order to expose the active site surface, the covering amino acids had to be removed from the top. Color code for surface representations: hydrophobic atoms in grey, and polar atoms in yellow, potentially charged atoms in red or blue (oxygen or nitrogen respectively), except for I112 and T306, which the hydrophobic atoms are colored deep grey and green, respectively. Also, the heme nitrogens are colored sky blue, the heme iron atom is pink, the heme propionate group oxygens are orange, and the iron oxene oxygen is purple. R96 and D116 are also circled in panels C and D, blue and red respectively.

Fig. 4. Proposed mechanism of substrate entrance inside the hamster P450c17 based on molecular dynamics trajectories. The tube and stick representation shows substrates entering the active site of hamster P450c17. The left and right panels are identical except for the point of view. The left panel in is the same point of view as Fig. 3A, and the right panel is rotated 90° clockwise in the plane of the page. Top: approaching substrate to the P450c17 putative substrate entrance, with recognition by R96 and D116 (D116 is omitted for simplicity). Middle: Entering substrate, directed by interactions of the C_{20}=O with T306 and the C_3-OH with R96. Bottom: Counter-clockwise rotation of substrate in the

P450c17 active site generates interactions with residues 110-112 (I112 is shown as a reference).

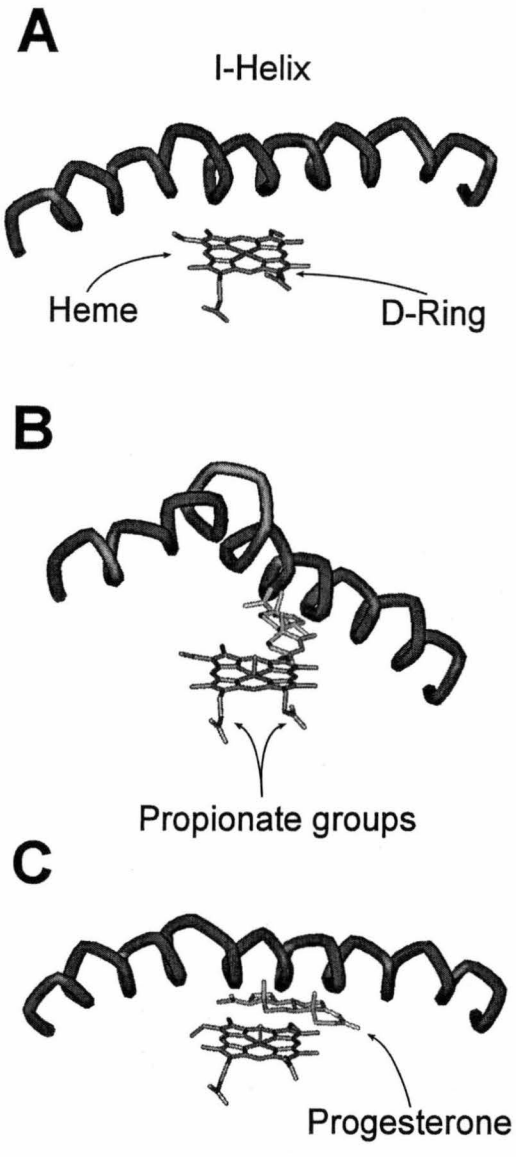
A
I-Helix
Heme
D-Ring
B
Propionate groups
C
Progesterone

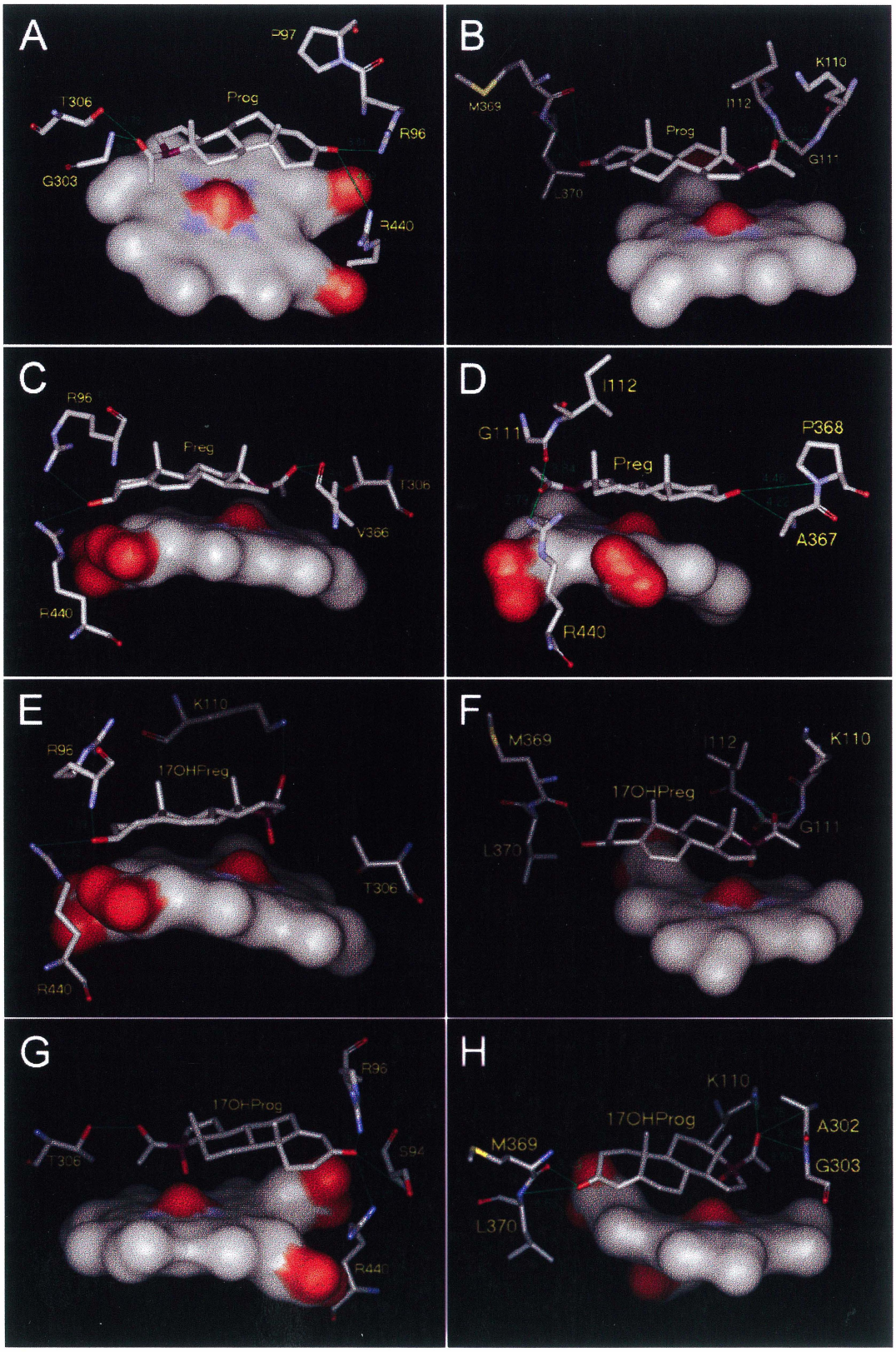
A
P97
T306
Prog
R96
G303
R440
B
K110
M369
I112
Prog
G111
L370
C
R96
Preg
T306
V366
R440
D
I112
G111
P368
Preg
A367
R440
E
K110
R96
17OHPreg
T306
R440
F
M369
I112
K110
17OHPreg
G111
L370
G
R96
17OHProg
T306
S94
R440
H
K110
17OHProg
A302
M369
G303
L370

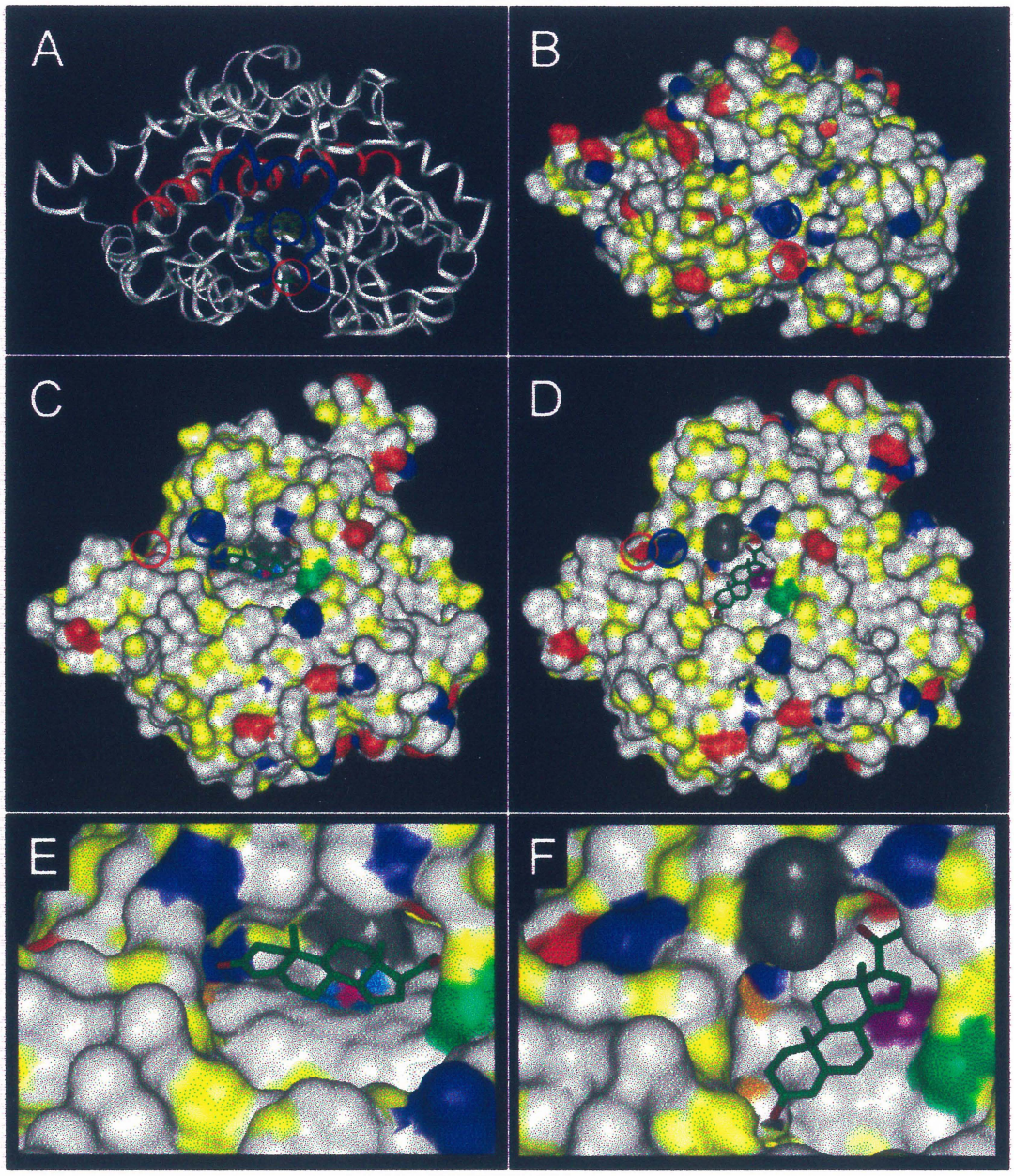
A
B
C
D
E
F

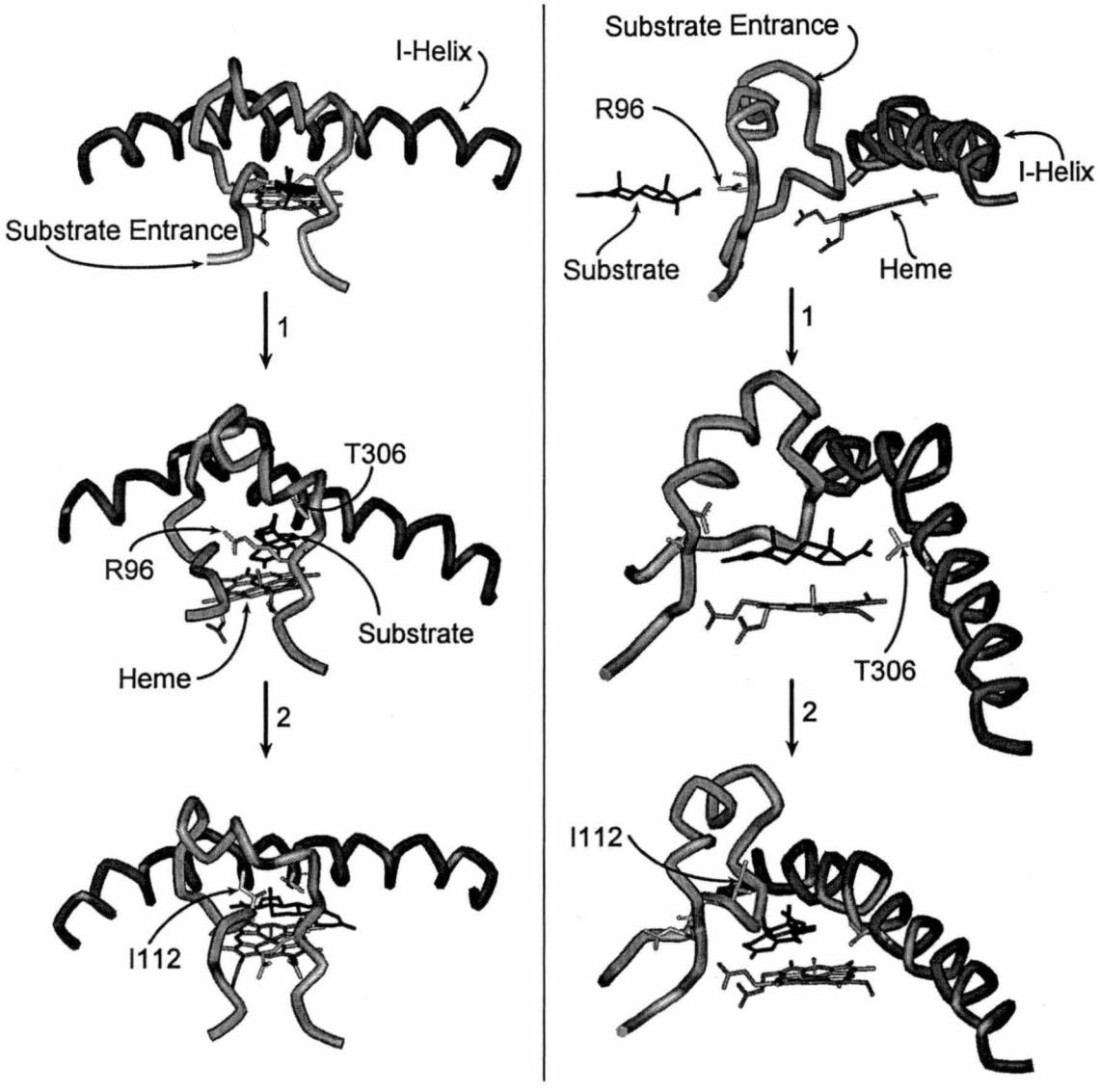
I-Helix
Substrate Entrance
1
T306
R96
Substrate
Heme
2
I112
Substrate Entrance
R96
I-Helix
Substrate
Heme
1
T306
2
I112

Table 1. Distances of the ferryl oxene to the sites of reaction on steroid substrates.

Substrate[a]	Set	H_{C17}-O_{Fe} (Å)	O_{C17}-O_{Fe} (Å)
Preg	1	2.40	NA
Preg	2	4.20	NA
17OHPreg	1	NA	2.48
17OHPreg	2	NA	2.45
Prog	1	3.55	NA
Prog	2	2.48	NA
17OHProg	1	NA	2.75
17OHProg	2	NA	2.41

[a]Abbreviations are those used in the text

H_{C17}-Fe = Distance between the hydrogen at substrate carbon 17 and the heme iron

O_{C17}-O_{FE} = Distance between the substrate hydroxyl oxygen at carbon 17 and the heme ferryl oxene

NA = Not applicable

Table 2. Summary of the important atomic interactions restraining substrate positioning in the hamster P450c17 models.

Substrate[a]	Set	Restraining Interactions	
		C_3-O (Å)	C_{20}=O (Å)
Preg	1	HProp (2.88)[H]	T306 (4.01)
		R440 (3.29)	V366 (5.16)
		R96 (3.11)	
Preg	2	A367 (4.22)	R440 (2.79)
		P321 (4.46)	G111 (3.84)
17OHPreg	1	HProp (2.84)[H]	
		R96 (3.39)[H]	K110 (2.92)[H]
		R440 (4.32)	
17OHPreg	2	M369 (2.78)	G111 (3.12)[H]
			I112 (3.15)[H]
Prog	1	R96 (3.61)	T306 (2.73)[H]
		R440 (4.09)	G303 (3.37)[H]
Prog	2	L370 (3.60)	G111 (3.08)[H]
		M369 (4.19)	I112 (3.46)
17OHProg	1	R96 (2.79)[H]	
		R440 (3.20)	T306 (2.73)[H]
		S94 (4.03)	
17OHProg	2	M369 (3.49)	K110 (2.75)
		L370 (4.63)	G303 (3.60)
			A302 (3.88)

[a]Abbreviations are those used in the text

C_3-O = Substrate oxygen at carbon 3 (Hydroxyl group for pregnenolone and ketonic group for progesterone)

C_{20}=O = Substrate ketonic group at carbon 20

[H]Possible hydrogen bonding

HProp = Heme D-ring propionate group

4. Discussion:

4.1. StAR:

4.1.1. Homology Modeling: The hamster and human StAR models were obtained by homology modeling based on the recent structural crystallographic data of the human MLN64 (Tsujishita and Hurley, 2000). As predicted by the strong homology of the amino acid sequences, the overall structure of the MLN64 and StAR models resemble to a great extent. The most notable difference between the models and the MLN64 crystal is the loss of the hydrophic tunnel in the StAR models, replaced by a closed hydrophobic cavity. This cavity therefore suggests that physical opening of StAR secondary structures is necessary to allow cholesterol inside, to transport cholesterol into mitochondria.

This hydrophobic cavity is characterized by an entire hydrophobic surface except for the presence of the salt bridge composed of amino acids E168 and R187 in the hamster model (E169 and R188 in the human – for simplicity, only the hamster model will be discussed unless stated otherwise – Chapter 2.1. Fig. 3B). As it turns out, this characteristic is crucial for StAR-dependent cholesterol transfer. Since water was trapped inside the MLN64 crystal, it is conceivable that water molecules are also present inside the StAR cavity. The contrast in properties between the polar water molecules and the hydrophobic cavity can be conceptualized as the driving force allowing the StAR to open, exposing the cavity and permitting cholesterol to bind. Indeed, according to our calculations, the presence of the water molecules inside the StAR cavity destabilizes StAR making a significant population of open unfolded StAR available for the transfer of cholesterol inside mitochondria. Moreover, the cavity took the shape of a cholesterol

molecule (Chapter 2.1. Fig. 3A), supporting the existence of the cavity in StAR and making it unambiguous to model a cholesterol molecule inside.

The cavity can be conceptualized as having two major functions: 1) acting as an anchor for proper cholesterol binding, and 2) serving as a locking-key to maintain proper minimal structure for cholesterol binding. The first function of the salt bridge is rather explicit; cholesterol is hydrophobic except for the 3β-hydroxyl group, matching the characteristics of the StAR cavity. It is not surprising that nature has developped the perfect environment in StAR for the transfer cholesterol. As a matter of fact, the salt bridge is perfectly positioned in the cavity such that when cholesterol is bound inside StAR, the salt bridge is located just the right distance from the cholesterol 3β-hydroxyl group to allow hydrogen bonding through one water molecule (Chapter 2.1. Fig. 4).

Since it is highly unfavourable to bury polar species inside a hydrophobic environment, the formation of the salt bridge is favoured to stabilize the charges on E168 and R187. Although some water molecules are certainly present inside the cavity, the nature of the cavity enviroment is principally hydrophobic (Chapter 2.1. Fig. 4). Therefore, the salt bridge can be visualized as a key feature responsible for maintaining a basic cavity structure for cholesterol binding. In fact, once StAR opens to allow cholesterol access to the cavity, the salt bridge is the only feature in the cavity that cannot change as the water molecules are displaced by cholesterol. It is imaginable that the hydrophobic residues in the cavity move as they interact with the entering hydrophobic cholesterol. On the other hand, the salt bridge can only interact with the 3β-hydroxyl group of cholesterol reducing the possibility of the salt bridge to dissociate as cholesterol enters the cavity. E168 and R187 are located on β-strands 5 and 6 respectively, basically

opposite the movable C-terminal α-helix and forming the pit of the bowl shape cavity. Thus it is foreseeable that the salt bridge maintains the cavity's bowl shape for proper cholesterol binding.

The importance of the salt bridge in StAR activity is demonstrated both *in vivo* and *in vitro* by mutagenesis. Indeed, previous studies show that the human StAR mutant E169G (corresponding to the hamster E168) is improperly folded and causes LCAH (Bose *et al.*, 1998). Here, we replaced the hamster salt bridge by hydrophobic residues of similar volume. When either E168L or R187M is co-expressed in COS-1 cells with the F2 construct (vector constaining all necessary enzymes for P450scc activity), all unstimulated StAR-dependent cholesterol transfer is lost without a change in the protein expression levels as compared to controls (Chapter 2.1. Fig. 5). Under stimulating conditions (Bu_2-cAMP = cAMP), the StAR-dependent cholesterol transfer never attains wild type activity (Chapter 2.1. Fig. 5). Taken together, it is unlikely that the mutants fold properly but it has not been verified. In the case that they do fold properly, their reduced activity can result from either of two possibilities: 1) StAR does not open to allow cholesterol to bind, or 2) cholesterol cannot exit StAR after binding inside the cavity.

Removal of the salt bridge results in a unified hydrophobic cavity, which is more stable than when the salt bridge is present, since burying a charged pair in a hydrophobic enviroment costs energetically. Our results show that replacement of a single amino acid of the charged pair is sufficient to stop all StAR activity (Chapter 2.1. Fig. 5). Although stabilization of the cavity by the replacement of a single charged amino acid cannot be as grand as the destabilization by the water inside the cavity, it seems that removing half of the change in the cavity is sufficient to reduce the population of open unfolded StAR.

Thus cholesterol will bind at much reduced rates. Also, the remaining charged amino acid might not be restrained in proper position to orient cholesterol suitably inside the cavity. If however cholesterol still manages to bind inside the StAR cavity, albeit at largely reduced rates, it is unlikely that cholesterol is released efficiently from StAR. As a matter of fact, it is envisionable that replacement of the water molecules by the hydrophobic cholesterol results is a stable complex. The combination of these two possibilities probably dictates the unoticable StAR-dependent cholesterol transfer inside mitochondria for the mutant StAR, as compared to StAR-independent cholesterol transfer (Bose *et al.*, 1996). Under stimulatory conditions (cAMP), it is possible that the phosphorylation of the mutant StAR conveys structural changes that may allow some cholesterol to bind StAR and be transferred into mitochondria as observed.

4.1.2. Phosphorylation: Undeniably, phosphorylation of StAR is important to convey structural changes that augment StAR's capacity to transfer cholesterol. As a matter of fact, phosphorylated species responding to ACTH were discovered before StAR was identified (Alberta *et al.*, 1989; Clark *et al.*, 1994; Epstein and Orme-Johnson, 1991a; Epstein and Orme-Johnson, 1991b; Pon *et al.*, 1986; Pon and Orme-Johnson, 1986; Pon and Orme-Johnson, 1988). Since the discovery of StAR, it has been demonstrated that the human StAR is phosphorylated on S57 and S195 (Arakane *et al.*, 1997), but that only the removal of the S195 phosphorylation site (S195A mutation – relatively S194 in the hamster) resulted in loss of StAR activity. As of yet, no systematic investigation has been undertaken to explore all putative phosphorylation control sites on StAR activity.

We have identified conserved StAR putative phosphorylation sites of thirteen vertebrate species (Chapter 2.2. Table 1), and as such, have developped a strategy to test

phosphorylation control of the hamster StAR. Our initial screening was based on the altered StAR activity when the phosphoryaltion site is removed by replacing the phosphorylable serine by an alanine. Effectively, alanine and serine have a similar volume, but the functional γ-hydroxyl group of serine is absent in alanine. Of the eleven putative phosphorylation sites tested, only three mutants altered StAR activity: S13A, S185A, and S194A. All three mutants decreased StAR activity; S13A decreased StAR activity the least, and S194A decreased StAR activity the most (Chapter 2.2. Fig. 2).

In agreement with previous studies of the human StAR (Arakane *et al.*, 1997), the hamster S194A dramatically decreased StAR function, resulting from a direct decrease in StAR phosphorylation (Chapter 2.2. Fig. 3). Yet, S194A decreased to a greater extent StAR function when expressed as the full length StAR versus the N-terminal 46 amino acid cleaved (N46) StAR lacking the mitochondrial import sequence (Chapter 2.2. Fig. 4). This suggests that although we show that the wild type N46-StAR is as functional as the full-length wild type StAR, S194 seems to be implicated in both the control of StAR function in the acute stimulatory responses and in the control of the mitochondrial targeting sequence processing. Since there is no need for processing of the N46-S194-StAR, S194 now only diminishes part of StAR function resulting in less decreased StAR function as compared to the full-length StAR. This is in agreement with previous studies showing that S195 phosphorylation is important for the acute response of the human StAR (Arakane *et al.*, 1997), and that phosphorylation and processing of the human StAR is rapid (Artemenko *et al.*, 2001).

S13A decreased basal StAR activity by 30% indicating that this amino acid is also important for StAR function (Chapter 2.2. Fig. 3). On the other hand, stimulated StAR

activity was not affected by this mutation showing that it is not important for the acute increased steroidogenesis response under stimulation. Moreover, when the double mutant S13A/S194A was tested, S13A decreased both the basal and stimulated S194A-StAR activities similarly (Chapter 2.2. Fig. 3). Therefore unlike S194, S13A seems only to be implicated in the control of the mitochondrial trageting sequence processing. This is also supported by the 2D-SDS-PAGE analyses where most of the different StAR bands of S13A versus wild type under cAMP stimulation, are located in higher molecular weights where the mitochondrial import sequence is present (Chapter 2.2. Fig. 6). In addition, comparison of the S13A and S194A 2D-SDS-PAGE results under cAMP stimulation supports the fact that there is synergy between the mitochondrial targeting sequence S13 with S194, as the bands that disappear for S13 also disappear for S194 (Chapter 2.2. Fig. 6).

Interestingly, S185A decreased StAR function for both full-length and N46, although only the full-length-S185A-StAR was stimulatable by cAMP (Chapter 2.2. Fig. 5). This suggests that S185A causes gross conformational changes in StAR when the mitochondrial targeting sequence is absent, insinuating that the mitochondrial targeting sequence might be important to maintain StAR conformation. This is also in accordance with the recent discovery that phosphorylation and mitochondrial targeting sequence processing are rapid (Artemenko *et al.*, 2001); the mitochondrial targeting sequence may only be important to maintain StAR conformation until StAR is phosphorylated. Surprisingly, S185A had practically no effect on the 2D-SDS-PAGE pattern (Chapter 2.2. Fig. 6 and 7), making its implication in StAR function control practically inexplicable at the time. Fortunately, we completed the hamster StAR model during the progress of this

analysis and the model showed that the hamster S185 was not accessible to solvent making it impossibe to be phosphorylated (Chapter 2.2. Fig. 10). Unlike S185, S194 is directly accessible to solvent and has been shown to be phosphorylated by ^{32}P incorporation in the human counterpart S195 (Arakane *et al.*, 1997). We therefore hypothesized that the activity alterations of S185A were due to alterations in protein geometry intrinsic to the amino acid properties instead of the possibility of phosphorylation.

As mentioned previously, serine and alanine have similar volumes, but they have different chemical properties: serine is non-charged polar and alanine is hydrophobic. To test the hypothesis that activity alterations of S185A were due to amino acid properties rather than its capacity to be phosphorylated, we mutated S185 to mimic a constitutive phosphorylated amino acid (negatively charged) and to a polar residue that cannot be phosphorylated. In order to mimic phosphorylation, we have changed S185 into and aspartate and glutamate (S185D and S185E, respectively) as both of these are charged negatively at physiological pH, and they have at least an additional atom at position δ mimicking the additional phosphate group when the amino acid is phosphorylated. Cysteine on the other hand, is identical to serine except that the hydroxyl oxygen in serine is replaced by sulfur in cysteine. Effectively, this maintains the non-charged polar nature of the residue although it cannot be phosphorylated (S185C). Therefore if StAR is phosphorylated at S185, S185D and/or S185E should be extremely active yet would not respond to stimulation. Also, S185C should be exactly the same as S185A. The activity profiles show that S185D and S185E result in a greater loss of StAR activity than S185A, while S185C partially recuperates S185A StAR function (Chapter 2.2. Fig. 9). Moreover,

S185C is stimulatable by cAMP, while S185D and S185D are not. This clearly suggests that S185 is not phosphorylated and its altered activity profile is a result of altered protein conformation. Furthermore, further examination of S185's spacial location revealed that it is located immediately "underneath" the E168-R187 salt bridge, helping to anchor the salt bridge through hydrogen bonding. Therefore, increasing the length of the S185 by aspartate and glutamate probably disturbed the orientation of the salt bridge resulting in the ablation of StAR function similarly to our E168L and R187M mutants. This also supports the importance of the salt bridge integrity in the hydrophobic cavity for proper StAR function. Since S185A probably caused distortion of this key feature of StAR functionality, it probably caused the gross conformational changes in StAR suggested when the mitochondrial targeting sequence is absent.

4.1.3. StAR-Dependent Cholesterol Transfer Mechanism: The next natural step with the StAR model is to shed light on the StAR mechanism for cholesterol transfer inside mitochondria. Unfortunately, the crystalized human MLN64 comprised only the START domain from 230-443 (Tsujishita and Hurley, 2000) corresponding to amino acids 66-279 of the hamster StAR (Chapter 2.1. Fig. 1). Modeling of the rest of the residues of the hamster StAR at this point would only be speculation. In addition to using modeling, it is possible to calculate the theoretical free energy of any protein with respect to the solvent accessible surface, so long as structural data is available *in silico*. From these structure-based thermodynamic calculations (Freire, 1993;Hilser and Freire, 1997), it is also possible to identify partially folded (unfolded) states of proteins in equilibrium with their native state and calculate theoretical binding constants of their ligands (Baker and Murphy, 1998; Hilser and Freire, 1997; Lavigne *et al.*, 2000). Conveniently, Pierre

Lavigne and collaborators have implemented the structure-based thermodynamic calculations in a computer program named STC.

Three mechanisms are presenlty proposed for StAR action: 1) desorption, 2) molten globule, and 3) intermembrane shuttle. Unfortunately, not one of these models can explain all experimental evidence collected to date. Desorption states that as StAR enters mitochondria *via* its mitochondrial targeting sequence, contact sites are created between the outer and inner mitochondrial membranes thus allowing for large quantities of cholesterol to diffuse from the cholesterol-rich outer mitochondrial membrane to the inner mitochondrial membrane where P450scc resides (Kallen *et al.*, 1998b). This can account for the rapid cholesterol transfer into mitochondria necessitating little StAR (Artemenko *et al.*, 2001), that StAR is located at "contact sites" of the inner and outer mitochondrial membranes (Pon *et al.*, 1989; Schwaiger *et al.*, 1987; Stocco and Clark, 1996), and the fact that StAR is quickly degraded by mitochondria (Clark *et al.*, 1994; Stocco and Clark, 1996). The greatest argument against this mechanism is the fact that StAR can still function without the mitochondrial targeting sequence as presented here and also previously (Arakane *et al.*, 1996; Arakane *et al.*, 1998), since the desorption mechanism is entirely dependent on the action of the mitochondrial targeting sequence's capacity to mediate StAR's entry inside mitochondria. The molten globule hypothesis is based on the observation that StAR looses tertiary structure while retaining secondary structure at low pH (Bose *et al.*, 1999; Christensen *et al.*, 2001). Through molten globular species, StAR can interact preferentially to membranes (Christensen *et al.*, 2001), acting on the cytosolic side of the outer mitochondrial membrane. Unfortunately, an acidic environment of pH 3.5-4.0 locally at the mitochondrial membrane has yet to be proven

and does not account for the fact that StAR was observed to be located in the intermembrane space of mitochondria (King *et al.*, 1995). Finally, the intermembrane shuttle mechanism is the child of the crystalized human MLN64 structure (Tsujishita and Hurley, 2000). The authors suggest that the hydrophobic tunnel discovered in the crystal is responsible for binding cholesterol inside StAR and thus shuttles from the outer mitochondrial membrane to the inner mitochondrial membrane, much like the mechanism of sterol carriers. They also suggest that the transfer mechanism necessitates conformational changes of the loops and or the C-terminal α-helix to allow cholesterol access to the hydrophobic tunnel since the openings are not large enough to let cholesterol pass. The greatest downfalls of this mechanism are the fact that the crystal does not account for the N-terminal region of StAR comprising the mitochondrial targeting sequence, and that shuttling of cholesterol from one membrane to the next would be fast enough as observed. These authors also suggest that StAR can enter into the mitochondrial intermembrane space without the mitochondrial targeting sequence based on the work of others (Derman *et al.*, 1993), although this has not been proven for StAR yet.

Since the StAR mechanism still remains a mystery, mostly due to the hydrophobic nature of StAR not allowing proper analysis of the protein, and contradicting experimental evidence exist, the notion of an amalgamated mechanism representing all these observations is growing. Recently, such a mechanism was presented (Stocco, 2000); StAR-mediated cholesterol transfer inside the mitochondria would be some sort of a "pore", which while interacting with both mitochondrial membranes, would change conformations through a molten globular form to expand the hydrophobic tunnel

extremities allowing cholesterol to pass. However, this is not supported by any new experimental evidence. This "pore" mechanism therefore merges the desorption and molten globular mechanisms, using the sterol carrier structure of MLN64. Unfortunately, this "pore" model is still dependent on the presence of the N-terminal mitochondrial targeting sequence and does not account for the observation that StAR can be located in the intermembrane space, other than at "contact sites". In addition, no protein interactions were successfully obtained for StAR as of yet (Kallen *et al.*, 1998a; Kallen *et al.*, 1998b).

Simultaneously, we present another vision. Following the key observations that the C-terminal region StAR is believed to conformationally change transiently for cholesterol binding (Tsujishita and Hurley, 2000), that upon binding of a cholesterol analogue causes StAR to loose α-helical structure (Petrescu *et al.*, 2001), that molten globular states of StAR are possible although artificially at low pH values (Bose *et al.*, 1999;Christensen *et al.*, 2001), and that the C-terminal α-helix entirely covers the cholesterol binding site and should be free for movement, we conceptualized that StAR function is mediated through various conformational states of the C-terminal α-helix (Chapter 2.1. Fig. 6 and 8). In order to test this hypothesis, we used theoretical structure-based thermodynamic calculations to determine the possibility of the existence of such species under normal physiological conditions. We show that an unfolded C-terminal α-helix StAR is theoretically plausible in a significant popoulation and should be important for StAR-mediated cholesterol transfer inside mitochondria.

Several key components come to mind for our novel "flipping StAR" mechanism. First of all, our model has a hydrophobic cavity instead of a hydrophobic tunnel as for the MLN64 crystal. Therefore StAR absolutely has to open to allow cholesterol access to the

binding site as suggested (Tsujishita and Hurley, 2000). Second, discovery of water molecules inside the MLN64 crystal is crucial as the driving force allowing StAR to open (Tsujishita and Hurley, 2000). Destabilization of StAR by the hydration of the hydrophobic cavity (by approximately 12 kcal/mol) makes a significant population of unfolded StAR (approximately 2%) available for cholesterol binding and transfer inside mitochondria, as calculated by structure-based thermodynamics (Freire, 1993; Lavigne *et al.*, 2000). Third, StAR activity is governed by the equilibrium of conformational states of StAR, along with the cholesterol gradient between mitochondrial membranes, resulting in the observed rapid adaptation of StAR to acute stimulation and inactivation (Clark *et al.*, 1994; Stocco and Clark, 1996). Fourth, due to our modeling and STC calculations, StAR is not limited by the presence of the mitochondrial targeting sequence and can be localized pratically anywhere solution, including in the intermitochondrial space or in proximity of the mitochondrial outer membrane in the cytosol. This allows for a rapid cholesterol transfer inside mitochondria as observed (King *et al.*, 1995) for the case of the intermembrane space shuttle mechanism, but does not exclude the possibility that StAR functions outside mitochondria. And fifth, our theoretical dissociation constant reflects a mechanism in which cholesterol will be released rapidly (Artemenko *et al.*, 2001).

On the other hand, one can argue that: 1) no experimental evidence shows that the C-terminal α-helix is the only structure that changes conformation for cholesterol binding and that anyhow, it refolds ontop of cholesterol between "trips", and 2) our modeling does not take into account phosphorylation and the N-terminal mitochondrial targeting sequence in the StAR mechanism. Here, we supply new *in silico* experimental data demonstrating that the StAR C-terminal α-helix can unfold to produce a significant

population molten globular species of StAR. We only simulated the movement of the C-terminal α-helix for simplicity and because it has been shown to be critical for StAR function (Bose *et al.*, 1996; Lin *et al.*, 1995). Moreover, the C-terminal α-helix is the only helix in proximity of StAR's cholesterol binding site, which can lead to the observed loss of α-helical content upon the ligation of the cholesterol analogue (Petrescu *et al.*, 2001). It is entirely possible that other structures, such as loop Ω1, simultaneously move with the C-terminal α-helix as previously suggested by Tsujishita *et al.* (Tsujishita and Hurley, 2000); STC calculations of this movement demonstrate that these conformational changes are beneficial to StAR molten globular populations, aiding to bind cholesterol. It is also possible that the C-terminal α-helix refolds ontop of cholesterol after it has bound to StAR, although this could significantly reduce the transfer rate as an additional step is required for effective cholesterol transfer. In addition, it has already been demonstrated that StAR looses much α-helical character when a cholesterol analogue binds (Petrescu *et al.*, 2001), and the C-terminal α-helix will only refold ontop of cholesterol if it can be shown that it's refolding is faster than cholesterol release from the binding site.

Finally, it is impossible to model the first 65 amino acids of StAR since the equivalent amino acids of MLN64 have not been crystalized. On the other hand, it seems that phosphorylation and N-terminal processing of StAR are rapidly obtained after StAR transcription, and are necessary for conveying StAR activity (Artemenko *et al.*, 2001). These authors conclude that wild type StAR is rapidly phosphorylated in the cytosol after transcription of the StAR mRNA, followed by import into the mitochondrial intermembrane space where the N-terminal mitochondrial targeting sequence is rapidly

cleaved. Therefore, what is the link between phosphorylation, N-terminal processing, and StAR function?

First of all, StAR phosphorylation seems to serve two functions. First, it interacts with the N-terminal mitochondrial targeting sequence. This would be especially important outside mitochondria where the mitochondrial targeting seqeunce is important to localize StAR in proximity of the outer mitochondrial membrane. Second, StAR phosphorylation would somehow increase StAR reactivity inside mitochondria, after the mitochondrial targeting sequence is rapidly cleaved (Artemenko *et al.*, 2001). Overall, phosphorylation may perform these tasks by simply augmenting StAR stability as suggested elsewhere (Clark *et al.*, 2000). On the other hand, it seems that the major function of the mitochondrial targeting sequence is to localize StAR in proximity of the outer mitochondrial membrane since no direct protein-protein interactions have been found for StAR, StAR is functional without the N-terminal mitochondrial targeting sequence, and the mitochondrial targeting sequence is rapidly removed after StAR import into mitochondria. Yet here, we show that there seems to be a possible interaction between the mitochondrial targeting sequence and phosphorylation suggesting that outside mitochondria, the mitochondrial targeting sequence may also be implicated in StAR stability.

4.2. P450c17:

4.2.1. Site-Directed Mutagenesis: In order to understand substrate selectivity of the P450c17, we mutated the hamster P450c17 at precise amino acids in the desire to change the hamster P450c17 into a more "human" type. Basically, we compared the amino acid

sequences of several species to rationaly choose residues that might be implicated in substrate selection and/or activity control the P450c17 (Chapter 3.2.). Since the hamster P450c17 produces both DHEA and androstenedione is relatively large amounts, it is conceivable that the primary amino acid sequence of the hamster resembles both the DHEA and androstenedione producing P450c17s, such as the human and rat P450c17s respectively. Therefore, this enables us to target specific amino acid that might convey human P450c17 specificity and/or activity profile.

Of all the possible hot spots, three key amino acids stood out: T202N, D240N, D407H. Interestingly, these three amino acids resulted in different patterns of the hamster P450c17 activity alterations. Three distinct patterns were obtained: 1) a general effector for all P450c17 activities, T202N; and 2) a particular P450c17 activity, D240N; and 3) a particular P450c17 activity for a specific pathway, D407H (Chapter 3.2. Table 2). Unfortunately, only the D407H mutant resulted in making the hamster P450c17 a bit more "human" as predicted.

Unlike the R200N guinea pig P450c17 mutant (Beaudoin *et al.*, 1998), the hamster T202 seem to be implicated in the overall reactivity of the hamster P450c17 since both the 17α-hydroxylase and 17,20-lyase activities were decreased for both pathways (DHEA and androstenedione pathways - Chapter 3.2. Table 2). On the other hand, the guinea pig mutant R200N specifically increased 17α-hydroxylation of pregenenolone and decreased 17,20-lyase of 17α-hydroxyprogesterone; this effectively makes the guinea pig P450c17 activities resemble more like the human P450c17 activity profile. Regrettably, the double mutant R200N/T202N did not result in further activity alteration.

Interestingly, the D240N mutation seemed to have perturbed the hamster P450c17 in such a way as to specifically decrease 17,20-lyase activity for both 17α-pregnenolone and 17α-hydroxyprogesterone (Chapter 3.2. Table 2). Yet, this mutation decreased the 17,20-lyase activity more for the DHEA pathway more than for the androstenedione pathway, suggesting that this mutation has a greater effect on the binding interactions of the 17α-hydroxylpregnenolone 3β-hydroxyl group than on the 3-keto group of 17α-hydroxyprogesterone; this is the only structural difference between these substrates.

Finally, D407H specifically reduced the 17α-hydroxylase activity for the androstenedione pathway for the hamster P450c17 (Chapter 3.2. Table 2). This is rather interesting since similar mutations in the human P450c17 resulted in decreased 17α-hydroxylase. Of particular interest, it was recently reported that the mutation P409R (Lam *et al.*, 2001) caused complete loss of 17α-hydroxylation in a patient harbouring this mutation. On the other hand, it was initially reported that the mutation F417C caused specific loss of 17,20-lyase activity (Biason-Lauber *et al.*, 2000b) although investigation of this mutation by others showed that it resulted in outright abolition of all P450c17 reactivity (Gupta *et al.*, 2001). The only way that the hamster P450c17 D407H mutation resembles more like the human P450c17 is in the fact that now, the hamster P450c17 harboring this mutation relatively produces more DHEA than androstenedione when each pathway is compared individually.

To our dismay, we were unable to convey complete human P450c17 activity to the hamster P450c17. To obtain this, we would have had to obtain an increased DHEA/androstenedione production ratio due to an elevated 17,20-lyase activity for the DHEA pathway as compared to the androstenedione pathway; the 17α-hydroxylase

activity should not have been altered. Then again, obtaining our present results enabled us to classify the function of amino acids in the substrate selection and P450c17 activity. But in order to obtain a complete understanding of their implication in these P450c17 characteristics, we opted for a molecular model of the hamster P450c17.

4.2.2. Modeling of the Hamster P450c17: Alignment of the hamster and human P450c17 was unambiguous and therefore made it relatively simple to model the hamster P450c17 by homology to the human coordinate data (Chapter 3.2. Fig. 2). In order to be able to compare discreet structural differences between these two models, it is necessary to perform the same energy minimizations and molecular dynamic calculculations when modeling. In effect, this is to reduce possible differences due to human manipulation. Upon completion of the hamster model, we first compared the overall structures and the active sites of the hamster and human P450c17 models, followed by modeling of the hamster mutants to visualize the effect of altering these amino acids on the conformational states of the hamster P450c17. Finally, we docked all the possible P450c17 substrates in the hamster P450c17 model to try to understand the P450c17 substrate specificity.

Overall, the hamster and human P450c17 structures resembled each other to great extend as we predicted. Yet, structural differences were evident. Three dissimilarities were discovered: 1) consolidation of the hydrophobic domain consisting of the α-helices A, F, and G, and the β-strands 1.1-1.3 and 2.1-2.2; 2) positioning of the J' α-helix; and 3) the structural environment of the active site (Chapter 3.2. Fig. 4A and 4B). The implication of these structural changes is not all clear, although it is certain that these ultimately change the conformation of the hamster P450c17 conveying the observed

activity profile. Specifically, it is imaginable that all these "global" structural changes outside the active site are responsible for the active site conformation. For example, when the active sites of the hamster and human structures are compared, the catalytically important T306, believed to be responsible for the homolysis of oxygen (Lee-Robichaud *et al.*, 1998), is kinked upwards from the floor of the active site composed of the heme. Moreover, this "kinking" positions the hamster P450c17 H-I loop closer to the putative substrate entrance than in the human structure, implying that this loop may be important for substrate recognition upon binding (Chapter 3.2. Fig. 4C and 4D).

Molecular modeling of the hamster P450c17 mutants shed light on their implication for P450c17 reactivity. Indeed, the mutant T202N is located in the F-helix (Chapter 3.2. Fig. 5), and interacts with V483 forming the roof of the active site. Even though asparagine has more volume than threonine (two δ-atoms vs one γ-atom, respectively), the T202N-V483 interaction still exists. Yet, T202N causes the roof of the P450c17 acitve site to drop, lowering the active site's "headroom". Since all the P450c17 substrates are virtually identical on the β-side of the steroids [formed by predominately by the methyl groups at position 18 and 19 for the interaction of the steroid and the roof of the active site (Auchus and Miller, 1999)], it is easily understandable that the mutation T202N reduces all of the hamster P450c17 activities. In addition, the T202N mutation caused I112 to move out of place; I112 seems a great deal implicated in substrate binding for reactivity.

D240N is located halfway in the G-helix at the junction of the G-, I- and B'-helices adjacent to the H-I loop (Chapter 3.2. Fig. 5). This mutation caused the I-helix to kink, raising T306 away from the heme plane, and lowering I112 closer to the heme. Yet the

most important alteration seems to be the stuffing of R96 and R440 towards the active site; these amino acids seem implicated in the initial substrate recognition upon substrate uptake into the active site. It is conceivable that alteration of these amino acids by the D240N mutation, results in the reduction of 17α-hydroxylation at two discrete levels. First, movement of I112, R96 and R440 towards the inside of the hamster P450c17 active site twists and shrinks the active site probably making it more difficult for the 17α-hydroxylated products to enter the active site. And second, it seems that the 17α-hydroxyl group of 17α-hydropregenenolone and 17α-hydroxyprogesterone interact with R96 and/or R440 as they enter to the active site. The fact that the only difference between the substrates for the 17α-hydroxylase and 17,20-lyase activities is the presence of the 17α-hydroxyl group for the 17,20-lyase substrates and the 17α-hydroxylase activity did not change with the mutation D240N, suggests that an interaction of the 17α-hydroxyl group with R96 and/or R440 is more important than the actual alteration in the hamster P450c17 active site conformation for this mutation. This is supported by other experimental results; recently, it was demonstrated that in cellular systems, the P450c17 steroid metabolism consists of two steps (Soucy and Luu-The, 2000). The first step is the production of 17α-hydroxylated products after which they are released from the P450c17. When enough 17α-hydroxyl products accumulate, they seem to compete for the P450c17 and thus shift reactivity. This suggests that although the K_M's for the human P450c17 activities are similar for all the substrates except 17α-hydroxyprogesterone (which is about 5-10 times higher than the others (Auchus *et al.*, 1998; Lee-Robichaud *et al.*, 1995)). In addition, as we determined the concentration of pregnenolone or progesterone necessary to have a linear correlation between 17α-hydroxylation and 17,20-lyase

activity, we discovered that there seemed to be a 17α-hydroxylated product/initial substrate concentration ratio (for example: 17α-hydroxyprogesterone/progesterone), where the 17α-hydroxyl product effectively competed for the P450c17 shifting the activities of the hamster P450c17 towards 17,20-lyase (unpublished results). Therefore, this suggests that although the rate of both P450c17 activities are similar (as dictated by the K_M's), differences in the binding affinities of the substrates influences P450c17 activity. Unfortunately, no binding assays are as yet performed for all P450c17 substrates but should be close at hand (personal communication with R.J. Auchus).

At first glance, it is less obvious why the mutation D407H specifically reduced 17α-hydroxylation for the androstenedione pathway. D407H is most remotely located mutant from the active site, positioned in the meander loop (Chapter 3.2. Fig. 5). Since loops are generally believed to move all about, it is unclear how this mutation can affect anything, yet it does. Upon a closer examination, D407 is located upstream of the heme binding C442 and during modeling, results in a shift in heme positioning and active site volume reduction. At this moment, we cannot explain how this active site conformational change leads to a specific reduction in either 17α-hydroxylase activity and/or progesterone binding. Yet, it is possible that if the hamster P450c17 is phosphorylated similarly to the human P450c17, this mutation could affect hamster P450c17 phosphorylation much like the F417C mutation in the human P450c17; in the case of the hamster, this alteration in P450c17 phosphorylation results in the reduction of 17α-hydroxylase activity specifically for porgesterone.

Due to the lack of time, we did not model the substrates in all of the modeled hamster P450c17 mutants. According to our substrate binding models, a total of 12 models would

have to be analyzed. Therefore, we cannot absolutely account for the effects of these mutants on substrate binding.

4.2.3. Substrate Uptake Mechanism for the Hamster P450c17: Before we can conclude about the effects of the mutants on the binding of the substrates, we must first have an understanding of the mechanism involved in the uptake of these substrates in the hamster P450c17. To be able to compare these results with the human P450c17 (Auchus and Miller, 1999), we docked the substrates in similar positions in the hamster model as in the human structure. Contrary to the human docked models, we obtained two sets of hamster P450c17 models for each docked substrate (Chapter 3.3. Fig. 1 and 2). Since similar patterns for the models were obtained, a molecular mechanism for substrate selectivity and uptake into the hamster P450c17 becomes apparent, a result not foreseable with the human docked models.

As the substrates were docked in the human P450c17 structure (Auchus and Miller, 1999), it was discovered that the active site was not large enough to allow a bi-lobal binding of the substrates conveying the two activities of P450c17 as previously described (Burke *et al.*, 1997; Laughton *et al.*, 1990; Lin *et al.*, 1994). Our results show that although a bi-lobal active site is not present in the hamster P450c17, but the substrates rotate in the active site in order to obtain optimal positioning for reactivity. Interestingly, similar patterns for the all the substrates were obtained except for the binding of pregnenolone.

Indeed, amino acids seemingly important for the binding and proper entry of the substrates in the hamster P450c17 active site were identifed. Briefly, two sets of amino acids were recognized as important for either directing the substrates as they enter the

P450c17, or placing them appropriately for reaction (Chapter 3.3. Fig. 2). The first set is composed mainly of residues surrounding T306 and R96; two residues directly opposite each other in the active site, and lined up with the volume of the empty acitve site. This set includes amino acids K110, G303, T306, and V366, along with S94, R96, and R440. The amino acids responsible for the proper binding of the substrates for reactivity are A302-G303, K110-I112, and R440 at one end, and P321 with A367-L370 for the other end; the only substrate functional groups capable of interacting strongly enough with P450c17 to maintain substrate positioning in the active site are the polar "oxygens" at either ends. It is not surprising that some residues are members of both these sets, as these are located in a position much like the corner where two walls meet, in the active site three-dimensional space.

These findings are supported by previous discoveries of human P450c17 mutants reported to change P450c17 reactivity due to supposed active site formation alterations. Most significantly, the R96W mutant (Laflamme *et al.*, 1996) and the duplication of I112 (Imai *et al.*, 1993) have been reported to abolish P450c17 activity. Moreover, our modeled hamster mutants also alter the positioning of these key amino acids supporting their implication in the mechanism of substrate uptake.

5. Conclusions

A tremendous amount of structural information is obtained from molecular modeling. This information can explain previously obtained data, such as site-directed mutagenesis, and open new exciting testable opportunities targeting specific objectives. Here, we used molecular modeling to shed light on the elusive mechanism of the StAR function and to

explain our structure/function analyses of the P450c17 in hamsters. Overall, we have successfully combined modern molecular modeling with more traditional structure/function analyses to develop testable models, assisting us to refine our understanding of these systems.

5.1. StAR:

According to our results presented here, we perceive StAR as having two distinct steps for reactivity after its transcription from mRNA: 1) cytosolic modification and localization to mitochondrial membranes, and 2) import into mitochondria for full reactivity. Of major importance, we propose a novel testable mechanism for StAR function, which can account for most of the StAR's observed characteristics. Together with the proposition of a "pore-like" StAR, we engage in new exciting experimentation to discover the true nature of StAR function.

Taken together, we have achieved our objectives in: i) obtaining a realistic model of StAR capable of ii) explaining our rational site-directed mutagenesis results for the putative phosphorylation sites, and used to identify important amino acids responsible for StAR function (*i.e.:* salt bridge) to iii) clarify current contradicting experimental results. Our work opens new exciting areas of research including the systematic identification of StAR phosphorylation sites and their implication in StAR function in all the species studied to date, and the elucidation of the actual StAR mechanism with respect to our proposed mechanism. Nuclear magnetic resonance and more classical thermodynamic studies will play a major part in the revelation of the actual StAR mechanism.

5.2. P450c17:

Although our research on the structure/function relationship of the hamster P450c17 was stunted by the attractive opportunity to elucidate the StAR mechanism of action, we have obtained an enormous amount of information on the selectivity and activity profiles of the hamster P450c17 versus the human P450c17. We conceptualize that the P450c17 mechanism is dependent on three key steps: 1) substrate recognition at the putative substrate entrance, mediated by residues R96 and D116; 2) admission of the substrates in a temporary orientation, directed by amino acids R96 and T306; and 3) rotational modification of the substrates position such that they are in optimal orientation for proper reactivity. Importantly, all the P450c17 residues play an essential role in this mechanism, either to: 1) maintain structural integrity of enzyme, 2) participate in heme binding, redox partner interactions, and catalysis, and/or 3) influence active site geometry and hence substrate selection.

Again, we met our objectives. We have:

i. Identified amino acids responsible for hamster P450c17 substrate for selectivity and have classified them accourding to functionality and degree of effect on overall substrate selection;

ii. Obtained a useful model of the hamster P450c17 capable of explaining our rational site-directed mutagenesis, as well as clarifying the human and hamster activity profile differences; and,

iii. Proposed a plausible P450c17 mechanism responsible for substrate uptake selectivity conferring the observed activity profiles.

As for any structure-function analyses, the increasing power of nuclear magnetic resonance and thermodynamic instruments will play a major role in the validation of any proposed mechanism. It can be thus envisioned that such experimental procedures will be undertaken to have a clear picture of the P450c17 functionality.

Acknowledgments

First of all, I would like to thank Dr. Jean-Guy LeHoux to have supervised me for the last 5 years and for his bottomless pit of knowledge. You have made me the researcher that I am today, a characteristic I profoundly cherish. Your support has taught me to persist and to perform to the full extent of my capacities, but most of all, how to take pleasure in scientific discovery without losing touch of reality and of my personal life. I'd also like to thank Dr. Richard Auchus to have initiated my entry into molecular modeling and to have spiked my enthusiasm into research. Also, I thank Dr. Pierre Lavigne to have shown me that molecular modeling is more than just computers and to have opened my eyes to a complete new world. In our brief work together, you have convinced me to continue to learn new perspectives, and your trust in me has given me the power to believe that I can attain higher levels and new roles in my future career. I look forward to working under your supervision to learn all that you can teach me. I also thank Andrée Lefebvre and Lyne Ducharme to have been there ensentially everyday, to support and advise me on how to do "everything" in the lab. Your presence has been tremendously loving and you always seem to be interested in everything I did, especially in the progress of my family. I also thank the Canadian Institutes of Heath research to have given me 5 full years of financial support.

Of course, I'd like to thank all the students I had the pleasure to meet and that have turned usual days into events to remember, in particular, Alain, Philippe, Eli, and Brian. Alain and Philippe, will we ever forget Adrenal Cortex 1998? The pool, the beer, "les petits pains chauds", and all the stupid things we said. We started with Quake Nights, only to discover the full potential of UT Nights – you guys got me hooked! Eli and Brian,

thanks for making our ski trips and the long hours of our LAN parties so nice. Oh yeah, I'd like to thank you also for your precious scientific advice ;o). As for the next generation, I wish Mireille and Julie the best of luck in the continuation of their projects, and success in whatever you'll do afterwards!

Final but absolutely not least, I'd like to thank my family for all their support during my studies, especially my wife Tayna, my son Kaleb, and our new baby to be. You complete me in every possible way.

References

Addison, T. (1849). On anaemia: disease of the supra-adrenal capsules. *Lond Med Gaz* 517-518.

Addison, T. (1855). *In* "On the constitutional and local effects of disease of the suprarenal capsules" Highly, London.

Alberta, J. A., Epstein, L. F., Pon, L. A., and Orme-Johnson, N. R. (1989). Mitochondrial localization of a phosphoprotein that rapidly accumulates in adrenal cortex cells exposed to adrenocorticotropic hormone or to cAMP. *J Biol Chem* **264**:2368-2372.

Arakane, F., Kallen, C. B., Watari, H., Foster, J. A., Sepuri, N. B., Pain, D., Stayrook, S. E., Lewis, M., Gerton, G. L., and Strauss, J. F., III (1998). The mechanism of action of steroidogenic acute regulatory protein (StAR). StAR acts on the outside of mitochondria to stimulate steroidogenesis. *J Biol Chem* **273**:16339-16345.

Arakane, F., King, S. R., Du, Y., Kallen, C. B., Walsh, L. P., Watari, H., Stocco, D. M., and Strauss, J. F., III (1997). Phosphorylation of steroidogenic acute regulatory protein (StAR) modulates its steroidogenic activity. *J Biol Chem* **272**:32656-32662.

Arakane, F., Sugawara, T., Nishino, H., Liu, Z., Holt, J. A., Pain, D., Stocco, D. M., Miller, W. L., and Strauss, J. F., III (1996). Steroidogenic acute regulatory

protein (StAR) retains activity in the absence of its mitochondrial import sequence: implications for the mechanism of StAR action. [see comments]. *Proc Natl Acad Sci U S A* **93**:13731-13736.

Arnold, A. (1998). Pathogenesis of endocrine tumors. *In* "Williams Textbook of Endocrinology" (J. D. Wilson, D. W. Foster, H. M. Kronenberg, and P. R. Larsen, Eds.), pp. 145-340, W.B. Saunders Company, Philadelphia.

Arnold, J. (1866). Ein Beitrag zu der feineren Structur und dem Chemismus der Nebennieren. *Arch Pathol Anat Physiol Klin Med* 64-107.

Artemenko, I. P., Zhao, D., Hales, D. B., Hales, K. H., and Jefcoate, C. R. (2001). Mitochondrial processing of newly synthesized StAR, but not total StAR, mediates cholesterol transfer to P450scc in adrenal cells. *J Biol Chem* M107815200.

Auchus, R. J. (2001). The genetics, pathophysiology, and management of human deficiencies of P450c17. [Review] [77 refs]. *Endocrinol Metab Clin North Am* **30**:101-119.

Auchus, R. J., Lee, T. C., and Miller, W. L. (1998). Cytochrome b5 augments the 17,20-lyase activity of human P450c17 without direct electron transfer. *J Biol Chem* **273**:3158-3165.

Auchus, R. J. and Miller, W. L. (1999). Molecular modeling of human P450c17 (17alpha-hydroxylase/17,20-lyase): insights into reaction mechanisms and effects of mutations. *Mol Endocrinol* **13**:1169-1182.

Baker, B. M. and Murphy, K. P. (1998). Prediction of binding energetics from structure using empirical parameterization. *Methods Enzymol* **295**:294-315.

Beaudoin, C., Lavallee, B., Tremblay, Y., Hum, D. W., Breton, R., de Launoit, Y., and Belanger, A. (1998). Modulation of 17alpha-hydroxylase/17,20-lyase activity of guinea pig cytochrome P450c17 by site-directed mutagenesis. *DNA Cell Biol* **17**:707-715.

Biason-Lauber, A., Kempken, B., Werder, E., Forest, M. G., Einaudi, S., Ranke, M. B., Matsuo, N., Brunelli, V., Schonle, E. J., and Zachmann, M. (2000a). 17alpha-hydroxylase/17,20-lyase deficiency as a model to study enzymatic activity regulation: role of phosphorylation. *J Clin Endocrinol Metab* **85**:1226-1231.

Biason-Lauber, A., Zachmann, M., and Schoenle, E. J. (2000b). Effect of leptin on CYP17 enzymatic activities in human adrenal cells: new insight in the onset of adrenarche. *Endocrinology* **141**:1446-1454.

Blair-West, J. R., Coghlan, J. P., Denton, D. A., Fei, D. T., Hardy, K. J., Scoggins, B. A., and Wright, R. D. (1980). A dose-response comparison of the actions of angiotensin II and angiotensin III in sheep. *J Endocrinol* **87**:409-417.

Bolté, E., Coudert, S., and Lefebvre, Y. (1967). Steroid production from plasma cholesterol. *J Clin Endocrinol Metab* **38**:394-400.

Borkowski, A. J., Levin, S., Delcroix, C., Mahler, A., and Verhas, V. (1967). Blood cholesterol and hydrocortisone production in man: quantitative aspects of the

utilization of circulating cholesterol by the adrenals at rest and under adrenocorticotropin stimulation. *J Clin Invest* **46**:797-811.

Bose, H. S., Baldwin, M. A., and Miller, W. L. (1998). Incorrect folding of steroidogenic acute regulatory protein (StAR) in congenital lipoid adrenal hyperplasia. *Biochemistry* **37**:9768-9775.

Bose, H. S., Pescovitz, O. H., and Miller, W. L. (1997). Spontaneous feminization in a 46,XX female patient with congenital lipoid adrenal hyperplasia due to a homozygous frameshift mutation in the steroidogenic acute regulatory protein. *J Clin Endocrinol Metab* **82**:1511-1515.

Bose, H. S., Sugawara, T., Strauss, J. F., III, and Miller, W. L. (1996). The pathophysiology and genetics of congenital lipoid adrenal hyperplasia. International Congenital Lipoid Adrenal Hyperplasia Consortium. *N Engl J Med* **335**:1870-1878.

Bose, H. S., Whittal, R. M., Baldwin, M. A., and Miller, W. L. (1999). The active form of the steroidogenic acute regulatory protein, StAR, appears to be a molten globule. *Proc Natl Acad Sci U S A* **96**:7250-7255.

Brière, N., Martel, D., Cloutier, M., and LeHoux, J. G. (1997). Immunolocalization and biochemical determination of cytochrome P450C17 in adrenals of hamsters treated with ACTH. *J Histochem Cytochem* **45**:1409-1416.

Brown-Séquard, C. E. (1856). Recherches expérimentales sur la physiology et la pathology des capsules surrénales. *Arch Gen Med* **5**:385-401.

Bulbrook, R. D., Hayward, J. L., and Spicer, C. C. (1971). Relation between urinary androgen and corticoid excretion and subsequent breast cancer. *Lancet* **2**:395-398.

Burke, D. F., Laughton, C. A., and Neidle, S. (1997). Homology modelling of the enzyme P450 17 alpha-hydroxylase/17,20-lyase--a target for prostate cancer chemotherapy--from the crystal structure of P450BM-3. *Anticancer Drug Des* **12**:113-123.

Caron, K. M., Soo, S. C., Wetsel, W. C., Stocco, D. M., Clark, B. J., and Parker, K. L. (1997). Targeted disruption of the mouse gene encoding steroidogenic acute regulatory protein provides insights into congenital lipoid adrenal hyperplasia. *Proc Natl Acad Sci U S A* **94**:11540-11545.

Christensen, K., Bose, H. S., Harris, F. M., Miller, W. L., and Bell, J. D. (2001). Binding of steroidogenic acute regulatory protein to synthetic membranes suggests an active molten globule. *J Biol Chem* **276**:17044-17051.

Chung, B. C., Picado-Leonard, J., Haniu, M., Bienkowski, M., Hall, P. F., Shively, J. E., and Miller, W. L. (1987). Cytochrome P450c17 (steroid 17 alpha-hydroxylase/17,20 lyase): cloning of human adrenal and testis cDNAs indicates the same gene is expressed in both tissues. *Proc Natl Acad Sci U S A* **84**:407-411.

Clark, B. J., Ranganathan, V., and Combs, R. (2000). Post-translational regulation of steroidogenic acute regulatory protein by cAMP-dependent protein kinase A. *Endocr Res* **26**:681-689.

Clark, B. J., Wells, J., King, S. R., and Stocco, D. M. (1994). The purification, cloning, and expression of a novel luteinizing hormone-induced mitochondrial protein in MA-10 mouse Leydig tumor cells. Characterization of the steroidogenic acute regulatory protein (StAR). *J Biol Chem* **269**:28314-28322.

Cloutier, M., Fleury, A., Courtemanche, J., Ducharme, L., Mason, J. I., and LeHoux, J. G. (1995). Cloning and expression of hamster adrenal cytochrome P450C17 cDNA. *Ann N Y Acad Sci* **774**:294-296.

Cloutier, M., Fleury, A., Courtemanche, J., Ducharme, L., Mason, J. I., and LeHoux, J. G. (1997). Characterization of the adrenal cytochrome P450C17 in the hamster, a small animal model for the study of adrenal dehydroepiandrosterone biosynthesis. *DNA Cell Biol* **16**:357-368.

Conaglen, J. V., Donald, R. A., Espiner, E. A., Livesey, J. H., and Nicholls, M. G. (1984). The effect of ovine corticotropin-releasing factor on catecholamine, vasopressin, and aldosterone secretion in normal man. *J Clin Endocrinol Metab* **58**:463-466.

Davis, L. G., Arentzen, R., Reid, J. M., Manning, R. W., Wolfson, B., Lawrence, K. L., and Baldino, F., Jr. (1986). Glucocorticoid sensitivity of vasopressin mRNA

levels in the paraventricular nucleus of the rat. *Proc Natl Acad Sci U S A* **83**:1145-1149.

Daynes, R. A., Dudley, D. J., and Araneo, B. A. (1990). Regulation of murine lymphokine production in vivo. II. Dehydroepiandrosterone is a natural enhancer of interleukin 2 synthesis by helper T cells. *Eur J Immunol* **20**:793-802.

DeBold, C. R., Sheldon, W. R., DeCherney, G. S., Jackson, R. V., Alexander, A. N., Vale, W., Rivier, J., and Orth, D. N. (1984). Arginine vasopressin potentiates adrenocorticotropin release induced by ovine corticotropin-releasing factor. *J Clin Invest* **73**:533-538.

DeFourcroy (1789). *Ann Chim Phys* **3**:242.

Derman, A. I., Puziss, J. W., Bassford, P. J., Jr., and Beckwith, J. (1993). A signal sequence is not required for protein export in prlA mutants of Escherichia coli. *EMBO Journal* **12**:879-888.

Dulbecco, R. (1991). "Encyclopedia of human biology," Academic Press, San Diego.

Dupont, E., Zhao, H. F., Rheaume, E., Simard, J., Luu-The, V., Labrie, F., and Pelletier, G. (1990). Localization of 3 beta-hydroxysteroid dehydrogenase/delta 5-delta 4- isomerase in rat gonads and adrenal glands by immunocytochemistry and *in situ* hybridization. *Endocrinology* **127**:1394-1403.

Eberwine, J. H., Jonassen, J. A., Evinger, M. J., and Roberts, J. L. (1987). Complex transcriptional regulation by glucocorticoids and corticotropin- releasing hormone of proopiomelanocortin gene expression in rat pituitary cultures. *DNA* **6**:483-492.

Epstein, L. F. and Orme-Johnson, N. R. (1991a). Acute action of luteinizing hormone on mouse Leydig cells: accumulation of mitochondrial phosphoproteins and stimulation of testosterone synthesis. *Mol Cell Endocrinol* **81**:113-126.

Epstein, L. F. and Orme-Johnson, N. R. (1991b). Regulation of steroid hormone biosynthesis. Identification of precursors of a phosphoprotein targeted to the mitochondrion in stimulated rat adrenal cortex cells. *J Biol Chem* **266**:19739-19745.

Eustachius, B. (1774). "Tabulae Anatomicae," Amsterdam.

Farkash, Y., Timberg, R., and Orly, J. (1986). Preparation of antiserum to rat cytochrome P-450 cholesterol side chain cleavage, and its use for ultrastructural localization of the immunoreactive enzyme by protein A-gold technique. *Endocrinology* **118**:1353-1365.

Fevold, H. R., Lorence, M. C., McCarthy, J. L., Trant, J. M., Kagimoto, M., Waterman, M. R., and Mason, J. I. (1989). Rat P450(17 alpha) from testis: characterization of a full-length cDNA encoding a unique steroid hydroxylase capable of catalyzing both delta 4- and delta 5-steroid-17,20-lyase reactions. *Mol Endocrinol* **3**:968-975.

Fleury, A., Ducharme, L., and LeHoux, J. G. (1998). In vivo effects of adrenocorticotrophin on the expression of the hamster steroidogenic acute regulatory protein. *J Mol Endocrinol* **21**:131-139.

Freire, E. (1993). Structural thermodynamics: prediction of protein stability and protein binding affinities. *Arch Biochem Biophys* **303**:181-184.

Fujieda, K., Tajima, T., Nakae, J., Sageshima, S., Tachibana, K., Suwa, S., Sugawara, T., and Strauss, J. F., III (1997). Spontaneous puberty in 46,XX subjects with congenital lipoid adrenal hyperplasia. Ovarian steroidogenesis is spared to some extent despite inactivating mutations in the steroidogenic acute regulatory protein (StAR) gene. *J Clin Invest* **99**:1265-1271.

Gelfman, N. A. (1964). Morphologic changes of the adrenal cortex in disease. *Yale J Biol Med* **37**:31-34.

Gell, J. S., Carr, B. R., Sasano, H., Atkins, B., Margraf, L., Mason, J. I., and Rainey, W. E. (1998). Adrenarche results from development of a 3beta-hydroxysteroid dehydrogenase-deficient adrenal reticularis. *J Clin Endocrinol Metab* **83**:3695-3701.

Gibbons, G. H., Dzau, V. J., Farhi, E. R., and Barger, A. C. (1984). Interaction of signals influencing renin release. *Annu Rev Physiol* **46**:291-308.

Gibson, D. M. and Paker, R. A. (1987). Hydroxymethylglutaryl-coenzyme A reductase. *In* "The Enzymes" (P. D. Boyer and E. G. Krebs, Eds.), pp. 179-215, Academic Press.

Gill, G. N. (1976). ACTH regulation of the adrenal cortex. *Pharmacol Ther [B]* **2**:313-338.

Graf, L., Bajusz, S., Patthy, A., Barat, E., and Cseh, G. (1971). Revised amide location for porcine and human adrenocorticotropic hormone. *Acta Biochim Biophys Acad Sci Hung* **6**:415-418.

Greenspan, F. (1991). "Basic and Clinical Endocrinology," Appleton & Lange Pub., Norwalk, Connecticut.

Griffin, J. and Ojeda, S. R. (1992). "Textbook of Endocrine Physiology," Oxford University Press, New York.

Gupta, M. K., Geller, D. H., and Auchus, R. J. (2001). Pitfalls in characterizing P450c17 mutations associated with isolated 17,20-lyase deficiency. *J Clin Endocrinol Metab* **86**:4416-4423.

Gwynne, J. T. and Strauss, J. F., III (1982). The role of lipoproteins in steroidogenesis and cholesterol metabolism in steroidogenic glands. *Endocr Rev* **3**:299-329.

Hanukoglu, I. (1992). Steroidogenic Enzymes: Structure, Function, and Role in Regulation of Steroid Hormone Biosynthesis. *J Steroid Biochem Mol Biol* **43**:779-804.

Hartigan, J. A., Green, E. G., Mortensen, R. M., Menachery, A., Williams, G. H., and Orme-Johnson, N. R. (1995). Comparison of protein phosphorylation patterns

produced in adrenal cells by activation of cAMP-dependent protein kinase and Ca-dependent protein kinase. *J Steroid Biochem Mol Biol* **53**:95-101.

Hilser, V. J. and Freire, E. (1997). Predicting the equilibrium protein folding pathway: structure-based analysis of staphylococcal nuclease. *Proteins* **27**:171-183.

Holmes, M. C., Catt, K. J., and Aguilera, G. (1987). Involvement of vasopressin in the down-regulation of pituitary corticotropin-releasing factor receptors after adrenalectomy. *Endocrinology* **121**:2093-2098.

Houssay, B. A. and Lewis, J. T. (1923). The relative importance to life of the cortex and medulla of the adrenal glands. *Am J Physiol* **64**:513-521.

Imai, T., Globerman, H., Gertner, J. M., Kagawa, N., and Waterman, M. R. (1993). Expression and purification of functional human 17 alpha-hydroxylase/17,20-lyase (P450c17) in Escherichia coli. Use of this system for study of a novel form of combined 17 alpha-hydroxylase/17,20-lyase deficiency. *J Biol Chem* **268**:19681-19689.

Ingle, D. J. and Kendall, E. C. Atrophy of the adrenal cortex of the rat produced by the administration of large amounts of cortin. Science 86, 245. 1937. Ref Type: Journal (Full)

International Union of Pure and Applied Chemistry (1972). Definitive rules for the nomenclature of steroids. *Pure Appl Chem* **31**:285-322.

Ishimura, K. and Fujita, H. (1997). Light and electron microscopic immunohistochemistry of the localization of adrenal steroidogenic enzymes. *Microsc Res Tech* **36**:445-453.

Itoi, K., Mouri, T., Takahashi, K., Murakami, O., Imai, Y., Sasaki, S., Yoshinaga, K., and Sasano, N. (1987). Suppression by glucocorticoid of the immunoreactivity of corticotropin- releasing factor and vasopressin in the paraventricular nucleus of rat hypothalamus. *Neurosci Lett* **73**:231-236.

Kallen, C. B., Arakane, F., Christenson, L. K., Watari, H., Devoto, L., and Strauss, J. F., III (1998a). Unveiling the mechanism of action and regulation of the steroidogenic acute regulatory protein. [Review] [51 refs]. *Mol Cell Endocrinol* **145**:39-45.

Kallen, C. B., Billheimer, J. T., Summers, S. A., Stayrook, S. E., Lewis, M., and Strauss, J. F., III (1998b). Steroidogenic acute regulatory protein (StAR) is a sterol transfer protein. *J Biol Chem* **273**:26285-26288.

Keller-Wood, M. E. and Dallman, M. F. (1984). Corticosteroid inhibition of ACTH secretion. *Endocr Rev* **5**:1-24.

Kennerson, A. R., McDonald, D. A., and Adams, J. B. (1983). Dehydroepiandrosterone sulfotransferase localization in human adrenal glands: a light and electron microscopic study. *J Clin Endocrinol Metab* **56**:786-790.

King, S. R., Liu, Z., Soh, J., Eimerl, S., Orly, J., and Stocco, D. M. (1999). Effects of disruption of the mitochondrial electrochemical gradient on steroidogenesis

and the Steroidogenic Acute Regulatory (StAR) protein. *J Steroid Biochem Mol Biol* **69**:143-154.

King, S. R., Ronen-Fuhrmann, T., Timberg, R., Clark, B. J., Orly, J., and Stocco, D. M. (1995). Steroid production after in vitro transcription, translation, and mitochondrial processing of protein products of complementary deoxyribonucleic acid for steroidogenic acute regulatory protein. *Endocrinology* **136**:5165-5176.

Laflamme, N., Leblanc, J. F., Mailloux, J., Faure, N., Labrie, F., and Simard, J. (1996). Mutation R96W in cytochrome P450c17 gene causes combined 17 alpha-hydroxylase/17-20-lyase deficiency in two French Canadian patients. *J Clin Endocrinol Metab* **81**:264-268.

Lam, C. W., Arlt, W., Chan, C. K., Honour, J. W., Lin, C. J., Tong, S. F., Choy, K. W., and Miller, W. L. (2001). Mutation of proline 409 to arginine in the meander region of cytochrome p450c17 causes severe 17 alpha-hydroxylase deficiency. *Mol Gen Metab* **72**:254-259.

Laughton, C. A., Neidle, S., Zvelebil, M. J., and Sternberg, M. J. (1990). A molecular model for the enzyme cytochrome P450 (17 alpha), a major target for the chemotherapy of prostatic cancer. *Biochem Biophys Res Commun* **171**:1160-1167.

Lavigne, P., Bagu, J. R., Boyko, R., Willard, L., Holmes, C. F., and Sykes, B. D. (2000). Structure-based thermodynamic analysis of the dissociation of protein

phosphatase-1 catalytic subunit and microcystin-LR docked complexes. *Protein Science* **9**:252-264.

Lee-Robichaud, P., Akhtar, M. E., and Akhtar, M. (1998). An analysis of the role of active site protic residues of cytochrome P-450s: mechanistic and mutational studies on 17alpha-hydroxylase-17,20-lyase (P-45017alpha also CYP17). *Biochem J* **330**:967-974.

Lee-Robichaud, P., Wright, J. N., Akhtar, M. E., and Akhtar, M. (1995). Modulation of the activity of human 17 alpha-hydroxylase-17,20-lyase (CYP17) by cytochrome b5: endocrinological and mechanistic implications. *Biochem J* **308**:901-908.

LeHoux, J. G., Hales, D. B., Fleury, A., Briere, N., Martel, D., and Ducharme, L. (1999). The in vivo effects of adrenocorticotropin and sodium restriction on the formation of the different species of steroidogenic acute regulatory protein in rat adrenal. *Endocrinology* **140**:5154-5164.

LeHoux, J. G. and Lefebvre, A. (1980). De novo synthesis of corticosteroids in hamster adrenal glands. *Journal of Steroid Biochemistry* **12**:479-485.

LeHoux, J. G., Mason, J. I., and Ducharme, L. (1992). In vivo effects of adrenocorticotropin on hamster adrenal steroidogenic enzymes. *Endocrinology* **131**:1874-1882.

Lin, D., Black, S. M., Nagahama, Y., and Miller, W. L. (1993). Steroid 17 alpha-hydroxylase and 17,20-lyase activities of P450c17: contributions of serine106 and P450 reductase. *Endocrinology* **132**:2498-2506.

Lin, D., Sugawara, T., Strauss, J. F., III, Clark, B. J., Stocco, D. M., Saenger, P., Rogol, A., and Miller, W. L. (1995). Role of steroidogenic acute regulatory protein in adrenal and gonadal steroidogenesis. [see comments]. *Science* **267**:1828-1831.

Lin, D., Zhang, L. H., Chiao, E., and Miller, W. L. (1994). Modeling and mutagenesis of the active site of human P450c17. *Mol Endocrinol* **8**:392-402.

Lundblad, J. R. and Roberts, J. L. (1988). Regulation of proopiomelanocortin gene expression in pituitary. *Endocr Rev* **9**:135-158.

Luo, X., Kiss, A., Rabadan-Diehl, C., and Aguilera, G. (1995). Regulation of hypothalamic and pituitary corticotropin-releasing hormone receptor messenger ribonucleic acid by adrenalectomy and glucocorticoids. *Endocrinology* **136**:3877-3883.

Migeon, C., Keller, A. R., Lawrence, B., and Shepart, T. H. (1957). Dehydroepiandrosterone and androsterone levels in the human plasma. *J Clin Endocrinol Metab* **17**:1051-1062.

Miller, W. L. (1997). Congenital lipoid adrenal hyperplasia: the human gene knockout for the steroidogenic acute regulatory protein. *J Mol Endocrinol* **19**:227-240.

Miller, W. L. (1999). The molecular basis of premature adrenarche: an hypothesis. *Acta Paediatrica* Supplement. **88**:60-66.

Morales, A. J., Nolan, J. J., Nelson, J. C., and Yen, S. S. (1994). Effects of replacement dose of dehydroepiandrosterone in men and women of advancing age. *J Clin Endocrinol Metab* **78**:1360-1367.

Mountjoy, K. G., Robbins, L. S., Mortrud, M. T., and Cone, R. D. (1992). The cloning of a family of genes that encode the melanocortin receptors. *Science* **257**:1248-1251.

Nafziger, A. N., Herrington, D. M., and Bush, T. L. (1991). Dehydroepiandrosterone and dehydroepiandrosterone sulfate: their relation to cardiovascular disease. *Epidemiologic Reviews* **13**:267-293.

Nakae, J., Tajima, T., Sugawara, T., Arakane, F., Hanaki, K., Hotsubo, T., Igarashi, N., Igarashi, Y., Ishii, T., Koda, N., Kondo, T., Kohno, H., Nakagawa, Y., Tachibana, K., Takeshima, Y., Tsubouchi, K., Strauss, J. F., III, and Fujieda, K. (1997). Analysis of the steroidogenic acute regulatory protein (StAR) gene in Japanese patients with congenital lipoid adrenal hyperplasia. *Hum Mol Genet* **6**:571-576.

Nakajin, S., Shively, J. E., Yuan, P. M., and Hall, P. F. (1981). Microsomal cytochrome P-450 from neonatal pig testis: two enzymatic activities (17 alpha-hydroxylase and c17,20-lyase) associated with one protein. *Biochemistry* **20**:4037-4042.

Namiki, M., Kitamura, M., Buczko, E., and Dufau, M. L. (1988). Rat testis P-450(17)alpha cDNA: the deduced amino acid sequence, expression and secondary structural configuration. *Biochem Biophys Res Commun* **157**:705-712.

Nebert, D. W. and Gonzalez, F. J. (1987). P450 genes: structure, evolution, and regulation. *Annu Rev Biochem* **56**:945-993.

Oki, Y., Peatman, T. W., Qu, Z. C., and Orth, D. N. (1991). Effects of intracellular Ca2+ depletion and glucocorticoid on stimulated adrenocorticotropin release by rat anterior pituitary cells in a microperifusion system. *Endocrinology* **128**:1589-1596.

Orentreich, N., Brind, J. L., Rizer, R. L., and Vogelman, J. H. (1984). Age changes and sex differences in serum dehydroepiandrosterone sulfate concentrations throughout adulthood. *J Clin Endocrinol Metab* **59**:551-555.

Orth, D. N. and Kovacs, W. L. (1998). The adrenal cortex. *In* "Williams Textbook of Endocrinology" (J. D. Wilson, D. W. Foster, H. M. Kronenberg, and P. R. Larsen, Eds.), pp. 517-664, W.B. Saunders Company, Philadelphia.

Petrescu, A. D., Gallegos, A. M., Okamura, Y., Strauss, J. F., and Schroeder, F. (2001). Steroidogenic acute regulatory protein binds cholesterol and modulates mitochondrial membrane sterol domain dynamics. *J Biol Chem* **276**:36970-36982.

Pon, L., Moll, T., Vestweber, D., Marshallsay, B., and Schatz, G. (1989). Protein import into mitochondria: ATP-dependent protein translocation activity in a submitochondrial fraction enriched in membrane contact sites and specific proteins. *J Cell Biol* **109**:2603-2616.

Pon, L. A., Hartigan, J. A., and Orme-Johnson, N. R. (1986). Acute ACTH regulation of adrenal corticosteroid biosynthesis. Rapid accumulation of a phosphoprotein. *J Biol Chem* **261** :13309-13316.

Pon, L. A. and Orme-Johnson, N. R. (1986). Acute stimulation of steroidogenesis in corpus luteum and adrenal cortex by peptide hormones. Rapid induction of a similar protein in both tissues. *J Biol Chem* **261**:6594-6599.

Pon, L. A. and Orme-Johnson, N. R. (1988). Acute stimulation of corpus luteum cells by gonadotrophin or adenosine 3',5'-monophosphate causes accumulation of a phosphoprotein concurrent with acceleration of steroid synthesis. *Endocrinology* **123**:1942-1948.

Privalle, C. T., Crivello, J. F., and Jefcoate, C. R. (1983). Regulation of intramitochondrial cholesterol transfer to side-chain cleavage cytochrome P-450 in rat adrenal gland. *Proc Natl Acad Sci U S A* **80**:702-706.

Provencher, P. H., Tremblay, Y., and Belanger, A. (1992). Effects of C19 steroids on adrenal steroidogenic enzyme activities and their mRNA levels in guinea-pig fasciculata-glomerulosa cells in primary culture. *J Endocrinol* **132**:269-276.

Regelson, W. and Kalimi, M. (1994). Dehydroepiandrosterone (DHEA)--the multifunctional steroid. II. Effects on the CNS, cell proliferation, metabolic and vascular, clinical and other effects. Mechanism of action? *Ann N Y Acad Sci* **719**:564-575.

Regelson, W., Loria, R., and Kalimi, M. (1994). Dehydroepiandrosterone (DHEA)--the "mother steroid". I. Immunologic action. *Ann N Y Acad Sci* **719**:553-563.

Rogerson, F. M., Courtemanche, J., Fleury, A., Head, J. R., Lehoux, JG, and Mason, J. I. (1998). Characterization of cDNAs encoding isoforms of hamster 3 beta-hydroxysteroid dehydrogenase/delta 5-->4 isomerase. *J Mol Endocrinol* **20**:99-110.

Schwaiger, M., Herzog, V., and Neupert, W. (1987). Characterization of translocation contact sites involved in the import of mitochondrial proteins. *J Cell Biol* **105**:235-246.

Shafagoj, Y., Opoku, J., Qureshi, D., Regelson, W., and Kalimi, M. (1992). Dehydroepiandrosterone prevents dexamethasone-induced hypertension in rats. *Am J Physiol* **263**:E210-E213.

Simpson, E. R. and Waterman, M. R. (1983). Regulation by ACTH of steroid hormone biosynthesis in the adrenal cortex. *Can J Biochem Cell Biol* **61**:692-707.

Simpson, E. R. and Waterman, M. R. (1988). Regulation of the synthesis of steroidogenic enzymes in adrenal cortical cells by ACTH. *Annu Rev Physiol* **50**:427-440.

Smith, P. E. Hypophysectomy and a replacement therapy in the rat. Am.J.Anat. 45, 205-273. 1930.

Soucy, P. and Luu-The, V. (2000). Conversion of pregnenolone to DHEA by human 17alpha-hydroxylase/17, 20-lyase (P450c17). Evidence that DHEA is produced from the released intermediate, 17alpha-hydroxypregnenolone. *Eur J Biochem* **267**:3243-3247.

Stocco, D. M. (2000). Intramitochondrial cholesterol transfer. *Biochim Biophys Acta* **1486**:184-197.

Stocco, D. M. and Clark, B. J. (1996). Regulation of the acute production of steroids in steroidogenic cells. *Endocrine Reviews* **17**:221-244.

Sviridov, D. (1999). Intracellular cholesterol trafficking. *Histol Histopathol* **14**:305-319.

Tee, M. K., Lin, D., Sugawara, T., Holt, J. A., Guiguen, Y., Buckingham, B., Strauss, J. F., and Miller, W. L. (1995). T-->A transversion 11 bp from a splice acceptor site in the human gene for steroidogenic acute regulatory protein causes congenial lipoid adrenal hyperplasia. *Hum Mol Genet* **4**:2299-2305.

Tremblay, Y., Fleury, A., Beaudoin, C., Vallee, M., and Belanger, A. (1994). Molecular cloning and expression of guinea pig cytochrome P450c17 cDNA (steroid 17 alpha-hydroxylase/17,20 lyase): tissue distribution, regulation, and substrate specificity of the expressed enzyme. *DNA Cell Biol* **13**:1199-1212.

Tsujishita, Y. and Hurley, J. H. (2000). Structure and lipid transport mechanism of a StAR-related domain. *Nature Structural Biology* 7:408-414.

Vale, W., Spiess, J., Rivier, C., and Rivier, J. (1981). Characterization of a 41-residue ovine hypothalamic peptide that stimulates secretion of corticotropin and beta-endorphin. *Science* **213**:1394-1397.

van Weerden, W. M., Bierings, H. G., van Steenbrugge, G. J., de Jong, F. H., and Schroder, F. H. (1992). Adrenal glands of mouse and rat do not synthesize androgens. *Life Sci* **50**:857-861.

Voet, D. and Voet, J. G. (1990). In: "Biochemistry," John Wiley & Sons, Inc., New Yrok.

Vulpian, E. F. A. (1856). Note sur quelques réactions propres à la substances des capsules surrénales. *C R Acad Sci Ser III* **43**:663-665.

Wheeler, T. D. and Vincent, S. (1917). The question as to the relative importance to life of the cortex and medulla of the adrenal bodies. *Trans R Soc Can* **11**:125-127.

White, P. C., New, M. I., and Dupont, B. (1987). Congenital adrenal hyperplasia. (1). *N Engl J Med* **316**:1519-1524.

Williams, D. L., Temel, R. E., and Connelly, M. A. (2000). Roles of scavenger receptor BI and APO A-I in selective uptake of HDL cholesterol by adrenal cells. *Endocr Res* **26**:639-651.

Williams, G. H. and Dluhy, R. G. (1983). Control of aldosterone secretion. *In* "Hypertension: Pysiopathology and Treatment" (J. Genest, O. Küchel, and P. Hamet, Eds.), pp. 320-327, McGraw-Hill, New York.

Wolf, O. T. and Kirschbaum, C. (1999). Actions of dehydroepiandrosterone and its sulfate in the central nervous system: effects on cognition and emotion in animals and humans. *Brain Research - Brain Research Reviews* **30**:264-288.

Youngblood, G. L. and Payne, A. H. (1992). Isolation and characterization of the mouse P450 17 alpha-hydroxylase/C17-20-lyase gene (Cyp17): transcriptional regulation of the gene by cyclic adenosine 3',5'-monophosphate in MA-10 Leydig cells. *Mol Endocrinol* **6** :927-934.

Zhang, L. H., Rodriguez, H., Ohno, S., and Miller, W. L. (1995). Serine phosphorylation of human P450c17 increases 17,20-lyase activity: implications for adrenarche and the polycystic ovary syndrome. *Proc Natl Acad Sci U S A* **92**:10619-10623.

Zuber, M. X., Simpson, E. R., and Waterman, M. R. (1986). Expression of bovine 17 alpha-hydroxylase cytochrome P-450 cDNA in nonsteroidogenic (COS 1) cells. *Science* **234**:1258-1261.

Zumoff, B., Rosenfeld, R. S., Strain, G. W., Levin, J., and Fukushima, D. K. (1980). Sex differences in the twenty-four-hour mean plasma concentrations of dehydroisoandrosterone (DHA) and dehydroisoandrosterone sulfate (DHAS)

and the DHA to DHAS ratio in normal adults. *J Clin Endocrinol Metab* **51**:330-333.

APPENDIX A: Enlarged Figures.

Chapter 2.1. Fig. 10. Proposed StAR mechanism in the mitochondrial intermembrane space (see page 98 for legend).

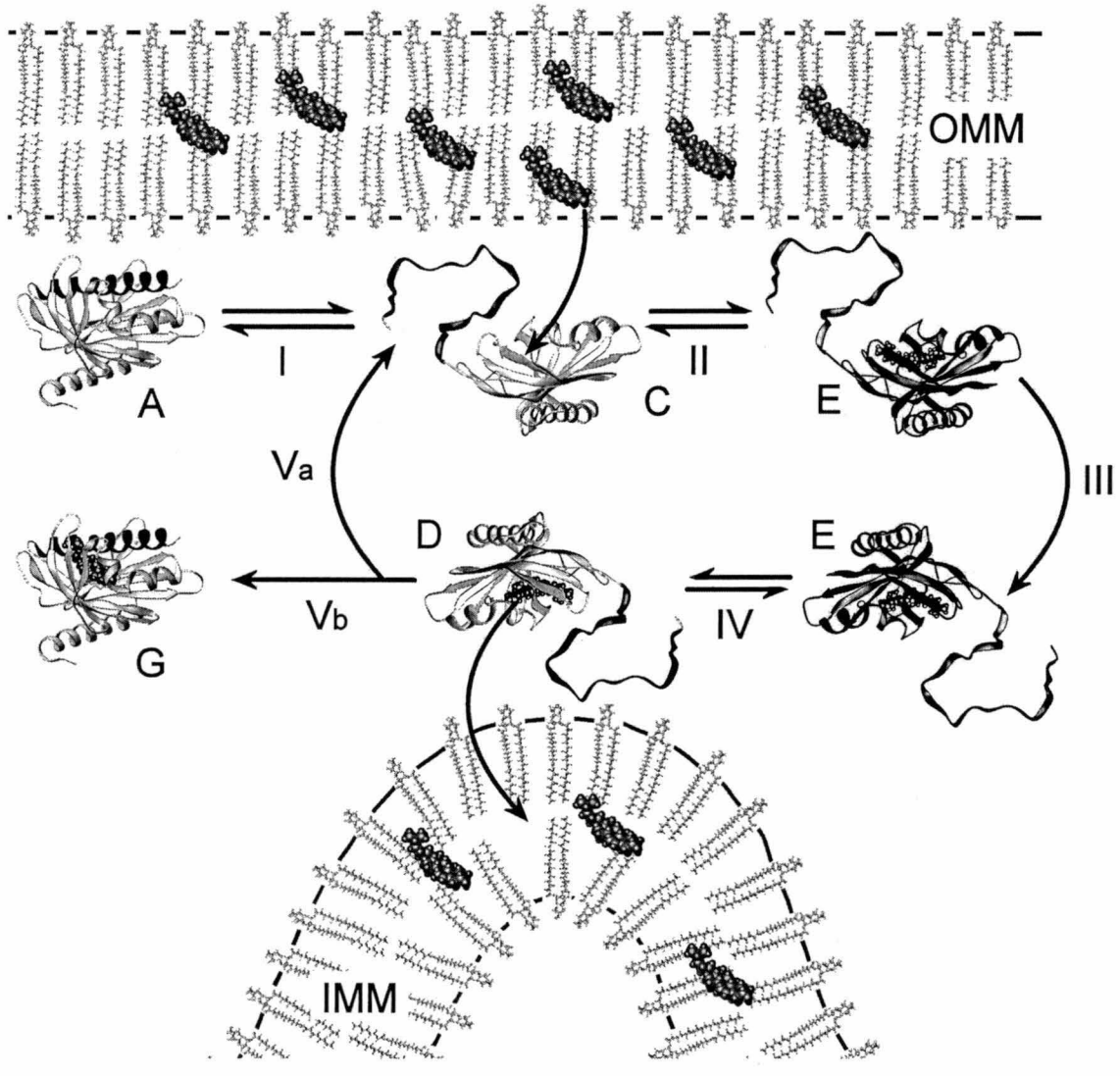

Chapter 2.1: Fig. 11. Proposed StAR mechanism in the cytosol (see page 99 for legend).

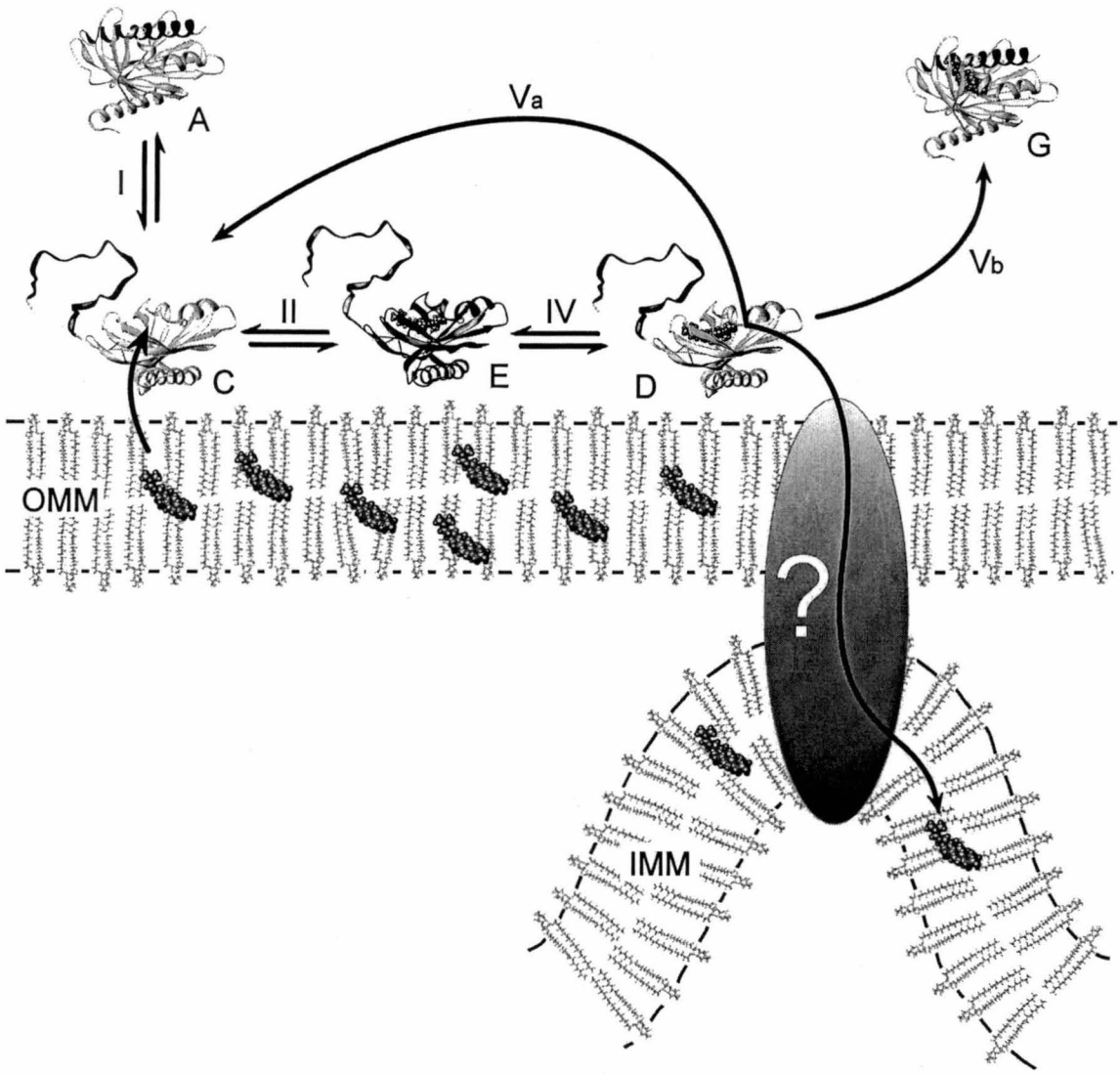

APPENDIX B:

Adrenocorticotropin Regulation of Steroidogenic Acute Regulatory Protein

†JEAN-GUY LEHOUX, AXEL MATHIEU, ‡PIERRE LAVIGNE AND ALAIN FLEURY

From the Department of Biochemistry, and ‡Pharmacology, Faculty of Medicine, University of Sherbrooke, Sherbrooke, Quebec, Canada, J1H 5N4.

Running title: ACTH StAR Regulation

Key words: Hamster, rat, COS-1 cells, adrenal, cAMP, 2D-PAGE

†To whom correspondence should be addressed: Department of Biochemistry, Faculty of Medicine, University of Sherbrooke, Sherbrooke, Quebec, Canada, J1H 5N4. Phone: (819) 564-5282; Fax: (819) 820-6852

E-mail: jlehou01@courrier.usherb.ca.

ABSTRACT **We have studied the effect of the adrenocorticotropin hormone (ACTH) on the expression of the Steroidogenic Acute Regulatory protein (StAR) *in vivo* in rat and hamster adrenals, also in transfection experiments using COS-1 cells. *In vivo*, ACTH increased the level of StAR mRNA within 30-60 minutes, and also increased the quantity of StAR but with a 2-3 hour delay. ACTH induced the formation of many acidic StAR species as analyzed by two-dimensional gel electrophoresis and immunoblotting. In the transfection experiments, $(Bu)_2$-cAMP also induced the formation of many acidic species for the hamster StAR; in COS-1 cells, StAR is phosphorylated mainly on serine (S) residue(s). When alanine (A) was substituted for serine, S13A, S185A and S194A mutants had decreased StAR activity compared to wild type, so determining the importance of these amino acid residues in StAR action. The full length WT, N46-truncated StAR lacking its mitochondrial import sequence, and N46-S194A had similar activities, whereas N46-S185A had completely lost its activity. Our results suggest that S194, but not S185, functions in association with the mitochondrial import sequence for the initiation of StAR activation. Further studies showed that S185 is implicated in salt bridge stability, not in StAR phophorylation, suggesting its importance for StAR folding. Thermodynamic calculations of the hamster StAR homology model based on MLN64, show that StAR can partially unfold to bind cholesterol and serve as a rapid transfer mechanism for eventual translocation into mitochondria. This is supportive of a StAR functioning either outside the mitochondria or in the mitochodrial intermembrane space.**

1. Pre-StAR (Steroidogenic Acute Regulatory protein) studies

1.1 *Studies that have lead to the discovery of phosphoproteins implicated in the acute response of ACTH stimulation.*

Early studies have shown that one action of adrenocorticotropin (ACTH) and 3', 5'-adenosine monophosphate on adrenocortical tissues was to increase the conversion of cholesterol to pregnenolone by the cytochrome P450 side chain cleavage (P450scc) enzyme system, considered as the rate-limiting step of the steroidogenesis pathway (Stone and Hechter, 1954; Karaboyas and Koritz, 1965). *In vitro* studies on different adrenal preparations have shown that ACTH acutely stimulated corticosteroid production within approximately 3 minutes (Farese, 1971; Kloppenborg et al., 1968; Urquhart and Li, 1968) and that the protein synthesis inhibitor cycloheximide prevented this stimulation *in vitro* (Haynes, 1959) as well as *in vivo* (Garren et al., 1965). It has also been established that removal of this inhibitor from incubation medium allows ACTH stimulation to occur again. Moreover, the rapid lost capacity of ACTH prestimulated adrenal cells to continue steroid production in the presence of cycloheximide indicated that these newly formed proteins are highly labile. Based on above results the concept of newly synthesized labile proteins has been proposed to mediate the acute steroidogenic response upon ACTH stimulation.

It was subsequently established that cycloheximide blocked the translocation of cholesterol from the outer membrane to the inner membrane (Privalle et al., 1983) where is located P450scc (Karaboyas and Koritz, 1965; Yago and Ichii, 1969), without affecting P450scc activity (Arthur and Boyd, 1974). The transport of cholesterol into mitochondria,

and not P450scc activity, was thus considered the rate-limiting step in the metabolism of cholesterol to pregnenolone and isocaproaldehyde.

A likely candidate for the postulated corticosteroid stimulatory protein (Furguson Jr, 1962) was pointed out by Krueger and Orme-Johnson (1983) who reported the discovery of a protein produced during acute ACTH stimulation in isolated rat adrenal cells. The synthetic time course and ACTH dose response of this protein were similar to those of corticosteroid production and they were concomitantly inhibited by cycloheximide. The subsequent work by the group of Orme-Johnson (Alberta et al., 1989; Epstein and Orme-Johnson, 1991; Krueger and Orme-Johnson, 1983; Pon et al., 1986b; Pon et al., 1986a; Pon and Orme-Johnson, 1986) covering the period of 1983-1991 clearly established the existence of a family of 28 to 32 kDa phosphoproteins in various steroidogenic tissues that fulfills the requirements of the postulated labile steroidogenic stimulatory protein. Their studies showed that these proteins all originated from a common 37 kDa precursor that was rapidly phosphorylated in response to cAMP, and cleaved during its import into mitochondria. These authors made the suggestion that this phosphoprotein could carry cholesterol inside mitochondria during its transit process (Epstein and Orme-Johnson, 1991).

2. Post-StAR studies

2.1 *Cloning of the StAR gene and its identification as the factor responsible for the acute steroidogenic response to ACTH stimulation.*

Phosphoproteins similar to those reported by the group of Orme-Johnson were analyzed by Stocco and Kilgore (1988) in MA-10 mouse Leydig tumor cells. They found in $(Bu)_2$-cAMP-stimulated cells four newly synthesized 30 kDa phosphoproteins with different pI localized into mitochondria. These phosphoproteins were shown to be identical by tryptic peptide analysis (Stocco and Chen, 1991). They also reported that phosphorylation was responsible for the more acidic forms of two of these proteins.

Purification of the 30 kDa proteins from MA-10 Leydig cells by Clark et al. (1994) followed by amino acid sequence analysis, allowed the cloning of its cDNA. These researchers demonstrated for the first time that expression of this protein in transfected MA-10 cells in the absence of hormonal stimulation was sufficient to induce steroid production (Clark et al., 1994). They have concluded that this novel protein is required in the acute regulation of steroidogenesis and they proposed to name it Steroidogenic Acute Regulatory protein.

The cloning of the human StAR was reported in 1995 (Sugawara et al., 1995), and Lin et al. (1995) discovered a mutated and non functional StAR in three individuals with congenital adrenal hyperplasia (LCAH), a disorder that is characterized by impaired gonadal and adrenal steroidogenesis. This provided the first genetic evidence that StAR is essential for normal adrenal and gonadal steroidogenesis. Another strong evidence that StAR is essential for steroid synthesis is the lipid accumulation and impaired steroidogenesis in steroidogenic tissues of StAR gene nullizygous mice (Caron et al., 1997b).

The cloning of StAR cDNA has been subsequently reported for other species, including pig (Pilon et al., 1997), hamster (Fleury et al., 1998b), rat (Ariyoshi et al.,

1998), cow (Rust et al., 1998), horse (Kerban et al., 1999), chicken (Bauer et al., 2000), frog (Bauer et al., 2000), zebra fish (Bauer et al., 2000), rainbow trout (Todo et al., 2000), brook trout (Goetz, 2000), and sheep (West et al., 2001). A high StAR sequence homology exists between these animal species. For example, the hamster StAR is 91.9% homologous to mouse and only slightly less with rat, human and other indexed species. As for the rodents, the hamster StAR protein contains 284 amino acid residues, one less than the human, bovine and porcine. The StAR from all the indexed species possess a mitochondrial recognition signal peptide. The hamster and mouse sequence signal cleavage site follows the consensus motif for a two-step cleavage site (Hendrick et al., 1989) whereas only one cleavage is predicted for sequences of other species.

In situ fluorescence hybridization placed the human StAR locus on chromosome 8p11.2, whereas a StAR pseudogene was mapped on chromosome 13 (Sugawara et al., 1995). Southern blot analyses suggest the presence of only one StAR gene in the hamster genome (Fleury et al., 1998b).

2.2 *Tissue distribution of StAR mRNA.*

StAR expression was detected mainly in steroidogenic tissues. For example, the hamster StAR mRNA (1.7 kb, 3.1 kb and 5.3 kb in size) was revealed in adrenals, ovary and testis, and not in other tissues (Fig.1) (Fleury et al., 1998b). The human StAR mRNA (1.6 kb, 4.4 kb and 7.5 kb) was detected in adrenals, testis, kidneys, but not in placenta (Sugawara et al., 1995). However, human StAR mRNA was detected in kidneys where StAR might be involved for the hydroxylation of vitamin D. The rat StAR mRNA (1.6 kb and 3.5 kb) was found in adrenals (Kim et al., 1997; LeHoux et al., 1998); *in situ*

hybridization studies revealed StAR transcripts in the rat cerebral cortex, hippocampus, dentate gyrus, olfactory bulb, cerebellar granular layer, and Purkinje cells (Furukawa et al., 1998), suggesting that StAR might be involved in neurosteroids synthesis.

2.3 *In vivo effects of ACTH on adrenal StAR mRNA expression*

The level of StAR mRNA in the adrenal *zona glomerulosa* ZG and *zona fasciculata* ZF were increased within thirty minutes after ACTH administration in rats (LeHoux et al., 1998) (Ariyoshi et al., 1998; Fleury et al., 1998a) and hamsters (Fleury et al., 1998b) indicating that ACTH regulates StAR mRNA synthesis. In other steroidogenic tissues, StAR mRNA levels were also induced by trophic hormones producing cAMP, suggesting that the cAMP-dependent protein kinase A pathway may induce StAR transcription. In human granulosa cells for example, the increase in StAR mRNA upon cAMP stimulation was associated with an increased transcription of the StAR gene that was blocked by actinomycin D (Kiriakidou et al., 1996). Deletion analyses of the human (Sugawara et al., 1996), mouse (Caron et al., 1997a), rat (Sandhoff et al., 1998), porcine (LaVoie et al., 1999), and bovine (Sugawara et al., 2001) StAR promoters indicate the existence of cAMP-responsive regions within 150, 254, 362, 60, and 342 base pairs from the transcriptional start site, respectively. All these data indicate that cAMP stimulates StAR gene trancription activity even though no consensus cAMP responsive element (CRE) sequences were found in these StAR gene promoters. This also suggests that the CRE binding protein does not bind directly on the StAR promoter and would rather exert its action in association with other transcription factors.

DNA motifs resembling binding sites for the steroidogenic factor 1 (SF-1) were identified in the human (Sugawara et al., 1996), mouse (Caron et al., 1997a; Clark et al., 1995), and rat (Sandhoff et al., 1998) gene promoters. Furthermore, the human StAR promoter is not active when expressed in SF-1 deficient cells. However, the introduction of SF-1 into these cells stimulated the promoter activity particularly in the presence of cAMP (Sugawara et al., 1996). This suggests that SF-1 plays a key role in controlling the basal and cAMP stimulated expression of the StAR gene. The activity of the rat StAR promoter, like that of the human, is responsive to cAMP stimulation involving SF-1 (Sandhoff et al., 1998). In the mouse, SF-1 is also required for activation of the StAR promoter but may not be the factor that confers cAMP responsiveness in steroidogenic cells (Caron et al., 1997a; Clark et al., 1995).

In SF-1 transfection experiments in a nonsteroidogenic cell line, CCAAT/enhancer binding protein β was reported to be involved in the basal and $(Bu)_2$-cAMP stimulated regulation of the mouse StAR gene transcription (Reinhart et al., 1999). Moreover, the transcription factor RIP 140 was recently shown to bind to SF-1 and DAX-1, negatively modulating the cAMP enhancing effect on the human StAR promoter activity (Sugawara et al., 2001). In the murine StAR promoter, a series of complex protein-DNA interactions were reported to occur within a cAMP responsive region containing C/EBPβ, SF-1, and AP-1 binding sites (Tsujishita and Hurley, 2000). Taken together these results clearly show that cAMP is effectively involved in the positive control of the StAR gene promoter activation. However, the interaction between known and unknown transcription factors involved in the complete cAMP action on the StAR promoter is yet to be unraveled.

2.4 *In vivo effects of ACTH on adrenal zonal and intracellular distributions of StAR; optical and electronic microscopy.*

Indirect immunofluorescence of rat adrenal paraffin sections revealed the presence of StAR in the *zonae glomerulosa, fasciculata* and *reticularis*. In control adrenals (Fig.2A), StAR was more concentrated in the thin *zona glomerulosa* (arrows) but more diffusely distributed in the *zona fasciculata* and *zona reticularis* (black bar). Five hours after ACTH treatment (Fig.2B), the intensity of the fluorescent signal was mainly increased in the *zona glomerulosa* (arrows) and *zona fasciculata* (black bar).

Colloidal-gold electron microscopic studies on thin rat adrenal sections revealed that more than 98% of positive StAR labeling was located over mitochondria (Fig.3) (LeHoux et al., 1999). It was determined that StAR is mainly localized in the intermembrane space and the intermembrane space side of the mitochondrial cristae membrane (King et al., 1995). ACTH administration lead to a significant increase of gold particles over mitochondrial *zona glomerulosa* and *zona fasciculata* cells, whereas it had no apparent increasing effect on the number of gold particles in the cytoplasm (LeHoux et al., 1999). These results indicate that upon ACTH stimulation, StAR does not accumulate in the cytoplasm and that it is either translocated into mitochondria or degraded in the cytoplasm. The level of StAR mRNA was increased in hamster (Fleury et al., 1996; Fleury et al., 1998b) and rat adrenals (Ariyoshi et al., 1998; Fleury et al., 1998a; LeHoux et al., 1998) within thirty to sixty minutes post *in vivo* ACTH administration. The increase in StAR protein levels was delayed compared to its mRNA

in rat adrenals (LeHoux et al., 1998; LeHoux et al., 1999), suggesting that the newly synthesized StAR mRNA was not completely translated into protein.

2.5 In vivo effects of ACTH on rat adrenal StAR processing; characterization by SDS-PAGE and immunoblotting.

Under ACTH stimulation the intensity of many rat adrenal specific StAR protein bands migrating between 29-39 kDa increased in mitochondrial and supernatant preparations (Fig.4). The expression of a 30 kDa band was only induced in mitochondria, its relative intensity being one tenth that of the major 29 kDa band. A 34 kDa protein band only increased in the supernatant of the ACTH-stimulated rats (LeHoux et al., 1999). All these increases were observed for the three to five hour treatments. Such an increase was not observed for the one hour treatment (not shown) even if plasma corticosteroid levels were already maximally elevated at that time of treatment (LeHoux et al., 1999).

Further characterization of the rat adrenal StAR by two-dimensional gel electrophoresis and immunoblotting showed the presence of four StAR species in the control homogenate preparation (Fig.5A, upper panel). The quantity of StAR was not increased in the ACTH treated group one hour after ACTH administration, whereas one band present in the control (arrow) disappeared in the treated group (Fig.5A middle panel). In agreement with these results, Artemenko et al. (2001) also did not find any noticeable increases in adrenal StAR expression between control and ACTH treated rats thirty minutes after treatment. These results clearly show that StAR does not quantitatively change much within the first hour of treatment during acute stimulation by

ACTH. Consequently, to explain the action of StAR during this acute stimulation period, one should look at minute changes in StAR characteristics.

Five hours after ACTH administration, however, many changes occurred in the number of StAR species as well as in StAR intensity as illustrated (Fig.5A, lower panel). Also, as seen in Fig.5B, two main StAR species (5.9/29 and 5.7/29) and four minor species were revealed in mitochondria of control preparations (upper panel). Five hours after ACTH administration, all the above mentioned species were increased in intensity and new mainly acidic StAR species were revealed in mitochondria. In the supernatant, ACTH treatment led to less apparent changes than in mitochondria. However, ACTH induced an increase in the 5.5/29 and 5.4/29 species and a reduction in the 5.4/28 species (Fig.5B lower panels). The latter species was observed only in supernatant but not in mitochondria. In agreement with our data Artemenko et al. (2001) reported the induction of many acidic StAR species in rat adrenals three hours after ACTH administration.

Taken together these results show that ACTH enhanced the formation and accumulation of many acidic species during StAR processing and importation into mitochondria.

3. Structure/Function of StAR

3.1 *Mutational analysis of StAR function in non-steroidogenic cells.*

The green monkey kidney COS-1 cell line was used to analyze the activity of wild type and mutated StAR. The assay consists of cotransfecting an expression plasmid harboring StAR cDNA and an F2 construct containing cytochrome P450scc-adrenodoxin

reductase-adrenodoxin cDNA (Harikrishna et al., 1993). The introduction of the cholesterol side chain system is essential since COS-1 cells are not steroidogenic. In this assay the pregnenolone secreted in incubation media reflects StAR activity. Using this system Lin et al. (1995) found that the plasmid containing normal human StAR cDNA synthesized 175 ng of pregnenolone per dish compared to 20 ng for the empty vector. Nineteen ng were secreted for the mutant Arg193Stop found in one LCAH patient and 25 ng for the mutant Gln258Stop found in two other LCAH patients. The 20 ng pregnenolone secreted in incubation media for the empty vector corresponds to StAR independent cholesterol transport into mitochondria. Using this assay we have studied the effect of increasing concentrations of the hamster wild type StAR-pcDNA3.1 on pregnenolone synthesis in the presence or absence of the stimulating agent $(Bu)_2$-cAMP. With a fixed concentration of the F2 construct, a maximum in pregnenolone secretion was obtained with 75 ng of WT StAR-pcDNA3.1.

We have thus studied the effect of $(Bu)_2$-cAMP on the characteristics of StAR by 2-dimensional gel analysis. Fig.6 shows that $(Bu)_2$-cAMP increased the number of mitochondrial StAR immunoreactive species in transfected COS-1 cells.

Two main immunoreactive StAR bands were revealed for control wild type (Ctr-WT) with pI of 5.9 and 5.7 migrating in the 30 kDa area (Fig.6A). StAR immunoreactive bands are also observed in the right portion of the figure. When $(Bu)_2$-cAMP was added in the incubation medium, the two main bands found in Ctr (panel A) were present with many induced additional StAR species (Fig.6, panel B). These data are in agreement with the *in vivo* long-term effects of ACTH discussed earlier, showing quantitative and qualitative differences in characteristics between Ctr and stimulated StAR preparations.

3.2 *Mutation of putative phosphorylation sites in the hamster StAR and StAR activity*

Pon et al. (1986b) used 2-dimensional gel electrophoresis to monitor proteins synthesized in control and ACTH- or cAMP-stimulated rat adrenal cells. They have identified four proteins with different pI having identical proteolytic peptide maps, now known as StAR. Two of these proteins were found in unstimulated cells and four after cell stimulation. They also found that ^{32}P-phosphate was incorporated into two of these proteins and that incubation with *E. coli* phosphatase caused a decrease of this incorporation. These authors established a correlation between the phosphorylation of these proteins and steroidogenesis upon ACTH stimulation in rat adrenal cells.

By amino acid sequence alignment of StAR from the thirteen different species indexed up to now, we have determined the presence of eleven putative phosphorylation sites in the hamster StAR which were conserved among most species. The eleven putative phosphorylation sites of the hamster StAR that were mutated are serine (S) S13, S55, S60, S90, S185, S194, S273 to alanine (A), and threonine (T) T5 and T262 to valine (V). The mutants S13A, S185A and S194A decreased StAR activity by 30%, 81% and 95% respectively, whereas the others did not result in any changes (Fleury et al., 2002). The secretion of pregnenolone was increased for WT and all mutants in the presence of $(Bu)_2$-cAMP. However, the increase was 40% and 89% lower for the stimulated S185A and S194A mutants compared to the stimulated WT. These results clearly show that it is the mutation S194A that affected StAR activity the most. The double S13A/S194A and S185A/S194A and the triple S13A/S185A/S194A mutants were thus engineered and tested on StAR activity. The activity of the double mutant S13A/S194A was further

decreased compared to that of the S194A mutant, yet still stimulated by $(Bu)_2$-cAMP. The StAR activity of the double S185A/S194A and triple S13A/S185A/S194A mutants were practically abolished demonstrating the importance of these three amino acid residues (Fleury et al., 2002).

The change in StAR activity of the above-mentioned mutants was not due to differences in StAR expression. In fact, the quantity of expressed protein was the same for unstimulated WT and mutant transfections. However, an increase in the quantity of StAR occurred when $(Bu)_2$-cAMP was added to the incubation media. This was also similar for WT and S185A, S194A and S185A/S194A mutants, although as mentioned above, the mutant StAR activity was considerably lower than that of WT. In the case of the double S185A/S194A mutant StAR activity was even abolished (Fleury et al., 2002). Given these results we conclude that altered mutants StAR activity is due to the mutation and not in different protein expression levels.

When analyzed by two-dimensional gel electrophoresis, the migration pattern of the S194A mutant in COS-1 cells stimulated by $(Bu)_2$-cAMP for 24 hours differed from the stimulated WT. Empty circles (Fig.6B) show the location of the main low pI StAR species present in WT and absent in the S194A mutant; many acidic StAR species present in WT were not revealed in the S194A preparation. These results are in agreement with those of Arakane et al. (1997) showing that the substitution of the human StAR amino acid residue S195 (equivalent to the S194 in hamster) by alanine, decreased steroidogenesis activity and did not yield the more acidic StAR species detected by two-dimensional immunoblotting. The conversion of the human S195 amino acid residue to an aspartic acid residue had no decreasing effect on steroidogenic activity, which is not

incompatible with the idea that a negative charge at this site could modulate StAR function. The migration pattern of the S13A and S185A mutant preparations stimulated by $(Bu)_2$-cAMP, however, did not differ much from WT (Fleury et al., 2002). The lack of effect by the S13A mutation on the migration pattern of StAR is not surprising since the part of the protein containing the amino acid S13 is removed when the leader peptide is cleaved by a mitochondrial protease. The lack of effect of the mutation S185A is more intriguing and is indicative that this amino acid residue might not be a phosphorylation site. To determine if S185 was effectively a true phosphorylation site, we have substituted the amino acid S185 by either glutamic acid or aspartic acid in order to mimic the presence of a negatively charged group on S185. These substitutions resulted in no increases, but rather a decrease in StAR activity. Furthermore, substitution of S185 by a cysteine residue, to replace the serine OH group by a SH group having similar characteristics but cannot be phosphorylated, nearly fully restored basal and $(Bu)_2$-cAMP stimulated activities (Fleury et al., 2002). Since the quantity of expressed StAR was similar between preparations, we can deduce that the hamster StAR S185 is not a site of phosphorylation.

3.3 *ΔN46 mutants and StAR activity.*

We have deleted the first N-terminal 46 amino acid residues of the hamster StAR to remove the mitochondrial import sequence. When coexpressed in COS-1 cells with the F2 construct, the truncated hamster N46-WT protein was as active as its full-length counterpart (Fleury et al., 2002). These data are in agreement with those of Arakane et al. (1996) suggesting that removal of the StAR mitochondrial import sequence does not

affect steroidogenesis. We took advantage of the fact that the truncated N-46 StAR was as active as the WT to study the effect of mutating the putative phosphorylation sites S185 and S194. The mutant N46-S185A and the double mutant S185AS/194A had no StAR activity; the pregnenolone found in the incubation media was the same as that of the empty vector transfection. Surprisingly however, the activity of the unstimulated N46-S194A mutant was as strong as that of the N46-WT, the quantity of StAR being similar for both preparations. When $(Bu)_2$-cAMP was added to the incubation media for N46-WT and N46-S194A preparations, the StAR mass increased in quantity. In contrast to the unstimulated preparations, the StAR activity of the stimulated N46-WT was significantly more elevated than that of the N46-S194A mutant (Fleury et al., 2002). These results thus indicate that modification of the hamster StAR S194 site affected the acute enhancing effect of $(Bu)_2$-cAMP on StAR activity even in the absence of its mitochondrial import sequence. This stresses the importance of this amino acid residue for StAR full activity.

3.4 *StAR phosphorylation.*

In order to further analyze StAR phoshorylation, the hamster WT StAR containing a myc-tag was isolated by immunoprecipitation with a specific anti-myc antibody. By immunoblotting with a specific anti-phosphoserine antibody, we were able to reveal phosphoproteins that co-localized with StAR. When a specific anti-threonine antibody was substituted to the anti-phosphoserine antibody only a faint signal was observed (Fleury et al., 2002). WT StAR transected COS-1 cells were also incubated with [^{33}P]orthophosphate. Following immunoprecipitation with an anti-StAR antibody,

analyzed by immunoblotting, we found two ^{33}P-labeled protein bands migrating at the same level as StAR (Fleury et al., 2002). These bands were cut and digested with HCl and separated by two-dimensional thin layer chromatography in the presence of internal serine, tyrosine and threonine standards. Almost all the radioactive amino acids comigrated with the internal serine standard, with only trace amounts with the threonine standard; no radioactivity was detected with the tyrosine standard. These results thus indicate that under conditions used, StAR was phosphorylated mainly on serine residues and to a much lower extent on threonine residues. Yet which serine(s) and/or threonine(s) are phosphorylated remains to be identified for the hamster StAR.

4. Mechanisms of StAR-Dependent Cholesterol Transfer

4.1 *Discussion of the pre- and post-MLN64 crystal models: desorption, molten globule, intermembrane shuttle and PBR-associated mechanisms.*

No clear concise picture can summarize all the experimental data reported to date. Therefore, it is not surprising that several models of StAR function exist in literature. Historically, these proposed mechanisms can be separated into two eras: pre- and post-MLN64 crystallographic data. Until the human MLN64 protein START domain was crystallized (Tsujishita and Hurley, 2000), no definite three-dimensional structural data was obtained to possibly elucidate the actual StAR mechanism. There are two key observations that have to be kept in mind wherever one tries to describe StAR function. These include: 1) the wild type StAR has a mitochondrial targeting sequence although it is not necessary for proper StAR activity, and 2) a minute amount of StAR is actually

needed to transfer large amounts of cholesterol inside mitochondria (Clark et al., 1994; Petrescu et al., 2001). Yet, the defining characteristic of StAR function is the fact that the hydrophobic cholesterol has to be translocated from the outer mitochondrial membrane, through the aqueous hydrophilic intermembrane space, to the inner mitochondrial membrane where P450scc resides for proper steroidogenesis.

In the initial proposed mechanism of StAR function by Kallen et al. (1998) pre-MLN64 crystallographic data, cholesterol would be transferred to the inner mitochondrial membrane where P450scc resides through a desorption mechanism. As StAR enters mitochondria *via* its N-terminal targeting sequence, the two mitochondrial membranes would merge thus allowing cholesterol to "freely" transfer from the cholesterol-rich outer mitochondrial membrane to the cholesterol-deprived inner mitochondrial membrane. This mechanism can account for the observation that StAR does co-localize to mitochondrial contact sites (Pon et al., 1989; Schwaiger et al., 1987; Stocco and Clark, 1996). Since the cholesterol gradient essentially drives its transfer inside mitochondria, large amounts of cholesterol could be transferred through this mechanism in little time, necessitating little amounts of StAR. Once inside the mitochondria matrix, mitochondrial enzymes would degrade StAR explaining its rapid turnover. Unfortunately to this date, there have not been any protein-protein interactions discovered between StAR and the mitochondrial import machinery to support this mechanism. Moreover, the desorption mechanism cannot explain the discovery that StAR can function without its mitochondrial targeting sequence (Arakane et al., 1996; Arakane et al., 1998; Fleury et al., 2002).

Another proposed StAR mechanism consists of molten globular states active on the cytosolic side of the outer mitochondrial membrane. This is due to the observation

that the 63-188 StAR fragment is protease resistant (Bose et al., 1999). Indeed, these authors have demonstrated that molten globular states of StAR are detected at low pH conditions (3.5-4.0), suggesting that these molten globular states are important for StAR function. Moreover, Christensen et al. (2001) have demonstrated that these molten globular states preferentially bind to cholesterol-rich membranes supporting their existence and their importance in StAR activity. On the other hand, the existence of acidic conditions immediately surrounding the outer mitochondrial membrane remains to be revealed in order to drive the observed StAR molten globular states.

Unfortunately, no StAR crystal has been obtained yet due to its highly hydrophobic nature. The closest approximation to the actual StAR three-dimensional structure is the recent crystal structure of the human MLN64 protein START domain (Tsujishita and Hurley, 2000). MLN64 is highly homologous to StAR and is believed to have a similar function to StAR in the human placenta, brain, and non-steroidogenic tissues (Bieche et al., 1996; Moog-Lutz et al., 1997; Watari et al., 1997). Straight from the crystallographic data, Tsujishita and Hurley (2000) suggest that MLN64 and thus StAR, function through an intermembrane shuttle mechanism. This comes from the observation that the MLN64 crystal is defined as a hydrophobic tunnel formed by a U-shaped β-barrel topped by a C-terminal α-helix; the openings of the hydrophobic tunnel are aligned to the poles of the capping α-helix. Moreover, these authors have demonstrated that both MLN64 and StAR bind one molecule of cholesterol per protein. They suggest that in order for cholesterol to bind, conformational changes of either the C-terminal α-helix and/or an adjacent loop have to occur since the hydrophobic tunnel's openings are not large enough to allow a cholesterol molecule through. Unfortunately, the

crystallographic data cannot describe any structural data for the mitochondrial targeting sequence as this segment was removed prior crystallization. Therefore, the importance of the mitochondrial targeting sequence in StAR remains elusive and cannot explain how StAR functions without it. These authors suggest that StAR could enter into the mitochondrial intermembrane space without the mitochondrial targeting sequence based on the work of others (Derman et al., 1993). On the other hand, electron microscopic studies of N62-StAR suggest no entry of this molecule in mitochondria (Arakane et al., 1996). The greatest downfall of this mechanism is that it is believed to be unfeasible that a shuttle mechanism transferring cholesterol, migrating from one membrane to the next, is rapid enough to support the observed cholesterol transfer inside mitochondria.

Recently it was shown that StAR and the peripheral-type benzodiazepine receptor (PBR) are localized in proximity of each other on the outer mitochondrial membrane (West et al., 2001). This observation, coupled to the fact that there is a reduction in steroidogenesis in the absence of PBR (Papadopoulos et al., 1997), suggests that these proteins could interact in the translocation of cholesterol inside mitochondria. This is supportive of the suggestion that StAR acts on or in the outer mitochondrial membrane, although, more studies are needed to confirm that this interaction is necessary for proper StAR function.

Finally, due to the lack of a single mechanism being able to explain all experimental data, the notion of "mixed mechanisms" is growing. Of particular interest, Stocco (2001) has recently suggested that StAR would function somewhat like a pore where StAR would take the three-dimensional structure described by the MLN64 crystal, be anchored at mitochondrial membrane contact sites, and sustain conformational

changes allowing cholesterol to pass through StAR's hydrophobic tunnel. However, there is no additional experimental data supplied for this hypothesis; this model is still dependent on the presence of the N-terminal mitochondrial targeting sequence and does not account for the observation that StAR can be located in the intermembrane space, other than at contact sites.

We have thus investigated a possible mechanism for StAR function set on homology modeling of StAR to the MLN64 crystal structure, and through the postulation of possible important molten globular states of StAR.

4.2 *Proposed mechanism for StAR action based on thermodynamic calculations.*

In addition to using molecular modeling to solve a protein's mode of action, it is possible to calculate the theoretical free energy of any protein with respect to the solvent accessible surface, so long as structural data is available *in silico*. From these structure-based thermodynamic calculations (STC) (Freire, 1993; Hilser and Freire, 1997), it is also possible to identify partially folded (unfolded) states of proteins in equilibrium with their native state and calculate theoretical binding constants of their ligands (Baker and Murphy, 1998; Hilser and Freire, 1997; Lavigne et al., 2000). Thus, we have used these tools to enlighten our understanding of the StAR function. Both the hamster and the human molecular models were obtained by homology modeling to the MLN64 crystallographic data, while STC simulations were performed on the hamster model. Yet, it is not the scope of this review to describe the molecular models or the actual STC simulations. These results are the subject of another publication (Mathieu et al., 2002).

We conceptualised that StAR function is mediated through various conformational states of the C-terminal α-helix following the following observations: 1) molten globular states of StAR are possible although artificially at low pH values (Bose et al., 1999; Christensen et al., 2001); 2) the C-terminal region of StAR is believed to transiently change conformations for cholesterol binding (Tsujishita and Hurley, 2000); 3) upon binding of a cholesterol analogue, StAR looses α-helical structure (Petrescu et al., 2001); 4) the C-terminal α-helix entirely covers the cholesterol binding site and should be free for movement; and 5) the StAR models had a hydrophobic cavity instead of a hydrophobic tunnel – the fact that a cavity is present instead of a tunnel, suggests that conformational changes are absolutely necessary for cholesterol binding. Through the production of various models of different conformational states of StAR, matched by STC calculations, we have shown that a StAR unfolded C-terminal α-helix is theoretically plausible in a significant population under normal conditions. This partially unfolded StAR should be important for StAR-mediated cholesterol transfer inside mitochondria (Mathieu et al., 2002). These observations become important for describing any StAR mechanism.

In the case of the intermembrane shuttle mechanism, it is believed that this mechanism is improbable due to the slow nature of protein diffusion in solution. STC calculations of the StAR models showed that the equilibrium between the folded and partially unfolded states (molten globular) of StAR is rapid, supporting a much faster intermembrane shuttle mechanism (Artemenko et al., 2001). This mechanism no longer necessitates StAR to unfold and refold to bind or release cholesterol. Therefore, a simple

rotational translation is needed to transfer cholesterol inside mitochondria at mitochondrial contact sites.

The partially unfolded states of StAR can also add insight into a mechanism where StAR functions on the cytosolic side of the outer mitochondrial membrane. In this case, the molten globular states of StAR may be useful to efficiently transfer cholesterol from the outer mitochondrial membrane to PBR, or another unidentified factor, which could transfer cholesterol inside mitochondria. Since the STC calculations were obtained with StAR in solution, the results are applicable to both the aqueous intermembrane space and the cytosol.

4.3 *Importance of the cholesterol binding site salt-bridge environment in the StAR mechanism.*

An interesting feature of StAR is the conserved E168-R187 salt-bridge pair (hamster StAR reference numbering) among animal species. In the StAR models, as well as for MLN64, this salt-bridge is located at the bottom of the U-shaped β-barrel opposite the movable C-terminal α-helix, indicating that it may serve an important function in StAR activity. In the molten globular intermembrane shuttle mechanism, this part of the hydrophobic cavity does not significantly change in the process of conformational change, nor during cholesterol binding. This salt-bridge can be envisioned as having two critical functions: anchoring for cholesterol binding and maintenance of minimal structure for the proper binding site definition. Through our modeling, we have shown that this salt-bridge can be implicated in hydrogen bonding of cholesterol to the binding site *via* one water molecule (Mathieu et al., 2002). In terms of maintaining minimal

structure definition for the binding site, burial of a salt-bridge in a generally hydrophobic pocket obviously costs energetically. Since this salt bridge is located on adjacent strands in the U-shaped β-barrel, it may thus help in maintaining the U-shaped β-barrel upon conformational changes of the C-terminal α-helix. Supporting this observation, the peptidase-resistant fragment of the human StAR is from 63-188 (Bose et al., 1999). Thus, the salt bridge may be implicated in this peptidase resistance.

Discovery of StAR salt-bridge mutations that abolish StAR activity (Mathieu et al., 2002) also support a critical role for this amino acid pair. In the event where only one amino acid of the salt-bridge is mutated for another non-charged amino acid, the remaining charged amino acid is too unstable in the hydrophobic environment and thus probably leads to improper protein folding (Bose et al., 1998). Moreover, our mutational analyses identified S185 as being important for StAR function. Upon a closer look, this amino acid is not solvent accessible and therefore cannot be phosphorylated unless major conformational changes occur. Therefore how can this amino acid alter StAR function to such an extent? In the hamster model, S185 is located directly beneath the salt-bridge pair, actually helping in maintaining the salt-bridge in position through hydrogen bonding. Thus, not only is the presence of the salt-bridge important for proper StAR function, but its environment and 3-dimensional space are critical as well.

4.4 *Overview of ACTH stimulation and StAR expression and function.*

The greatest challenge in explaining StAR function resides in unifying phosphorylation and leader peptide modulation to StAR molecular mechanisms. Although contradicting results suggest that StAR functions on the cytosolic side of the

outer mitochondrial membrane instead of the intermembrane space, our thermodynamic calculations support either of these models. Thus, only two steps seem necessary for StAR activation: 1) leader peptide modulation possibly *via* phosphorylation, allowing 2) StAR partially unfolded states for cholesterol transfer. As suggested previously (Christenson and Strauss III, 2001), phosphorylation could entice leader peptide modulation before or after actual contact to mitochondria. In either case, these are not inconsistent with the StAR partially unfolded states.

In the case where StAR functions in the mitochondrial intermembrane space, the leader peptide modulation *via* phosphorylation leads to StAR's import into the intermembrane space where it can now function through the shuttle mechanism (Fig 7A). On the other hand, if StAR functions outside mitochondria (Fig 7B), modulation of the leader peptide by phosphorylation should lead to StAR mitochondrial targeting for which StAR partially unfolded state becomes necessary for cholesterol binding, mediating cholesterol transfer to an undetermined factor mediating cholesterol entry into mitochondria.

These mechanisms are consistent with StAR without its leader peptide since these experiments have all been performed in transfection assays expressing large amounts of N-terminally cleaved StAR. The true test would be to verify if knock out animals would be viable in the event where the WT StAR would be replaced with a leader deficient StAR.

Acknowledgments

This work was supported by a grant from the Medical Research Council of Canada, grant MT-10983 (to J.G.L.), and the Heart and Stroke Foundation of Canada (to J.G.L.), and from the Natural Sciences and Engineering Research Council of Canada to P.L.. J.G.L. is *Chercheur boursier de carrière* du *Fonds de la recherche en santé du Québec,* and P.L. is the recipient of a c*hercheur-stratégique* Scholarship from *le Fonds pour la Formation de Chercheurs et l'Aide à la Recherche.* We would also like to thank Dr. Dale Buchanan Hales for the anti-StAR antibodies, Dr. Walter Miller for the F2 construct, Lyne Ducharme for technical assistance and Dr. Normand Brière for advice.

REFERENCES

Alberta JA, Epstein LF, Pon LA, Orme-Johnson NR. 1989. Mitochondrial localization of a phosphoprotein that rapidly accumulates in adrenal cortex cells exposed to adrenocorticotropic hormone or to cAMP. J Biol Chem 264:2368-2372.

Arakane F, Kallen CB, Watari H, Foster JA, Sepuri NB, Pain D, Stayrook SE, Lewis M, Gerton GL, Strauss III JF. 1998. The mechanism of action of steroidogenic acute regulatory protein (StAR). StAR acts on the outside of mitochondria to stimulate steroidogenesis. J Biol Chem 273:16339-16345.

Arakane F, King SR, Du Y, Kallen CB, Walsh LP, Watari H, Stocco DM, Strauss III JF. 1997. Phosphorylation of steroidogenic acute regulatory protein (StAR) modulates its steroidogenic activity. J Biol Chem 272:32656-32662.

Arakane F, Sugawara T, Nishino H, Liu Z, Holt JA, Pain D, Stocco DM, Miller WL, Strauss III JF. 1996. Steroidogenic acute regulatory protein (StAR) retains activity in the absence of its mitochondrial import sequence: implications for the mechanism of StAR action. Proc Natl Acad Sci USA 93:13731-13736.

Ariyoshi N, Kim YC, Artemenko I, Bhattacharyya KK, Jefcoate CR. 1998. Characterization of the rat Star gene that encodes the predominant 3.5-kilobase pair mRNA. ACTH stimulation of adrenal steroids in vivo precedes elevation of Star mRNA and protein. J Biol Chem 273:7610-7619.

Artemenko IP, Zhao D, Hales DB, Hales KH, Jefcoate CR. 2001. Mitochondrial processing of newly synthesized steroidogenic acute regulatory protein (StAR), but not total StAR, mediates cholesterol transfer to cytochrome P450 side chain cleavage enzyme in adrenal cells. J Biol Chem 276:46583-46596.

Arthur JR, Boyd GS. 1974. The effect of inhibitors of protein synthesis on cholesterol side-chain cleavage in the mitochondria of luteinized rat ovaries. Eur J Biochem 49:117-127.

Baker BM, Murphy KP. 1998. Prediction of binding energetics from structure using empirical parameterization. Methods Enzymol 295:294-315.

Bauer MP, Bridgham JT, Langenau DM, Johnson AL, Goetz FW. 2000. Conservation of steroidogenic acute regulatory (StAR) protein structure and expression in vertebrates. Mol Cell Endocrinol 168:119-125.

Bieche I, Tomasetto C, Regnier CH, Moog-Lutz C, Rio MC, Lidereau R. 1996. Two distinct amplified regions at 17q11-q21 involved in human primary breast cancer. Cancer Res 56:3886-3890.

Bose HS, Baldwin MA, Miller WL. 1998. Incorrect folding of steroidogenic acute regulatory protein (StAR) in congenital lipoid adrenal hyperplasia. Biochemistry 37:9768-9775.

Bose HS, Whittal RM, Baldwin MA, Miller WL. 1999. The active form of the steroidogenic acute regulatory protein, StAR, appears to be a molten globule. Proc Natl Acad Sci USA 96:7250-7255.

Caron KM, Ikeda Y, Soo SC, Stocco DM, Parker KL, Clark BJ. 1997a. Characterization of the promoter region of the mouse gene encoding the steroidogenic acute regulatory protein. Mol Endocrinol 11:138-147.

Caron KM, Soo SC, Wetsel WC, Stocco DM, Clark BJ, Parker KL. 1997b. Targeted disruption of the mouse gene encoding steroidogenic acute regulatory protein provides insights into congenital lipoid adrenal hyperplasia. Proc Natl Acad Sci USA 94:11540-11545.

Christensen K, Bose HS, Harris FM, Miller WL, Bell JD. 2001. Binding of steroidogenic acute regulatory protein to synthetic membranes suggests an active molten globule. J Biol Chem 276:17044-17051.

Christenson LK, Strauss III JF. 2001. Steroidogenic acute regulatory protein: an update on its regulation and mechanism of action. Arch Med Res 32:576-586.

Clark BJ, Soo SC, Caron KM, Ikeda Y, Parker KL, Stocco DM. 1995. Hormonal and developmental regulation of the steroidogenic acute regulatory protein. Mol Endocrinol 9:1346-1355.

Clark BJ, Wells J, King SR, Stocco DM. 1994. The purification, cloning, and expression of a novel luteinizing hormone-induced mitochondrial protein in MA-10 mouse Leydig tumor cells. Characterization of the steroidogenic acute regulatory protein (StAR). J Biol Chem 269:28314-28322.

Derman AI, Puziss JW, Bassford PJ, Jr., Beckwith J. 1993. A signal sequence is not required for protein export in prlA mutants of Escherichia coli. EMBO J 12:879-888.

Epstein LF, Orme-Johnson NR. 1991. Regulation of steroid hormone biosynthesis. Identification of precursors of a phosphoprotein targeted to the mitochondrion in stimulated rat adrenal cortex cells. J Biol Chem 266:19739-19745.

Farese RV. 1971. Stimulation of pregnenolone synthesis by ACTH in rat adrenal sections. Endocrinology 89:958-962.

Fleury A, Cloutier M, Ducharme L, Lefebvre A, LeHoux J, LeHoux JG. 1996. Adrenocorticotropin regulates the level of the steroidogenic acute regulatory (StAR) protein mRNA in hamster adrenals. Endocr Res 22:515-520.

Fleury A, Ducharme L, Hales DB, Stocco DM, LeHoux JG. 1998a. Acute in vivo effects of ACTH on the expression of steroidogenic acute regulatory protein in rat adrenal. Endocr Res 24:571-574.

Fleury A, Ducharme L, LeHoux JG. 1998b. In vivo effects of adrenocorticotrophin on the expression of the hamster steroidogenic acute regulatory protein. J Mol Endocrinol 21:131-139.

Fleury A, Mathieu AP, Ducharme L, Hales DB, LeHoux JG. 2002. Phosphorylation and function of the hamster adrenal steroidogenic acute regulatory protein (StAR). Unpublished

Freire E. 1993. Structural thermodynamics: prediction of protein stability and protein binding affinities. Arch Biochem Biophys 303:181-184.

Furguson JJ. 1962. Puromycin and adrenal responsiveness to adrenocorticotropic hormone. Biochim Biophys Acta 57:616-617.

Furukawa A, Miyatake A, Ohnishi T, Ichikawa Y. 1998. Steroidogenic acute regulatory protein (StAR) transcripts constitutively expressed in the adult rat central nervous system: colocalization of StAR, cytochrome P-450SCC (CYP XIA1), and 3beta-hydroxysteroid dehydrogenase in the rat brain. J Neurochem 71:2231-2238.

Garren LD, Ney RL, Davis WW. 1965. Studies on the role of protein synthesis in the regulation of corticosterone production by adrenocorticotropic hormone in vivo. Proc Natl Acad Sci USA 53:1443-1450.

Goetz FW. 2000. Charactherization of the brook trout StAR and MLN64 homologs. Unpublished

Harikrishna JA, Black SM, Szklarz GD, Miller WL. 1993. Construction and function of fusion enzymes of the human cytochrome P450scc system. DNA Cell Biol 12:371-379.

Haynes RC. 1959. Influence of adenosine 3',5'-monophosphate on corticoid production by rat adrenal glands. J Biol Chem 234:1421-1423.

Hendrick JP, Hodges PE, Rosenberg LE. 1989. Survey of amino-terminal proteolytic cleavage sites in mitochondrial precursor proteins: leader peptides cleaved by two matrix proteases share a three-amino acid motif. Proc Natl Acad Sci USA 86:4056-4060.

Hilser VJ, Freire E. 1997. Predicting the equilibrium protein folding pathway: structure-based analysis of staphylococcal nuclease. Proteins 27:171-183.

Kallen CB, Billheimer JT, Summers SA, Stayrook SE, Lewis M, Strauss III JF. 1998. Steroidogenic acute regulatory protein (StAR) is a sterol transfer protein. J Biol Chem 273:26285-26288.

Karaboyas GC, Koritz SB. 1965. Identity of the site of action of 3',5'-adenosine monophosphate and adrenocorticotropic hormone in corticosteroidogenesis in rat adrenal and bovine adrenal cortex slices. Biochemistry 4:462-468.

Kerban A, Boerboom D, Sirois J. 1999. Human chorionic gonadotropin induces an inverse regulation of steroidogenic acute regulatory protein messenger ribonucleic acid in theca interna and granulosa cells of equine preovulatory follicles. Endocrinology 140:667-674.

Kim YC, Ariyoshi N, Artemenko I, Elliott ME, Bhattacharyya KK, Jefcoate CR. 1997. Control of cholesterol access to cytochrome P450scc in rat adrenal cells mediated by regulation of the steroidogenic acute regulatory protein. Steroids 62:10-20.

King SR, Ronen-Fuhrmann T, Timberg R, Clark BJ, Orly J, Stocco DM. 1995. Steroid production after in vitro transcription, translation, and mitochondrial processing of protein products of complementary deoxyribonucleic acid for steroidogenic acute regulatory protein. Endocrinology 136:5165-5176.

Kiriakidou M, McAllister JM, Sugawara T, Strauss III JF. 1996. Expression of steroidogenic acute regulatory protein (StAR) in the human ovary. J Clin Endocrinol Metab 81:4122-4128.

Kloppenborg PW, Island DP, Liddle GW, Michelakis AM, Nicholson WE. 1968. A method of preparing adrenal cell suspensions and its applicability to the in vitro study of adrenal metabolism. Endocrinology 82:1053-1058.

Krueger RJ, Orme-Johnson NR. 1983. Acute adrenocorticotropic hormone stimulation of adrenal corticosteroidogenesis. Discovery of a rapidly induced protein. J Biol Chem 258:10159-10167.

Lavigne P, Bagu JR, Boyko R, Willard L, Holmes CF, Sykes BD. 2000. Structure-based thermodynamic analysis of the dissociation of protein phosphatase-1 catalytic subunit and microcystin-LR docked complexes. Protein Sci 9:252-264.

LaVoie HA, Garmey JC, Veldhuis JD. 1999. Mechanisms of insulin-like growth factor I augmentation of follicle-stimulating hormone-induced porcine steroidogenic acute regulatory protein gene promoter activity in granulosa cells. Endocrinology 140:146-153.

LeHoux JG, Fleury A, Ducharme L. 1998. The acute and chronic effects of adrenocorticotropin on the levels of messenger ribonucleic acid and protein of steroidogenic enzymes in rat adrenal in vivo. Endocrinology 139:3913-3922.

LeHoux JG, Hales DB, Fleury A, Briere N, Martel D, Ducharme L. 1999. The in vivo effects of adrenocorticotropin and sodium restriction on the formation of the different

species of steroidogenic acute regulatory protein in rat adrenal. Endocrinology 140:5154-5164.

Lin D, Sugawara T, Strauss III JF, Clark BJ, Stocco DM, Saenger P, Rogol A, Miller WL. 1995. Role of steroidogenic acute regulatory protein in adrenal and gonadal steroidogenesis. Science 267:1828-1831.

Mathieu AP, Fleury A, Ducharme L, Lavigne P, LeHoux JG. 2002. Molecular modeling of the human and hamster adrenal steroidogenic acute regulatory (StAR) protein: Insight on cholesterol transfer into mitochondria. Unpublished

Moog-Lutz C, Tomasetto C, Regnier CH, Wendling C, Lutz Y, Muller D, Chenard MP, Basset P, Rio MC. 1997. MLN64 exhibits homology with the steroidogenic acute regulatory protein (STAR) and is over-expressed in human breast carcinomas. Int J Cancer 71:183-191.

Niswender GD. 2002. Molecular control of luteal secretion of progesterone. Reproduction 123:333-339.

Papadopoulos V, Amri H, Li H, Boujrad N, Vidic B, Garnier M. 1997. Targeted disruption of the peripheral-type benzodiazepine receptor gene inhibits steroidogenesis in the R2C Leydig tumor cell line. J Biol Chem 272:32129-32135.

Petrescu AD, Gallegos AM, Okamura Y, Strauss III JF, Schroeder F. 2001. Steroidogenic acute regulatory protein binds cholesterol and modulates mitochondrial membrane sterol domain dynamics. J Biol Chem 276:36970-36982.

Pilon N, Daneau I, Brisson C, Ethier JF, Lussier JG, Silversides DW. 1997. Porcine and bovine steroidogenic acute regulatory protein (StAR) gene expression during gestation. Endocrinology 138:1085-1091.

Pon L, Moll T, Vestweber D, Marshallsay B, Schatz G. 1989. Protein import into mitochondria: ATP-dependent protein translocation activity in a submitochondrial fraction enriched in membrane contact sites and specific proteins. J Cell Biol 109:2603-2616.

Pon LA, Epstein LF, Orme-Johnson NR. 1986a. Acute cAMP stimulation in Leydig cells: rapid accumulation of a protein similar to that detected in adrenal cortex and corpus luteum. Endocr Res 12:429-446.

Pon LA, Hartigan JA, Orme-Johnson NR. 1986b. Acute ACTH regulation of adrenal corticosteroid biosynthesis. Rapid accumulation of a phosphoprotein. J Biol Chem 261:13309-13316.

Pon LA, Orme-Johnson NR. 1986. Acute stimulation of steroidogenesis in corpus luteum and adrenal cortex by peptide hormones. Rapid induction of a similar protein in both tissues. J Biol Chem 261:6594-6599.

Privalle CT, Crivello JF, Jefcoate CR. 1983. Regulation of intramitochondrial cholesterol transfer to side-chain cleavage cytochrome P-450 in rat adrenal gland. Proc Natl Acad Sci USA 80:702-706.

Reinhart AJ, Williams SC, Clark BJ, Stocco DM. 1999. SF-1 (steroidogenic factor-1) and C/EBP beta (CCAAT/enhancer binding protein-beta) cooperate to regulate the murine StAR (steroidogenic acute regulatory) promoter. Mol Endocrinol 13:729-741.

Rust W, Stedronsky K, Tillmann G, Morley S, Walther N, Ivell R. 1998. The role of SF-1/Ad4BP in the control of the bovine gene for the steroidogenic acute regulatory (StAR) protein. J Mol Endocrinol 21:189-200.

Sandhoff TW, Hales DB, Hales KH, McLean MP. 1998. Transcriptional regulation of the rat steroidogenic acute regulatory protein gene by steroidogenic factor 1. Endocrinology 139:4820-4831.

Schwaiger M, Herzog V, Neupert W. 1987. Characterization of translocation contact sites involved in the import of mitochondrial proteins. J Cell Biol 105:235-246.

Stocco DM. 2001. Tracking the role of a star in the sky of the new millennium. Mol Endocrinol 15:1245-1254.

Stocco DM, Chen W. 1991. Presence of identical mitochondrial proteins in unstimulated constitutive steroid-producing R2C rat Leydig tumor and stimulated nonconstitutive steroid-producing MA-10 mouse Leydig tumor cells. Endocrinology 128:1918-1926.

Stocco DM, Clark BJ. 1996. Regulation of the acute production of steroids in steroidogenic cells. Endocr Rev 17:221-244.

Stocco DM, Kilgore MW. 1988. Induction of mitochondrial proteins in MA-10 Leydig tumour cells with human choriogonadotropin. Biochem J 249:95-103.

Stone D, Hechter O. 1954. Studies on ACTH action in perfused bovine adrenals: the site of action of ACTH in corticosteroidogenesis. Arch Biochem Biophys 51:457-469.

Sugawara T, Abe S, Sakuragi N, Fujimoto Y, Nomura E, Fujieda K, Saito M, Fujimoto S. 2001. RIP 140 modulates transcription of the steroidogenic acute regulatory protein gene through interactions with both SF-1 and DAX-1. Endocrinology 142:3570-3577.

Sugawara T, Holt JA, Driscoll D, Strauss III JF, Lin D, Miller WL, Patterson D, Clancy KP, Hart IM, Clark BJ. 1995. Human steroidogenic acute regulatory protein: functional activity in COS-1 cells, tissue-specific expression, and mapping of the structural gene to 8p11.2 and a pseudogene to chromosome 13. Proc Natl Acad Sci USA 92:4778-4782.

Sugawara T, Holt JA, Kiriakidou M, Strauss III JF. 1996. Steroidogenic factor 1-dependent promoter activity of the human steroidogenic acute regulatory protein (StAR) gene. Biochemistry 35:9052-9059.

Todo T, Kusakabe M, McQuillan J, Young G. 2000. Molecular cloning of steroidogenic acute regulatory (StAR) protein cDNA from rainbow trout. Unpublished

Tsujishita Y, Hurley JH. 2000. Structure and lipid transport mechanism of a StAR-related domain. Nat Struct Biol 7:408-414.

Urquhart J, Li CC. 1968. The dynamics of adrenocortical secretion. Am J Physiol 214:73-85.

Watari H, Arakane F, Moog-Lutz C, Kallen CB, Tomasetto C, Gerton GL, Rio MC, Baker ME, Strauss III JF. 1997. MLN64 contains a domain with homology to the

steroidogenic acute regulatory protein (StAR) that stimulates steroidogenesis. Proc Natl Acad Sci USA 94:8462-8467.

West LA, Horvat RD, Roess DA, Barisas BG, Juengel JL, Niswender GD. 2001. Steroidogenic acute regulatory protein and peripheral-type benzodiazepine receptor associate at the mitochondrial membrane. Endocrinology 142:502-505.

Yago N, Ichii S. 1969. Submitochondrial distribution of components of the steroid 11 beta-hydroxylase and cholesterol sidechain-cleaving enzyme systems in hog adrenal cortex. J Biochem 65:215-224.

Figures legends

Fig.1 Tissue distribution of hamster StAR mRNAs. Lines 1'-and 2': ovary and testis with a film exposure time of 72h. Lines 1-8: ovary, testis, female kidney, male kidney, female liver, male liver, female adrenal and male adrenal, respectively with a film exposure time of 24h (Fleury et al., 1998b).

Fig.2 Indirect immunofluorescence micrograph of paraffin sections of rat adrenals at 0 (A) and 5 h (B) after ACTH stimulation. C: Capsule; ZG: *zona glomerulosa*; ZF: *zona fasciculata*; ZR: *zona reticularis* (LeHoux et al., 1999).

Fig.3 Colloidal-gold electron microscopic studies of thin rat adrenal sections. A, In *the zona glomerulosa* (ZG) of the control glands, StAR was detected over MT. A few particles are localized in the cytoplasm, whereas the nucleus (N) is negative (x 40,000). B, The number of gold particles is increased over MT in the adrenal ZG in rats 5 h after ACTH stimulation. The detection of StAR remained unchanged in the cytoplasm and negative in the N (x 40,000). Similar results were obtained for the zona fasciculata cells. C, Higher Magnification of mitochondrion (*) appearing in A and B (x 80,000) (LeHoux et al., 1999).

Fig.4 Effects of ACTH on the level of StAR in rat ACTH-stimulated rats whole adrenals. Two groups of three male rats were injected with ACTH and were killed 5 h after treatment; two other groups served as controls. Immunoblotting analyses were performed

on 40 μg of mitochondrial and supernatant preparations, obtained by differential centrifugation and submitted to SDS-PAGE (LeHoux et al., 1999).

Fig. 5 Effects of ACTH on the level of StAR. A) Male rats were injected with ACTH and then killed 1 h and 5 h after treatment, respectively; another group served as control, analyses were performed on *zona glomerulosa* (ZG) preparations. B) One group of male rats was injected with ACTH and then killed 5 h after treatment; another group served as control. Proteins from whole adrenal homogenates (HOM) panel A, mitochondria (MT) and supernatant (SN) panel B preparations were separated by electrofocusing and electrophoresis, and transferred onto nitrocellulose membrane. Western blotting analysis was performed using a specific anti-StAR antibody. The *bottom panel* is a schematic that shows the mobility of the different StAR species. Species are expressed as pI over MW (in kDa) (LeHoux et al., 1999).

Fig.6 COS-1 cells co-transfected with the F2 construct and WT StAR-pcDNA3.1 plasmids were incubated for 24 hours. $(Bu)_2$-cAMP (cAMP) (1 mM) was present in B medium. Fifty μg mitochondrial proteins of each preparation were separated on two-dimensional polyacrylamide gels, first by electrofocusing and then electrophoresis. Proteins were then transferred on membranes and revealed by an anti-StAR antibody (Fleury et al., 2002).

Fig. 7 StAR partially unfolded states are necessary for StAR activity. This figure adds StAR partially unfolded states either to the intermembrane shuttle mechanism (A) or in

the case where StAR functions outside mitochondria (B). In both cases, StAR mRNA is transcribed from the genome, translated into StAR protein, which is rapidly phosphorylated to modulate leader peptide activity (adapted from Christenson and Strauss III (2001); encircled + signs denote steps which can be stimulated by cAMP. **A)** The intermembrane shuttle mechanism. Once StAR is phosphorylated, the leader peptide is activated, leading to a protein-dependent or –independent import pathway (I - grey pentagon). The exact nature of the StAR mitochondrial import mechanism remains to be elucidated. Once inside mitochondria, StAR can function through the intermembrane shuttle mechanism where conformational changes through partially unfolded states become important for proper StAR function. **B)** StAR functions outside mitochondria. Again, StAR protein is produced and phosphorylated rapidly, allowing the leader peptide to interact with the outer mitochondrial membrane (either lipid- or protein-dependent) to target StAR near a functional mitochondrial cholesterol transporter system (T – grey hexagon); a possible candidate is PBR (West et al., 2001). Near the outer mitochondrial membrane, StAR can function through partially unfolded states allowing either cytoplasmic (Niswender, 2002) or OMM cholesterol to bind, and transferring cholesterol to T. In either mechanism, StAR can function without its leader peptide so long as: 1) StAR can enter the mitochondria without its leader peptide in the intermembrane shuttle mechanism (leader peptide-independent import), or 2) N-truncated StAR associates to mitochondrial cholesterol rich membranes (Christensen et al., 2001). OMM, outer mitochondrial membrane; IMM, inner mitochondrial membrane; I, unidentified mitochondrial import mechanism for StAR; T, unidentified mitochondrial cholesterol transport mechanism (ie: PBR); grey circles, cholesterol.

Fig.1

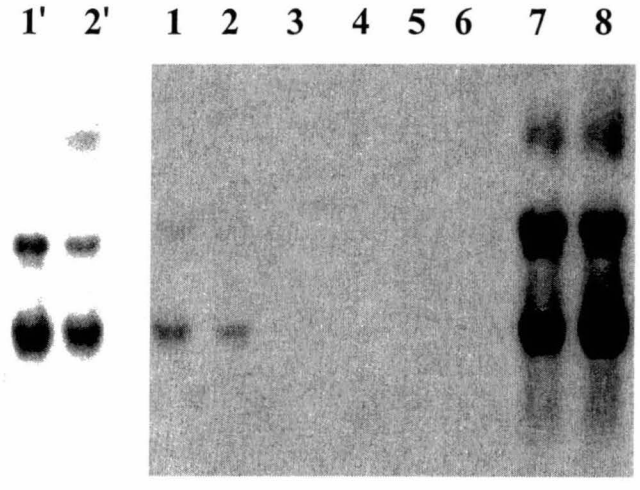

Fig.2

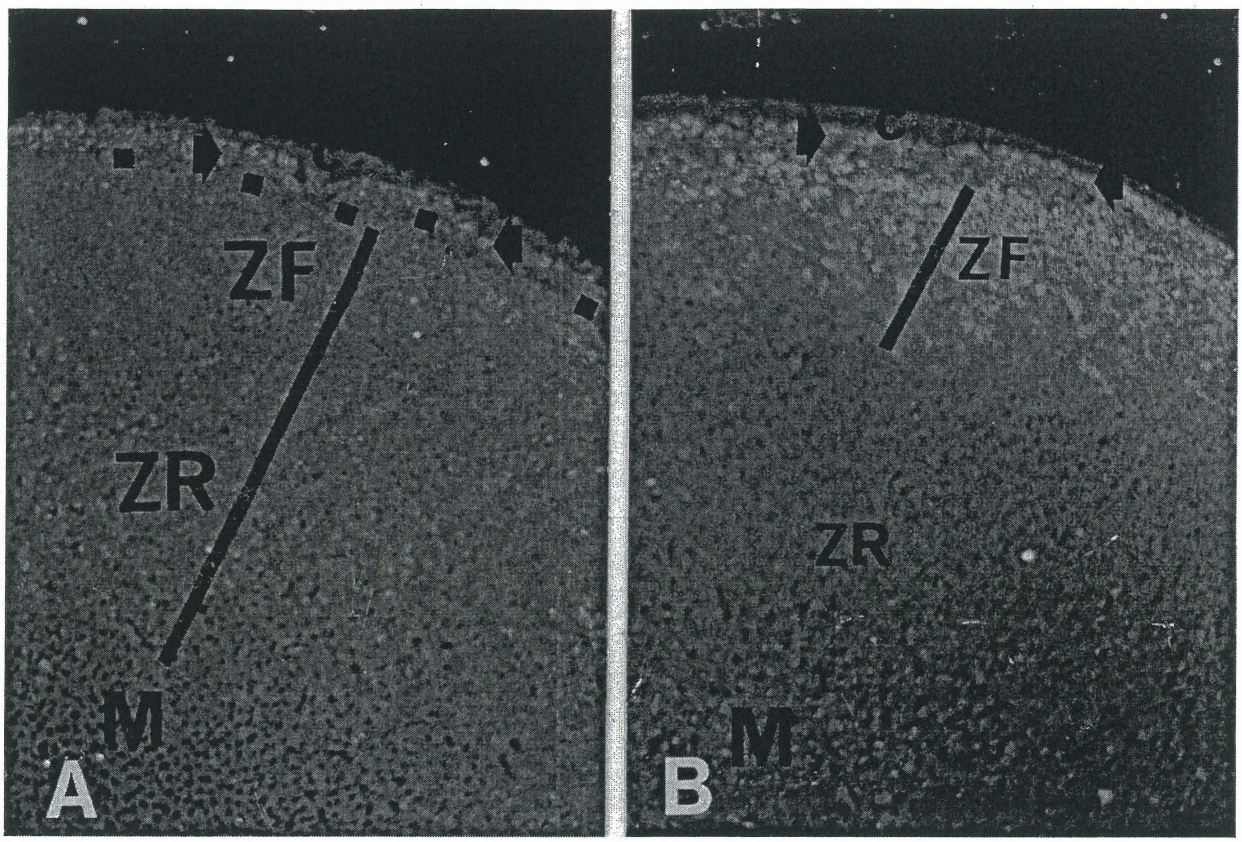

Fig.3

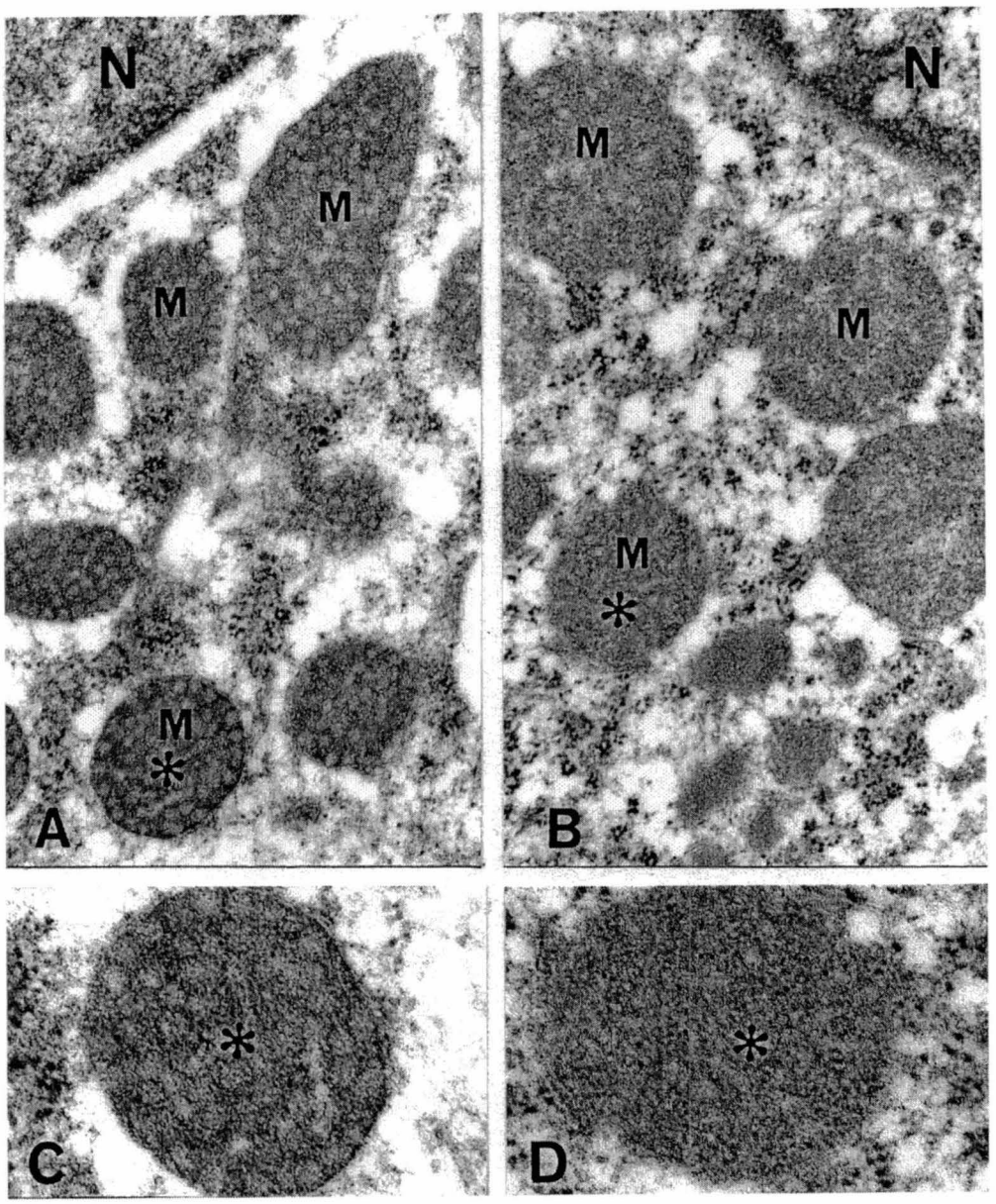

Fig.4

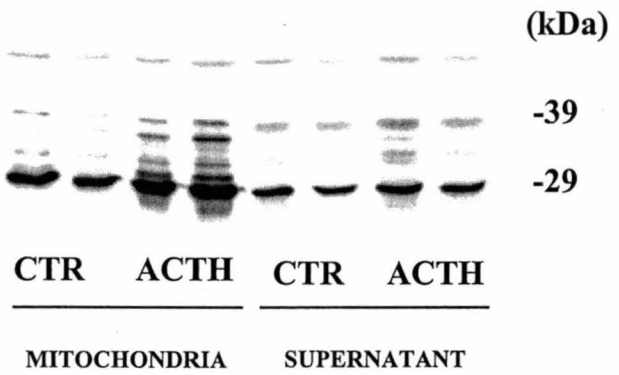

Fig.5

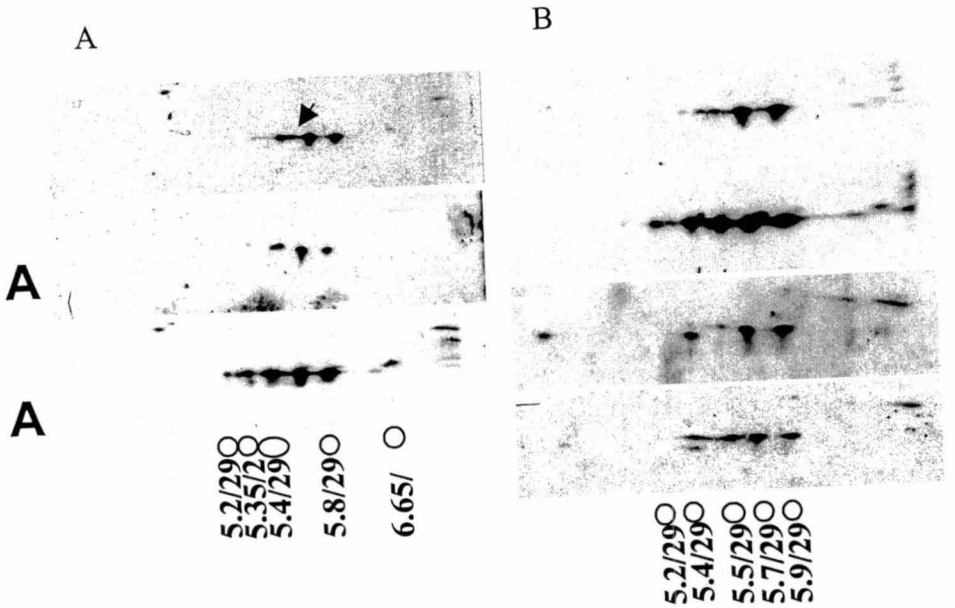

Fig.6

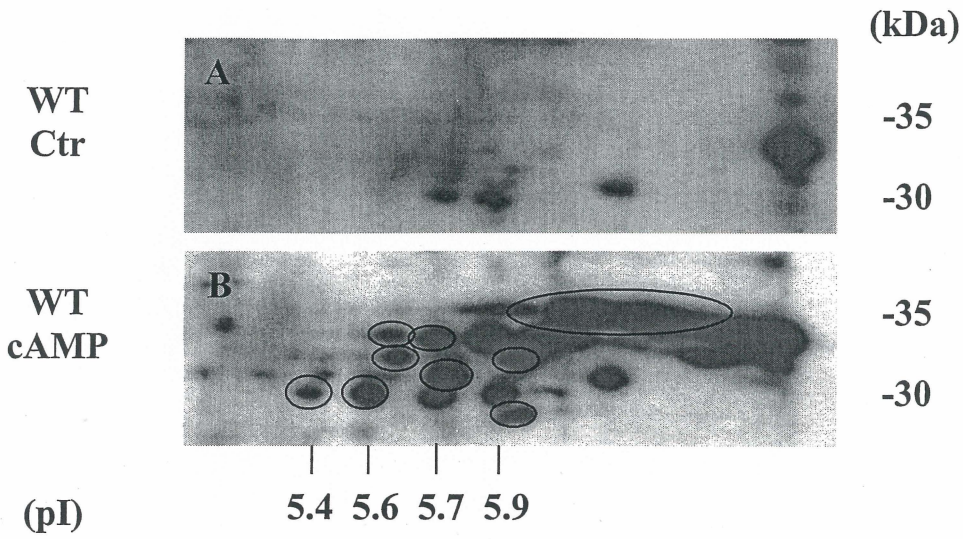

Fig.7